

**SOURCE APPORTIONMENT OF AIRBORNE
PARTICULATE MATTER IN A CHINESE
MEGACITY: MODELLING COMPARISON**

by

Zhe Tian

**A thesis submitted to the University of Birmingham for the degree of DOCTOR OF
PHILOSOPHY**

Division of Environmental Health and Risk Management

School of Geography, Earth and Environmental Science

University of Birmingham, B15 2TT

United Kingdom

March 2018

UNIVERSITY OF
BIRMINGHAM

University of Birmingham Research Archive

e-theses repository

This unpublished thesis/dissertation is copyright of the author and/or third parties. The intellectual property rights of the author or third parties in respect of this work are as defined by The Copyright Designs and Patents Act 1988 or as modified by any successor legislation.

Any use made of information contained in this thesis/dissertation must be in accordance with that legislation and must be properly acknowledged. Further distribution or reproduction in any format is prohibited without the permission of the copyright holder.

Abstract

Jinan is one of the most industrialised mega-cities in North China Plain. Like Beijing, Jinan has suffered from heavy haze pollution, particularly in the winter. This is primarily due to the high levels of PM_{2.5} in the ambient air. A quantitative understanding on the sources of PM_{2.5} is a prerequisite to develop effective measures to control the severe PM_{2.5} pollution. However, this is poorly known in Jinan. In this project, 103 PM_{2.5} samples were collected in central Jinan and their chemical composition, including water-soluble ions, trace metals, organic carbon, elemental carbon and organic molecular markers (i.e., *n*-alkanes, hopanes, polyromantic hydrocarbons and sterols), were measured. Mass closure analysis reveals that Organic Matter (OM) (29%), sulphate (18%), nitrate (10%), ammonium (9%) and geological material (9%) are the major chemical components in PM_{2.5} in Jinan. The data were fed to both PMF and CMB models for source apportionment and uncertainty analysis. PMF and CMB have identified secondary inorganic aerosol (41%; 31%), coal burning (10%; 16%), biomass burning (20%; 17%), vehicle emission (16%; 14%) and mineral dust (10%; 6%) as the major PM_{2.5} sources in Jinan, respectively. CMB also identified the metallurgic plant (11%) production as a potentially important source of Jinan's PM_{2.5}. The results were also compared with those reported in Beijing, which is also located in the North China Plain. Furtherwork needs to be done including using other source identifications such as back trajectory, chemical transport model and remote sensing to help identify the source even more accurately. Longer sampling periods is also recommended and establishing the local source profile is vital for the source apportionment in Jinan in the near future.

Acknowledgement

The four-year-long PhD study has been shaped me to be a better person. It has also been a journey that makes myself to have a better understanding of science, environment and what I really would like to achieve in the future. I am deeply grateful to all the people who have guided me in the past four years.

Firstly, I would love to express my sincere gratitude to my both supervisors Dr Zongbo Shi and Professor Roy Harrison OBE who have spent a lot of their valuable time and patience on my work and guided me to be a better researcher. Their enthusiasm for their work and research has deeply inspired me and will continue inspiring me in the future.

Besides, I also would like to thank the research group directed by Professor Li Weijun for their massive support on sampling campaign in Jinan. It has been a great time with Professor Li and the students when we delivered a decent team work and gained a great friendship. I am also very grateful to the support by the laboratory managers Dr Maria Thompson and Dr Eimear Orgill who have been always understanding and caring.

I thank my PhD colleague in both laboratory and office as well as my housemates in Birmingham along the last a couple years. And also a special thanks to Mary Harding and Gretchel Coldicott. You are all so amazing. The life would not be such colourful without you and I have learnt some amazing spirits from your stories a lot.

My sincere thanks and love also go to my wife Cheng Cheng and my family back in China. There have been quite a lot of tough moments during this study. I am stronger when I am on all your shoulders.

Last but not the least, I would like to thank the air quality team at Atkins too who have been very caring and supportive for my PhD work during the write-up stage.

The toughness of last four years is one of most valuable treasures that have been left to me. The advance never stops and the new beginning is just ahead. I will keep thriving further and many thanks to all the people again who support me along the way.

Table of Contents

Abstract.....	2
Acknowledgement	3
List of Tables	10
List of tables	15
Abbreviations	16
1 Chapter One – Introduction and Literature Review	1
1.1 Background	1
1.2 Fundamentals of receptor models.....	3
1.3 Current related study in China	5
1.4 Geographic distribution of study locations and their PM concentration level	11
1.5 Main sources identified in China and their markers used in receptor model	12
1.5.1 Tracers and organic molecular markers	12
1.5.2 Coal combustion	13
1.5.3 Marine salt	14
1.5.4 Road Traffic	15
1.5.5 Secondary Inorganic Aerosols	16
1.5.6 Mineral Dust.....	16
1.5.7 Industrial sources	17
1.5.8 Biomass Burning	18

1.5.9 Secondary Organic Aerosols and Organic Molecular Markers	19
1.6 The source profiles availability in China	20
1.6.1 Fugitive dust	23
1.6.2 On-road sources	24
1.6.3 Biomass burning.....	26
1.6.4 Cooking.....	27
1.6.5 Other sources	28
1.7 The choice and the use of receptor models	30
1.7.1 Overview	30
1.7.2 Source categories and outcomes comparison.....	33
1.7.3 Certain PM fraction source apportionment	36
1.8 Highlight points and issues.....	37
1.8.1 Sampling sites – urban, suburban and background	37
1.8.2 Analytical Chemistry – latest techniques.....	38
1.8.3 Quality Control on the modelling results: the uncertainty analysis	41
1.9 Other methods coupled with receptor modelling – New trend.....	42
1.9.1 Receptor models coupled with back trajectory	42
1.9.2 The use of organic markers in PMF.....	43
1.9.3 Inter-comparison of between different receptor models.....	44
1.9.4 Enlightenment based on previous studies and other research experiences in other countries – U.S.A. and EU	45

1.10 Source apportionment in Jinan and objectives of this project.....	47
1.10.1 Current research status and motivation.....	47
1.10.2 The structure of this thesis.....	48
2 Chapter Two Methodology	49
Abstract.....	49
2.1 Offline Sampling campaign in Jinan	49
2.1.1 TH-16A PM Sampler (Wuhan Tianhong Instruments Co.Ltd)	51
2.1.2 TH-150F Automatic Medium Volume Sampler	52
2.1.3 Weather station	52
2.2 Physical and Chemical Analysis of Deposited PM _{2.5} Filters in the Laboratory.....	53
2.2.1 Filters and its processing	53
2.2.2 Water soluble ions analysis by Ion Chromatography (IC)	54
2.2.3 Trace metal analysis by XRF	54
2.2.4 Organic Carbon (OC) and Elemental Carbon (EC) analysis.....	55
2.2.5 Organic Molecular Markers Analysis by GC-MS	56
2.3 Fundamentals of Source apportionment and Receptor modellings	69
2.4 The modelling criteria of CMB and PMF	72
2.4.1 CMB criteria	72
2.4.2 PMF criteria.....	72
2.5 Models Performance and Outcomes Evaluations	73
3 Chapter Three Mass Concentration of PM _{2.5} and its constituents n Jinan, China ...	75

Abstract.....	75
3.1 Introduction.....	75
3.3 Results and Discussion	76
3.3.1 PM _{2.5} concentration	76
3.3.2 Chemical species concentration.....	79
3.4.3 Mass Closure Analysis.....	113
3.6 Conclusion.....	114
4 Chapter Four Positive Matrix Factorisation Modelling Of PM _{2.5} Samples in Jinan	116
Abstract.....	116
4.1 Introduction.....	116
4.2 Models Parameters Setting.....	118
4.4 Modelling Results.....	121
4.4.1 Three factors	121
4.4.2 Four factors.....	122
4.4.3 Five factors	125
4.4.4 Six factors	126
4.4.5 Seven factors	128
4.5 Discussions	131
4.5.1 Further Biomass Burning's Contribution Analysis.....	131
4.5.2 Biomass burning contribution estimation by other means	132
4.5.3 PMF Uncertainty Analysis	132

4.6.3 Sources Contribution and Mass Closure	138
4.7 Conclusions	140
5 Chapter Five Chemical Mass Balance Modelling on Jinan's PM _{2.5} Dataset	142
Abstract.....	142
5.1 Introduction.....	143
5.2 Methodology	144
5.2.1 Chemical Mass Balance Model	144
5.2.2 Sampling and Chemical Analysis	144
5.2.3 Model Parameters and Settings and Evaluation Criteria	144
5.3 Source Profiles Used in the Modelling.....	145
5.3.1 Soil dust.....	149
5.3.2 Biomass Burning	150
5.3.3 Coal burning	151
5.3.4 Secondary sulphate and nitrate.....	152
5.3.5 Diesel and petrol vehicle emissions.....	153
5.3.6 Metallurgic Plant.....	153
5.4 Modelling Results and Model Performance	157
5.4.1 Annual source apportionment of PM _{2.5} in Jinan	157
5.4.2 Seasonal variation of source contributions to PM _{2.5} in Jinan.	159
5.4 Comparison between CMB modelling result and mass closure analysis	161
5.5 Further work.....	162

5.6 Conclusion.....	162
6 Chapter Six PMF and CMB Modelling Results Comparison.....	164
Abstract.....	164
6.1 Introduction.....	164
6.2 The PMF and CMB results comparison in this study.....	165
6.2.1 Profile Comparison	165
6.2.2 Annual Source Contribution	176
6.2.2 Seasonal Source Contribution and Daily Source Contribution	179
6.3 The Receptor Modelling results comparison between other studies in Jinan ..	189
6.4 The similarity and difference of PM2.5 sources between Jinan and Beijing....	193
6.5 Conclusion	194
7 Chapter Seven Conclusion	196

List of Tables

Figure 1-1 number of publications on PM source apportionments using receptor models in the last decade in China (Web of Science) from 2004 to 2014. NB: 1) A topic search of (“source apportionment” and “China” and “PM” or “particular matter” or “PMF” or “positive matrix factorization” or “CMB” or “chemical mass balance”) and (“particle*” or “particulate*” or “particulate matter*” or “aerosol*” or “PM”) and (“China” or “Chinese”)), refined by categories of (“meteorology atmospheric sciences” or “environmental sciences” or “geosciences multidisciplinary” or “engineering environmental” or “geochemistry geophysics”) b) the papers on source apportionment of VOCs or source apportionment of PM by other means are also included.	6
Figure 1-2 Source apportionment study by receptor models for PM _{2.5} and/or PM ₁₀ in China from 2004 to 2014	7
Figure 1-3 the location distribution statistics of source apportionment of PM across China	11
Figure 1-4 a) The use of different receptor models in China; b) the frequency of use of different receptor models in China.	32
Figure 1-5 Summary of mean source contributions to PM _{2.5} in Beijing from 2005-2014 and their uncertainties, based on the reviewed literatures.	34
Figure 1-6 Markers that were used for the PM _{2.5} source apportionment in Beijing.....	35
Figure 2-1 Map showing the location of Jinan City and sampling site	50
Figure 2-2 Photo and schematic diagram of TH-16A Ambient Particulate Sampler.....	51
Figure 2-3 Photo and schematic diagram of TH-150F Ambient Particulate Sampler (....	52
Figure 2-4 Summary of the whole chemical analysis processes.	67
Figure 2-5 Recovery rate for all internal standards.....	68

Figure 3-1 Daily PM _{2.5} concentration in Jinan during the whole sampling campaign.....	77
Figure 3-2 Seasonal mean PM _{2.5} concentration in Jinan	77
Figure 3-3 Annual mean concentration of measured water-soluble ions	85
Figure 3-4 Ion Balance analysis of water-soluble ions measured from Jinan's PM _{2.5} sample	87
Figure 3-5 annual mean concentration of all measured trace elements in PM _{2.5} in Jinan	88
Figure 3-6 Seasonal variation of trace metals in PM _{2.5} in Jinan.....	89
Figure 3-7 Enrichment Factor Analysis	90
Figure 3-8 Annual mean PAHs concentration.....	93
Figure 3-9 Seasonal variation of PAHs mass concentration.	94
Figure 3-10 Annual Mean n-Alkanes concentration in Jinan	95
Figure 3-11 seasonal variations of n-alkenes in Jinan.....	96
Figure 3-12 Annual Mean hopanes concentration in Jinan	98
Figure 3-13 Seasonal variation of hopanes in Jinan	100
Figure 3-14 Correlations between ^{K+} and levoglucosan in the four seasons	103
Figure 3-15 a) the correlation of K ⁺ and SO ₄ ²⁻ during the five sampling period; b) the correlation of K ⁺ and Cl ⁻ during the five sampling period.....	104
Figure 3-16 the correlation of levoglucosan and OC during the five sampling period.....	106
Figure 3-17 a) the correlation of K ⁺ and levoglucosan during the five sampling period; b) the correlation of levoglucoan and OC during the five sampling period.....	108
Figure 3-18 Wind rose analyses on wind speed and direction in Jinan a) winter; b) spring; c) summer; d) autumn	112
Figure 3-16 Mass reconstruction and contribution percentage of the chemical components for PM _{2.5} in Jinan	114

Figure 4-1 Factor profiles when three factors was set before the model run.....	121
Figure 4-2 Factor profiles when four factors was set before the model run	124
Figure 4-3 Factor profiles when five factors was set before the model run	126
Figure 4-4 Factor profiles when six factors was set before the model run	128
Figure 4-5 Factor profiles when seven factors was set before the model run	129
Figure 4-6: G-space plot of factor 3 and factor 7.....	130
Figure 4-7 Time series of sources contribution during the sampling campaign.....	134
Figure 4-8 Uncertainties of each species contribution in each profile due to random error mainly	135
Figure 4-9 Obs/Pred time series analysis of model run	137
Figure 4-10 a) Source contribution modelled by PMF; b) mass closure analysis.....	139
Figure 5-1 Chemical characterisation of soil profile in Tianjin, Northern China (Provided by College of Environmental Science and Engineering, NKU).	150
Figure 5-2 Chemical characterisation of biomass burning profile in Xiamen, Eastern China (Zhang et al. 2016).	151
Figure 5-3 Chemical characterisation of coal burning profile China (Hao, 2008).....	152
Figure 5-4 Source profile of secondary sulphate and nitrate (Zhang et al. 2016).	152
Figure 5-5 Chemical characterisation of vehicle exhaust profile in Xiamen, Eastern China.	153
Figure 5-6 Chemical characterisation of metallurgic plant profile in Jinan, Northern China (Provided by College of Environmental Science and Engineering, NKU).....	154
Figure 5-7 PM _{2.5} apportionment by CMB v8.2 in Jinan coupled with the PM _{2.5} profiles from China	158
Figure 5-8 Seasonal variations of source contributions to PM _{2.5} in Jinan.....	160

Figure 5-9 Annual PM _{2.5} Mass Closure analysis in Jinan	161
Figure 6-1 a) Source (or factor) profiles of soil or mineral dust comparison (Provided by College of Environmental Science and Engineering, NKU); b) species abundances correlations between measured and PMF-generated profiles for soil/mineral dust	166
Figure 6-2 a) Source (or factor) profiles of secondary nitrate comparison (Zhang et al. 2016) species abundances correlations between measured and PMF-generated profiles for secondary nitrate.....	168
Figure 6-3 a) Source (or factor) profiles of secondary sulphate comparison (Zhang et al. 2016); b) species abundances correlations between measured and PMF-generated profiles for secondary sulphate.....	169
Figure 6-4 a) Source (or factor) profiles of biomass burning comparison (Zhang et al. 2016); b) species abundances correlations between measured and PMF-generated profiles for biomass burning emissions.....	171
Figure 6-5 a) Correlation between PMF modelled biomass burning and measured biomass burning profile; b) G-plot between PMF modelled biomass burning and secondary sulphate; PMF modelled biomass burning and coal burning.....	173
Figure 6-6 a) Source (or factor) profiles of coal burning comparison; b) species abundances correlations between measured and PMF-generated profiles for coal burning.....	174
Figure 6-7 a) Source (or factor) profiles of petrol car/vehicle exhaust comparison; b) species abundances correlations between measured and PMF-generated profiles for petrol car/vehicle exhaust.....	176
Figure 6-8 Comparison of source apportionment of PM _{2.5} results by CMB and PMF model run	177
Figure 6-9 the G-plot of biomass burning against secondary sulphate factor	178

Figure 6-10 a) – f) Comparison of seasonal variations of PM _{2.5} apportionments for vehicle emission, soil/mineral dust, coal burning, industrial emission, secondary sulphate and secondary nitrate, respectively, by CMB and PMF.....	183
Figure 6-11 a) Source apportionment of PM ₁₀ by CMB in 2002 (Bi et al. 2007); b) Source apportionment of PM _{2.5} by CMB in this study.	190
Figure 6-12 a) Source apportionment of PM _{2.5} by PMF in 2002 (Yang et al., 2012); b) Source apportionment of PM _{2.5} by PMF in this study.....	192
Figure 6-13 PM _{2.5} source contribution in Jinan compared with source contributions to PM _{2.5} in Beijing from 2005-2014 based on the reviewed literatures.	193

List of tables

Table 2-1 The measured PAHs and their basic physical properties	56
Table 2-2 GC-MS sample injection programming for <i>n</i> -alkanes & hopanes	62
Table 2-3 GC-MS sample injection programming for PAHs	63
Table 2-4 GC-MS sample injection programming for Levoglucosan & Cholesterol.....	64
Table 2-5 Limit of detections (LoD) for all chemical species	65
Table 3-1 Seasonal and periods mean concentration of all measured chemical species. .	79
Table 3-2 Mean OC, EC and PM _{2.5} concentration for all periods in Jinan	83
Table 3-3 Mean seasonal total PAHs concentration and its range.	92
Table 3-4 Mean concentration and range of total <i>n</i> -alkanes	96
Table 3-5 Seasonal mean mass concentration of total hopanes and their ranges at each season.....	99
Table 3-6 Summary of levoglucosan and cholesterol measurement in PM _{2.5} , Jinan ...	101
Table 3-7 Summary of Wind Speed, Wind direction and RH during the sampling period in Jinan.....	110
Table 4-1 Input Data Statistics for PMF Modelling.	119
Table 5-1 Mass concentrations of source profiles that used in the CMB modelling.....	146
Table 5-2 Mass concentration uncertainties of source profiles that used in the CMB modelling (% mass)	148
Table 5-3 the list of rejected profiles that have been used during the receptor modelling in CMB (% mass)	163
Table 6-1 Seasonal Source Apportionment of PM _{2.5} in Jinan by both CMB and PMF	180

Abbreviations

AQG	Air Quality Guideline
CMB	Chemical Mass Balance
CTM	Chemical Transport Modelling
CPF	Conditional Probability Function
EI	Emission Inventory
GC-MS	Gas Chromatography-Mass Spectrometry
HPLC	High-performance liquid chromatography
HMW	High Molecular Weight
ICP-MS	Inductively Coupled Plasma-Atomic Emission Spectrometer
IC	Ion Chromatography
LMW	Low Molecular Weight
ME-2	Multiple Engine 2
NCP	North China Plain
POMs	Particulate Organic Matters
PRD	Pearl River Delta
PM ₁₀	air borne particulate matter with aerodynamic diameter less than 10 micron
PM _{2.5}	air borne particulate matter with aerodynamic diameter less than 2.5 micron
PMF	Positive Matrix Factorisation
PSCF	Potential Source Contribution Function
PCA	Principle Component Analysis
RM	Receptor Modelling
RTA	Residence Time Analysis
SQTBA	Simplified Quantitative Trajectory Bias Analysis
TSP	Total Suspended Particles
USEPA	United States Environmental Protection Agency
VOC	Volatile Organic Carbons
WHO	World Health Organisation
XRF	X-ray fluorescence spectrometer
YRD	Yangtze River Delta

1 Chapter One – Introduction and Literature Review

1.1 Background

Chinese megacities have suffered from poor air quality for more than two decades (Chan , 2008; Ma et al. 2012; Yao et al. 2009). The expansion of population and industrialization have resulted in large increase in energy consumption, leading to more air pollutant emission (Chan, 2008). The huge increase in the number of vehicles on roads in the last 20 years also contributes to the severe air pollution in China (Zhang et al. 2014). PM₁₀, PM_{2.5}, NO_x, CO, O₃ and SO₂ are the major pollutants in the ambient air in China today (Ma et al. 2012). Meanwhile, four major haze regions have been found in China, which is North China Plain (NCP), Yangtze River Delta (YRD), Sichuan Basin and Pearl River Delta (PRD) (Pui et al. 2014; Li et al. 2017). NCP is, however, the most polluted region in terms of PM_{2.5} in China (Li et al. 2017). In 2008, only 19 of 113 major cities in China met the requirements of WHO Interim target-1 (IT-1), which is 35 µg·m⁻³ for annual mean concentration for PM_{2.5} (WHO, 2005; Zheng, Mei et al. 2014). Moreover, only six cities met the IT-2 and none of them meets the IT-3 and Air Quality Guideline (AQG), where the annual mean PM_{2.5} concentration is 25 and 15 µg·m⁻³, respectively (WHO, 2005; Zheng, Mei et al. 2014). Furthermore, compared to London smog and Los Angeles smog, Chinese smog seems more complex, formed by emission of coal combustion, vehicle exhaust, domestic biomass burning as well as other secondary pathways, e.g. photochemical

pollution and secondary aerosol formations (He et al., 2011). The Chinese smog has resulted in a far-reaching impact on public health service and economy sector (Ma et al., 2012). Li et al. (2016) estimated that the health-related economic loss caused by PM₁₀ and SO₂ accounted for 1.6 and 2.3% of the GDP based on the data from 74 cities in 2015. To combat air pollution, it is essential to accurately quantify the sources of these pollutants.

Source apportionment is a technique to identify and quantify the emission contribution from different sources at receptor site, which is the base of air pollution control and an increasingly important component in air quality planning and management (Hopke 2016). In general, there are three major ways to find the sources of ambient pollutants, Emission Inventory (EI), Receptor Modelling (RM) and Chemical Transport Modelling (CTM) (Hopke 2003; Cao et al. 2011; Hopke 2016). EI and CTM are bottom-up methods. The CTM can conclude or deduce the pollution from many point sources by simulating the meteorology, source emission rate and chemical reactions during the transport (Hopke 2016). While emission inventory investigates and summarizes the emission factor and emission rate of each source and find their contribution (Cao et al. 2011). On the other hand, receptor modelling is a top-down method which focused on how the sources in the study region contribute the pollution level at the receptor site (Hopke 2016). This method is based on mass conservation and statistics. There following major and popular receptor models in use today, including Chemical Mass Balance (CMB), Principle Component Analysis (PCA), Positive Matrix Factorisation (PMF), Multiple Engine 2 (ME-2) and Unmix etc. (Belis et al., 2014). Normally, both methods, that is, receptor models and CTM, are recommended to be applied together in order to offset the weakness of each approach (USEPA, <https://www3.epa.gov/scram001/models/receptor/EPA-CMB82Manual.pdf>,

no date). Some other researchers also evaluate the pollution by the routine monitoring data, for example, the correlation between wind direction with local measured components concentration, back trajectory analysis and correlation of gaseous pollutants with particular matter components to identify the associated sources etc. (Zhang et al. 2014). All of these methods have been applied in some certain source apportionment study in China.

Anyhow, a proper and detailed source apportionment can be vital for policymakers to refine the current mitigation methods as well as monitoring the air quality improvement and evaluate the previous efforts. Until today, there have been hundreds of publications related to source apportionment about Chinese urban ambient pollutants since the late 1990s. However, the methodology between different authors and research group can be largely different, for example, the length of sampling, the sampler type, the place of interest, how the pollutants have been characterized by the analytical method and the choice of models and its execution. Meanwhile, it is also lack of enough parallel comparisons between the different studies too. Since there is still a strong need for air quality data, especially more source apportionment works across the country, it is vital to extract more potential valuable information from the previous works, which is helpful for the future study of experimental design, comparability analysis, policy and public health assessment etc.

1.2 Fundamentals of receptor models

This project is mainly focused on receptor models such as CMB and PMF. The details of theory on these methods can be found in the other reviews and it will be presented in chapter two (Hopke 2003; Viana et al. 2008; Pant & Harrison 2013; Hopke 2016). There are a couple of review papers describing the sampling and chemical analysis instruments

and techniques for particular matter used in China elsewhere, which is also not repeated in this Chapter (Pui et al. 2014; Zheng et al. 2014; Liang et al. 2016)

In brief, no matter which kind of receptor models, they are all based on the principle of mass balance, which is assumed that the mass of pollutants is in conservation between the emission and receptor site. In this case, the following mass equation can be written to account for all m species in the n samples contributed from p independent sources (Hopke 2016):

$$x_{ij} = \sum_{k=1}^p g_{ij} f_{kj} \quad (1.1)$$

where x_{ij} is the j^{th} chemical species concentration measured in the i^{th} sample, f_{kj} is the concentration of the j^{th} species in emission from the k^{th} source contributing to the i^{th} sample. This conceptual model and equation can be fitted to the varies of available data and solved differently in the real model such as CMB and PMF (Hopke 2016). Usually, the PM samples are collected in a daily basis so that the daily mean concentration can be measured. The samples will also be analysed by analytical chemical instruments so that different chemical species can be identified and quantified so that the data input can be prepared. In some cases, the source profile is also compulsory for the model run so that it should be also prepared prior to the modelling, for example, CMB.

1.3 Current related study in China

It is always helpful to understand the current research status of source apportionment in China before the new project so that the lessons can be learnt from the previous experiences in order to achieve the improvements. The data mining of source apportionment related papers from 2004 to 2016 has been preceded on the Web of Sciences. Overall, there has been increasing research intensity on source apportionment of PM in China. According to the database on Web of Science, there are 154 papers containing the detailed information on source apportionment in total have been found between this decade (*See Figure 1-1*). According to figure 2.1, there is a limited number of publications in the first five years on source apportionment of air pollutants. However, there has been a significant increase in publication since 2009. In addition, it is found that most of the studies only employed one source apportionment approach for one type of pollutants before 2009, for example, by using one type of models to apportion sources' contribution to PM_{2.5} in Hong Kong (Ho et al. 2006). There is an increasing number of source apportionment on air pollutants by different methods after 2009. Moreover, there is a clear increasing trend that studying the sources of both PM₁₀ and PM_{2.5} by different methodologies have become the hot-spot in China. However, it has to be noted that only about half of these publications are mainly based on receptor models.



Figure 1-1 number of publications on PM source apportionments using receptor models in the last decade in China (Web of Science) from 2004 to 2016. NB: 1) A topic search of (“source apportionment” and “China” and “PM” or “particular matter” or “PMF” or “positive matrix factorization” or “CMB” or “chemical mass balance”) and (“particle*” or “particulate*” or “particulate matter*” or “aerosol*” or “PM”) and (“China” or “Chinese”)), refined by categories of (“meteorology atmospheric sciences” or “environmental sciences” or “geosciences multidisciplinary” or “engineering environmental” or “geochemistry geophysics”) b) the papers on source apportionment of VOCs or source apportionment of PM by other means are also included.

Therefore, 50 papers which use receptor models (including CMB, PMF, ME-2, UNMIX and PCA) have been selected from the data mining and their details are summarized in Table 1-1 below. The location of study, the choice of receptor model, the choice of pollutants, the average concentration of pollutants and source apportionment results are presented.

Table 1-1 The source apportionment study by receptor models for PM_{2.5} and/or PM₁₀ in China from 2004 to 2014

Ref	Location	Method	Pollutants	Annual PM _{2.5} and/or PM ₁₀ Concentration (µg/m ³)	PM _{2.5} or PM ₁₀ Source Contribution (%)								
					Coal Burning	Marine	Vehicle	Secondary Aerosols	Mineral Dust	Industry	Biomass Burning	SOC	Other
Lei et al. (2004)	Beijing	PMF	PM _{2.5}	-	-	-	-	-	-	-	-	-	-
Sun et al. (2004)	Beijing	Factor Analysis	PM _{2.5} & PM ₁₀	77.3	3.6	-	5.7	53.7	13.3	4.9	-	-	12.6
Okuda et al. (2004)	Beijing	CMB	PM ₁₀	171.0	25.0	-	22.0	16.0	37.0	0.0	-	-	-
Zhang et al. (2005)	Beijing	CMB	PM _{2.5}	101.0	14.0	-	7.0	33.0	20.0	26.0	25.0	-	-
Wang et al. (2006)	Guangzhou	CMB	PM ₁₀	90.9	26.0	4.0	38.4	20.0	10.0	-	-	-	-
Querol et al. (2006)	Wuhan	PCA	PM ₁₀	156.0	31.0	-	16.0	-	-	28.0	-	-	-
Song, et al. (2006a)	Beijing	PCA	PM _{2.5}	96.1	26.7	-	6.0	23.3	7.2	6.6	-	-	26.4
Song, Y. et al. (2006b)	Beijing	PMF	PM _{2.5}	96.1	19.0	-	6.0	31.0	9.0	6.0	-	-	12.0
Lu et al. (2007)	Beijing	Factor Analysis	PM ₁₀	71---319-	11.2	-	-	-	52.4	25.6	-	-	-
Bi et al. (2007)	Jinan etc.	CMB	PM ₁₀	115.0	19.0	-	9.0	9.0	55.0	-	-	-	-
Zhang, et al. (2007)	Beijing	CMB/PMF	PM _{2.5} & PM ₁₀	141.9	20;14	-	26;28	15;19	19;20	6;5	15;20	-	0;2
Feng, et al. (2007)	Jiaozuo	CMB	PM ₁₀	326.0	13.9	-	6.1	-	76.4	0.5	-	-	3.2
Wang, et al. (2008)	Beijing	PMF	PM _{2.5}	-	28.5	-	5.9	17.4	15.9	-	8.8	-	13.7
Guo et al. (2009)	Hong Kong	PCA	PM _{2.5}	-	-	7.0	23.0	28.0	10.0	-	-	-	13.0
Wang, et al.(2009)	Beijing	PMF	PM _{2.5} & PM ₁₀	102.0	25.0	-	4.0	45.0	2.0	9.0	15.0	-	-

Ref	Location	Method	Pollutants	Annual PM _{2.5} and/or PM ₁₀ Concentration (µg/m ³)	PM _{2.5} or PM ₁₀ Source Contribution (%)								
					Coal Burning	Marine	Vehicle	Secondary Aerosols	Mineral Dust	Industry	Biomass Burning	SOC	Other
Wu, et al. (2009)	Kaifeng	CMB	PM ₁₀	116.0	17.0	26.2	10.5	19.0	12.0	-	-	5.8	4.8
Li et al. (2010)	Changsha	PCA	PM ₁₀	101.0	7.0	-	14.7	13.3	33.0	6.7	11.0	-	-
Kong et al. (2010)	Tianjin	CMB	PM _{2.5} & PM ₁₀	70.9	16.0	7.0	34.0	-	10.0	-	-	-	33.0
Gao et al. (2011)	Jinan etc.	PCA	PM _{2.5}	-	-	13.0	45.0	15.0	-	-	-	-	-
Huang et al. (2011)	Harbin	CMB	PM ₁₀	63.6--- 306.1	16.3	-	11.0	17.7	14.4	12.0	-	7.2	14.9
Han et al. (2011)	Wuxi	CMB	PM ₁₀	106.5	14.6	-	9.4	9.0	57.0	2.0	-	5.0	3.0
Wang et al. (2012)	Ordos	PCA-MLR	PM _{2.5} & PM ₁₀	51.8	4.6	-	22.7	32.4	35.8	-	-	-	-
Qiu et al. et al. (2012)	Longyang	CMB	PM ₁₀	100.0	6.4	7.4	15.4	20.8	8.7	5.4	-	-	-
Kong et al. (2012)	Fushun	PCA	PM ₁₀	130.2	27.7	-	20.7	-	21.5	18.2	5.8	-	-
Ni et al. (2012)	Shenyang etc. in Liaoning Province	CMB	PM ₁₀	188.1	35.6	-	14.1	-	37.4	16.9	-	-	3.9
Cheng, S.Y. et al. (2013)	Beijing	PCA	PM _{2.5}	-	17.7	4.9	15.4	-	27.4	14.2	13.4	-	-
Wu. G. et al. (2013)	Shenzhen	PCA	PM ₁₀	108.4	54.5	-	8.0	-	-	11.4	-	-	-
Zhang, et al. (2013)	Beijing	PMF	PM _{2.5}	135.0	14.0	-	3.0	26.0	16.0	28.0	13.0	-	-
Li, et al. (2013)	Kinmen and Xiamen	PCA	PM ₁₀	75.0	14.0	16.5	-	-	42.8	7.0	-	-	-

Ref	Location	Method	Pollutants	Annual PM _{2.5} and/or PM ₁₀ Concentration (µg/m ³)	PM _{2.5} or PM ₁₀ Source Contribution (%)								
					Coal Burning	Marine	Vehicle	Secondary Aerosols	Mineral Dust	Industry	Biomass Burning	SOC	Other
Hu et al. (2013)	Nanjing	PCA	PM _{2.5} & TSP	76.4	26.3	15.2	13.7	-	25.7	-	-	-	-
Yu et al. (2013)	Beijing	PMF	PM _{2.5}	55.4	16.0	-	17.1	26.5	23.1	6.0	11.2	-	-
Wang (2013)	Northern Yellow Sea	PMF	TSP	123.2	10.0	9.3	-	42.1	-	2.6	11.5	-	-
Geng et al. (2013)	Zhengzhou	PMF	PM _{2.5}	175.0	44.0	-	16.0	41.0	46.0	8.0	23.0	-	-
Yang, et al. (2013)	Jinan	PMF	PM _{2.5}	148.7	21.0	-	6.1	51.2	9.3	2.9	4.6	-	1.1
Huang et al. (2013)	Qingyuan	PMF	PM _{2.5}	111.2	12.6	-	7.6	39.1	8.2	13.3	3.2	-	-
Dai, et al. (2013)	Shen Zhen	PMF-OMM	PM _{2.5}	101.6	-	-	-	-	-	-	-	-	-
Li et al. (2014)	Suixi	PMF	PM _{2.5}	110.7	6.1	-	5.4	28.4	10.4	0.7	44.9	-	8.5
Huang, X.F. (2014)	Shenzhen	PMF	PM _{2.5}	42.2	-	-	26.9	39.3	-	-	9.8	17.6	-
Liu et al. (2014)	Beijing	PMF	PM ₁₀	-	-	-	25.5	34.7	20.3	19.5	-	-	-
Huang et al. (2014)	Beijing etc.	CMB and PMF	PM _{2.5}	159.0	26.1	-	5.6	25.3	10.0	-	5.6	25.8	26.9
Tao et al. (2014)	Chengdu	PMF	PM _{2.5}	119.0	22.0	-	-	46.0	10.0	25.0	15.0	-	-
Wei et al. (2014)	Southern Hebei Province	PMF	PM _{2.5}	160.1	25.9	-	7.7	21.8	10.9	16.2	-	-	-
Liu et al. (2015)	Hangzhou	PMF	PM _{2.5}	108.2	12.8	-	17.2	27.9	-	10.1	-	-	-
Hua et al. (2015)	Nanjing	CMB	PM _{2.5}	-	5	-	15	55	4	5	19	-	-
	Suzhou	CMB	PM _{2.5}	-	7	-	6	50	7	4	26	-	-

Ref	Location	Method	Pollutants	Annual PM _{2.5} and/or PM ₁₀ Concentration (µg/m ³)	PM _{2.5} or PM ₁₀ Source Contribution (%)								
					Coal Burning	Marine	Vehicle	Secondary Aerosols	Mineral Dust	Industry	Biomass Burning	SOC	Other
	Ningbo	CMB	PM _{2.5}		5		22	43	2	2	21		
	Shanghai	CMB	PM _{2.5}		11		8	58	2	1	16		
Yao et al. (2016)	North China Plain	PMF	PM _{2.5}	80.9			5.2	54.3	8.3	15.6	15.8		
Li et al. (2016)	Nanjing	PMF	PM _{2.5}	142	12.4	4.5		64.1	10.6	8.45			
Wang et al. (2016)	Guangzhou	CMB	PM _{2.5}	138	24.6		14.1				5.6	15.9	
Liu et al. (2016)	Taian	PMF	PM _{2.5}	70.8	17.9		16.7	27.47	9.4	19.6			
Tao et al. (2017)	PDR	PMF	PM _{2.5}	47	15		10	50	7				

NB: It has to notice that only the works based on PMF, CMB and related methods including PCA etc. for particular matter only are shown above. If there is more than one method or particular matter size has been studied, PMF and CMB are preferable in terms of method and PM_{2.5} is preferable in this table.

1.4 Geographic distribution of study locations and their PM concentration level

Except the research activity on this topic in the last a couple of years, there are following main features worth addressing based on table one: 1) the latest $PM_{2.5}$ and PM_{10} concentration level; 2) the geographic distribution of study locations; 2) the methods applied in Chinese source apportionment of PM and the major sources that have been identified by these research.

Based on the data summarized in table one, it can be found that most of the case study on source apportionment of PM is in north China, accounting for 60% over a total number of case study (See Figure 1-2). Among these 60% northern Chinese cities, 16 out of 27 case studies were in Beijing so that Beijing has become the most studied city on PM source apportionment in China.

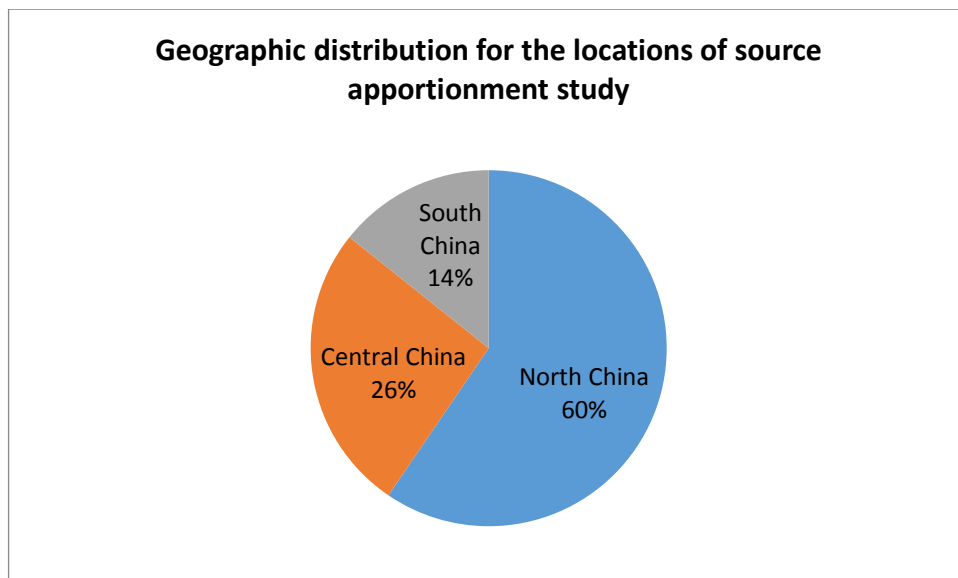


Figure 1-2 the location distribution statistics of source apportionment of PM across China

Moreover, according to Table 1-1, all the mean concentration of $PM_{2.5}$ or PM_{10} during the sampling campaign is more than 35 and 75 $\mu\text{g}\cdot\text{m}^{-3}$, respectively, which is greater than the

second tier concentration of PM_{2.5} and PM₁₀ in the latest national ambient air quality standards of China (MEP, 2012). It is also much higher than the WHO guidelines on ambient PM_{2.5} and PM₁₀ level that can be suggested have very low risk to human health as mentioned earlier. Therefore the PM pollution is still a very common issue not only in major big cities such as Beijing but in from moderate size to mega-city across the country. As suggested in the other publications, it has become a regional pollution issue (Huang et al. 2014).

1.5 Main sources identified in China and their markers used in receptor model

In the majority of published papers on source apportionment of Chinese megacities, there are five major sources including 1) coal combustion; 2) vehicle exhaust and road dust; 3) secondary inorganic aerosols; 4) industrial emission and 5) biomass burning as shown in Table 1-1. Meanwhile, waste incineration and marine salt are also occasionally identified depending on the location and the use of technique (Zhang et al. 2013). In this section, the major sources found in China and which tracers that have been used for apportioning the sources will be discussed.

1.5.1 Tracers and organic molecular markers

The chemical signatures of measured chemical species from the sample are vital to the receptor models to apportion the sources of these particular matters (Lin et al. 2010). The receptor models use these signatures from both sources emissions (or source profiles) and ambient samples to identify the specific sources and then it helps to quantify its contribution (Bullock et al. 2008). The ideal tracer (or called organic molecular markers) is regard as the chemicals that:

“Must be characteristic of some sources but not others and must react slowly enough in the atmosphere that they will survive transport from their source to receptor air monitoring stations.”

(Cass, 1998)

They are also should not be formed by atmospheric chemical reactions or can be evaporated to gas phase from liquid or solid phase during the transport to the receptor site (Cass, 1988). In this case, if the source profile is provided, as the sample is regarded as a linear combination of these tracers compounds distributions present in the effluent from the contributing sources based on mass balance principle, these tracers amount in the samples can be used to estimate the relative contribution from the corresponding sources (Cass, 1988), for example, CMB. Alternatively, they can also be helpful when it is used for determining the type of source in a qualitative way in other models such as PMF. It is crucial to choose a distinctive compound in a source as a tracer and have a good knowledge of the ratio between the total particle mass emission rate and tracer mass emission rate in order to make this approach work correctly (Cass 1998).

1.5.2 Coal combustion

Coal combustion is the major combustion of PM sources in China (Yao et al. 2009). In China, coal is particularly widely used for domestic heating in local combustion appliances from mid-November to late March in the majority of Northern China as well as one of the major resources for power plants (Ziková et al. 2016). Another study suggests that 3.81 million tonnes of coal are burnt per year in total by the coal-fired power plants in mainland China that may contribute 44.6% of the total PM emission by mass (Yao et al. 2009). Coal combustion can be also related to the industrial boilers as it is a very important energy supply in the China's heavy industry as well as local small workshops (Hao et al., 2008). Coal combustion is one the most frequently apportioned and quantified source according

to Table 1-1 where 82% of studies found that the coal combustion is one of the major sources of PM in the local region. The average of coal combustion contribution is around 19% in these 42 case studies. As the most studied cities, the contribution of coal combustion to PM_{2.5} is between 15-25% according to Table 1-1, which is fairly consistent to the estimation suggested by Yao et al. (2009) with the value between 15 to 20%.

While apportioning the coal combustion source in China, Cl, As and Se are the most commonly used as inorganic tracers (Song et al. 2006; Zhang et al. 2007; Wang et al. 2009; Zhang et al. 2013; Yu et al. 2013). Cl is particularly regarded as an important inorganic tracer is because due to direct emission as HCl from coal burning (Huang et al. 2014).

1.5.3 Marine salt

Only a few study apportioned a considerable amount of marine salt in PM₁₀ rather than any PM_{2.5} source apportionment in China. This is not only due to the locations where the cities such as Beijing is far away from the coast but also due to the size fraction of sea spray of which its coarse mode accounting for more than 90% of the total mass (Fitzgerald 1991). Ni et al. (2012) found the sea salt accounts for 4% of total PM₁₀ mass in Huludao in North-eastern China. Li et al. (2013) discussed the sea salt contribution to PM₁₀ in Xiamen where at the southeast coast and there is not distinctive seasonal variation and it accounts about 3.6% on average all year around. The data are comparable with other case study in the other places (Amato et al. 2016). Normally Na and Mg are used as tracers for sea salt as they are predominant chemicals (Huang et al. 2014).

1.5.4 Road Traffic

Road traffic is another important PM_{2.5} sources in China and it generally makes a great contribution to total PM in urban areas. Road traffic normally consists of two major parts, the exhaust emissions from the tailpipe and the non-exhaust emission to wear and tear of automobile components such as brake-wear, tyre-wear and re-suspension of road dust etc. (Pant & Harrison 2013). Unfortunately, due to a lack of understanding of this source and unclear definition on “road traffic”, it shows great uncertainty presented across all the literature. Some common elemental tracers such as Zn, Cu, Ba, Sb, Fe and organic molecular makers including some particular PAHs and n-alkanes (Amato et al. 2012; Fabretti et al. 2009; Harrison et al. 2012) are also used in China, but the choice of tracers also varies in different study. Among them, Zn and Cu are the most frequently used tracer for vehicle exhaust is due to its existence in lubricant oil while Zn can be also found in brake ware and tyre ware (Yu et al. 2013). The ratio of OC and EC is also a popular choice for vehicle emission as they have a very high amount of its emission. Zhang et al. (2007) also deployed CH₃CHOO[·] and HCOO[·] for identifying automobile.

On the other hand, it is common that the source of “road traffic” is not generally all split into exhaust emission and non-exhaust emission in some studies in China. However, it is a better practice to separate the vehicle exhaust and road dust as they may have some distinctly different chemical profiles, which road dust is mainly minerals though it is related to the traffic (Yu et al. 2013).

1.5.5 Secondary Inorganic Aerosols

Secondary inorganic aerosols is another major source of PM in China, especially playing a very important role in PM_{2.5} (Li et al. 2013b). Ammonium, nitrate and sulphate are the dominant species in secondary inorganic aerosol which they commonly in the form of (NH₄)₂SO₄ and NH₄NO₃ (Long et al. 2014). In general, nitrate is formed by its precursor NO_x, which comes from some primary sources such as fossil fuels combustion, reacting with OH· while ammonium is participated in the reactions so that the equilibrium between the gas phase to the solid phase may form. While the sulphate come from the oxidation of SO₂ and then neutralized by the ammonium in the ambient air. Secondary nitrate and sulphate are relatively easier to identify in receptor models, especially PMF, as the modelling factor profile will show distinctive high concentration of nitrate, sulphate and ammonium loading. For example, there is a good agreement in sulphate proportion in Beijing's PM_{2.5}, which is around 17% according to table 1.1. However, the uncertainty for nitrate is larger ranging from 8% to 27% with average of 14% accounting the total mass of PM_{2.5}. This may due to the formation of nitrate is more sensitive to temperature because of its saturation vapour pressure property.

1.5.6 Mineral Dust

Mineral dust is also a common sources of both PM_{2.5} and PM₁₀ in Chin's urban area and normally they are the mixes of desert and loess dust, local fugitive dust, construction and re-suspended road dust (Zhang et al. 2013). Dust storm is generally seasonal and it is most severe in spring in northern China while the construction dust without controlling measures in many cities in China is the issue all year around (Chan Yao, X. 2008). Therefore, Ca and other elemental tracers including Al, Mg, Fe, Ti and Si are usually used

in the receptor models(Song et al. 2007). In some cases, it is also regarded as “road dust” in some circumstances (Wang et al. 2009). Perhaps, mineral dust is the factor that has highest agreement in the source apportion in Beijing as an example, which accounts for about 19% on average.

1.5.7 Industrial sources

The emission from industrial sites has complicated compositions including trace metals, OC, EC and PAHs and they are the important contributions to both PM_{2.5} and PM₁₀ (Taiwo et al. 2014). In China, industrial emission is also widely apportioned in receptor modelling. For example, Zhang et al. (2013) used OC, EC, Zn, Mn and Cr as tracers and found “industry” accounting for 25% of total annual mass of PM_{2.5} in Beijing as the high content of Zn and Cr may imply the emission from smelters and metallurgical industries. Yang et al. (2013) used Ni and Cr for typical indicator for residual fuel oil combustion, oil-fired power plants and steam boilers. The high loading of Ni, Cr, Co and Sc mixing with other trace species such as Zn, Pb and Fe could also be suggested the industrial emission (Yang et al. 2013). Moreover, Huang et al. (2014) used Zn for metallurgical industry and V for oil combustion sources. Wang et al. (2009), however, thought Al and Fe may not only come from the soil dust but also implies the emission from welding and cutting of metal working from local workshop.

However, it is worth pointing out that the so called ‘industrial emission’ is normally not specific or even misleading as it is the source which is very difficult to apportion since the source profile from different industrial sites can be massive due to difference manufacturing processes. And this has been suggested by the difference choice on tracer species for

industrial emission source in the different studies mentioned above. Taiwo et al. (2014) proposed that “*a general classification of the source ‘industry’ is rarely appropriate for PM source apportionment.*” And different industrial processes should be classified in more details by putting any single efforts to achieve their source profile and use multiple models to minimize the modelling uncertainties (Taiwo et al. 2014).

1.5.8 Biomass Burning

Biomass burning emission study is a hot topic in the recent years in China. Chen et al. (2016) recently reviewed the impact of biomass burning to the local and regional air quality, public health and climate. Chen et al. (2016) addressed that the rice, wheat and corn straws burning is the major source of biomass burning in China. Though they are temporal and spatially dependent, it can deteriorate the air quality in a relatively very short time and the its contribution to SOA in mass during the biomass burning related pollution episode can account for up to 60% (Chen et al. 2016). There are usually three major biomass burning periods throughout the year in China, namely the ‘summer harvest season’ from late May to the end of June; 2) crop burning in October; and 3) Winter heating (Chen et al. 2016).

Though there are fewer studies reported biomass burning than other sources, more than half of papers in the table 1.1 identified the biomass burning in their modelling. The average contribution of biomass burning in mass from these studies is around 14%.

In general, like other source apportionment elsewhere, K^+ or K is the major tracer for biomass burning due to its large amount of emission from the biogenic residuals burning (Chen et al. 2016; Song et al. 2007; Wang et al. 2009; Zhang et al. 2013). Cl^- and Sr are used as the inorganic tracer for biomass burning in China too (Zhang et al. 2007; Yang et

al. 2013). Pb may also coexisted with biomass burning in China as they are burnt with some local waste together (Huang et al. 2014). Except for these inorganic tracers, levoglucosan and mannosan are also widely used for biomass burning organic molecular markers (Fu et al. 2008; Cheng et al. 2013). However, there are also some studies use levoglucosan for cooking emission in China as it can be also released when the vegetable is heated (Jiang et al. 2009).

1.5.9 Secondary Organic Aerosols and Organic Molecular Markers

The secondary organic aerosols (SOA) is formed via photochemical reaction processes after the primary organic matter is emitted to the atmosphere (Huang et al. 2014). Due to its high degree of complexity on chemical characteristics, there is currently no direct method to measures its contribution (Huang et al. 2014). Therefore it is normally difficult for CMB model to estimate the SOA contribution due to lack of source profile (Pant & Harrison 2013; Pant et al. 2014; Pant 2014; Lee et al. 2008). In PMF model, however, SOA normally will get involved with other factors together such as SIA and vehicle emission due to the high loading of OC (Huang et al. 2014). Normally, the OC/EC ratio method is introduced to estimate the SOA concentration in the ambient air indirectly in the Chinese literature like elsewhere. The secondary organic carbon is estimated based on the OC and EC data by using the following equation (1.2):

$$\text{SOC} = \text{OC} - (\text{OC}/\text{EC})_{\text{primary}} \times \text{EC} \quad (1.2)$$

Where: $(\text{OC}/\text{EC})_{\text{primary}}$ is equivalent to the minimum OC/EC ratio during the sampling campaign. This method uses EC as a tracer to estimate the secondary organic carbon formation indirectly (Zhang et al. 2012; Han et al. 2011).

Some researchers have started discovering the appropriate organic molecular marker for SOA in receptor model. For example, Wang et al. (2012) used 2-methylerythritol for the SOA formation from isoprene and applied in the PMF in Rochester, NY. Wang et al. (2012) also found that *n*-heptacosanoic acid and *n*-octacosanoic acid are also associated with SOA in PMF. Zhang et al. (2009) deployed some organic molecules such as 2-methylglyceric acid, pinic acid, 3-Acetyl pentanedioic etc. together with other fatty acids, hopanes, PAHs and *n*-alkanes to apportion the isoprene SOA, α -pinene SOA and β -caryophyllene SOA in the PMF in the mid-western region in U.S.A. However, it is lack of similar study applying organic molecular markers for SOA in receptor models in China.

But Zheng et al. (2005) are one of the very first authors reported using a set of organic molecular markers rather than inorganic tracers only in receptor model (CMB in her research) to apportion the PM_{2.5} in Beijing. By using GC-MS, Zheng et al. (2005) detected and quantified the *n*-alkanes, PAHs, *n*-alkanoic acids, *n*-alkenoic acids, resin acids, aliphatic and aromatic dicarboxylic acids and levoglucosan etc. in the PM_{2.5} samples. Unfortunately, the similar source apportionment is not the majority before by 2014. More source apportionment by using organic molecular markers should be encouraged in China.

1.6 The source profiles availability in China

Local source profile is crucial for receptor models, particularly CMB and result verification for PMF etc., which can directly determine how robust the results of receptor models could be. Or using the profiles from literature may result in substantial bias in CMB for example as the profiles for the same type of source in the literature may not completely reflect the chemical characteristics at the local study area (Kong et al. 2011). Unfortunately, there is

not a comprehensive database for PM₁₀ and PM_{2.5} in China as same as SPECIATE in U.S.A. or SPECIEUROPE in EU. Some comprehensive source profiles measured in China's literature are summarised below.

Table 1-2 listed the recent publications on PM source profiles, covering fugitive dust, vehicle exhaust, industrial fly ash, cooking, straw burning and biomass burning. Fortunately, the currently available reports cover a broad range of sources and both inorganic and organic compounds have been addressed and measured.

Table 1-1 the study of source profile in China

Author	Year	Size of PM	Source	Main markers or analyzed chemicals
He et al	2006	PM _{2.5}	Vehicle exhaust	n-alkanes, PAHs, Hopanes, n-fatty acids
Zhang. et al	2007	PM _{2.5}	Cereal straw burning	OC, EC, levoglucosan, Methyloxylated phenol, guiacyl, syringyl
Cao et al.	2008	TSP, PM ₁₀ and PM _{2.5}	Fugitive dust	Al, Si, K, Ca, Fe, Cl, Ammonium, K
Hou et al.	2008		Charcoal Broiling	Linoleic acids (more); stearic acid (less)
Wang et al	2008	PM _{2.5} /PM ₁₀	Rural biomass burning	ACY, ACE, FLU, PHE, ANT, FTH, PYR, BaA, CHRY, BbF, BkF, BaP, IcdP, DahA, BghiP
Shen et al	2010	PM ₁₀	Road Dust	OC, EC, BaP, Ca, Sulphate, Nitrate, IP, BghiP
Kong et al	2011	PM ₁₀	Soil Dust	Si, Ca
Chen et al	2013	PAHs in PM ₁₀	Vehicle exhaust in Fu Gui-shan Tunnel	BghiP, BkF, BaA, BaP
Han et al.	2014	PM ₁₀	Geological Sources (including soil dust, road	Si, Al, Ca, Fe, Pb, OC, Sulphate, Cr, Ni, Cu, Zn, Cd, Sn, Sb, OC, EC

Author	Year	Size of PM	Source	Main markers or analyzed chemicals
			dust and construction derived dust)	
Han et al.	2014	PAHs in PM ₁₀	Road Dust	4-6 rings PAHs including PHE, ANT, FLU, PYR, CHR, PER, B[k]F, B[a]P, D[bah]A, B[ghi]P, IND
Kong et al	2014	PM _{2.5} /PM ₁₀ /TSP	Fugitive dust	Ca, Si, OC, Al, Fe, Sulphate
Zhang et al	2014	<100 micron	Fugitive dust	Al, Si, Ca, Fe
Zhang et al	2015	PM _{2.5}	Diesel Lorry	OC,EC,Sc, Sulphate, Ca, Ni, Cr, Mo, Ti, Cu, Mn, Se, Zn, Ba and Pb
Zhao et al	2015	PM _{2.5}	Chinese residential cooking	Fatty acids, sterols, monosachharide anhydride, polyols.
Pei et al.	2016	PM _{2.5}	coal-fired boiler	High abundances of sulfate, Ca, Al, Fe, S, OC and geological materials
Wu et al	2016	PM _{2.5}	Diesel Lorry	Sulphate, Cl, Na, Ti, V, Cr, Mn, Co, Ni, Cu, Ga, As, Sr, Pb and U,OC,EC
			Industrial Fly Ash	Si, Ca, Al, Fe, Na, SO ₄ ,
			Vehicle exhaust	Sulphate, OC, EC, Cd, Nitrate
			Coal combustion	OC, EC, Sulphate, Ca, Si, Fe, Al
			Road Dust	Si, Al, Ca, Mg, Na, Fe, OC, EC, Cr, Sulphate
			Construction derived dust	Ca, Si, Al
			Coal combustion	Si, Ca, Al, Pb, Cr, OC, EC
			Iron Smelt plant	Si, Ca, Al, Mg, OC, EC
			Industrial raw material and production pile	Si, Ca, Al

Author	Year	Size of PM	Source	Main markers or analyzed chemicals
			Coal Storage pile	Si, Al, Ca, Fe, Na, Zn, Cr, OC

Sources : (He et al. 2006; Zhang et al. 2007; Cao et al. 2008; Hou et al. 2008; Wang et al. 2008; Shen et al. 2010; Kong et al. 2011; Chen et al. 2013; Han et al. 2014; Kong et al. 2014; Zhang et al. 2014; Zhang et al. 2015; Zhao et al. 2015; Pei et al. 2016; Wu et al. 2016)

1.6.1 Fugitive dust

The fugitive dust is the re-suspended mineral that may consist of road dust, construction derived dust and soil dust etc. It is the most studied source profile in China in both PM₁₀ and PM_{2.5} size range (Cao et al. 2008, Kong et al., 2011 and 2014, Han et al., 2014, Zhang et al., 2014) and they show a high degree of agreements. Cao et al. (2008) used the samples from the Loess Plateau where is one of the major sources of mineral dust in Eastern Asia and North Pacific Ocean while the major trace metal, water-soluble ions and EC, OC were measure. It turns out that Al, Si, K Ca and Fe were found the most abundant trace metals in all size range from TSP to PM1.0, which matches the composition of mineral compositions (clay and feldspar) in Loss Plateau (Cao et al., 2008; Liu, 1985). Other studies also found Al, Si, Ca and Fe are the most abundant elements in the soil dust while Ca is also abundant in road dust, construction derived dust and cement plant (Kong et al., 2011 and 2014, Han et al., 2014, Zhang et al., 2014). Therefore, these five elements can be used as markers for this type of sources in receptor model in the China's source apportionment with confidence. And since this fugitive dust is common in Northern China, therefore it could be a good source profile input data in many northern Chinese cities, especially for the short-term dust storm pollution episode source apportionment.

On the other hand, it should not be ignored that these geological sources may have also been affected by the anthropogenic chemical. For example, some unexpected high concentration for some specific water-soluble ions and carbon fraction including K^+ and NH_4^+ were also found (Cao et al., 2008), showing the contamination from biomass burning and possible fertilization. And regarding road dust, there is also a considerable amount of sulphate, nitrate and OC appeared (Shen et al., 2010, Han et al., 2014). This implies the complexity of source profile and different sources may be interlinked and the deposition of other anthropogenic pollutants should be considered while discussing the simulated source profile by the PMF.

1.6.2 On-road sources

Both vehicle exhaust and road dust can be regarded as on-road sources. Several source profiles regarding the vehicles exhaust and/or road dust and tire and brake abrasion have been assessed. Most of them were undertaken within tunnels as it provides a decent condition to show a more real-world traffic emission with low dispersion rate, less input from other sources and no affect from sunlight (Pant et al., 2014; Keyte et al., 2016). For instance, He et al. (2006) measured the $PM_{2.5}$ in Wutong tunnel, Shenzhen, which is the longest tunnel in China. The $PM_{2.5}$ in the tunnel has distinctive difference with the ambient $PM_{2.5}$ that EC, OC, and nitrate accounts for 63.7%, 34.2% and 0.9% to the total $PM_{2.5}$ and alkanes, PAHs, hopanes, fatty acids and dicarboxylic acids are the major identified OC (He et al. 2006). Furthermore, *n*-alkanes are the most abundant and the carbon number is from 15 to 31 while *n*-Tricosane is at the peak level among the *n*-Alkanes (He et al., 2006). Hopane was also proved to be a very good tracer in receptor modelling in this study not only it constitute 5.3% of the total OC in the $PM_{2.5}$ but also its characteristics are consistent

with those in the petrol and diesel vehicles emissions (He et al., 2006). Meanwhile, Chen et al (2012) focused on the PAHs in the Fu Gui-shan Tunnel in Nanjing, China. Benzo[ghi]perylene (B[ghi]P), benzo[k]fluoranthene (B[k]F), benz[a]anthracene (B[a]A) and benzo[a]pyrene (B[a]P) are the four most abundant particular phase PAHs in PM₁₀. This is quite different from the previous study in the Wutong tunnel where pyrene, fluoranthene and phenanthrene are the three major PAHs. This could be caused by the percentage of diesel powered heavy-duty vehicles and petrol cars.

On the other hand, other researchers move the interest on the road dust. Shen et al. (2010) collects the PM₁₀ at the roadside during the heavy traffic period in Xi'an. Chemical compositions including OC, EC, water-soluble ions and PAHs have been conducted (Shen et al. 2010). The dominant inorganic species are Ca²⁺, SO₄²⁻, NO₃⁻ while B[ghi]P has the highest level in this study as the measured organic molecule and B[a]A, B[b]F, Chr, B[k]F, B[a]P, IP, dB[ah]A also have significant contribution in OC and turns out a reliable fingerprint for the source apportionment (Shen et al. 2010). Han et al. (2014) put more efforts on the trace elements on road dust. Except finding a big amount of contributions from Si, Ca, Al, Fe, Ca²⁺ and SO₄²⁻, trace elements including Cr, Ni, Cu, Zn, Cd, Sn, Sb are also enriched compared to the soil dust, indicating the depositions from industrial and vehicle emissions, especially the tyrewear and brakewear. However, since road dust is a non-exhaust particulate emission greatly depend on site and particle size and it is closely related to fugitive dust, the use of profile will be really careful (Chen et al. 2013).

1.6.3 Biomass burning

As mentioned earlier, the biomass combustion from straw burning plays a significant role in the PM emission. Some efforts also have been made recently on this source. For example, Wang et al. (2008) measured the PAHs emission from biomass burnt for domestic cooking in the Chinese rural area. 16 USEPA priority PAHs have been measured in PM₁₀. It is found that there is high emission rate during the cooking while this biomass is burnt and five- and six-ring PAHs dominates the emission (Wang et al. 2008).

Zhang et al. (2007) focused on the cereal straw burning and the carbonaceous compounds were measured in both smouldering and flaming phase which was simulated in a burning chamber. Gas Chromatography–Mass Spectrometry (GC-MS) were employed for the organic species analysis, including n-alkanes, n-alkanols, organic acids, PAHs, sugars, sterols, Methyloxylated phenols etc. and OC and EC were measured by Sunset thermal-Optical analyser (Zhang et al., 2007). Apart from the common tracers mentioned in the previous studies such as levoglucosan and mannosan (Simoneit, 1999; Simoneit et al., 2002), methyloxylated phenols is also discovered as one of the primary particulate organic matters (POMs) from the straw burning in China, which accounts for 8.7% of mass of the fine particles (Zhang et al., 2007), which can be good indicator for the Chinese cereal straw burning too. Other organics such as sugars, Methyloxylated phenols, Sterols, n-Alkanes, PAHs, n-Fatty acids, dicarboxylic acids. n-Alkanes and PAHs show a good similarity with the previous study (Simoneit, 2002; Simoneit et al., 1999) while the author claims that levoglucosan in cereal burning has a very similar mass proportion in its fine particles which is not helpful enough to distinguish the source of wood burning or cereal burning. Overall 141 organic molecular have been measured provided a detailed profile for the users of

CMB, which provided a detailed profile for the users of CMB. More study on source profile of at least other types of biomass burning such as wood burning is still required.

1.6.4 Cooking

The cooking can be really variable and the emissions will be consequently different with each cuisine (He et al. 2004). A couple of publications show the source profile for Chinese cooking and how it differs from the American cooking, which suggests it is essential to establish the local cooking source profile in China. For example, He et al. (2004) took the sample from the cooking fume at the exhaust exit on the roof of a Hunan cuisine and Cantonese cuisine restaurants, which both are very popular cooking method in China. All the major organics including n-alkanes, fatty acids, dicarboxylic acids, PAHs, steroids etc. have been measured by GC-MS. It has been found that the majority of chemicals are organics with minor constituents of EC and water-soluble ions. Overall, the components of fatty acids, PAHs and steroids are quite different with western cooking and the linoleic acid and pyrene are predominate and C27-C29 sterols were detected in Chinese cooking due to different ingredients (He et al., 2009). Even the Hunan and Cantonese foods are also a bit different in organics emission amount while Hunan cuisine release 81.6 % of organics but the Cantonese food only emits 52.6%, which again shows how crucial the local source profile is if they will be used in the receptor models.

Meanwhile, Hou et al. (2008) completed a simulation of charcoal broiling, aiming to work out the contribution from the street food in China, which is becoming more and more popular and could be distinctive to normal Chinese cooking and may make a significant contribution to the winter night. He mainly focused on PAHs, fatty acids, levoglucosan

and cholesterol. The profile of PAHs shows the differences with the cooking by natural gas, where fluoranthene and pyrene have the highest emission rate (Hou et al., 2008). In addition, fatty acids dominate the organic compounds during the cooking process particularly oleic acid and palmitic acid which are the products of hydrolysis and thermal oxidation, showing the agreement with the previous study (Hou et al., 2008; Rogge et al., 1991; Schauer et al., 1999). The author claimed that fatty acids were more important emission rather than PAHs after comparing his charcoal cooking profile and the corresponding ambient source profile that was sampled at the meantime, due to Benzo[b, k]fluoranthene and other HMW 5- and 6-ring PAHs dominates within the ambient aerosol rather than fluoranthene, Pyrene and other LMW 4-ring PAHs (Hou et al., 2008). On the other hand, fatty acids characterisation shows more consistency between charcoal cooking source profile and ambient source profile. Moreover, it should be addressed that both cholesterol and levoglucosan were both detected. This is mainly because the vegetables are also fried with oil in China. As mentioned earlier, levoglucosan is generally regarded as the organic marker for biomass combustion and but this reminds the researcher again to be cautious while using this marker. Nevertheless, these source profiles can be very helpful and more reliable rather using the other country's cooking profile.

1.6.5 Other sources

Last but not the least, Han et al. (2014) finished a comprehensive study on the source profile on some other sources including cement plant, coal combustion, construction dust and industrial fly ash. It has been noticed that Al, K, Fe, Ca^{2+} are relatively abundant in the emission from both of construction and cement plant while construction site contains more Si while the cement plant emits more Ca (Han et al., 2014). The construction process will also produce some particles with a relatively high amount of Mg while SO_4^{2-} is more

dominant in cement plant emissions (Han et al., 2014). The coal combustion source profile is dominant by OC, EC, SO_4^{2-} , Ca, Si, Fe and Al (Han et al., 2014). However, there are more varieties on the chemical characterisation on industrial fly ash as the compositions differ due to production processes, combustion processes and pollution control device (Han et al., 2014) and it is difficult to produce a general source profile for “industrial emission”.

Zheng et al. (2013) also established the industrial emission in Shanghai. They found the chemical composition from coal combustion and mixed fuels power plant emit the similar pollutants except for the differences in Ca, Al, Fe and SO_4^{2-} percentage (Zheng et al., 2013). Much more significant difference between sintering plant and metallurgic plant were found due to more different industrial process.

In summary, it is found that though many emissions inventories have been developed within the last decade, for example, the Multi-resolution Emission Inventory for China (MEIC, 2016), far few studies reported chemical profiles of PM sources in China. It could be partially because that obtaining PM source profiles is technically difficult and time-consuming (Hao et al., 2009). Nevertheless, it should be addressed that lacking enough source profile data in China could be a big obstacle for a more accurate source apportionment and this might be another reason why the uncertainty of modelling in the same city can be still significant. Many more other source categories should be studied and reported for the future receptor modelling requirements.

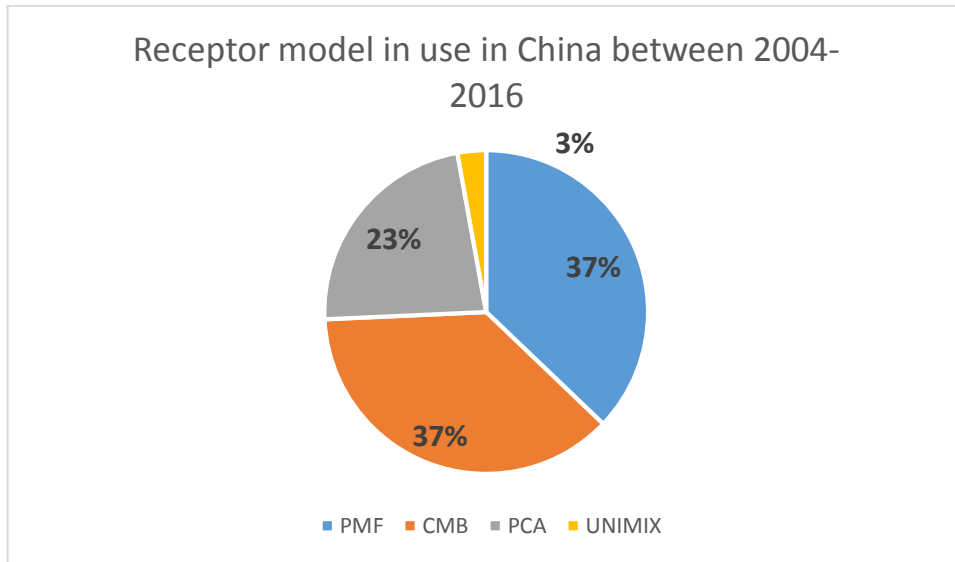
1.7 The choice and the use of receptor models

1.7.1 Overview

Based on the literature research and Figure 1-3, a clear pattern of the choice of receptor models and its trend can be revealed. Both PMF and CMB play almost equally important roles in the past decade while Principle Component Analysis (PCA) also has contributed massively to the source apportionment study in China at the earlier stage. Furthermore, there is a clear trend that PMF has become more popular in the recent years. This is probably due to that PMF model does not require the source profile for the analysis and there is no limitation on sources numbers in theory (Hopke 2003; Zhang et al. 2013). Secondly, the efforts on verifying one source profile can be huge and may not be realistic to all the research groups (Song et al. 2006). On the other hand, for the most CMB modelling case study, since there is not enough source profile data, some assumptions and estimations have to be made prior to the CMB modelling or other source profiles which were not similar to the local source profile were employed so that bigger errors may be made (Okuda et al. 2004). Therefore, PMF has gradually become the mainstream of receptor modelling in China which can perform the source apportionment analysis in a reasonable time and cost (Song et al. 2006). However, what should not be overlooked that CMB could apportion some sources which are very difficult to PMB by using some certain source profiles and organic molecular markers. For example, Zheng et al. (2005) combined the local dust, coal combustion etc. and vehicle emission profile from North America and successfully quantified the contribution from vegetative detritus, cigarette smoke etc. which have not been reported from PMF modelling results. If possible, much more efforts should be put to establish comprehensive local source profiles so that more detailed apportionment is much more likely to be achieved.

Last but not the least, AMS has become another means to analysing the source contribution in China in the recent years. Ge et al. (2017) and Ye et al. (2017) have found that traffic, cooking and biomass burning have played the key role in water soluble organic matter in $PM_{2.5}$. Thanks to its advantage in real-time high resolution sampling, AMS will play an even greater role in the future to understand the complex aerosol source in the urban area.

a)



b)

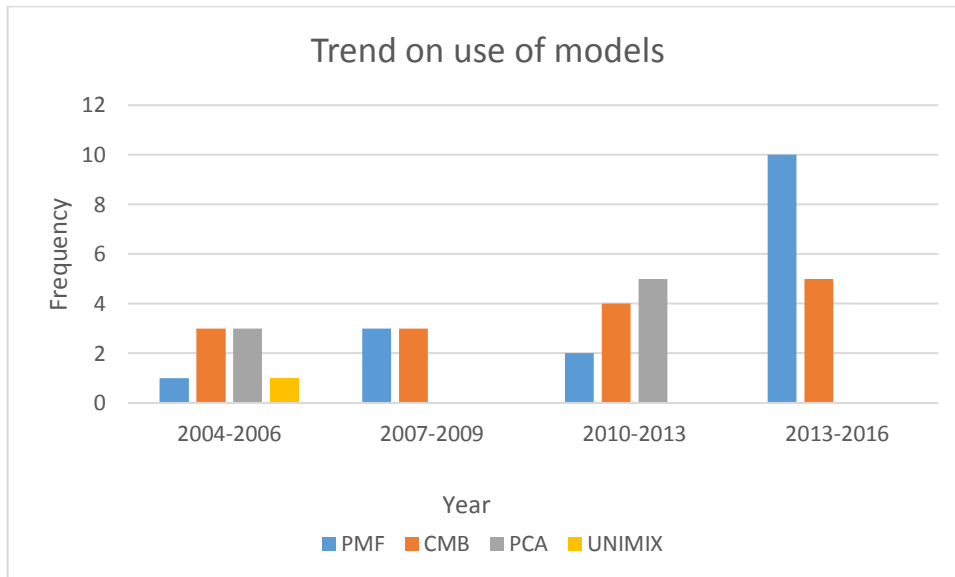


Figure 1-3 a) the use of different receptor models in China; b) the frequency of use of different receptor models in China.

1.7.2 Source categories and outcomes comparison

According to Table 1-1, the following source categories have been summarized from the literatures on China's source apportionment, which are coal, sea salt, vehicle emissions, including exhaust and non-exhaust, secondary inorganic aerosols, which are mainly secondary nitrate and sulphate, crustal matter, industrial emission, biomass burning and SOA. These eight source categories are the most frequently reported sources in China, especially the fossil fuel combustion, vehicles, secondary inorganic aerosols, mineral dust and industrial emission and biomass burning.

However the uncertainty for some sources contribution remains high. Beijing, where is the most studied city, is chosen as an example for discussion so that the comparison could be as comparable as possible.

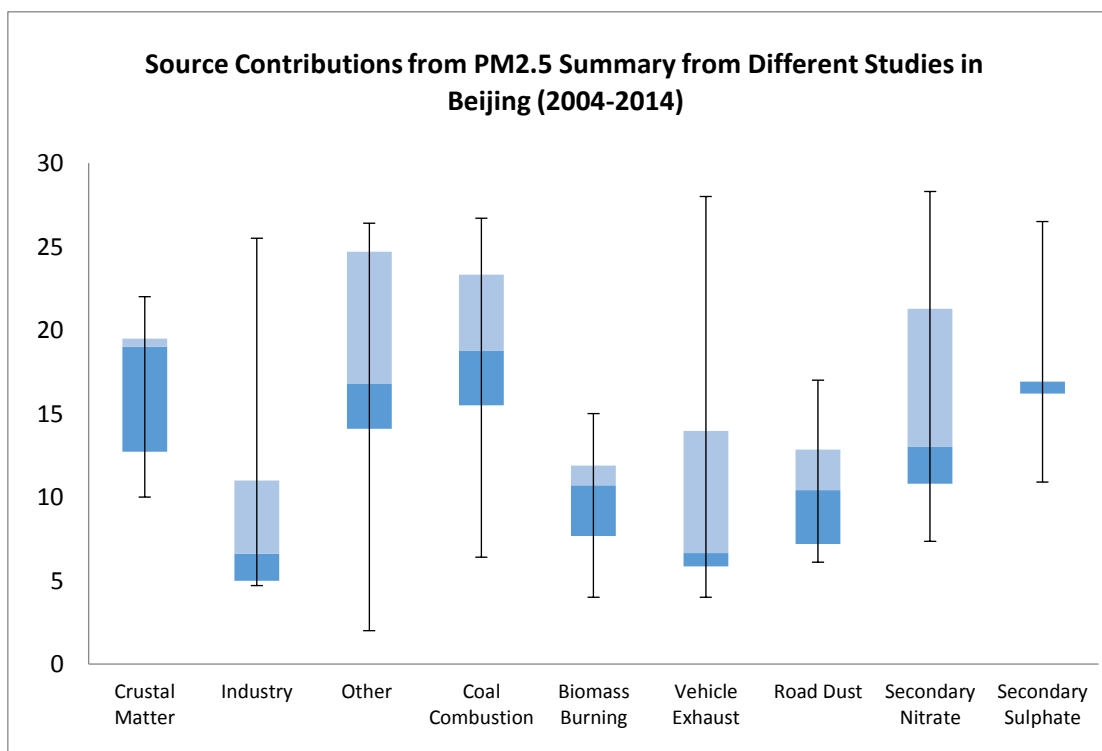


Figure 1-4 Summary of median source contributions to PM_{2.5} in Beijing from 2005-2014 and their uncertainties, based on the reviewed literatures. Sources: (Okuda et al. 2004; Zheng et al. 2005; Zhang et al. 2007; Wang et al. 2009; Zhang et al. 2013; Huang et al. 2014; Liu et al. 2014; Huang et al. 2014;; Song et al. 2006a; Song et al. 2006b; Wang et al. 2008;)

Figure 1-4 shows the average source contribution to the PM_{2.5} in Beijing from 2004 to 2014. According to this graph, crustal matter, biomass burning and road dust have relatively small uncertainty where the rest of apportioned sources have big uncertainties. Many factors may result in the big uncertainties such as the time of sampling, meteorological conditions, the chemical analysis methods and the model execution. Despite the objective reasons, one common issue about the source apportionment in China and elsewhere is that the definition of each source and the standards or reference on identifying the same source might be different. For example, there are more agreements on the choice of inorganic and organic markers for and mineral dust, road dust and biomass burning while executing the models. For instance, all the researchers from the reviewed literatures used K⁺ or K and

levoglucosan as markers and the mineral dust are also mainly defined by some elemental markers including Si, Ca, Al, Fe etc. (Zhang et al. 2013; Song et al. 2006; W. Zhang et al. 2007; Zíková et al. 2016). However, the choice of markers industrial sources and vehicles emission is far more different and diverse (See Table 1-2).

Table 1-2 the markers which were used for the PM2.5 source apportionment in Beijing

Ref	Method	PM	Factors							
			Coal Burning	Biomass Burning	Vehicle Exhaust	Road Dust	Secondary Nitrate	Secondary Sulphate	Industry	Soil
Song, Y. et al. (2007)	PMF	PM2.5	OC, Cl, K		Pb, Zn	Al, Si, Ca, Ti, Fe, Mg	Nitrate, Ammonium	Sulphate, Ammonium	Ni	
Liu, Q.Y. et al. (2014)	PMF	PM10			EC, OC and nitrate		Nitrate, Ammonium	Sulphate, Ammonium	Cu, Fe, Pb, V	Al, Ca, Fe
Sun, Y.L. et al. (2004)	FA	PM2.5			Ni, Cu		Nitrate, Ammonium	Sulphate, Ammonium	Fe, Mn, As, Zn, Pb, Cd	Mg, Ca, Ti, Al
Zhang, W. et al. (2007)	PMF&CMB	PM2.5	As, Pb, Cd, Sb, Se	K, Cl	CH ₃ CHOO-, HCOO-		Nitrate, Ammonium	Sulphate, Ammonium	Cu, Ni, Zn	Al, Fe, Se, Ti, Ca, Sr
Zhang, R.J. et al. (2013)	PMF	PM2.5	Cl, Na, OC, EC	K	Nitrate, EC, Cu, Zn, Cd, Pb, Mo, Sb, Sn				OC, EC, Zn, Mn, Cr	Al, Ca, Fe, Mg, K, Ti
Wang, H.L. et al. (2009)	PMF	PM2.5	As, Cl, sulphate	K	Zn, Pb, Cu, Zn	Ni, Cr, Na, Mg	Nitrate, Ammonium	Sulphate, Ammonium	Al, Fe	Mn, Mg, Ca, Ti

Sources: (Zhang et al. 2007; Wang et al. 2009; Zhang et al. 2013; Liu et al. 2014; Song et al. 2007; Sun et al. 2004)

Therefore, more efforts should be put in rediscover some certain source profiles including all the major sources such as coal burning, vehicles emission, different type of industries etc. where possible. In addition, a careful selection of markers during running models should be taken.

1.7.3 Certain PM fraction source apportionment

Some efforts also have been put on source apportionments from the different chemical fraction. The most popular study in this area is about discussing the sources of carbonaceous aerosol, PAHs and/or VOCs's sources and apportion the sources by PCA (Yuan et al. 2009; Cao et al. 2005; Dameng et al. 2008; Hu et al. 2012; Wang et al. 2015). For instance, Cao et al. (2005) measured the OC, EC, and TC in Xi'an and the relationship between the OC and EC in autumn and winter have discussed. Four major sources including petrol vehicle, diesel vehicle, residential coal burning and biomass burning have been found and petrol engine exhaust accounts for the major OC emission in Xi'an (Cao et al. 2005). Based on Cao et al. (2005)'s method, Wang et al. (2015) have also taken into account of SOC estimation, gases phases pollutants including NO_x, O₃ and SO₂. Wang et al. (2015) found that coal combustion and diesel vehicle exhaust contribute much more than Xi'an. Liu et al. (2010) and Hu et al. (2012) collected the total suspended particles (TSP) in Shenzhen and Guiyang. They have measured the PAHs by High-performance liquid chromatography (HPLC) and PCA was applied to apportion the sources of PAHs from the TSP. Vehicles, coal combustion and waste incineration were the major sources of PAHs in these two cities (Liu et al. 2010; Hu et al. 2012). In order to avoid the complexity of PAHs phases partitioning, the measured gas and particulate phase of PAHs were combined (Liu et al. 2010). Furthermore, Wang et al. (2014) applied PMF to find out the

sources of PAHs from PM_{2.5}. Five major sources were found including petrol and diesel engine emission, coal combustion, biomass burning and air-surface exchange. Newer method such as ¹⁴C which has been mentioned and Aerosol Mass Spectrometer (AMS) were also started to be used in source apportionment. He et al. (2011) used the high time resolution obtained from AMS in PMF to apportion the sources of organic aerosol (OA) in PM₁, hydrocarbon-like (HOA), biomass burning and two oxygenated OA (LV- and SV-OOA) are the major apportioned compounds from the model, implying the potential significant contribution of fossil fuel burning, biomass burning and SOA (Xiao et al. 2011). The advantage of AMS is that the efficiency on data collection and high time resolution can be achieved rather than the traditional daily average data, which may more helpful for some short pollution episode study, for example, the diurnal variations.

1.8 Highlight points and issues

Based on the reviewed papers, the latest features of receptor modelling in China in terms of sampling site, relevant chemical analysis and the execution of models are discussed below.

1.8.1 Sampling sites – urban, suburban and background

The choice of sampling site is important as it is not only representing the contribution of the source at the receptor (citywide, for example) but also depends on what is the purpose of the project. Most of the sampling sites in China are allocated in the urbanised region. The benefit is that it aims at the maximum population exposure possible (Viana et al. 2008) and it provides the convenience to the sampling management as the sites are normally established within the research institutes. However, it should not be overlooked that other places may also play important roles, for example, the rural and/or suburban area and an

even particular site such as industrial park if the aim is to evaluate the impact from industrial emission (Taiwo et al. 2014). Since some locations, such as rural area, represent the background pollution compared to the urban area, it could be extremely useful to explain the origins of some pollution sources and quantify the long-range transported PM (Viana et al. 2008), which is fairly unclear in many case study in China.

Some works, however, did make efforts to this particular point. For instance, Liu et al. (2014) collected the PM₁₀ sample during the non-dust and dust storm days in Beijing in both urban and background site where is 30 km north-west of city centre. It has been turning out that this measure is not only help to distinguish the different impacts of different sources at each site and highlight which source is originated within the urban area, but also helps to assess the impact of dust storm which is common in spring in Beijing. Yuan et al. (2009) also used two sampling site in both urban and rural environment and tell the difference on petrol car emissions. Song et al. (2007) synthesize six sampling site with half of them within the urban environment where the other located at three different directions in the suburban area of Beijing and the differences between urban and suburban areas turn out very useful for determining the origin of biomass burning and industrial orientated source contributions from nearby region (Song et al. 2007).

1.8.2 Analytical Chemistry – latest techniques

Variety of analytical techniques have been applied for the determination of water-soluble ions, trace metals, OC/EC and organic molecular markers and even radioactive element (e.g. ¹⁴C). Both offline and online methods are popular in China, particularly the attempts of aerosol mass spectrometry (AMS), Single Particle Aerosol Mass Spectrometry (SPAMS)

and Carbon-14. The use of these methods has been summarized and discussed in great detail in another review by Zheng et al. (2014), which is not repeated here. However, what should be addressed is that, though researchers have already been able to achieve numbers of datasets on all these species by Ion Chromatography (IC), X-ray fluorescence spectrometer (XRF), Inductively Coupled Plasma-Atomic Emission Spectrometer (ICP-MS), Inductively Coupled Plasma-Mass Spectrometer (ICP-MS), Thermal-Optical Analyser and Gas Chromatography-Mass Spectrometry (GC-MS) etc., the number of study which have full spectrum of all major species measurements are still limited. Majority of published papers in China focuses on either inorganic species or carbonaceous aerosols (Wang et al. 2006; Song et al. 2006; Yang et al. 2013; Han et al. 2011; Geng et al. 2013; Bi et al. 2007; Q. Wang et al. 2009; Ziková et al. 2016). Since there is extensive studies to use inorganic compounds data as input for the receptor models, the addition of organic compounds should be encouraged. Lin et al. (2010) reviewed the development of organic markers in $PM_{2.5}$ and their use for source apportionment. The organic molecular marker plays more and more important roles in using receptor models as it can differentiate various carbon related sources better, for example, distinguish the diesel and petrol vehicles emission, the contribution from meat cooking, cigarette smoke, vegetative detritus, natural gas heating (Lin et al. 2010).

Fortunately, some efforts have been made in both PMF and CMB models in China with combinations of both inorganic and organic dataset to apportion more sources in the PM. For instance, Li et al. (2013) measured the fatty acids and PAHs in the $PM_{2.5}$ and PM_{10} in Beijing and used to identify the combustion sources. And Wang et al. (2009) measured the

n-alkanes, hopanes and sterols, which found that the Chinese cooking contribute significantly in the total OC in Beijing.

In addition, as ^{14}C measurement is able to distinguish the fossil and non-fossil fuels in the PM samples, this technique has also applied in a couple of study in China. Liu et al. (2013) discussed the fossil and non-fossil sources of OC and EC in $\text{PM}_{2.5}$ in a background site in East China by both radiocarbon measurement and levoglucosan. It was found that 59% of water-insoluble OC came from biomass burning and biogenic sources where fossil fuel is the dominant contributor to the EC, which accounts for 78%. Zhang et al. (2014) used the same method in another background site on Hainan Island, South China where the fossil sources contribute 51% to EC and biogenic and biomass burning contribute 56% and 44%, respectively, which is similar to Liu et al. (2013)'s research. On the other hand, Zhang et al. (2015) also measured the ^{14}C in fine carbonaceous aerosols in four urban areas in China during the haze episode, including Beijing, Xi'an, Shanghai and Guangzhou. Again, the contribution of non-fossil fuel to OC is significant, accounting 55% and the primary biomass burning account for 48%, 40%, 53% and 65% in these four cities respectively. EC is also dominated by the fossil fuel with mean contribution of 75% for the four cities (Zhang et al. 2015). By using K^+ and levoglucosan, it was turn out that the major source of biomass burning is mainly from the combustion of crops residues and there is a big fraction of OC is secondary rather than primary (Zhang et al. 2015). These studies do help to extract further useful information from the carbonaceous aerosols and help the judgement on receptor modelling. However, more measurements on radiocarbon are required since these studies in China are still scarce.

1.8.3 Quality Control on the modelling results: the uncertainty analysis

For the most popular receptor models that have been used in China, namely, PCA, CMB and PMF, PMF is one of the model which is able to provide reliable uncertainty analysis for the modelling results by “bootstrapping”, which is an method that randomly replaces n samples from the dataset to create new dataset and a new execution of model will be based on this new dataset (Reff, 2012). Similar multivariable models such as ME-2 and UNMIX also contain this function. This is vital for the modelling results, especially for QA/QC purpose. However, few publications have detailed discussion on modelling results uncertainty and even how to treat the data including the missing data; the data below detection limit etc., even the change of Q value are not clearly mentioned. These measure should be encouraged to be applied and presented in the publication to show the robustness of the results (Viana, et al. 2008). Fortunately, Wang et al. (2015) made some outstanding efforts on modelling results evaluation by discussing the sensitivity of the results to imposition of some constraints, which are the *a priori* source characteristics knowledge. The utility of organic markers in the PMF is also discussed by the different choice of markers in the input data. These attempts are the very helpful experience for the future work on how to use the constraints more properly and how to choose the markers in some certain study area so that the modelling results can be more robust.

1.9 Other methods coupled with receptor modelling – New trend

1.9.1 Receptor models coupled with back trajectory

Back trajectory is a method that can trace back the position of the sampled air in time from the receptor point from various starting time throughout the sampling interval (Hopke 2003). A few methods have been developed for relating the collected PM with trajectory at receptor site including residence time analysis (RTA), conditional probability function (CPF), Potential Source Contribution Function (PSCF) and Simplified Quantitative Trajectory Bias Analysis (SQTBA) (Hopke 2003; Hopke 2016). The benefit of incorporating back trajectories with these methods is that not only where the major air parcel at certain period will be known but also the transport pathway of certain composition can be also identified (Zhang et al. 2013) This analysis is helpful to understand the locations of the sources through long range transport, which is also useful to interpret the factors in the receptor models. In China, PSCF has been popularly involved with the receptor model and some efforts have been made. For instance, Zhang et al. (2013) used PSCF based on the back trajectories clusters and found the secondary inorganic aerosols from the PM_{2.5} in Beijing normally come from East to South direction while OC and EC may also come from northwest as well as mineral dust etc. Ziková et al. (2016) achieve similar results to Zhang et al. (2013)'s research by using PSCF and CPF together. In addition, they also found traffic source is mainly local in Beijing but biomass burning was coming from ENE to ESE, particularly in summer and there is also significant signal that long-term transport may also play the role in coal combustion from the southeast of China. Zhao et al. (2015a) used the PSCF and found that the PM_{2.5} contribution was more likely from the local emission in Shanghai while the long-term transport plays greater role in the rest of the year.

1.9.2 The use of organic markers in PMF

Applying more organic molecular markers in the PMF instead of using CMB when there is not enough robust source profile is also another trend. The most common examples are using levoglucosan and mannosan in the PMF for apportioning the biomass burning more accurately. For example, Cheng et al. (2013) examined the biomass burning contribution in Beijing by using K^+ , levoglucosan and mannosan and found the biomass burning contribution was significant throughout the year and almost 50% of OC was associated with biomass burning in Beijing. Similarly, Qiao et al. (2016) also used levoglucosan and mannosan as markers and found about 16% of $PM_{2.5}$ contribution may from biomass burning and coal combustion. Wang et al. (2015), however, examined much more organic molecular markers including n-alkanes (C27-C33), PAHs and biomass burning markers levoglucosan and mannosan were used in PMF for OC and EC source apportionment in Dongguan, PRD, to see the their feasibility. The utility of organic markers turn out massively in PMF and levoglucosan and mannosan were important input to distinguish biomass burning from coal burning. Hopanes and 1,3,5-triphenylbenzene was found useful for vehicle exhaust and plastic burning and C27-C33 n-alkanes and other PAHs can also influence the source profile markedly (Wang et al. 2015). By using these organic molecular markers, it helps to identify that biomass and coal combustion are the two major contributions to the OC and EC in PDR while industrial and shipping emission and secondary OC are also important (Wang et al. 2015).

1.9.3 Inter-comparison of between different receptor models

The inter-comparison between the different receptor model's performances in China has been attempted in a few studies. Song et al. (2006) was one of the earliest research group compared the modelling results on PM_{2.5} sampling data in 2000 in Beijing by PCA, CMB, PMF and UNMIX comprehensively. CMB and PMF apportion more sources than PCA and UNMIX. All the models have relatively high agreement on coal combustion and motor vehicles. However, CMB underestimate the contribution from coal burning, which may be due to the source profile. While UNMIX overestimate the motor vehicles, this could be the reason that the secondary sulphate may mix with motor vehicles in the UNMIX. Overall, the results between CMB and PMF are similar while PCA and UNMIX are more comparable. Zhang et al.(2007) also accessed the results between CMB and PMF based on the source apportionment of PM_{2.5} in Beijing. The results from CMB and PMF have very high agreements on most of apportioned sources including coal combustion, vehicle, soil dust and biomass burning on annual average level. Qiu et al. (2012) measured the trace metal composition in PM₁₀ in Longyan in Fujian Province and apportion the sources by both CMB and PCA. The results are, however, not that matches each other properly. Unfortunately, we lacksome recent discussion on the inter-comparison between different receptor models. It should be addressed that it is very valuable to compare the results between different approaches, not only because it may test the accuracy of modelling but also different receptor models have its own advantages and drawbacks. It is even worth rediscovering the old data and analysing them by using another receptor model and test whether any similar outcomes can be obtained. It is always ideal to maximize their strength while minimize their limit at the same receptor site source apportionment.

1.9.4 Enlightenment based on previous studies and other research experiences in other countries – U.S.A. and EU

Both air quality communities in the United States of America and the European Union have accumulated much experience on source apportionment of particulate matter. Some measures they have taken is worth considering to China and helpful to establish a long-term plan and strategy on air pollution mitigation since the air quality is so poor in China. First of all, establish an updated source profile database is crucial for receptor modelling, especially for CMB modelling. The USEPA has created their own source profile database suitable for majority of North America called “SPECIATE” for decades and the database is updated every two or three years. The latest version is SPEVIATE 4.5 released in September 2016. It contains both PM and VOCs source profiles which is very helpful for creating speciated emissions inventories for regional air quality modelling, estimating the air pollutant emissions from the primary source, providing CMB data input and also for verifying the derived profiles from PMF modelling (USEPA, 2016, https://www.epa.gov/sites/production/files/2016-09/documents/speciate_4.5.pdf).

Similarly, the Forum for air quality modelling in Europe (FAIRMODE) under the European Union developed a brand new PM emission source profile database appropriate for Europe, SPECIEUROPE, in 2016 (Pernigotti et al. 2016). Like SPECIATE, it also cover large variety of sources including fuel oil burning, ship emissions, coke burning, wood burning etc. (Pernigotti et al. 2016). It also involves some composite profiles, calculated and derived profiles based on stoichiometric composition and modelling, which might be helpful for sensitivity test. More sources categories and area coverage are

expected to be added in. Both databases are free and opened to the public which are very beneficial to the relevant researchers all over the world.

On the other hand, FAIRMODE also organised an exercises of source apportionment models inter-comparison and they established a new method to evaluate the performance and uncertainty based on different modelling results from different executions (Belis et al. 2015). The evaluation framework that they have designed set a very good example on how the source apportionment communities may make full use of their all advantages at national and even regional scale to produce the modelling results as robust and accurate as possible and assess the modelling uncertainty in another solid way. The exercises itself also benefits from the FAIRMODE framework so that the research resources can be massively networked and certain bigger group works can be executed efficiently, which is also very enlightening.

Last but not the least, the education for the new generation and driving force from the society should not be overlooked. For example, it is really intriguing that the Joint Air Quality Initiative put some efforts even after the Joaquin Project ended. They created an online game that younger generation can learn what the air pollution is about and what their impact to the environment and health during the game. This is a very good example about how scientific community linked their work to the society.

1.10 Source apportionment in Jinan and objectives of this project

1.10.1 Current research status and motivation

Jinan, the capital of Shandong Province in NCP where the hub of coal-fired power plant in China, is a highly urbanised and industrial city with more than eight million population is located in a semi-enclosed region by Mount Tai and Mount Lu range. Based on the review of previous literature on source apportionment in China, NCP is the most polluted region in terms of many kinds of air pollutants including $PM_{2.5}$ and PM_{10} . However, majority of study in northern China has focused on Beijing but no other surrounding places including Jinan, another typical polluted megacity in this region. Some study has shown that Jinan might be even more polluted than Beijing and it is one of the most polluted city on average in China (Yang et al. 2013). There is some research has been taken in this city to evaluate its PM pollution and the sources of these PM. The earliest study is done by Bi et al. (2007b) who have investigated the sources of PM_{10} in six northern cities, including Jinan, in China by CMB. This is the first receptor model that conducted and reported for Jinan. Later, the sources identification for PM has also been attempted by other means such as trajectory statistical methods (Cheng et al. 2011; Yang et al. 2012). Gao et al. (2011) also applied PCA with semi-continuous measurement of water-soluble ions in $PM_{2.5}$. Yang et al. (2012) first applied PMF model in Jinan to apportion the sources of $PM_{2.5}$. These studies reveal that the major source of PM_{10} is mineral dust but coal combustion, SIA and traffic contribute to the $PM_{2.5}$ significantly too. However, there is no other research available and there is lack of source apportionment with multiple modelling in Jinan. And there is lack of research on source apportionment with detailed uncertainties analysis or applying organic molecular markers in the receptor model.

Under this background, this project aims to compare the results of receptor modelling for apportioning PM_{2.5} by both CMB and PMF. It is aimed to find out how different or similar the results could be by two methods and try to understand the causes. It is also aimed to understand what the advantage and disadvantage of both methods are for apportioning the PM_{2.5}. Water-soluble ions, trace metal, OC and EC and some selected organic molecular markers will be measured after the sampling of PM_{2.5} in urban Jinan. The author believes this will be helpful to have a source apportionment result with more confidence and will be not only helpful to control the emission of PM_{2.5} in this city itself but also help to understand the regional PM_{2.5} pollution in NCP better.

1.10.2 The structure of this thesis

The thesis chapters are organized as follows:

Chapter 2 describes the general methods of sampling, analytical chemical experiments and modelling in this project

Chapter 3 describes results of the raw data obtained from the sampling campaign and experiments

Chapter 4 describes results of PMF modelling based on the experimental data input

Chapter 5 describes results of CMB modelling based on the experimental data input

Chapter 6 compares the results from the two different models and discusses the causes of similarity and differences

Chapter 7 describes the conclusions from the current study and provides recommendation for future work.

2 Chapter Two Methodology

Abstract

In this chapter, the sampling methods and the analytical chemical analyses are introduced, including describing the offline sampling instruments used in Jinan for PM_{2.5} sampling, the usage of filters and treatments for the deposited filters. Medium volume sampler and a parallel four-channel sampler are the major samplers during the campaign.

In addition, analytical chemical analysis plays an important role in the data preparation as model input after sampling and different analytical chemistry techniques have been deployed to discover the physical and chemical characterisation of sampled PM_{2.5}. In brief, the mass concentration of PM_{2.5} were achieved by weighing the pre and post-sampling filters; Si, Fe, Al and other trace elements abundances were measured by using X-ray Florescence (XRF); Organic carbon (OC) and elemental carbon (EC) were detected by Sunset thermal and optical analyser and the organic molecular markers were found by Gas Chromatography–Mass Spectrometry (GC-MS).

2.1 Offline Sampling campaign in Jinan

Jinan (36°40' N; 117°00' S) is an industrial megacity located at the heart of North China Plain. Jinan has humid continental climate (*Dwa*) where it is hot and wet in the summer but cold and dry in the winter. The city is surrounded by the mountain range in the south, east and west, which has an adverse topography for dispersing the air pollutants. Unlike Beijing, Jinan is also surrounded by other industrial cities nearby. The location of samplers and weather station was chosen to be on the roof of teaching building at the Shandong University Central Campus,

which is at the central area of Jinan. The teaching building is about 30 metres high and there are urban main road networks and commercial areas nearby and industrial hub in the north west of the campus (See Figure 2.1).

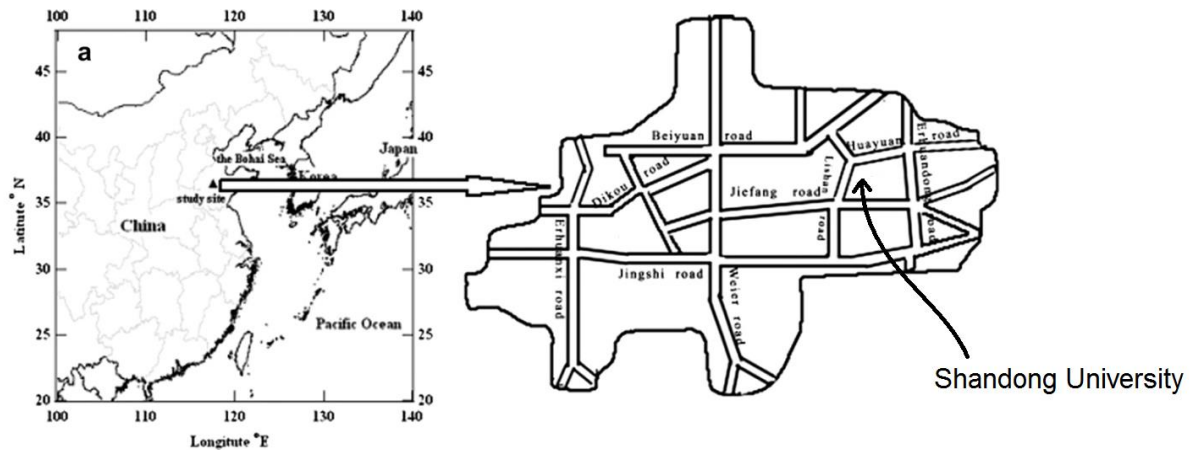


**Figure 2-1 Map showing the location of Jinan City and sampling site within Jinan
【Adapted from Yang et al., (2013)】**

The PM_{2.5} sampling was conducted by TH-16A four-channel sampler with Whatman[®] PTFE membrane filters (47 mm Dia., 1.0 µm pore size, WTP type) and TH-150F Medium Volume Sampler with Whatman[®] QM-A quartz filters. A Kestrel 4500 Applied Ballistics Meter was attached with the TH-16A sampler so that the wind speed and direction, temperature, relative humidity (RH) and atmospheric pressure (a.t.m.) were recorded simultaneously. Due to the schedule of instrument bookings, maintenance and time availability of collaborators, five periods of sampling was decided and performed, including from January to early February (Winter-1, also abbreviated as P1), mid-May to mid-June (Early Summer, abbreviated as P2), early July to early August (Late Summer, abbreviated as P3) and late November to early

December (Late autumn, called “Autumn” in the rest of thesis, abbreviated as P4) in 2015 and mid to the end of January in 2016 (Winter -2, abbreviated as P5). In total, 103 valid PM_{2.5} samples have been achieved. The following sections elaborate the two sampling instruments in details.

2.1.1 TH-16A PM Sampler (Wuhan Tianhong Instruments Co.Ltd)

The TH-16A PM sampler is an classic cyclone sampler using the filtration method with four channels which can conduct the sampling simultaneous with same or different configurations (Wuhan Tianhong Instruments Co.Ltd., http://en.thyb.cn/products_detail/productId=54.html , no date). There is a holder for one cassette magazine which can be placed with 47 mm Ø filter at each channel in this sampler. At work, the constant flow rate is 16.7 L·min⁻¹ and each sampling stint is 23 hours and a half per day. In Jinan’s PM_{2.5} campaign, two channels out of four have been used and two PM_{2.5} sampling head have been equipped (See Figure 2-2). The filters in the first channel will be used for water soluble ions determination while the other filter in the second channel will be used for trace metal element determination.

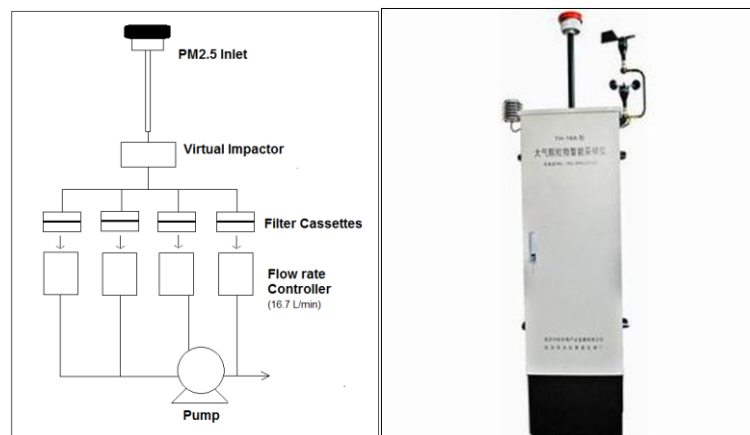


Figure 2-2 a picture and schematic diagram of TH-16A Ambient Particulate Sampler (Wuhan Tianhong Instruments Co.Ltd., http://en.thyb.cn/products_detail/productId=54.html , no date)

2.1.2 TH-150F Automatic Medium Volume Sampler

The other sampler used in this campaign is TH-150F automatic medium volume sampler by using the principle of filtration too. There is a filter cassette magazine for 90 mm Ø filter and the flow rate of TH-150F has been maintained at 100 L·min⁻¹ at work. Each sampling stint is also 23 hours and a half per day (Figure 2-3).

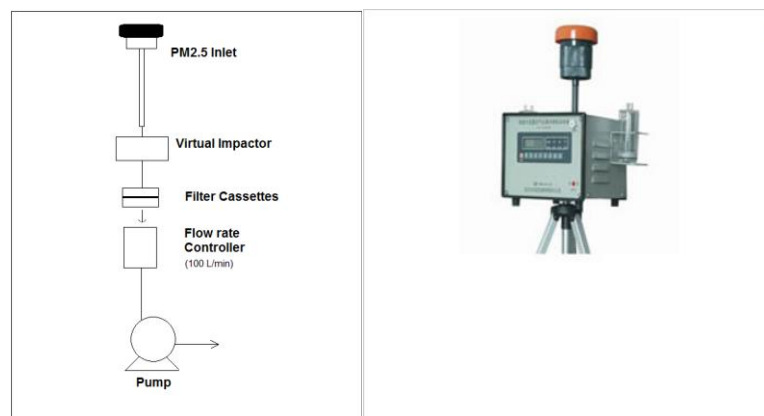


Figure 2-3 a picture and schematic diagram of TH-150F Ambient Particulate Sampler (Wuhan Tianhong Instruments Co.Ltd., http://en.thyb.cn/products_detail/productId=74.html, no date)

2.1.3 Weather station

A Kestrel 4500 Ballistics Meter was attached with the TH-16A sampler so that the wind speed and direction, temperature, RH and a.t.m. pressure were recorded simultaneously. The meteorological data is automatically saved as .csv file and then downloaded to the PC from the instrument. The details of Kestrel 4500 Applied Ballistics Meter can be found at: <https://kestrelmeters.com/products/kestrel-4500nv-applied-ballistics-meter>.

Due to the schedule of instrument bookings, maintenance and time availability of collaborators, five periods of sampling was decided and performed, including from January to early February (P-1), mid-May to mid-June, early July to early August (P-3) and late

November to early December (P-4) in 2015 and mid to the end of January in 2016 (P-5). For the convenience of data analysis, P-1 and P-5 are combined together to represent winter.

2.2 Physical and Chemical Analysis of Deposited PM_{2.5} Filters in the Laboratory

2.2.1 Filters and its processing

Two different types of filters have been used in Jinan's PM_{2.5} sampling campaign. The filters used in the TH-16A sampler are the Whatman® PTFE membrane filters (47 mm Dia., 1.0 µm pore size, WTP type) while the other filters are the Whatman® QM-A quartz filters (90 mm Dia., 2.2 µm pore size), which have been placed in the TH-150F sampler. The Whatman® PTFE membrane filters are used for PM_{2.5} mass concentration determination, water-soluble ions and trace metal analysis. The Whatman® QM-A quartz filters are used for organic carbon (OC), elemental carbon (EC) and organic molecular markers analysis. Each type of filter were conditioned for more accurate measurements in the later analysis prior to the sampling. The Whatman® PTFE membrane filters are firstly pre-conditioned for 24 hours at 25 ± 5°C and 40 ± 10 % R.H. in the clean weighing room and then remove the surface static by the ionizing blower and weighted by Sartorius microbalance (MC-5) and the mass before the sampling $m_1(i)$ can be found. The Same process is conducted again after sampling so that the mass afterwards $m_2(i)$ are found. The difference mass $\Delta m_{PM_{2.5}}(i)$ of m_1 and m_2 for each PTFE filter are the PM_{2.5} mass accumulated during the daily sampling, namely:

$$\Delta m_{PM_{2.5}}(i) = m_2(i) - m_1(i) \quad (2.1)$$

Moreover, each filter is stored in the 47 mm Dia. size plastic petri dish and sealed in a small plastic bag for storage and logistics before and after sampling.

Regarding Whatman® QM-A quartz filters, they are baked in the furnace at 500 °C for six hours to remove any carbonaceous residual left during the manufacturing operations. Then they are packed with aluminium foil and stored in the clean sealing plastic bags for storage and logistics before and after sampling. Before any analysis, they are stored in the freezer at -20 °C.

2.2.2 Water soluble ions analysis by Ion Chromatography (IC)

Since two channels of TH-16A samplers are used during the sampling campaign in Jinan. Two portions of simultaneously deposited PTFE filters are obtained. One portion is used for analysing the major water-soluble ions within Jinan's PM_{2.5} including Na⁺, NH₄⁺, K⁺, Mg²⁺, Ca²⁺, Cl⁻, NO₃⁻, SO₄²⁻, PO₄³⁻ and C₂O₄²⁻ by Dionex ICS 500 and Dionex ICS 2000, which are the IC instruments for cations and anions, respectively. Before the sample injection, the PTFE filters are firstly placed in the graded plastic finger test tube and rinsed by 0.3 ml 2-Propanol and then added with 10 ml distilled deionized water (DDW). The capped test tube with filter soaked in the mixture solution is then shaken by the mechanical shaking machine at 240 r/min for half an hour. Afterwards, the leachate is transferred to the IC sample vials and placed on the IC autosampler, which is ready for injection and analysis. Each ions calibration is established by known concentration standards solutions in the range of 0.5 to 20.0 ppm before the sample's analysis and six blank filters are also run in the sequence to minimize the impact of background components concentration.

2.2.3 Trace metal analysis by XRF

The other portion of PTFE filters were posted to the University of Massachusetts, Amherst in U.S.A. for X-ray fluorescence analysis by Pallavi Pant from Department of

Environmental Health Sciences, School of Public Health Amherst Centre. XRF is a non-destructive analytical technique for determining the elemental compositions by measuring the fluorescent or secondary X-ray emitted from the trace element after it has been excited by the primary X-ray (Thermo-Fisher Scientific, 2016). Several quality controls have been taken measures to secure the accuracy and precision of the results, including: 1) Annual single element calibration- Standards are run for each element, and calibration curves are updated; 2) Energy calibration- performed every week to ensure that the energy levels being used for the analysis are correct; 3) Multi-element standard- A multi-element (5 elements- Si, Mg, Cd, Pb, Fe) standard is run with each batch (9 samples + 1 standard); and 4) Blank filters are also run to keep a check on the measurements. During the analysis Amherst, Ag, Cd, In, Sn, Sb, Te, I, Rh, Ti, V, Cr, Mn, Fe, Co, Ni, Cu, La, Ce, Sm, Eu, Tb, Hf, Ba, Pr, Nd, Gd, , Er, Tm, Yb, Lu, Ge, Zn, Ga, As, Se, Br, Rb, Sr, Y, Zr, Nb, Mo, W, Ir, Au, Hg, Pb, Pd, Pt, Tl, U, Cs, Bi, Na, Mg, Al, Si, P, S, Cl, K, Ca, Sc have been measured by the Thermo Scientific ARL™ QUANT'X EDXRF Spectrometer.

2.2.4 Organic Carbon (OC) and Elemental Carbon (EC) analysis

OC and EC are analysed by using the Sunset Laboratory Thermo-Optical Carbon Aerosol Analyser. One 1 cm² piece of quartz filter is punched and placed into the instrument. The EUSAAR2 (European Supersites for Atmospheric Aerosol Research) protocol is applied. During the analysis, the OC is thermally desorbed from the quartz filter under inert helium gas followed by oxidation in the oven by the catalyst MnO₂ to CO₂ (Sunset Laboratory Inc., 2000). Finally, the CO₂ is converted to CH₄ under hydrogen gas with heated nickel catalyst so that the equipped Flame Ionization Detector (FID) can be measured and quantified by its internal standard CH₄ gas flow (Yin et al. 2010; Pant, P 2014). And EC is determined by its optically absorbing property while laser transmits through the filter. A






calibration curve of OC is achieved by analysing known concentration sucrose water solution for quality control purposes. Six blank filters are measured to minimize the background impurity effect.

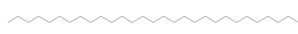






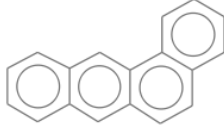
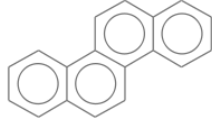
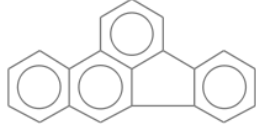
2.2.5 Organic Molecular Markers Analysis by GC-MS



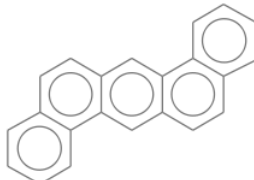
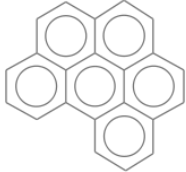
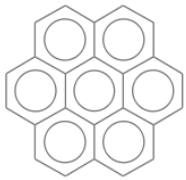
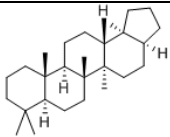
n-Alkanes, hopanes, PAHs, levoglucosan and cholesterol have been chosen for the organic molecular makers for fossil fuel combustion sources, biomass burning, vegetation and cooking (Zhao et al. 2015; Cheng et al. 2013; Li et al. 2010; Zheng et al. 2014; Lin et al. 2010; Yanlin Zhang et al. 2015; He et al. 2006; Ke, Liu, Wang, Russell, et al. 2008; Yin et al. 2015; Cass 1998; Wang et al. 2012; Simoneit 2002; Simoneit et al. 1991; Zhang et al. 2009b; Pant et al. 2014; Bullock et al. 2008).

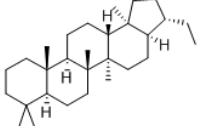
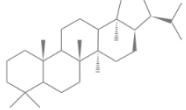
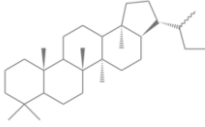
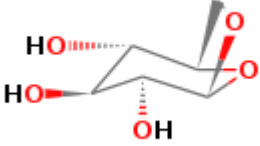
The name, abbreviation and their basic physical property and molecular structures are listed in the following table here.

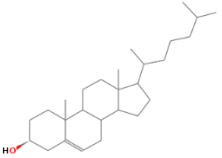
Table 2-1 the measured OMM and their basic physical properties

Name	Abbreviation	Formula/Molecular Weight (1)	Structure
n-Tetracosane	C24	$C_{24}H_{50}$; 338	
n-Pentacosane	C25	$C_{25}H_{52}$; 352	
n-Hexacosane	C26	$C_{26}H_{54}$; 366	
n-Heptacosane	C27	$C_{27}H_{56}$; 377	
n-Octacosane	C28	$C_{28}H_{58}$; 395	

Name	Abbreviation	Formula/Molecular Weight (1)	Structure
n-Nonacosane	C29	$C_{29}H_{60}$; 408	
n-Triacontane	C30	$C_{30}H_{62}$; 423	
n-Hentriacontane	C31	$C_{31}H_{64}$; 437	
n-Dotriacontane	C32	$C_{32}H_{66}$; 451	
n-Tritriacontane	C33	$C_{33}H_{68}$; 465	
n-Tetratriacontane	C34	$C_{34}H_{70}$;	
Retene	-	$C_{18}H_{18}$; 234.34	
Benz[a]anthracene	BaAnt	$C_{18}H_{12}$; 228.29	
Chrysene	Chr	$C_{18}H_{12}$; 228.29	
Benzo[b]fluoranthene	BbF	$C_{20}H_{12}$; 252.31	

Name	Abbreviation	Formula/Molecular Weight (1)	Structure
Benzo[a]pyrene	BaPyr	C ₂₀ H ₁₂ ; 252.31	
Indeno[1,2,3-cd]pyrene	Ipyre	C ₂₂ H ₁₂ ; 276.33	
Dibenzo[a,h]anthracene	DBahAnt	C ₂₂ H ₁₄ ; 278.35	
Benzo[g,h,i]perylene	BghiPer	C ₂₂ H ₁₂ ; 276.34	
Coronene	COR	C ₂₄ H ₁₂ ; 300.35	
17 α (H)- 22,29,30- Trisnorhopane	C _{27α}	C ₂₇ H ₄₆ ; 371	

Name	Abbreviation	Formula/Molecular Weight (1)	Structure
17 α (H),21 β (H)- 30-norhopane	C _{29$\alpha\beta$}	C ₂₉ H ₅₀ ; 399	
17 α (H),21 β (H)- Hopane	C _{30$\alpha\beta$}	C ₃₀ H ₅₂ ; 413	
22S- 17 α (H),21 β (H)- 30- Homohopane	C _{31$\alpha\beta$S}	C ₃₁ H ₅₄ ; 427	
22R-17 α (H),21 β (H)- 30-Homohopane	C _{31$\alpha\beta$R}	C ₃₁ H ₅₄ ; 427	
Levoglucosan	Levo	C ₆ H ₁₀ O ₅	

Name	Abbreviation	Formula/Molecular Weight (1)	Structure
Cholesterol	Chol	C ₂₇ H ₄₆ O	

These analytes from the samples are pre-processed by extraction, concentration and derivation before the sample injection to the GC-MS. For analyte mass quantification, internal calibration is used in this experiment and internal standard (IS) is added while extraction is being taken place.

Extraction: Firstly, $\frac{1}{4}$ of quartz filter is placed in a cleaned 250 ml glass bottle and spiked with 50 μ l of 10 ppm internal standard mix-all (ISALL, including octacosane-d58 and hexatriacontane-d74 for n-alkanes; aaa-20R-cholestane-d4 for hopanes; chrysene-d12 and dibenzo(ah)anthracene-d14 for PAHs; Methyl-beta-D-xylopyranoside for levoglucosan and cholesterol-2,2,3,4,4,6-d6 for cholesterol). Then it is left in the fume hood for about 30 minutes for evaporation. Afterwards, it is ready for extraction by adding 30 ml mixture solvent of 2:1 Dichloromethane (DCM) and methanol and place in the ultrasonic water bath for 15 minutes sonication. The extracted solution is then transferred to a turbo evaporator tube for further concentration under nitrogen gas blow and heating by warm water in the instrument. This step is repeated one more time and the 250 ml glass bottle is rinsed three pipettes of 2:1 DCM and methanol mixture solvent so that more than 60 ml of total volume of extracted solvent are obtained before the concentration.

Concentration: more than 60 ml of total volume of extracted solvent are concentrated to 500 µl by two stage of concentration for the convenience of internal calibrations. The first stage is using turbo evaporator to blow down to 5 ml. Then the extracts were then filtered through pre-cleaned glass wool and sodium sulphate (Na₂SO₄) columns and collected in pre-cleaned 15 ml glass finger vial. The samples were then concentrated to 500 µl under a gentle stream of oxygen-free nitrogen and transferred to three pre-cleaned GC vials equipped with insert with about 160 µl each. The samples are stored in the freezer at -20 °C until analysis. The first two vials are used directly for n-alkanes & hopanes and PAHs analysis, respectively while the third vial is required derivation before its levoglucosan and cholesterol analysis.

Derivation: Cholesterol and levoglucosan are polar component. Therefore, a reagent N,O-Bis(trimethylsilyl)trifluoroacetamide plus 1% trimethylchlorosilane (BSTFA-TMCS) is chosen for the silylation. First of all the 166 µl of final extract is blown down to near dryness under gentle nitrogen gas stream again and Add 166 µl of BSTFA-TMCS to the vials containing samples until mark line. Heat the vial on a dry heater block at 80°C for 1 hour. Allow the vial to cool in a desiccator for 1 hour and then they are immediately subjected to GC-MS analysis.

GC-MS sample injection and programming is shown as follows: These three programmes (SIM methods) are used for n-alkanes, hopanes, PAHs, levoglucosan and cholesterol analysis by Agilent GC- 6890N plus MSD-5973N fitted with an HP-5MS (30 m, 0.25 mm diameter, 0.25 µm thickness) column.

The settings of GC-MS is shown below while the whole process of chemical species measurement is summarized in figure 2.3.

Table 2-2 GC-MS sample injection programming for *n*-alkanes & hopanes

GC and MS conditions	Column Type: HP-5MS Column (30 m, 0.25 mm Diameter, 0.25 µm film thickness)
GC Conditions	
Injector Temperature (°C)	300
GC/MS Interface Temperature (°C)	300
Initial Oven Temperature (°C)	65
Initial Oven Hold Time (min)	5
Oven Temperature Ramp Rate 1 (°C/min)	10
Oven Temperature end 1 (°C)	250
Oven Hold Time 1 (min)	0
Oven Temperature Ramp Rate 2 (°C/min)	5
Final Oven Temperature (°C)	300
Final Oven Temperature Hold Time (min)	26.5
Carrier Gas	Helium
Carrier Gas Flow rate (ml/min)	1.0
Injection Mode	Splitless
MS Conditions	
Solvent Delay (min)	22
Data Collection Mode	SIM (ions: 57, 71, 85, 66, 82, 98; 191, 221)
Dwell Time (ms)	50

Table 2-3 GC-MS sample injection programming for PAHs

GC and MS conditions	Column type: HP-5MS Column,_(30 m, 0.25 mm Diameter, 0.25 µm film thickness)	
GC Conditions		
Injector Temperature (°C)	300	
GC/MS Interface Temperature (°C)	300	
Initial Oven Temperature (°C)	65	
Initial Oven Hold Time (min)	2	
Oven Temperature Ramp Rate 1 (°C/min)	5	
Oven Temperature end 1 (°C)	100	
Oven Hold Time 1 (min)	0	
Oven Temperature Ramp Rate 2 (°C/min)	10	
Final Oven Temperature (°C)	300	
Final Oven Temperature Hold Time (min)	28	
Carrier Gas	Helium	
Carrier Gas Flow rate (ml/min)	1.0	
Injection Mode	Splitless	
MS Conditions		
Solvent Delay (min)	5	
Data Collection Mode	Scan	
Scan Range (amu)	50-650	
Solvent Delay (min)	10	
Data Collection Mode	SIM(Ions One:59,100,114,115,129,143,157; Two: 129,171,163,194,152,185; Three: 221, 241,239)	Group Group Group
Dwell Time (ms)	50,50,100	

Table 2-4 GC-MS sample injection programming for Levoglucosan & Cholesterol

GC and MS Conditions	Column type: HP-5MS Column,(30 m, 0.25 mm Diameter, 0.25 µm film thickness)
<p style="text-align: center;">GC Conditions</p> <p>Injector Temperature (°C) 300</p> <p>GC/MS Interface Temperature (°C) 300</p> <p>Initial Oven Temperature (°C) 65</p> <p>Initial Oven Hold Time (min) 10</p> <p>Oven Temperature Ramp Rate (°C/min) 10</p> <p>Final Oven Temperature (°C) 300</p> <p>Final Oven Temperature Hold Time (min) 26.5</p> <p>Carrier Gas Helium</p> <p>Carrier Gas Flowrate (ml/min) 1.0</p> <p>Injection Mode Splitless</p> <p style="text-align: center;">MS Conditions</p> <p>Solvent Delay (min) 15</p> <p>Data Collection Mode SIM(ions:204,217,333,368,374,458,464)</p> <p>Dwell time (ms) 50h</p>	

The LoD is calculated as three times of concentration level measured via travel blanks from all the samples.

Table 2-5 Limit of detections (LoD) for all chemical species

Instrument Limits of Detection (LoD)	
Species	LoD
Water Soluble Ions	(µg/m)
Chloride	0.063830
Nitrate	0.063830
Sulphate	0.063830
Phosphate	0.024830
Carbonate	0.027064
Sodium	0.010021
Ammonium	0.000000
Potassium	0.006383
Magnesium	0.023936
Calcium	0.026106
Trace Metals	(µg/cm ³)
Cd	0.003955
Sn	0.070283
Sb	0.039925
Ti	0.014591
V	0.002672
Cr	0.020577
Mn	0.013950
Fe	0.009995
Co	0.000000
Ni	0.004115
Cu	0.007269
Ba	1.625692
Pr	0.061410
Zn	0.008231
As	0.005665
Se	0.002031
Br	0.004703
Sr	0.003795
Mo	0.008177
Pb	0.003848
Na	0.134739
Mg	0.040139

Instrument Limits of Detection (LoD)	
Species	LoD
Al	0.122286
Si	0.000000
Cl	0.003367
K	0.002352
Ca	0.001122
Sc	0.018813
Carbon	($\mu\text{gC}/\text{cm}^2$)
OC	0.059566
EC	0.002489
Organic Molecular Markers	($\mu\text{g}/\text{ml}$)
Levoglucosan	0.257362
Cholesterol	0.051472
n-Tetracosane (C24)	0.000766
n-Pentacosane (C25)	0.000766
n-Hexacosane (C26)	0.000766
n-Octacosane (C28)	0.000255
n-Nonacosane (C29)	0.000766
n-Triacontane (C30)	0.001021
n-Hentriacontane (C31)	0.001021
n-Dotriacontane (C32)	0.001021
n-Tritriacontane (C33)	0.000766
n-Tetratriacontane (C34)	0.000766
n-Pentatriacontane (C35)	0.000766
17a(H)-22,29,30-Trisnorhopane	0.001021
17a(H),21b(H)-30-norhopane	0.001021
17a(H),21b(H)-Hopane	0.001021
22S-17a(H),21b(H)-30-Homohopane	0.001021
22R-17a(H),21b(H)-30-Homohopane	0.001021
22S-17a(H),21b(H)-30-Bishomohopane	0.001021
22R-17a(H),21b(H)-30-Bishomohopane	0.001021
22S-17a(H),21b(H)-30,31,32-trishomohopane	0.001021
22R-17a(H),21b(H)-30,31,32-trishomohopane	0.001021
Retene	0.001532
Benzo[a]Anthracene	0.000766
Chrysene	0.000511
Benzo[b]Fluoreathene	0.000511
Benzo[k]Fluorathene	0.000255
Benzo[a]Pyrene	0.001021

Instrument Limits of Detection (LoD)	
Species	LoD
Indeno[1,2,3-cd]Pyrene	0.000511
Dibenzo[a,h]Anthracence	0.001021
Benzo[g,h,i]Perylene	0.000511
Coronene	0.000766

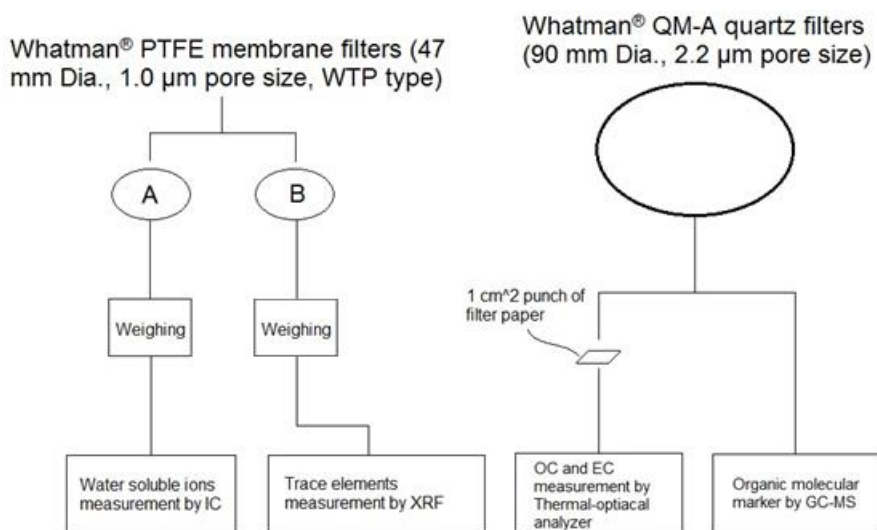


Figure 2-4 Summary of the whole chemical analysis processes.

Finally, the internal standard recovery rates were determined after the GC-MS analysis. The average recovery rate of IS for all analyzed species are all lied in the range from 30% to 150%, which is acceptable (See Figure 2-5). The recovery rate is calculated by the following equation:

$$\% \text{ IS Recovery} = \left[\left(\frac{A_{IS}}{A_{RDS}} \right)_S \times \left(\frac{A_{RDS}}{A_{IS}} \right)_{STD} \times \left(\frac{C_{IS}}{C_{RDS}} \right)_{STD} \times \left(\frac{C_{RDS}}{C_{IS}} \right)_S \right] \times 100$$

Where $(A_{IS}/A_{RDS})_S$ = ratio of internal standard peak area to recovery determination standard peak area in the sample; $(A_{RDS}/A_{IS})_{STD}$ = ratio of recovery determination standard

peak area to internal standard peak area in the calibration standard (the average of values obtained for both calibration standards run for a batch of samples is used); $(C_{IS}/C_{RDS})_{STD}$ = ratio of concentration of internal standard to concentration of recovery determination standard in the calibration standard; and $(C_{RDS}/C_{IS})_S$ = ratio of concentration of recovery determination standard to concentration of internal standard in the sample (assuming 100% recovery).

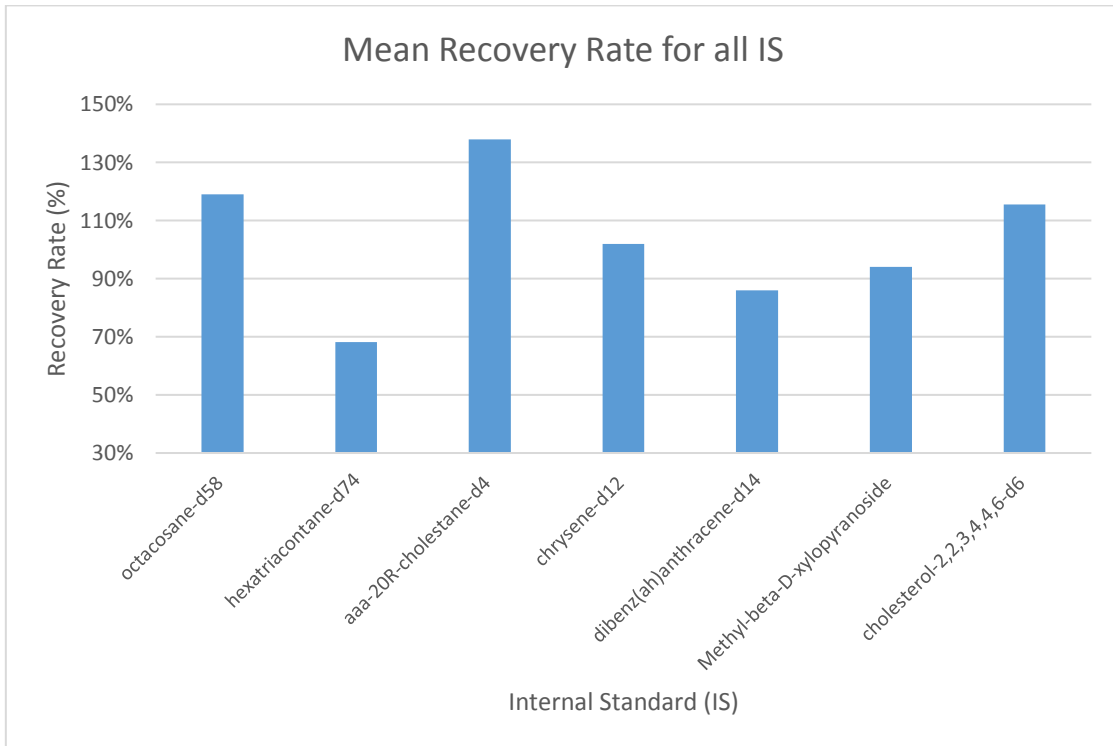


Figure 2-5 Recovery rate for all internal standards

2.3 Fundamentals of Source apportionment and Receptor modellings

2.3.1 Scientific basis

In this project, the two receptor models, Positive Matrix Factorization (PMF) and Chemical Mass Balance (CMB) have been employed. The method based on mass conservation and statistics and they are aimed to evaluate the contribution of different sources to ambient PM (Pant 2014). The details are as follows.

In general, the purposes of receptor models (RMs) includes the following three major components: 1) to interpret the physical and chemical ambient particles at the sampling site (receptor); 2) to interpret the precursors of these particles and therefore deduce the possible sources; 3) and finally conclude the contribution of all sources in a quantitative way. To achieve these goals, a critical assumption is made, which the mass of the bulk ambient particles are conserved during the transport in the air and the principle of mass conservation has been applied, as mentioned earlier in the Chapter one (Hopke, P., 1991).

Again, mathematically,

$$x_{ij} = \sum_{k=1}^p g_{ij} f_{kj} \quad (2.1)$$

where x_{ij} is the j^{th} chemical species concentration measured in the i^{th} sample, f_{kj} is the concentration of the j^{th} species in emission from the k^{th} source contributing to the i^{th} sample.

For instance, for the elemental carbon (EC) from an ambient air samples with pollutant P coming from different sources 1, 2, 3 etc., the total amount of EC in pollutant P on the deposited filter or at the receptor will be $P_{\text{total EC}} = P_{1\text{EC}} + P_{2\text{EC}} + P_{3\text{EC}} + \dots + P_{k\text{EC}}$ (2) where k is the k^{th} of sources. Furthermore, since P is a complex mixture and if f is defined as the

mass fraction of EC for one part of pollutant P from a specific source and g is defined as the mass concentration of the part of pollutant P from this specific source within the ambient air samples. Equation (1) can be rewritten as $P_{\text{total EC}} =$ (3). Finally, if equation (3) is applied to j chemical species from i samples, $x_{ij} = \sum_{k=1}^p g_{ij} f_{kj}$ (4). In this terms, the receptor model will identify the factors (or sources) by solving the equation (4) and a large amount of dataset matrix of which consisting of chemical constituents collected from a number of samples are required and preferred (Belis et al. 2013). Based on this principle, a few quantitative methods including, Chemical Mass Balance (CMB), Positive Matrix Factorization (PMF), Multilinear Engine (ME) have been developed since then.

However, the solution of mass conversion equation of CMB and PMF are solved in a slightly different way so that the data requirements and preparation are different in the later project. Based on the conceptual framework that presented as equation (1). Miller et al. (1972) proposed the following mass balance equation that used in the CMB and PMF models later:

$$x_j = \sum_{k=1}^p \alpha g_{ij} f_{kj} + e_{ij} \quad (2.2)$$

where x_j is the concentration of chemical species j measured in the sample of interest, f_{kj} is the concentration of the chemical species j from the source k , g_k is the mass contribution of source k to the sample of interest, e_{ij} is the un-modelled portion of the variation and α_j is the coefficient of fractionation for species j that indicates the amount of that species remaining in the particulate matter after transport to the sampling site while it is usually assumed to be unity due to the difficulty in estimating the differential reactivity of the various species in a given profile (Miller et al. 1972; Hopke 2016).

Hopke (1991) discussed the assumptions to CMB model and how the solution to the mass balance equation is solved. One of the biggest features of CMB is that it requires the source profile, which is the term f_{kj} in the equation (4) for the model run. In 1990s, Paatero & Tappert (1993; 1994) proposed the concept of PMF model which an explicit least-squares formulation of the mass balance is utilised so that it solves the equation by minimizing a weighted objective function given by the following Q value equation:

$$Q = \sum_{i=1}^n \sum_{j=1}^m \left(\frac{e_{ij}}{s_{ij}} \right)^2 = \sum_{i=1}^n \sum_{j=1}^m \left[\frac{x_{ij} - \sum_{k=1}^p g_{ik} f_{kj}}{s_{ij}} \right]^2 \quad (2.3)$$

Where s_{ij} is an estimate of the uncertainty for the j^{th} species in the i^{th} sample. The advantage of PMF's algorithm is that it does not require the source profiles as the data input. These methods have been successfully applied in many cases study where CMB and PMF are one of the most popular used methodology in nowadays (Belis et al. 2013). In this project, the USEPA CMB v8.2 and PMF v5.0 is used for the modelling processes. However, PCA has not used in this thesis as it has not been widely accepted as a receptor model today (Hopke, 2004). In addition, the latest version of PMF is also considered more advanced than UNMIX so that this model is also not applied in this thesis (Hopke, 2016). On the other hand, ME-2 algorithm is more suitable for large dataset obtained by continuous real-time high-resolution sampler but it is an option in the further study (Crippa et al. 2014).

2.4 The modelling criteria of CMB and PMF

2.4.1 CMB criteria

In CMB, the following performance measures have been established to assess the how well the model has performed, which is consist of the following parameters: 1) R-square value (r^2); 2) chi-square value (χ^2); 3) t-stat value and 4) Calculated/Measured Ratio (C/M) (USEPA, 2004).

Briefly, r^2 and χ^2 the parameter for the least squares calculation where r^2 is the fraction of the variance in the measured concentration that is explained by the variance in the calculated species concentrations and χ^2 is the weighted sum of the squares of the differences between the calculated and measured fitting species concentrations (USEPA, 2004). If r^2 is between 0.8 and 1 while χ^2 is less than 4, the results are acceptable (USEPA, 2004)

T-statistic (Tstat) is the ratio of the source contribution estimate to the standard error (USEPA, 2004). If Tstat value is less than two, which implies that the source contribution estimate is at or below the detection limit that likely due to collinearities between sources profiles (UESEPA, 2004).

Additional performance measures include C/M and R/U. If C/M is between 0.75 and 1.5 while R/U value is between -2 and 2, the results are acceptable (USEPA, 2004).

2.4.2 PMF criteria

Based on the PMF v5.0 manual and beyond, the best standards and practice on how to evaluate the model performance and assessing the physical significance of the mathematical solution by the PMF model have also been in-depth reviewed (Reff et al. 2007; Belis et al., 2014; Belis et al., 2015; Brown et al., 2015; Hopke, 2016). Based on these

recommendations, the best solution of PMF model run in this study is judged by the following criteria: 1) the solutions between 3 to 7 factors will be investigated; 2) by assessing the stability and minimization of Q value and Q expected value over multiple run; 3) by assessing the G-space plot and scaled residuals; 4) by evaluating the modelling uncertainties by Bootstrap(BS) and Displacement (DISP); 5) by assessing whether the modelled total variable perdition is matched with measurement data ($R^2 > 0.9$ and gradient ≈ 1.0) etc. (Masiol et al. 2017).

2.5 Models Performance and Outcomes Evaluations

A framework of modelling results evaluations is introduced as follows.

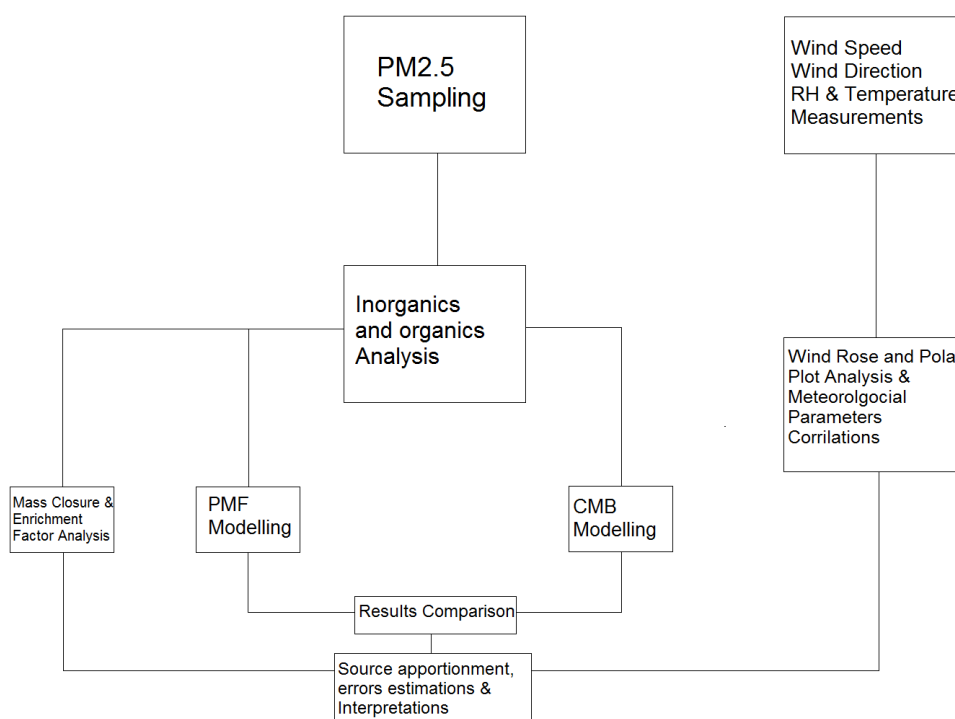


Figure 2.5 The framework of data analysis, modelling results comparison and source apportionment.

The core results and data analysis are the outcomes comparison between PMF and CMB analysis. While interpreting the results, other analysis including the mass closure analysis, enrichment factor and meteorological data analysis are also applied. Microsoft Excel 2010, R (with OpenAir Package, USEPA PMF5.0 and CMB 8.2 are used for the entrie numerical analysis.

3 Chapter Three Mass Concentration of PM_{2.5} and its constituents in Jinan, China

Abstract

This chapter reports the chemical composition of PM_{2.5} in an urban area of Jinan city, northern China from early 2015 to early 2016. PM_{2.5} samples were collected on the roof of teaching building on the central campus of Shandong University. Meteorological parameters were monitored by a simple met station. The PM_{2.5} concentration was highest in winter. Autumn was another season when it was heavily polluted while early summer and late summer were less polluted in Jinan with respect to PM_{2.5}. PM_{2.5} samples were analysed by using IC, XRF, Thermal-Optical analyser and GC-SM. Ion balance analysis showed that the ambient air in Jinan was almost neutral, which implies the influence of ammonium in the ambient air and also reflects the reliability of the dataset. Mass closure analysis indicated that secondary inorganic aerosols (SIA), mineral dust, OC and EC were the major chemical components of PM_{2.5}.

3.1 Introduction

Jinan has suffered by the severe air pollution for a couple of decades and today's PM_{2.5} concentration level remains high (Cheng et al. 2011; Gu et al. 2014). The annual mean PM_{2.5} concentration was around 150 µg·m⁻³ in 2010 (Gu et al. 2014), which was 10 times greater than the WHO PM_{2.5} annual mean guideline (WHO, 2006). In terms of chemical composition, secondary sulphate, nitrate, ammonium, OC and EC were found as the major substance in the ambient air, which is very similar to the other mega city's pollution in China (Gao et al. 2011; Huang et al. 2014). In order to execute a comprehensive source

apportionment study for the latest pollution status in the urban area of Jinan with limited budget, it is vital to collect a sufficient number of samples which can be used to not only quantify the current $PM_{2.5}$ concentration but also characterize both inorganic and organic compounds of $PM_{2.5}$ by the available instruments within a limited time. Therefore, both quartz and Teflon filters were used for the $PM_{2.5}$ sampling in Jinan to meet the requirements of chemical analysis. A simple weather station was also employed to record the wind speed (ws), wind direction (wd), temperature (T), relative humidity (RH) and atmospheric pressure (P) so that the impact on $PM_{2.5}$ from meteorological condition could be assessed. This section aims to discuss the $PM_{2.5}$ concentration, the concentration of analysed chemical compositions, the relationship between the weather and $PM_{2.5}$ and also the relationships between the different chemical species during this sampling period.

3.3 Results and Discussion

3.3.1 $PM_{2.5}$ concentration

The daily $PM_{2.5}$ concentration and seasonal mean $PM_{2.5}$ concentration are shown below in Figure 3-1 and Figure 3-2, respectively. Jinan has a humid subtropical (Cwa) climate. The city is dry and nearly rainless in spring from March to May and hot and rainy in summer from June to August, dry and cold with little snow in autumn (September to November) and winter from December to February. According to these two figures, the $PM_{2.5}$ concentration in spring and summer were the lowest, and there were a few days with fairly good air quality. However, the $PM_{2.5}$ pollution was much worse in late autumn (P4) and both winter sampling periods (P1 & P5). Both the mean concentration and frequency of pollution episodes were greater than the other two seasons (P2 & P3).

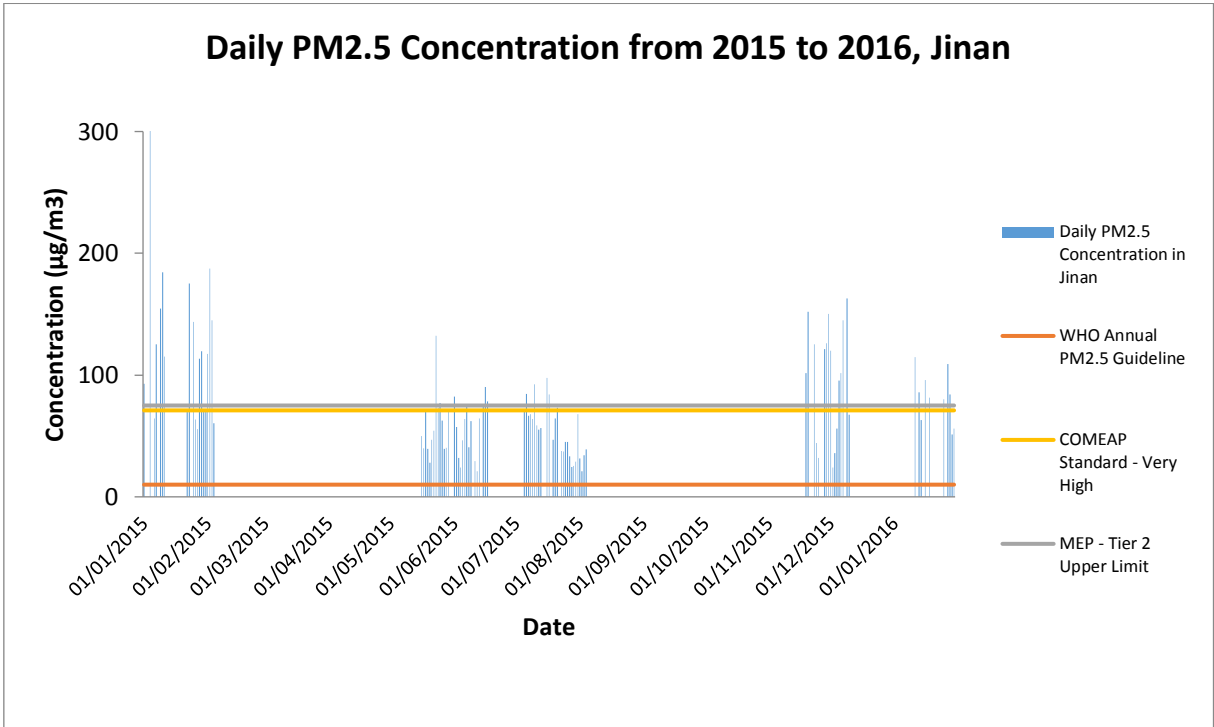


Figure 3-1 Daily PM_{2.5} concentration in Jinan during the whole sampling campaign.

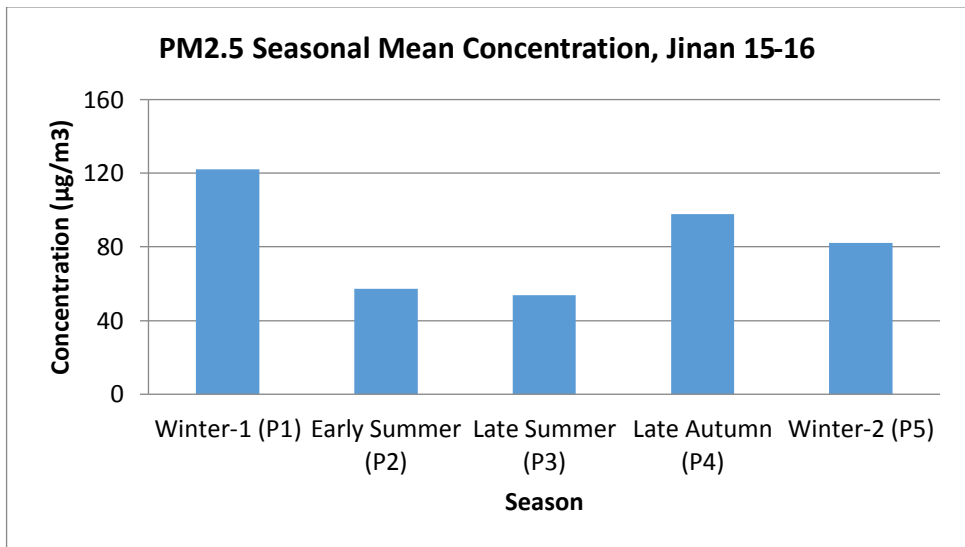


Figure 3-2 Seasonal mean PM_{2.5} concentration in Jinan

Overall, the mean $PM_{2.5}$ concentration in winter (P1 & P5), early summer (P2), late summer (P3) and autumn (P4) were $108.8 \mu\text{g}\cdot\text{m}^{-3}$, $57.4 \mu\text{g}\cdot\text{m}^{-3}$, $53.4 \mu\text{g}\cdot\text{m}^{-3}$ and $97.7 \mu\text{g}\cdot\text{m}^{-3}$, respectively, while the mean concentration in P1 is $122.1 \mu\text{g}\cdot\text{m}^{-3}$ and P5 is $82.1 \mu\text{g}\cdot\text{m}^{-3}$. The variation of $PM_{2.5}$ concentration is probably because of two main reasons. The weather in North China Plain is usually influenced by the anticyclone in winter while inversion layer will be formed so that inhibiting the $PM_{2.5}$ diffusion. On the other hand, the monsoon in summer and precipitation helps the wet deposition and helps to scavenge (Cheng et al. 2011). Meanwhile, the heating period for domestic use normally takes place from late November to late March in Jinan so that coal burning will be an important source of ambient particulate matter (Ni et al. 2012).

According to COMEAP (UK) recommendations of $PM_{2.5}$ index, it will be considered as “very high” level of $PM_{2.5}$ pollution if its 24-hour mean concentration is above or equal to $71 \mu\text{g}\cdot\text{m}^{-3}$, which is considered as having acute health effects for all general population (Ayres et al., 2011). Under this circumstance, 73%, 21%, 19% and 65% days of winter, early summer, late summer and autumn, respectively had severe air pollution in Jinan. The mean $PM_{2.5}$ based on this sampling campaign was $79.3 \mu\text{g}\cdot\text{m}^{-3}$, which is more than five times higher than the WHO annual guidance. It is even still much higher than the slightly less strict tier 2 limit of $PM_{2.5}$ in the ambient air quality standards of China (MEP, 2012). Hence, although the $PM_{2.5}$ concentration was significantly lower than another case study about five years ago, Jinan is still a very heavily polluted city in terms of fine particles.

3.3.2 Chemical species concentration

The following tables and figures in this section summarise the mean concentration of each measured species of PM_{2.5}. Overall, the mean concentration in each sampling periods and total concentration is summarised in Table 3-1 below.

Table 3-1 the seasonal and periods mean concentration of all measured chemical species (OC, EC and water soluble ions are in unit of µg/m³ while the rest is in ng/m³)

	P1	P2	P3	P4	P5	Mean
OC	16.9	12.3	12.3	21.0	20.7	15.1
EC	3.5	2.5	2.7	3.7	4.4	3.1
Na ⁺	0.45	0.30	0.27	0.55	0.38	0.37
NH ₄ ⁺	5.64	7.72	8.06	7.07	4.49	7.14
K ⁺	1.03	2.21	1.82	2.05	1.83	1.81
Mg ²⁺	0.07	0.10	0.10	0.28	0.09	0.12
Ca ²⁺	1.05	0.49	0.43	0.84	0.52	0.65
Cl ⁻	1.78	0.34	0.79	3.38	3.10	1.41
NO ₃ ⁻	6.97	4.74	7.39	14.65	11.04	7.94
SO ₄ ²⁻	8.83	17.51	17.21	11.84	9.66	14.32
C ₂ O ₄ ²⁻	0.22	0.47	0.35	0.24	0.19	0.33
Al	0.78	0.43	0.24	0.57	0.75	0.48

	P1	P2	P3	P4	P5	Mean
Si	1.61	1.01	0.27	0.91	1.21	0.92
Ti	0.07	0.04	0.02	0.04	0.03	0.04
V	0.01	0.01	0.00	0.01	0.00	0.01
Cr	0.03	0.02	0.01	0.03	0.08	0.02
Mn	0.06	0.04	0.02	0.07	0.12	0.05
Fe	1.28	0.69	0.37	1.11	1.35	0.82
Ni	0.03	0.02	0.02	0.04	0.05	0.02
Cu	0.07	0.05	0.06	0.09	0.11	0.06
Zn	0.22	0.16	0.16	0.37	0.53	0.22
As	0.01	0.01	0.01	0.02	0.03	0.01
Se	0.01	0.01	0.00	0.02	0.03	0.01
Pb	0.09	0.06	0.05	0.14	0.19	0.09
Sr	0.01	0.00	0.00	0.00	0.00	0.00
Mo	0.01	0.00	0.00	0.01	0.01	0.00
Cd	0.01	0.01	0.01	0.01	0.03	0.01
Sb	0.04	0.04	0.04	0.06	0.04	0.04

	P1	P2	P3	P4	P5	Mean
Ba	0.40	0.26	0.51	0.63	0.43	0.43
Na	1.39	1.26	1.57	2.26	2.67	1.59
Mg	0.27	0.24	0.24	0.34	0.35	0.27
K	1.24	1.51	1.94	2.19	2.58	1.73
Ca	2.03	1.00	0.40	1.27	1.66	1.11
Sc	0.18	0.10	0.05	0.13	0.16	0.11
Sn	0.03	0.04	0.04	0.06	0.03	0.04
Levogluconan	0.38	0.12	0.23	0.65	0.65	0.31
Cholesterol	0.02	0.01	0.00	0.01	0.02	0.01
Retene	0.005	0.002	0.003	0.006	0.008	0.004
Benzo[a]Anthracene	0.011	0.007	0.008	0.014	0.017	0.009
Chrysene	0.014	0.002	0.006	0.019	0.019	0.009
Benzo[b]Fluoreathene	0.021	0.008	0.012	0.026	0.023	0.015
Benzo[k]Fluorathene	0.012	0.003	0.007	0.021	0.018	0.010
Benzo[a]Pyrene	0.016	0.008	0.009	0.017	0.019	0.012
Indeno[1,2,3-cd]Pyrene	0.004	0.003	0.003	0.009	0.004	0.004

	P1	P2	P3	P4	P5	Mean
Dibenzo[a,h]Anthracence	0.001	0.000	0.000	0.002	0.001	0.001
Benzo[g,h,i]Perylene	0.003	0.001	0.002	0.019	0.005	0.005
Coronene	0.000	0.000	0.000	0.002	0.001	0.001
C24	0.067	0.023	0.042	0.118	0.071	0.056
C25	0.059	0.026	0.045	0.128	0.078	0.058
C26	0.048	0.028	0.042	0.099	0.062	0.050
C27	0.057	0.059	0.050	0.114	0.067	0.066
C28	0.039	0.036	0.039	0.071	0.047	0.044
C29	0.074	0.114	0.059	0.113	0.068	0.089
C30	0.041	0.038	0.040	0.054	0.042	0.042
C31	0.055	0.080	0.050	0.065	0.050	0.063
C32	0.029	0.028	0.036	0.091	0.055	0.043
C33	0.036	0.041	0.042	0.106	0.069	0.053
C34	0.032	0.033	0.033	0.079	0.043	0.041
r17aTNohop	0.008	0.012	0.028	0.033	0.030	0.020
17aNohop	0.029	0.024	0.017	0.020	0.017	0.022

	P1	P2	P3	P4	P5	Mean
17ahop	0.018	0.018	0.027	0.028	0.027	0.023
22SabHH	0.025	0.025	0.022	0.023	0.023	0.024
22RabHH	0.022	0.027	0.045	0.045	0.044	0.035

3.3.2.1 OC and EC

Table 3-2 the mean OC, EC and PM_{2.5} concentration for all periods in Jinan

	P1	P2	P3	P4	P5
OC ($\mu\text{g}\cdot\text{m}^{-3}$)	24.1	11.8	13.4	22.8	23.6
EC ($\mu\text{g}\cdot\text{m}^{-3}$)	4.9	2.5	3.1	3.4	5.9
OC/EC	4.9	4.3	4.3	6.7	4.0

Table 3-2 summarises the mean concentration of OC and EC in each season. The concentration of OC and EC follows the trend of PM_{2.5} concentration where winter and autumn had the highest concentration of OC and EC and spring and summer experienced the lowest concentration in both OC and EC. Overall, the OC and EC account for about 20% and 4% of PM_{2.5} total mass annually.

The secondary organic carbon (SOC) is normally the low-volatility products formed by the oxidation of gas-phase precursors which have low vapour pressure to condense upon volatile organics on existing aerosol particles (Castro et al. 1999; Seguel A. et al. 2009).

SOC is difficult to measure directly due to its complex compositions and formation mechanism (Zhou et al. 2012), it is estimated based on the OC and EC data by using the following equation (3.1):

$$\text{SOC} = \text{OC} - (\text{OC}/\text{EC}_{\text{primary}}) \times \text{EC} \quad (3.1)$$

Where: $(\text{OC}/\text{EC}_{\text{primary}})$ is equivalent to the minimum OC/EC ratio during the sampling campaign (Zhou et al. 2012). This method uses EC as a tracer to estimate the secondary organic carbon formation indirectly (Zhang et al. 2012). The annual mean SOC is $6.77 \mu\text{g}\cdot\text{m}^{-3}$, which accounts for 37.5% of total organic aerosol mass, suggesting a high degree of SOA formation in Jinan all year round.

3.3.2.2 *Water Soluble Ions*

Water-soluble ions were also the important constituents of $\text{PM}_{2.5}$ in Jinan, including ammonium, potassium, calcium, chloride, nitrate and sulphate. They may come from primary precursors such as SO_2 and NO_x emitted from fossil fuel burning and industrial emission or agriculture (Wu et al. 2013; Gu et al. 2014). According to figure 3.5, sulphate, nitrate and ammonium were the three dominant constituents in $\text{PM}_{2.5}$. Potassium, calcium and chloride also had reasonable high concentration, though their amount was a magnitude less than the three major ions. Sodium, magnesium and oxalate ions were also measured by IC but there is relatively minor contribution than the rest constituents (Figure 3-3).

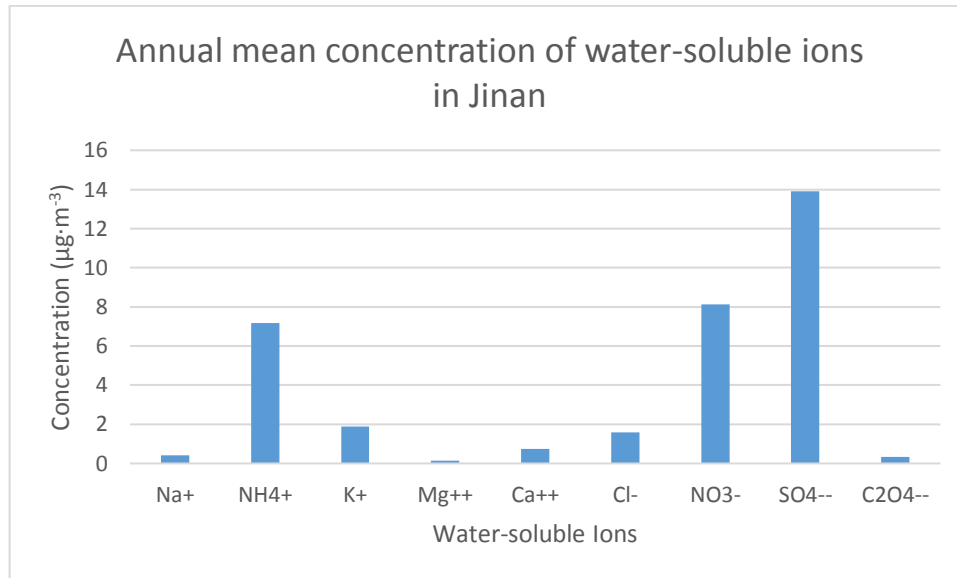


Figure 3-3 annual mean concentration of measured water-soluble ions

According to Figure 3-3 annual mean concentration of measured water-soluble ions, sulphate, ammonium and nitrate account for 41%, 22% and 21% of total water-soluble mass, which dominate the total mass of water-soluble ions. First of all, the non-sea salt sulphate ($\text{SO}_4^{2-}_{\text{nss}}$) is calculated by equation (3.2) where $[\text{SO}_4^{2-}_{\text{nss}}] = [\text{SO}_4^{2-}] - [\text{Na}^+] \times 0.252$ (Long et al. 2014). The non-sea salt sulphate accounted for 99% of total sulphate. Since Jinan is an industrialised and urbanised mega-city, the amount of these major secondary inorganic aerosols (SIA) implies the high intensity of anthropogenic emission from this city rather than from the sea salt at all. Therefore, the contribution from the sea is negligible. On the other hand, the nitrate to sulphate ratio ($\text{NO}_3^- / \text{SO}_4^{2-}$) (in $\mu\text{g}/\text{m}^3$) is a good indicator for assessing whether mobile source or coal combustion is the predominance emission at the place of interest (Kong et al. 2010). The annual $\text{NO}_3^- / \text{SO}_4^{2-}$ is 0.58, which further implies coal combustion related industry is a major source of $\text{PM}_{2.5}$ in Jinan (Kong et al. 2010). Furthermore, there is a clear seasonal variation for nitrate and sulphate. The nitrate has much higher concentrations in autumn and winter while it decreases substantially in spring and summer. This is very likely due to the phase partition of NO_3^- , which largely

depends on the temperature, humidity and ammonia concentration (Yao et al. 2002). As the average temperature in spring and summer are much higher than autumn and winter, a significant amount of nitrate may have transferred to the gas phase. However, there is more sulphate in spring and summer rather than autumn and winter in Jinan which is not that typical compared to other studies (Wang et al. 2009; Zhang et al. 2007; Zhang et al. 2013; Song et al. 2007; Zíková et al. 2016). It generally has higher sulphate in autumn and winter due to the domestic heating supplied by coal burning in China (Yao et al. 2002; Dai et al. 2013). However, similar trend has been found in the earlier study in Jinan and Yang et al. (2012) suggested that the low RH in winter and autumn does not favour heterogeneous aqueous reactions and a higher concentration of ozone and stronger sunlight accelerate the secondary conversion of SO₂ to sulphate via oxidation. This is also supported by the latest findings on secondary sulphate formation mechanism that the severe haze pollution in China is largely caused by SO₂ oxidation and sulphate formation where the high reaction rate principally depends on the water content in the ambient air (Cheng et al. 2016; G. Wang et al. 2016).

Ion balance analysis is applied for assessing both the measurement error of water-soluble ions and acidity of secondary inorganic formation in Jinan. According to figure 3.6, the PM_{2.5} in Jinan was close to neutral, which was the same as what was reported by Cheng et al. (2011b). The correlation coefficient R² is 0.939 (P≥0.001) and gradient is 0.995, which show a good degree of ion balance in PM_{2.5}.

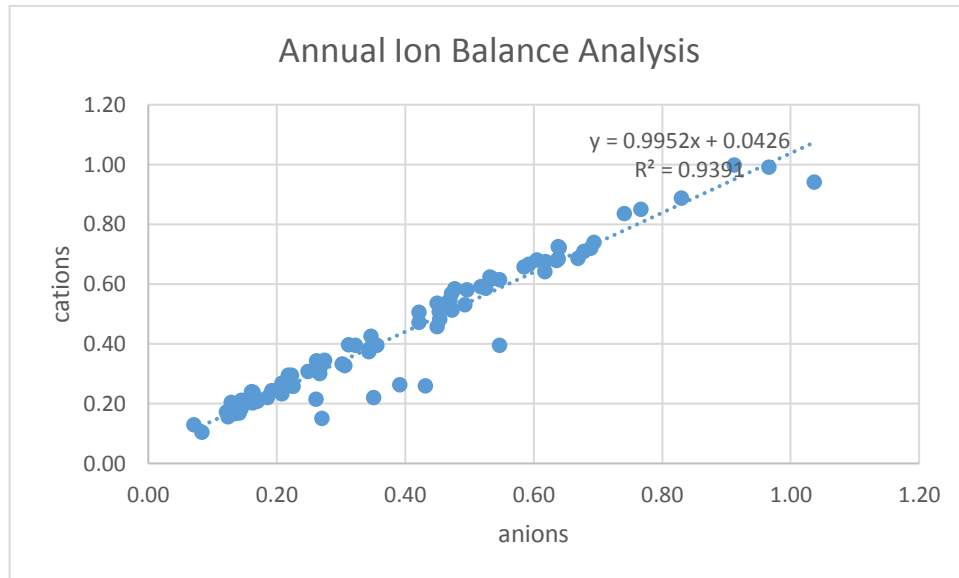


Figure 3-4 Ion Balance analysis of water-soluble ions measured from Jinan’s PM_{2.5} sample

The ion balance analysis also suggests that acids are almost neutralised in Jinan’s ambient air throughout the whole sampling campaign since the gradient of this curve is close to one. It may imply that the acid rain problem has been remitted in the recent years. This could be due to a large amount of ammonium emission in China today. Wang et al. (2016) suggested that there are 22 Tg S y⁻¹, 19 Tg N y⁻¹ and 15 Tg N y⁻¹ of SO₂, NO_x, NH₃, respectively emitted in China every year where a large amount of ammonium coming from the use of nitrogen fertiliser. This ammonium naturalizes the fine PM in the ambient eventually.

3.3.2.3 Trace metal

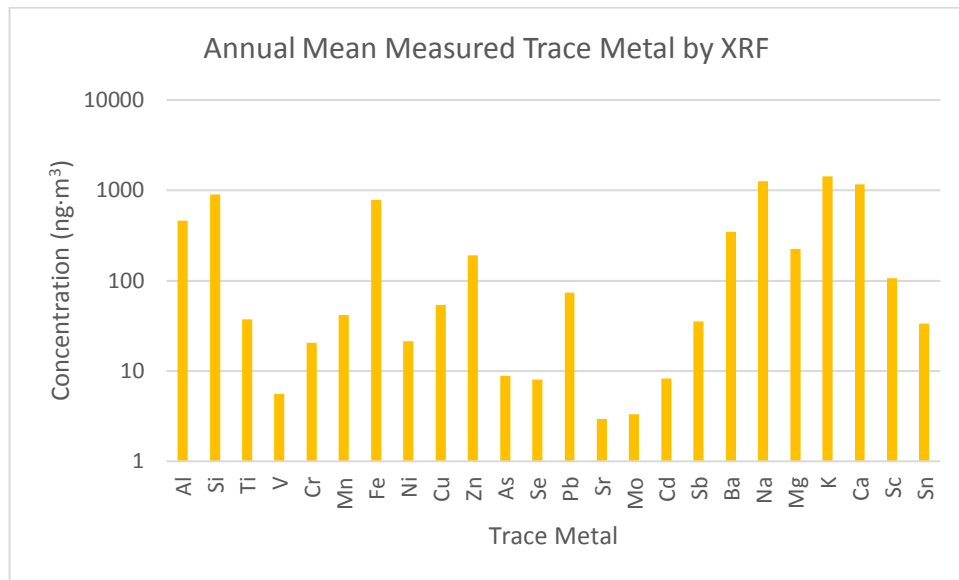


Figure 3-5 annual mean concentration of all measured trace elements in PM_{2.5} in Jinan

Trace metals can be very useful for the receptor modelling as some of them are closely related to anthropogenic emission such as Ni and V, which are normally regarded as the tracer for the heavy oil industry (Viana et al. 2008). 24 trace elements which majority of their daily concentration were greater than the lowest of detection (LoD) are presented in Figure 3-5 annual mean concentration of all measured trace elements in PM_{2.5} in Jinan. Apart from the total sodium, magnesium, potassium and calcium, aluminium, silicon, iron, zinc and barium had a higher absolute value of concentration in the PM_{2.5} compared with rest of other trace metal.

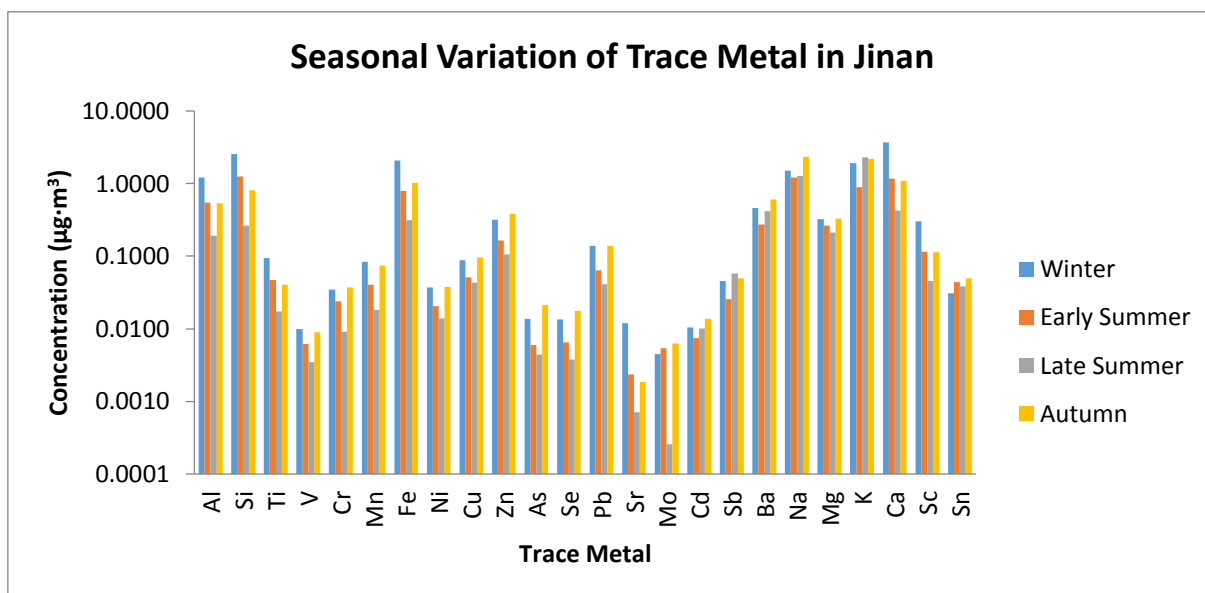


Figure 3-6 Seasonal variations of trace metals in PM_{2.5} in Jinan

Figure 3-6 Seasonal variations of trace metals in PM_{2.5} in Jinan shows the seasonal variation of trace metal in Jinan. A majority of species concentration follows the trends of PM_{2.5} concentration. Major elements including Al, Si, Fe and Ca had the highest concentration in winter rather than early summer, which implies that the sandstorm from Gobi desert may not be the major contribution of mineral dust in Jinan this year in the early summer (Sun et al. 2005). However, fly ash or cement, and other construction-related sources could influence the concentration of these elements (Gu, et al. 2014). In addition, the highest concentration of K appeared in late summer and autumn; this might be due to the biomass burning activity during these two periods (Chen et al. 2016).

Enrichment factor analysis was conducted here to determine the degree of anthropogenic impact on the trace metal (Figure 3.8). The enrichment factor (EF) is defined according to the equation (3.3) below (Wang et al. 2006):

$$EF = (X/Y)_{\text{sample}} / (X/Y)_{\text{crust}} \quad (3.3)$$

Where : X is the trace element of interest, Y is the reference element, and $(X/Y)_{\text{sample}}$ and $(X/Y)_{\text{crust}}$ are the ratios between the concentration of the trace element of interest in the $PM_{2.5}$ and crust, respectively. In this study, Si and Al are used for the reference element in the analysis. If the value of EF of the interest is over 10, it suggests that anthropogenic emissions have a significant impact on it.

Based on the results from figure 3.8, it turns out that Ni, Cu, Zn, Se, Pb, Cd, Sb, Sc and Sn could have been affected by the anthropogenic pollution in the ambient air while rest of elements have fewer influences from the human-made emission as their enrichment factors value are more than 10.

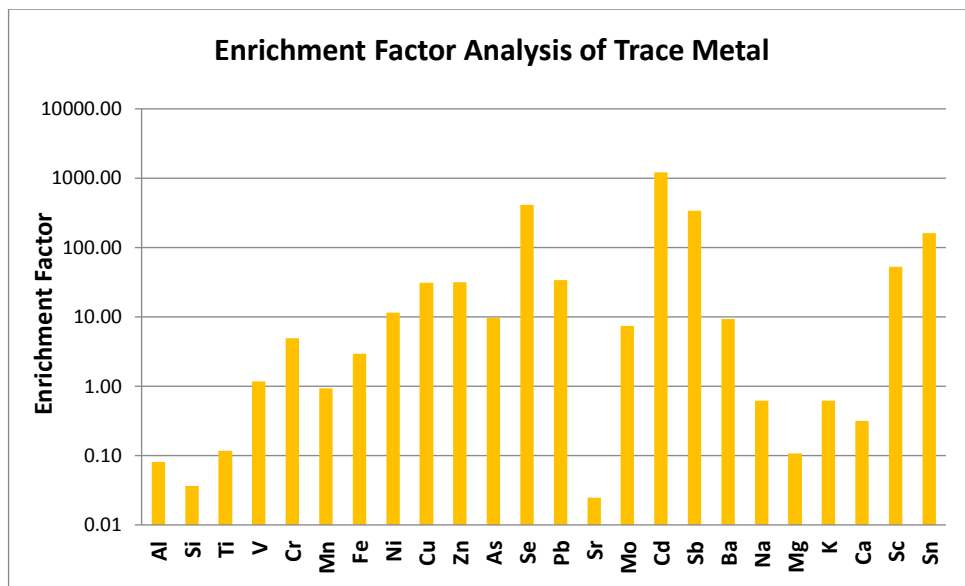


Figure 3-7 Enrichment Factor Analysis

This can be an important clue for the later receptor modelling as these are the potential trace metal that can be used as tracers in the modelling. Based on the previous study, Cu, Zn, Sb and Ba is very likely due to the traffic-related source emissions such as tyre wear (Wählín et al. 2006).

Overall, compared to another two available case study in Jinan reported by Cheng et al. (2011a) and Gu et al. (2014), there is some decline in terms of total PM_{2.5} concentration, OC, EC and water-soluble ions but the trace metal level are still similar to the previous years. Ni might be the sign of oil refinery related industrial emission (Viana et al. 2008). Si, Al, Ca, Mg, Fe and Ti in the coarse mode are also commonly used for identifying mineral dust (Song, Zhang, et al. 2006) while Mn and Cr are also frequently used as tracers for industrial sources (Zhang et al. 2013).

3.3.2.4 Polycyclic Aromatic Hydrocarbons (PAHs)

Generally, PAHs are mostly colourless, white or pale yellow solids with high melting point and environmentally persistent and toxic to human beings, which are associated with incomplete combustion of organic materials, especially the emissions of vehicles, coal combustion and industrial process in the urban ambient air (Yin et al. 2010). PAHs are very important constituents of OC, however, they are much less studied in Jinan. Table 3-3 Mean seasonal total PAHs concentration and its range. presents the mean total PAHs concentration and its range throughout the year.

Similar to a majority of inorganics, OC and EC, PAHs also had a highest mean concentration in winter. Autumn was another season when Jinan experienced a high concentration of PAHs while early summer and summer had the lowest concentration of PAHs.

Table 3-3 Mean seasonal total PAHs concentration and its range.

Season	Winter	Early summer	Late Summer	Autumn
Total PAHs Concentration in ng·m³	162.5	37.9	31.7	90.9
Range (ng·m³)	64.95-556.45	26.47-78.97	26.18-41.34	40.71-207.23

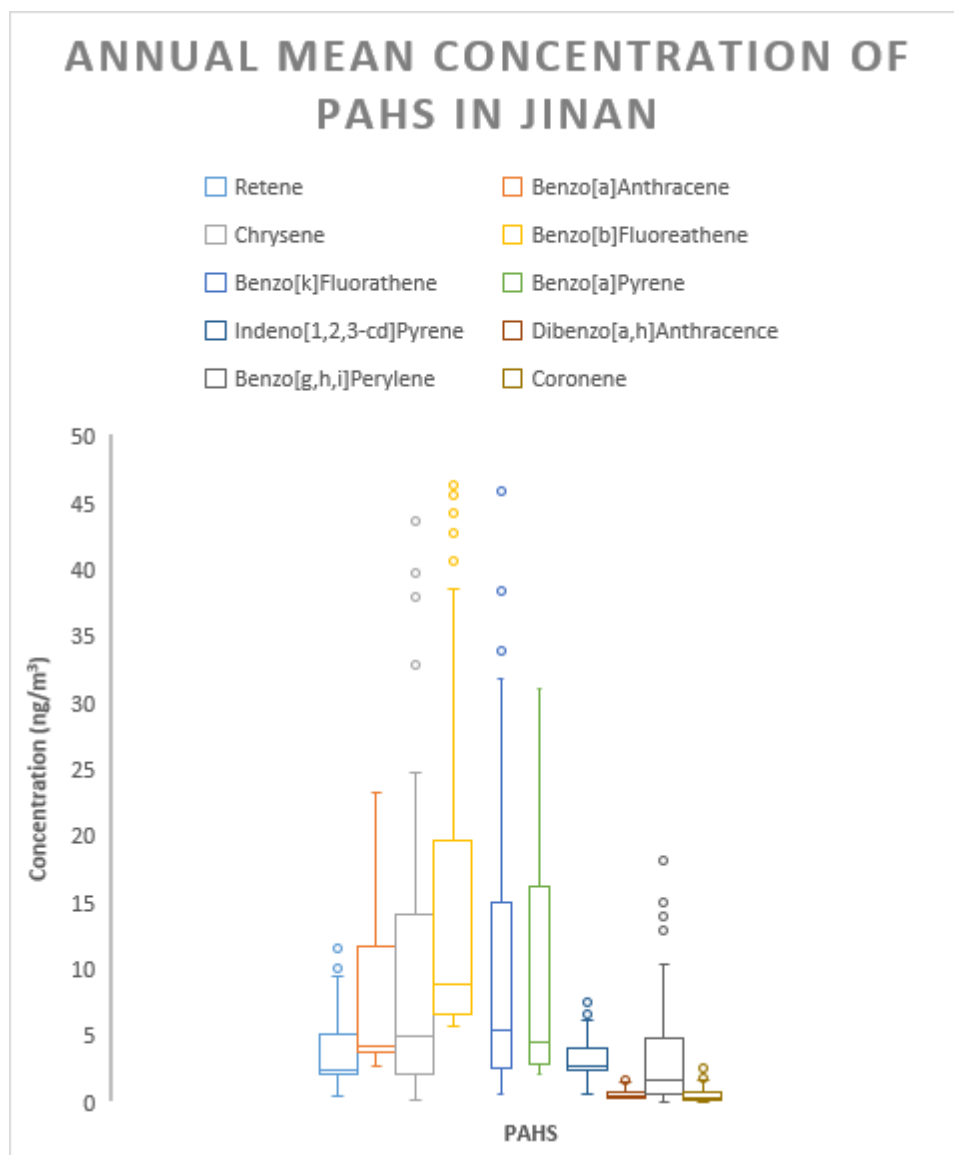


Figure 3-8 annual mean PAHs concentration

Figure 3-8 annual mean PAHs concentration shows the mean mass concentration of PAHs including retene, BaAnt, Chr, BbPyr, BaPyr, Ipyre, DBahAnt, BghiPer and COR. BaAnt, Chr, BbPyr and BaPyr have much higher concentration than other PAHs ($\sim 12 \text{ ng}\cdot\text{m}^{-3}$) while DBahAnt and COR had a lower concentration than a majority of measured PAHs ($\sim 2 \text{ ng}\cdot\text{m}^{-3}$). In comparison, the PAHs concentration is similar to Beijing-Tianjin urban region reported by Wang et al. (2011). However, it is about two to three times higher than Harbin and Guangzhou in North-eastern China and Southern China, respectively (Ma et

al. 2010; Li et al. 2006), which shows Jinan is heavily polluted by PAHs. Figure 3.10 shows the average level of PAHs and their seasonal variations that found in Jinan. One of the important feature of PAHs in the ambient air is that typically the lower molecular weight, the higher vapour pressure and vice versa, though the vapour pressure of PAHs is relatively low in most cases (Abdel-Shafy & Mansour 2015). Therefore, the lower molecular weight PAHs is more likely in gas phase while some higher molecular weight PAHs is more likely in the solid phase in the ambient particulate matter. Therefore, the temperature could result in the seasonal variation of PAHs mass distribution.

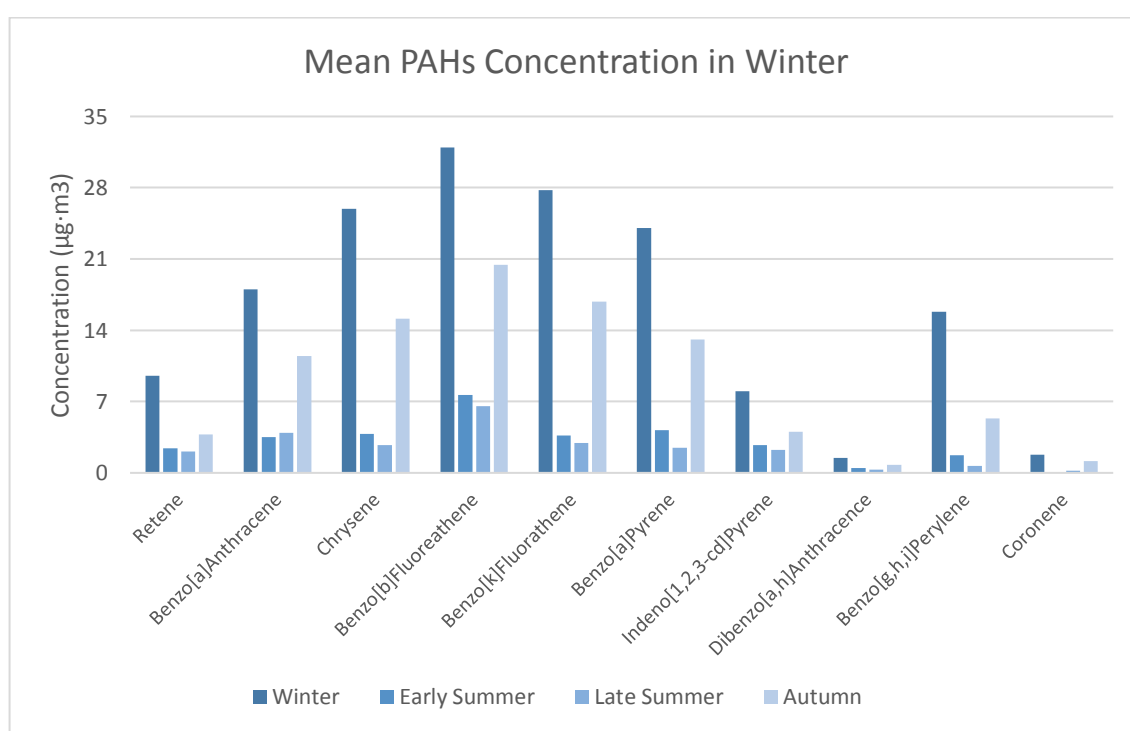


Figure 3-9 seasonal variations of PAHs mass concentration.

High level of BaAnt, Chr, BbPyr, BaPyr, BghiPer implies that both the coal combustion and vehicle exhaust may play an important role in contributing PM_{2.5} level in the ambient air (Hu et al. 2012; Shen et al. 2010). These species could be helpful for apportioning the

oil fuel burning related sources in the PMF or CMB if the profiles which contain PAHs are provided.

3.3.2.5 *n*-Alkanes

Normal alkanes (*n*-alkanes) are another other important organic compounds in the ambient air. They may not only come from both anthropogenic sources such as fossil fuel combustion, biomass burning or cooking but may also from the biogenic emissions such as plant wax (Li et al. 2010). Their mass distribution can suggest the contribution from anthropogenic or biogenic sources based on the different *n*-alkanes mass distribution.

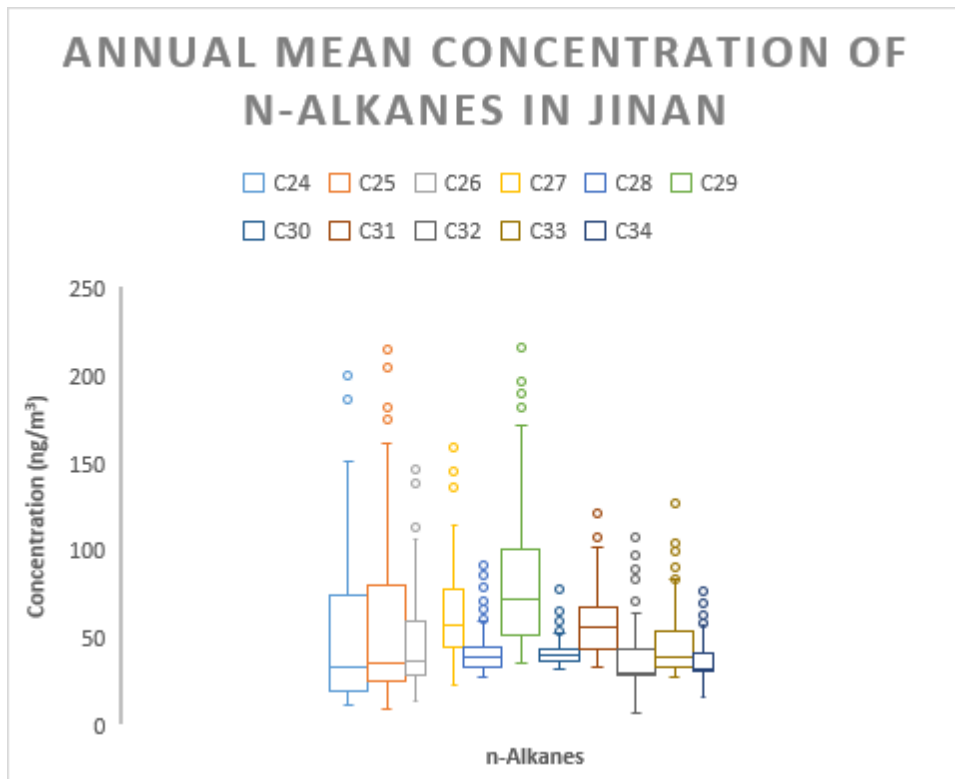


Figure 3-10 Annual Mean *n*-Alkanes concentration in Jinan

Table 3-4 the mean concentration and range of total n-alkanes

Season	Winter	Early summer	Summer	Autumn
Total n-alkane Concentration (C₂₄ to C₃₄) in ng·m³	815.5	544.14	365.2	942.0
Range (ng·m³)	436.7-2240.1	409.6-895.5	294.2-508.0	398.5-1473.5

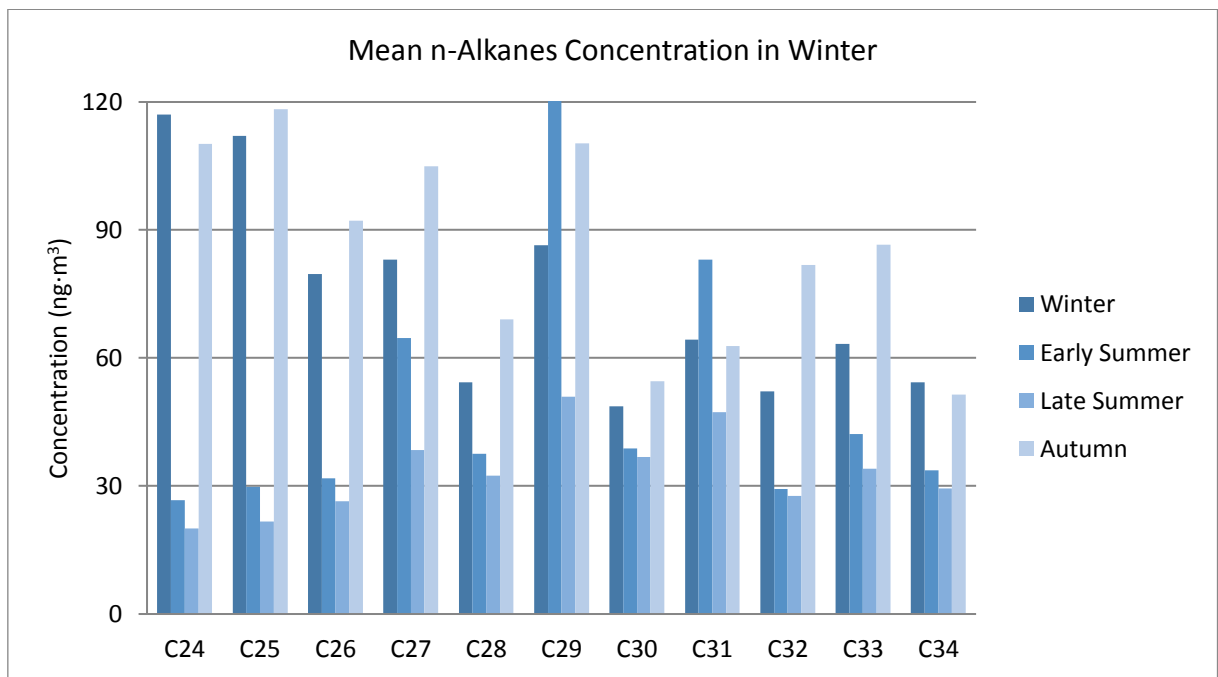


Figure 3-11 seasonal variations of n-alkenes in Jinan.

Figure 3-11 seasonal variations of n-alkenes in Jinan. and Figure 3-10 Annual Mean n-Alkanes concentration in Jinan shows the total periods mean n-alkanes mass concentration and mass concentration distribution in different periods from C₂₄ to C₃₄ while Table 3-4 the mean concentration and range of total n-alkanes presents the mean concentration, the

range of total n-alkane and mass concentration distribution of each n-alkanes. Again, the results show that both winter and autumn were the most polluted period while early summer is much less polluted and summer had the lowest n-alkanes concentration overall. In addition, the peak concentration of n-alkanes appeared at carbon number C₂₄ or C₂₅ in winter and autumn, where the lower molecular weight n-alkanes (C₂₄ to C₂₈) had higher mass concentration than the rest of n-alkanes. On the contrary, during the early summer and late summer, the mass concentration distribution shows a unimodal distribution where the peak appeared at C₂₉. Similar to PAHs, the temperature at different seasons could be the major cause of the seasonal variation since n-Alkanes were also temperature dependent due to its semi-volatile property (W. Li et al. 2010). Furthermore, the coal combustion in winter and autumn could be another cause as the fossil fuel combustion was related with n-alkanes with carbon number predominance C_{max} at C₂₂-C₂₅ (Rogge et al. 1993). While the peak at C₂₉ in early summer and late summer was very likely due to the plant wax release into the atmosphere as it consists mainly high molecular weight compounds including odd-even carbon number of C_{max} at between C₂₇ and C₃₁ (Simoneit 1999; Li et al. 2010).

Carbon preference index (CPI), which is the ratio of odd to even carbon number n-alkanes, has been used for evaluating the contribution of anthropogenic and biogenic sources (Simoneit 1999). Odd number n-alkanes are normally found in fossil fuels while even carbon number n-alkanes are found in the plants. If the CPI value is close to unity, it suggests that anthropogenic emission is the major sources; when CPI over 2.0, it indicates a major influence from biogenic sources (Li et al. 2010). The CPI of n-alkanes is 1.16, 2.11, 1.25 and 1.38 in winter, early summer, late summer and autumn in Jinan, which suggests

a strong impact on n-alkanes from anthropogenic sources except for early summer while plan wax also played an important role.

3.3.2.5 Hopanes

Hopanes are triterpenoid hydrocarbons that are primarily derived from bacteria as bacteriohopanols and also can be anthropogenic, i.e., from fossil fuel combustion. They are abundant in coal, crude oil and lubricant oil and vehicle exhaust (Wang et al. 2009; Yin et al. 2010). Therefore, they are widely used as organic molecular markers for coal combustion and traffic emissions (Fu et al. 2008). In this study, the following hopanes including: $17\alpha(\text{H})$ -22,29,30-Trisnorhopane ($\text{C}_{27\alpha}$), $17\alpha,21\beta(\text{H})$ -30-norhopane ($\text{C}_{29\alpha\beta}$), $17\alpha(\text{H}),21\beta(\text{H})$ -Hopane ($\text{C}_{30\alpha\beta}$), 22S- $17\alpha(\text{H}),21\beta(\text{H})$ -30-Homohopane($\text{C}_{31\alpha\beta\text{S}}$) and 22R- $17\alpha(\text{H}),21\beta(\text{H})$ -30-Bishomohopane ($\text{C}_{31\alpha\beta\text{R}}$) have been analysed.

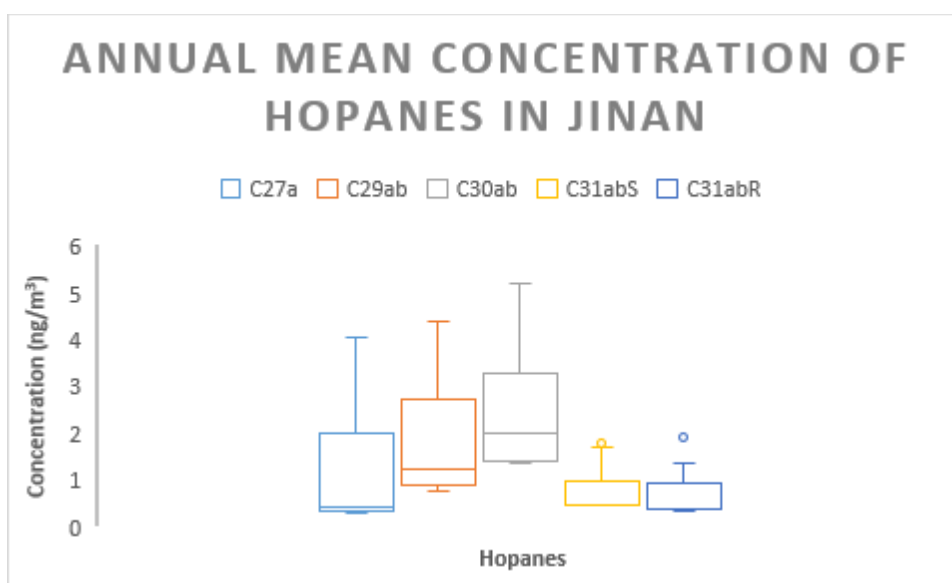


Figure 3-12 Annual median hopanes concentration in Jinan

The mean total hopanes mass concentration and their ranges in the four seasons are shown in Figure 3-12 and Table 3-5. The seasonal concentration is shown in Figure 3-13. Winter

and autumn experienced much higher concentration of hopanes than early summer and late summer. This is similar to the other case study of hopanes measurement in other places in China (Wang et al. 2006).

Table 3-5 the seasonal mean mass concentration of total hopanes and their ranges at each season

Seasons	Mean Total Hopanes (ng·m ³)	Range (ng·m ³)
Winter	11.84	8.39-18.46
Early summer	4.32	4.15-4.69
Late summer	3.47	3.37-3.58
Autumn	10.99	9.84-13.15

In terms of concentration, the values are at the same order of magnitude with other studies in Beijing, Tianjin and Changchun (Wang et al. 2006). Among the five hopane species in this study, the three most abundant compounds were C_{27α}, C_{29αβ} and C_{30αβ}, which are closely related to coal combustion and vehicle exhaust. C_{29αβ} is considered as the dominant hopane compound from coal combustion emission in China, C_{30αβ} is more likely to be from vehicle exhausts; similarly, C_{27α} is also more likely to be from coal combustion rather than vehicle emissions (Zhang et al. 2008). The ratios of C_{29αβ} to C_{30αβ} in four seasons (winter to autumn) are 0.83, 0.60, 0.59 and 0.74, respectively. The higher ratio implies the impact from coal combustion while the lower ratio reflects the influence from vehicles (Zhang et al. 2008). The relative abundance of C_{27α} also increased during the winter and autumn which was in accordance with the heating period when the coal combustion could be enormous.

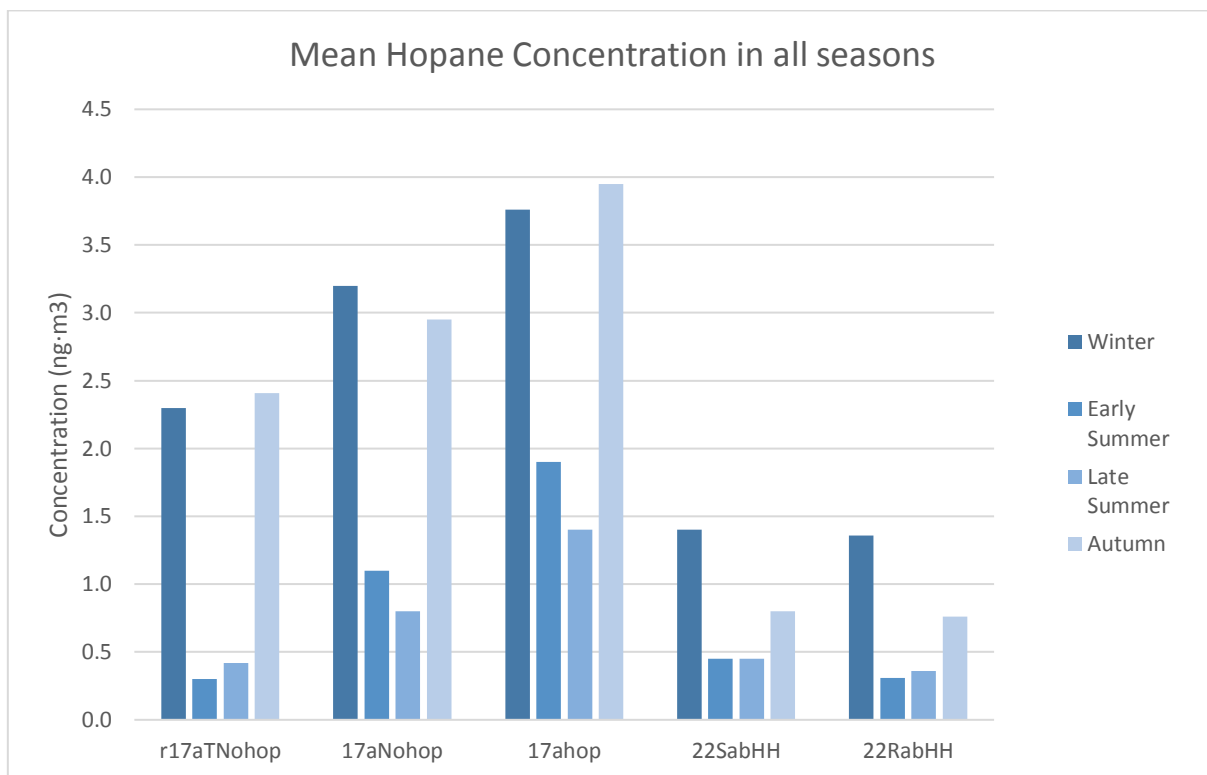


Figure 3-13 Seasonal variations of hopanes in Jinan

3.3.2.6 Levoglucosan and Cholesterol

Two sterols were analysed in this study, namely levoglucosan and cholesterol. Levoglucosan is normally considered as a tracer for biomass burning sources since it is emitted at very high concentration during cellulose combustion (Simoneit et al. 1999; Simoneit 1999; Lin et al. 2010), which is widely used in China (Liu et al. 2013; Cheng et al. 2013; Chemistry et al. 2013). While cholesterol exists in all the body tissues in higher animals by biosynthesis and it is an important emission during the meat cooking, which is therefore used as the tracer for cooking (He et al. 2004). Table 3-6 shows the mean concentration and its seasonal variations of these two sterols.

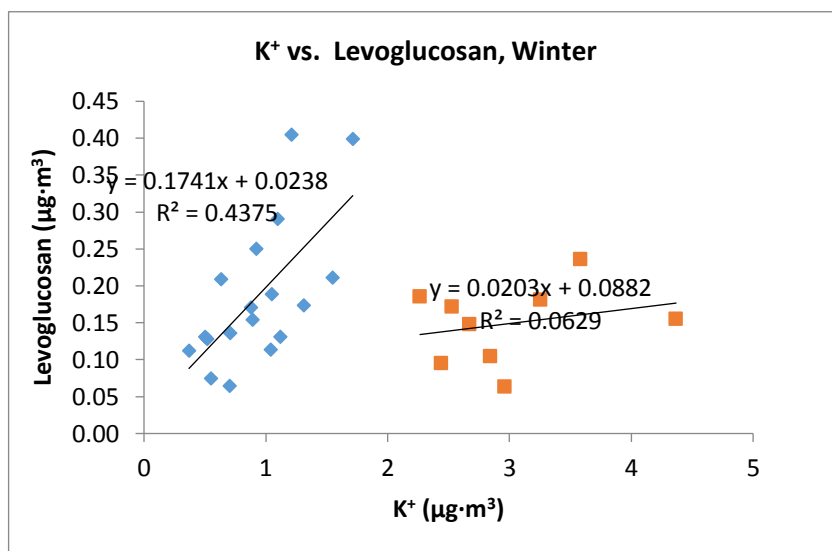
Table 3-6 Summary of levoglucosan and cholesterol measurement in PM2.5, Jinan

Seasons	Levoglucosan mean concentration (ng·m³)	Concentration range of Levoglucosan (ng·m³)	Cholesterol mean concentration (ng·m³)	Concentration range of Cholesterol (ng·m³)
Winter	233.0	62.9-1595	2.3	0.5-10.4
Early summer	33.7	13.5-113.7	0.4	0.2-2.2
Late Summer	27.6	26.4-30.5	0.3	0.0-0.8
Autumn	158.3	29.0-339.8	0.3	0.1-0.6

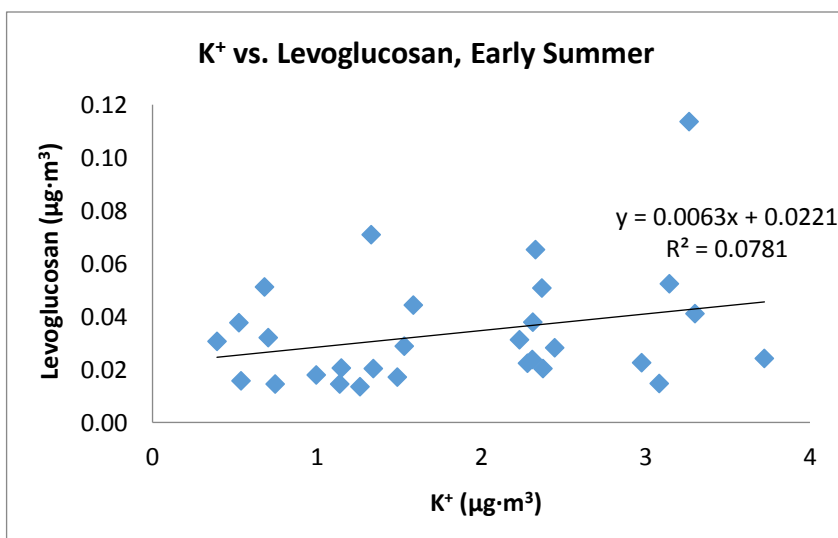
Both levoglucosan and cholesterol peaked in the winter reaching 1595 ng·m³ and 10.4 ng·m³, respectively. Autumn was also another period with high levoglucosan concentration, but the cholesterol remained at low level. This could be due to the biomass burning in autumn when there would be corn residuals burning during October in northern China (Chen et al., 2016). Levoglucosan concentration in this study is much higher than that reported in Beijing and Shanghai in terms of annual mean concentration reported by Jiang et al. (2009) and at the background site in East China by Liu et al. (2013). However, it is similar to the level in Beijing year season by Cheng et al. 2013) but much lower than the study by (Zhang et al. 2008) annually. This is likely due to the special distribution of levoglucosan is varied from site to site and time to time (Hedberg et al. 2006).

As water-soluble potassium is also usually used as an inorganic tracer for biomass burning which is usually used in PMF, the correlations between levoglucosan and potassium in the four seasons are analysed below.

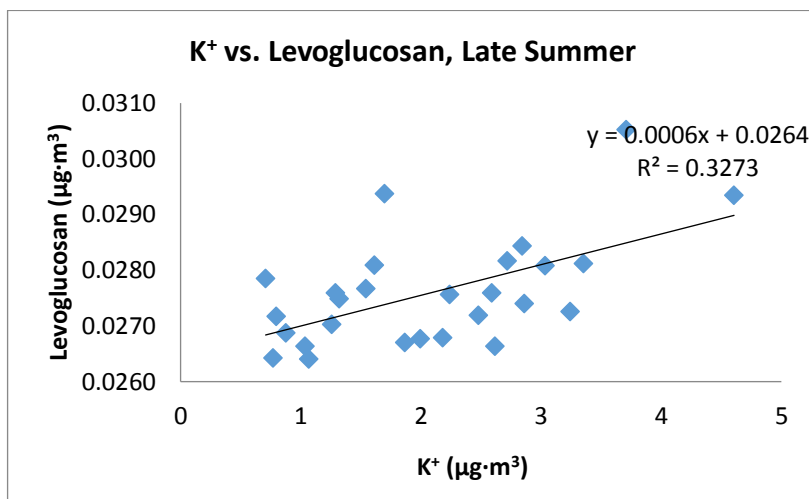
a)



b)



c)



d)

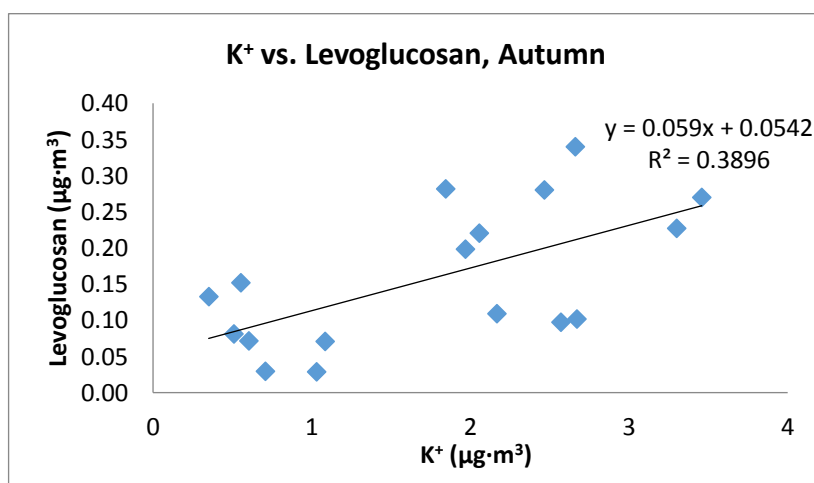
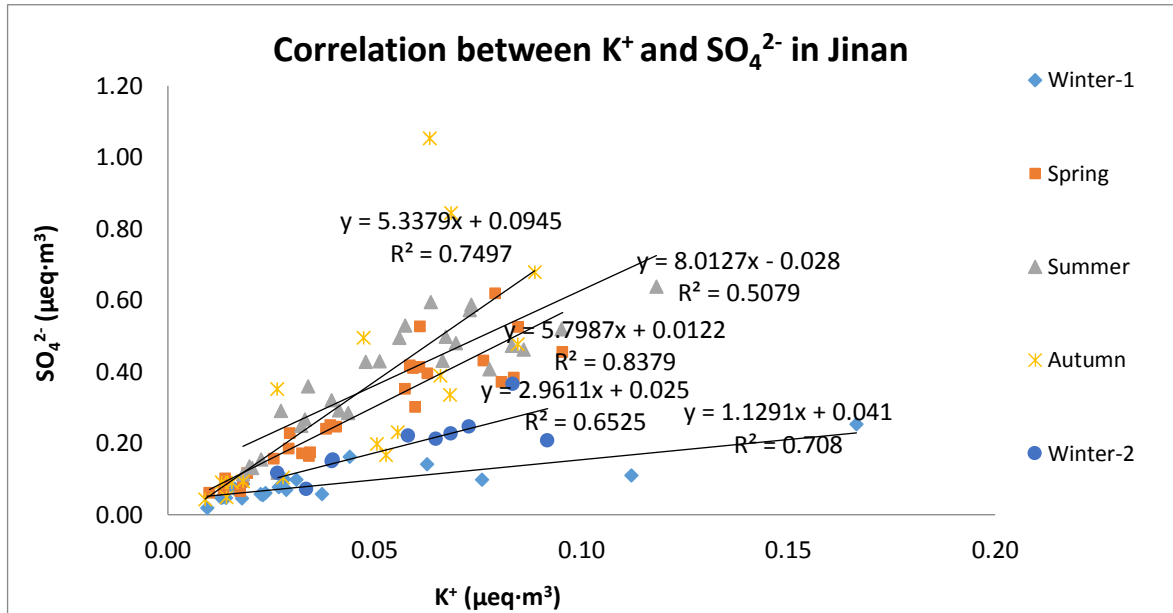


Figure 3-14 the correlations between K⁺ and levoglucosan in the four seasons

Summer and autumn have shown some degree of correlation between water-soluble potassium and levoglucosan. However, the source of K⁺ in winter seems more complex, one of the cause could be from crustal materials (Cheng et al. 2013). Alternatively, K⁺ may also have got involved in secondary aerosol formation. On the other hand, there was no strong correlation in early summer. It may be because the biomass was not that active in May during P3. Overall, winter and autumn experienced the greater correlation between K⁺ and levoglucosan while summer and early summer experienced lower correlation. This trend

is similar to the study of Beijing's biomass burning reported by Cheng et al. (2013). In order to further investigate the poor correlation between K^+ and levoglucosan, the following correlations have been also performed.

a)



b)

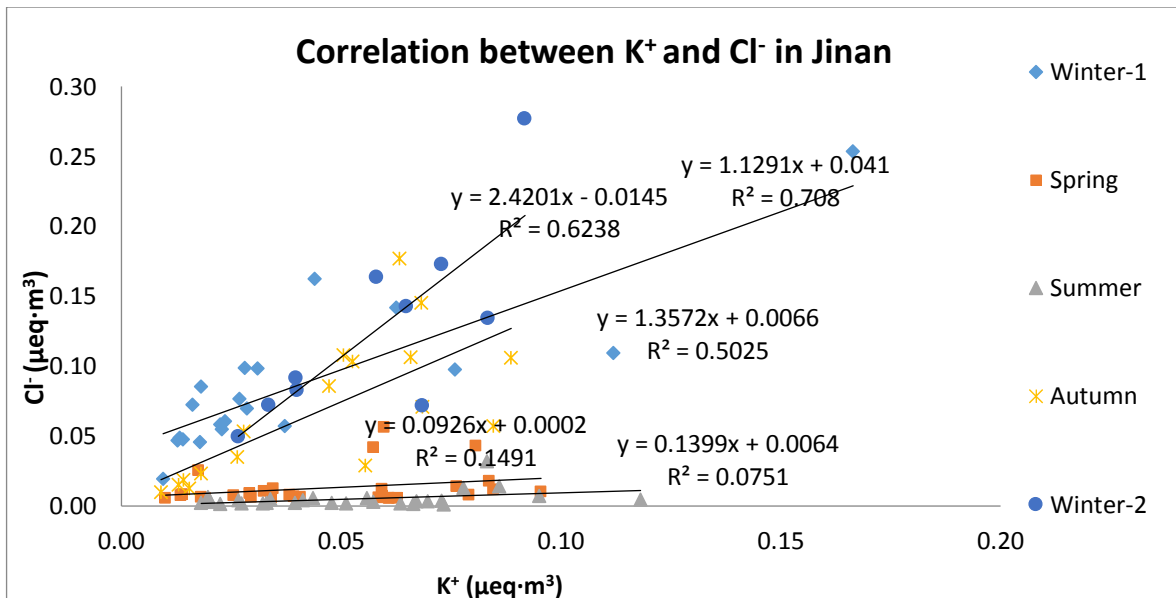


Figure 3-15 a) the correlation of K^+ and SO_4^{2-} during the five sampling period; b) the correlation of K^+ and Cl^- during the five sampling period

Figure 3-15 shows the correlation between K^+ and SO_4^{2-} or Cl^- during the five different sampling periods. Reasonable correlations between K^+ and SO_4^{2-} have shown in all five sampling period across the year. On the contrary, there is almost no correlation between K^+ and Cl^- in summer. This is very likely due to the temperature-induced volatilization during the early summer and summer sampling period as the temperature was up to 35 °C. Therefore K^+ could be in the form of either KCl or K_2SO_4 in Jinan as well as other salts such as KNO_3 . However, KCl would be largely decomposed during hot weather but K_2SO_4 remained relatively stable. In addition, the heterogeneous reactions between K^+ and H_2SO_4 , HCl and HNO_3 may both happen during the emission of coal combustion and biomass burning. Therefore, the K^+ emission from the biomass burning might have become K_2SO_4 while arriving the receptor, which has been suggested by a related study in China (Li et al. 2016).

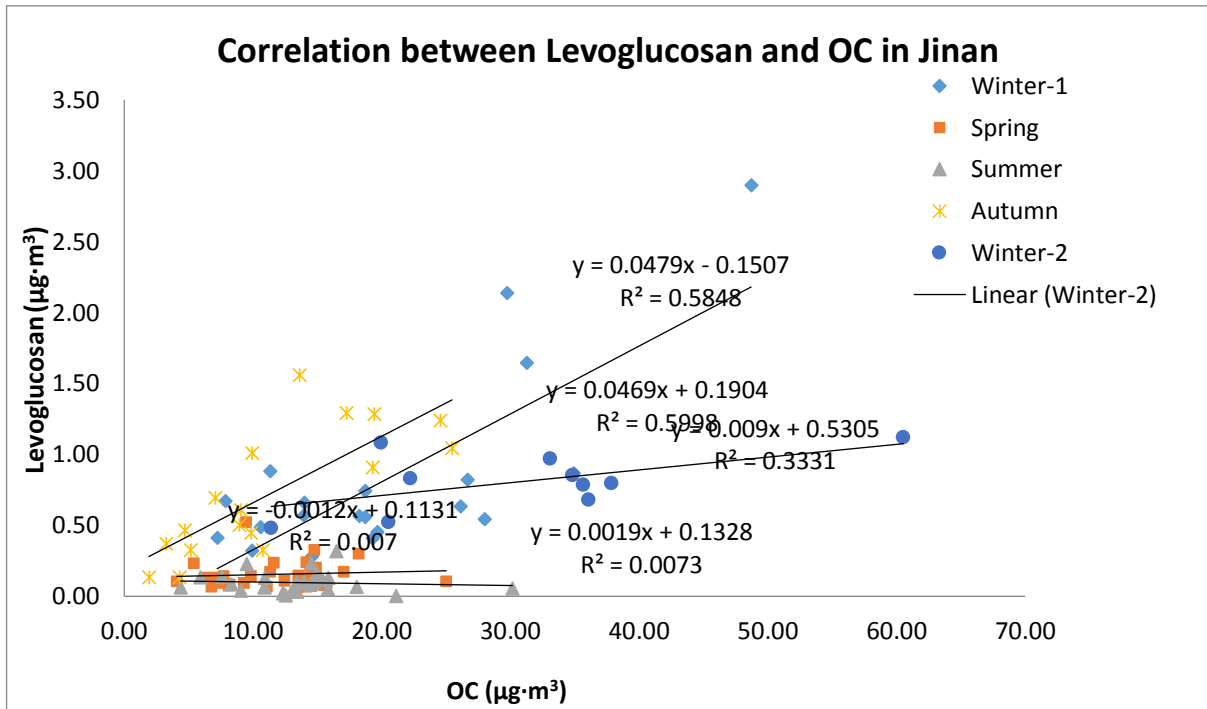


Figure 3-16 the correlation of levoglucosan and OC during the five sampling period.

On the other hand, since levoglucosan has been widely reorganized and used as the organic molecular marker for biomass burning. If the K^+ comes from the biomass burning, it may have a relatively high degree of correlation with levoglucosan (Urban et al. 2012). Both linear and exponential fit could be found during the biomass burning episode (Urban et al. 2012; Cheng et al. 2013) and this has been evaluated in chapter three. Again, according to Figure 3-16, levoglucosan and OC have significant correlation in the first wintery sampling period and autumn sampling period and there is a high correlation between levoglucosan and K^+ in P1 too. These imply that some K^+ may come from the biomass burning indeed. There have been some studies shown that the levoglucosan to K^+ could increase during the prevailing biomass burning period (Schkolnik et al. 2005; Caseiro et al. 2009).

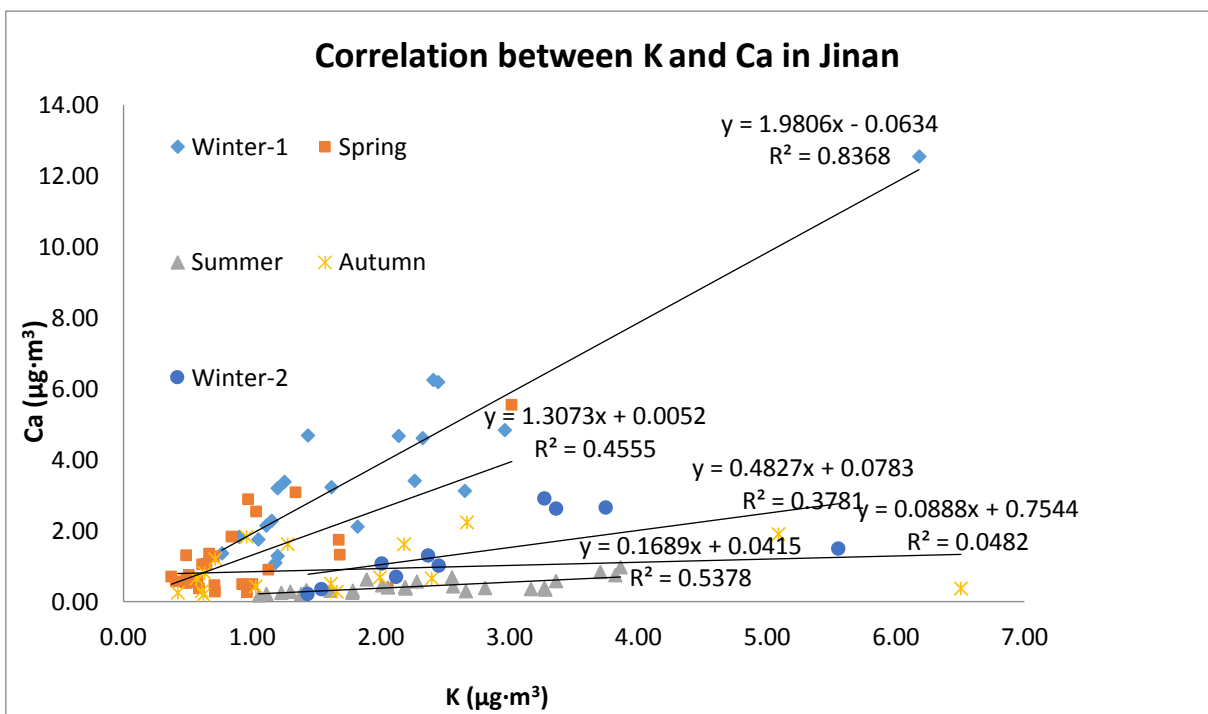
Table 3-7 Levoglucosan to K⁺ concentration ratio during all the sampling periods

Sampling Period	Winter-1	Early summer	Summer	Autumn	Winter-2
Levo/K ⁺	0.54	0.08	0.32	0.38	0.35

But it is also worth addressing that both levoglucosan and cholesterol can be released from the cooking in China and both species have high loading together by the same factor in the PMF modelling (Zhao et al. 2015). Therefore, the influence from other sources to levoglucosan should also be concerned in the source identification judgement.

Finally, some K⁺ may also come from the soil rather than entirely from biomass burning. The Figure 3-17 below assesses whether the K⁺ may come from the soil dust.

a)



b)

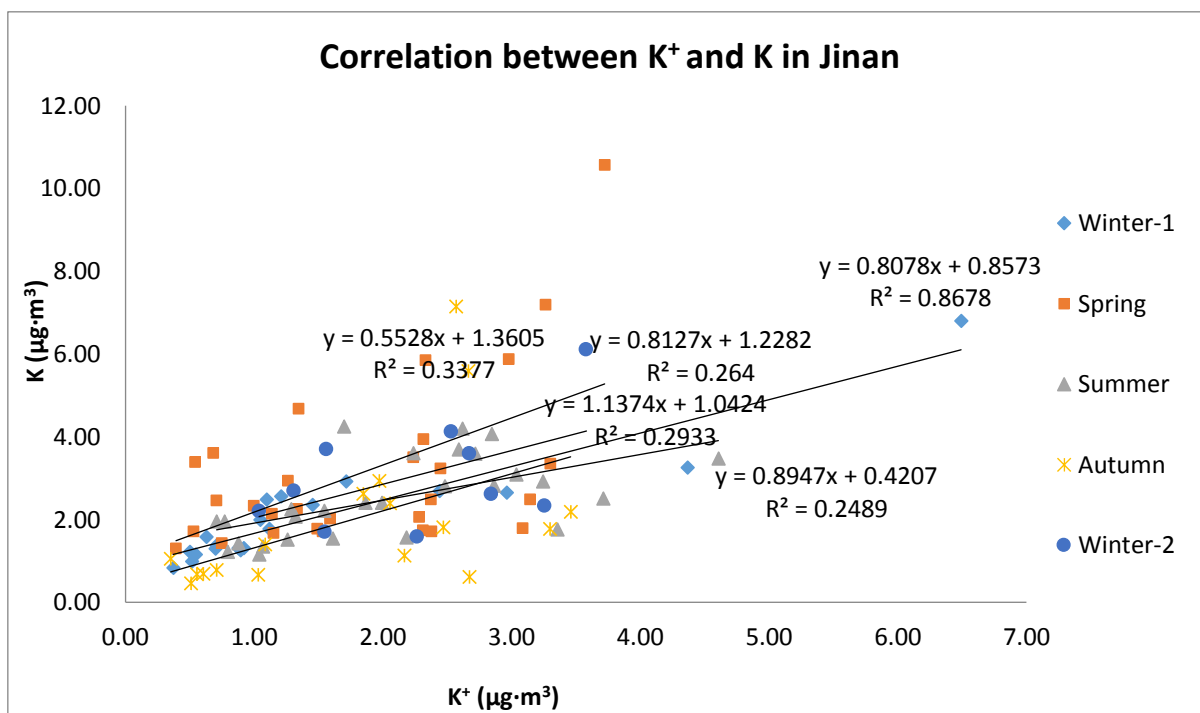


Figure 3-17 a) the correlation of K^+ and levoglucosan during the five sampling period; b) the correlation of levoglucosan and OC during the five sampling period.

Ca is normally from soil and other mineral dust. Therefore, high correlations between Ca and K may suggest that K could come from soil. The correlations between Ca and K have been conducted. According to Figure 3-17, the total potassium (K) has significant correlations with Ca during early summer and summer. Meanwhile, K and K^+ have some moderate correlations throughout the year too. Hence, the K^+ during the early summer and summer could be more due to the soil dust contribution. However, it should be noticed that K also have strong correlation with Ca during the winter. This suggests that the source of K^+ during the winter may both comes from biomass burning and soil dust.

On the other hand, Cl^- to NO_3^- ratio is helpful to determine whether Cl^- comes from coal combustion or not. Similar to $[NO_3^-]/[SO_4^{2-}]$, $[Cl^-] / [NO_3^-]$ can be helpful to indicate or tell the increment of Cl^- may come from stationary sources such as coal combustion power plant with respect to relatively stable mobile sources emission throughout the year (Yao et

al. 2002). Table 3.7 shows the $[Cl^-] / [NO_3^-]$ during the five sampling periods while both winter sampling periods have the highest ratio. It seems that coal combustion could be an important source of Cl^- in Jinan.

Table 3-7 Cl^- to NO_3^- concentration ratio during all the sampling periods

Sampling Period	Winter-1	Early Summer	Late Summer	Autumn	Winter-2
$[Cl^-] / [NO_3^-]$	0.32	0.12	0.03	0.17	0.32

To sum up, the Cl^- signal appearing in the biomass burning factor could be also influenced from coal burning. Meanwhile, K^+ in the secondary sulphate factor may come from the primary emission of both biomass burning and soil dust during different time of year. There is evidence showing that the biomass burning contributed the $PM_{2.5}$ pollution in Jinan is likely due to the long-range transport from nearby region. There is also sign that levoglucosan may also come from cooking emission too in Jinan but further work required to clarify this deduction.

3.4.3 Meteorological Data

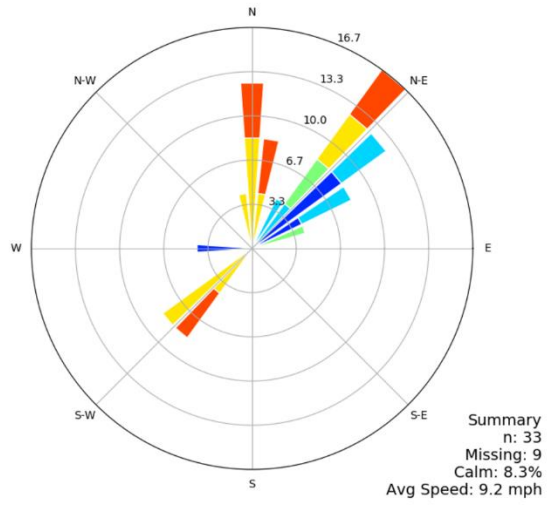
During the sampling campaign, wind speed, wind direction, temperature, RH and a.t.m. pressure were also recorded simultaneously by the simple weather station. Unfortunately, the thermometer and barometer sensors were not working properly during the sampling periods, only the mean values of ws , wd and RH are summarised below in Table 3.8.

Table 3-8 Summary of Wind Speed, Wind direction and RH during the sampling period in Jinan

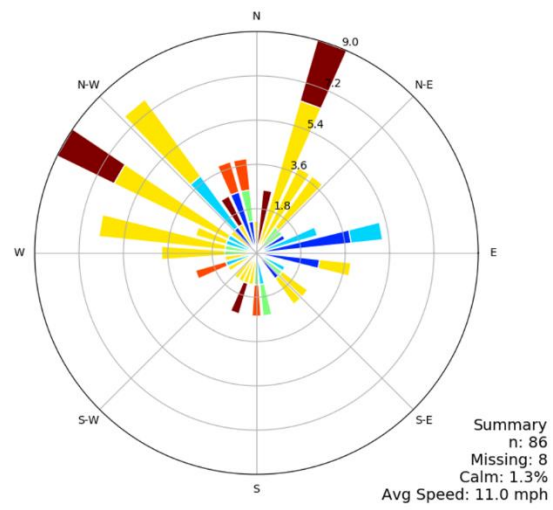
Seasons	Wind Speed (m/s)	Prevailing Wind Direction	RH (%)
Winter (P1&P5)	4.1	NE	48.5
Early summer (P2)	4.9	N	54.4
Summer (P3)	4.6	SW	73.0
Autumn (P4)	1.8	NE	66.8

The meteorological condition based on Table 3-8 Summary of Wind Speed, Wind direction and RH during the sampling period in Jinan shows that the wind condition in Jinan was calm throughout the year which contributes to PM_{2.5} accumulation in the ambient air. It was also generally dry in Jinan except for the summer period. Autumn was also relatively mild and steady. Moreover, Figure 3-15 Wind rose analyses on wind speed and direction in Jinan a) winter; b) early summer; c) late summer; d) autumn shows the wind rose analysis by Iowa State University (iastate, 2018).

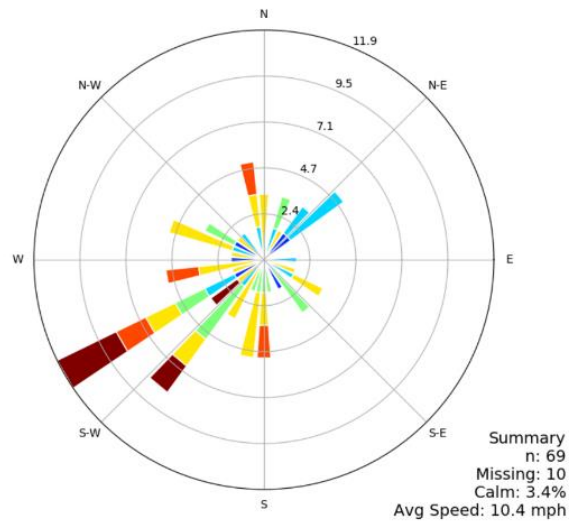
a)



b)



c)



d)

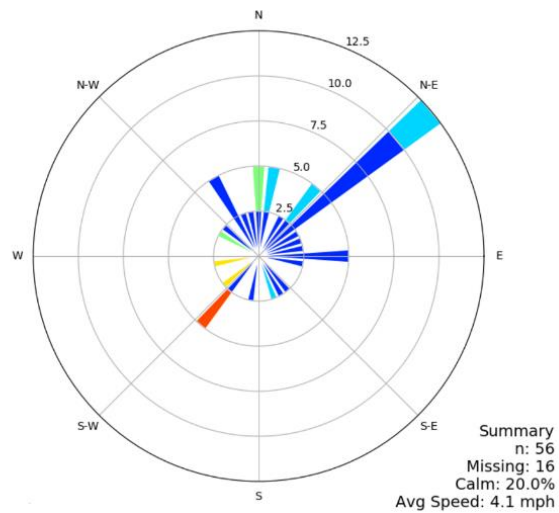


Figure 3-15 Wind rose analyses on wind speed and direction in Jinan a) winter; b) early summer; c) late summer; d) autumn

It turns out that the prevailing wind in Jinan mainly coming from three directions, namely NE and SW or from north in May and June. The wind from NE may bring the pollutants from the industrial zone at the suburban area of Jinan while the SW and northerly wind

may get involved in the regional transport of pollutants from the Southern Shandong Province, Henan, Anhui and Jiangsu Province or Hebei Province.

3.4.3 Mass Closure Analysis

Mass closure (or mass reconstruction) is a useful measure for understanding the temporal and spatial variations of the chemical composition of $PM_{2.5}$, which is very helpful for the source apportionment judgement and also validating the consistencies and addressing uncertainties of mass and chemical measurements by the laboratory analysis (Chow et al. 2015). The reconstructed $PM_{2.5}$ is the sum of mass consisting of the following seven representative chemical compounds, namely 1) inorganic ions; 2) organic matter (OM); 3) elemental carbon (EC); 4) geological minerals; 5) sea salt; 6) trace elements and 7) other (Chow et al. 2015). In details, inorganic ions is calculated as the sum of sulphate, nitrate and ammonium; $OM = 1.4 \times OC$; geological minerals = $1.89Al + 2.14Si + 1.4Ca + 1.43Fe$; trace elements is the sum of all the measured trace metal elements excluding S, Al, Si, Ca, and Fe plus Na^+ and Mg^{2+} (Solomon et al. 1989). Hence, the mass closure of $PM_{2.5}$ in Jinan is reconstructed by this means. The results are shown below.

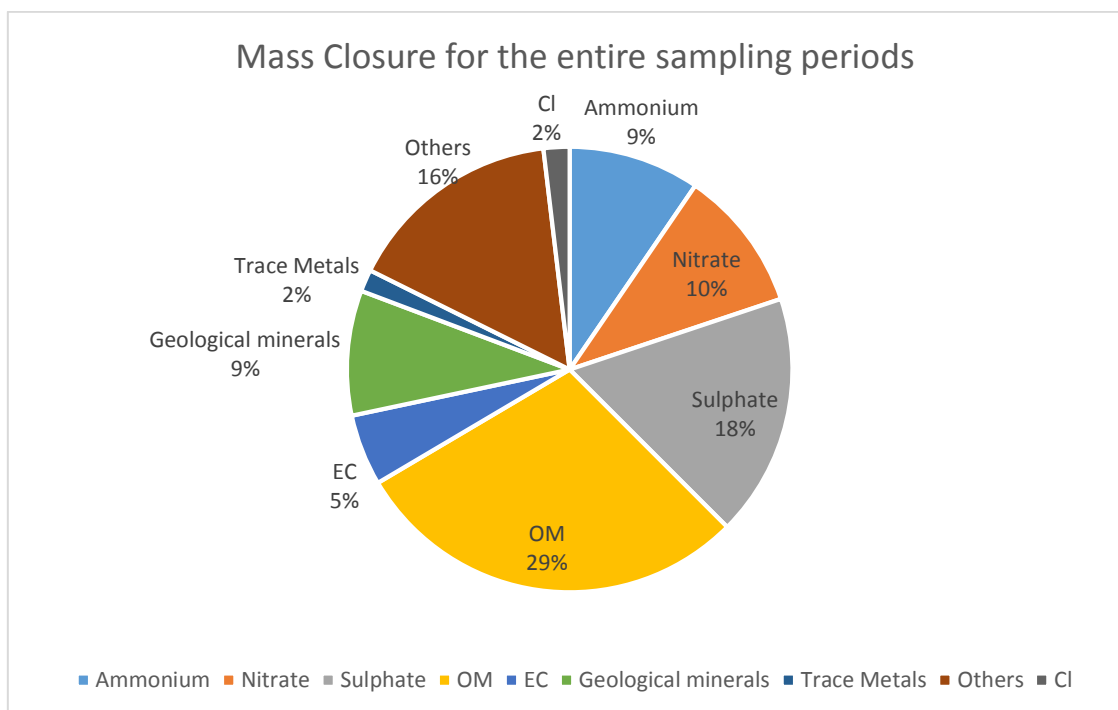


Figure 3-16 PM_{2.5} mass closure in Jinan

According to figure 3.16, the nine categories of chemical species explain about 84% of total mass of PM_{2.5}. OM, secondary inorganic aerosols, geological materials and EC contributes the majority of PM_{2.5} in the city. Compared to the previous study of Jinan in 2007, there is a decline in sulphate. This could be due to the decrease of primary sulphate emissions (Chan, 2008).but the contribution from OM is increased substantially from 13% in 2007 to 29% in 2015 (Gu, et al. 2014). Furthermore, 16% of total PM_{2.5} mass has not yet interpreted. This could be due to unmeasured aerosol water and other species (Chow et al. 2015).The results of mass closure analysis will be helpful in the further receptor modelling data analysis and assessment.

3.6 Conclusion

The data of physical and chemical characterisation of PM_{2.5} has presented above. The meteorological data is also presented. OC, EC, water-soluble ions, trace elements and

some important organic molecular markers have been quantified. According to the chemical quantification and mass closure analysis, the $PM_{2.5}$ concentration in Jinan has declined in the last decade including some major chemical components including SIA. However, OM has become another new major pollutant in the $PM_{2.5}$ and the annual mean concentration of $PM_{2.5}$ remained high and is much greater than the WHO guideline. Also, both inorganic and organic compounds quantification, including emission factor analysis etc. have suggested there is still a significant impact from coal burning and mobile sources to $PM_{2.5}$ in this city. Jinan is still suffered by the severe air pollution in the recent year. The data will be used in receptor models for further analysis.

4 Chapter Four Positive Matrix Factorisation Modelling Of PM_{2.5} Samples in Jinan

Abstract

A couple of source identification studies have been conducted in Jinan by using various means including back trajectory, Principle Component Analysis (PCA) and receptor models including PMF and CMB. However, none of them applied organic molecular markers while apportioning the sources of the PM_{2.5} in Jinan. This chapter discusses the modelling process and results by PMF on the PM_{2.5} sample collected in Jinan by using molecular organic markers. Six factors (sources) were resolved from the models, including secondary sulphate (32 %), secondary nitrate (9 %), coal burning (10 %), biomass burning (20%), vehicle exhaust (16 %) and mineral dust (10 %) and other sources (3%). The rotational ambiguity due to the fact that there is no unique solution in PMF model and uncertainty have also been assessed. There is no significant rotational and excessive error found in the model run. Secondary sulphate and biomass burning may be overestimated by the model compared to the results estimated by alternative empirical equation.

4.1 Introduction

Jinan is heavily polluted city due to its urbanisation and industrialisation in the last a couple of decades and the coal burning and steel and cement production may play an important role to the air pollution in Jinan (Yang et al. 2012). Jinan is surrounded by the mountains in the east, west and south side. Due to its semi-enclosed topography and stable air mass in winter, the pollution level of PM_{2.5} could be very high and it has been one of the most polluted cities in the world (Yang et al. 2012). However, it has been less addressed

in terms of air pollution study compared to other cities such as Beijing. Fortunately, some efforts have been made on discussing the pollutants formation and their variation. Gao et al. (2011) conducted an intensive semi-continuous measurement of water-soluble ions by ambient ion monitor. It was found that there was more local extensive secondary sulphate and nitrate formation in summer than other seasons. While Xu et al. (2011) discussed the size distribution of aerosol in Jinan and compared the difference between urban area of Jinan and rural areas, they suggested that Jinan has high number concentration of accumulation-mode parties with the diameter between 100 to 500 nm but relatively lower number concentration of ultrafine parties (10 to 100 nm) and inactive new particle formation was observed in Jinan. This is probably due to the high existing particles which inhibit the new nanoparticle formation (Xu et al. 2011). In addition, there is also a high correlation between the surface concentration and NO_x in all seasons, which implies the importance of traffic to the pre-existing particles in Jinan. On the other hand, other efforts have also been made to find out the sources of PM in Jinan. Bi et al. (2007) sampled the PM_{10} in Jinan and five other northern Chinese cities and established the local source profiles including re-suspended dust, soil dust, coal combustion fly ash and vehicle exhaust. Bi et al. (2007) also firstly applied the CMB based on the local source profile to quantify the contribution of sources in Jinan. While Yang et al. (2013) firstly apportioned the $\text{PM}_{2.5}$ by PMF and other approaches have also been employed including PCA, CPF and PSCF (Gu et al. 2014; Gao et al. 2011). The findings from all of these studies pointed out that coal combustion, SIA, mineral dust and vehicles are the major emission sources in Jinan. Other sources including cement production, biomass burning, industrial sources have also been apportioned (Yang et al. 2013; Bi et al. 2007; Gu et al. 2014). However, there are some disagreements on the source categories from the modelling results and uncertainties

remain. In addition, it is lack of inter-comparison between different receptor models in the previous studies and organic molecular markers are advised to input into the models to possibly achieve more robust results. In this project, two different receptor models, PMF and CMB were used and organic molecular markers have been applied. This chapter will mainly focus on the PMF model run and its results.

4.2 Models Parameters Setting

For PMF models, two datasets input is essential for the modelling, which are the chemical species concentration data and the corresponding concentration uncertainty data. Two datasets were organised by MS Excel 2010 in daily format and saved as .xlsx file. The uncertainty is calculated as follows by equation 4.1 (Adam Reff 2012):

$$Uncertainty = (0.05 \cdot x_{ij}) + DL_{ij} \quad (4.1)$$

where x_{ij} and DL_{ij} are the concentration and detection limit of the j^{th} species in the i^{th} sample, respectively. The following preliminary data quality checks were also done before the model run, including mass closure, ion balance mentioned in Chapter three as well as signal-to-noise ratio. The signal-to-noise ratio $(S/N)_j$ is interpreted as the relationship between certain portion of the concentration that exceeds the uncertainty. The signal-to-noise ratio is one of the vital references to decide which species (or variable) should be selected for the model run (Paatero & Hopke 2003). In most cases, the species with signal-to-noise ratio below 0.2 were excluded and the species with the signal-to-noise ratio between 0.2 to 2 were generally marked as weak. Therefore, 24 species were used in the model run, which is shown in below.

Table 4-1 Input Data Statistics for PMF Modelling.

Species	Category	Signal-to-noise ratio
PM _{2.5}	Weak	0.0
OC	Strong	10
EC	Strong	10.0
NH ₄ ⁺	Strong	10.0
K ⁺	Weak	10.0
Cl ⁻	Weak	5.6
NO ₃ ⁻	Strong	9.5
SO ₄ ²⁻	Strong	10.0
Al	Strong	2.5
Si	Weak	10.0
Ti	Weak	1.6
Mn	Weak	2.0
Fe	Strong	9.8
Ni	Strong	3.6
Cu	Strong	4.9
Zn	Strong	8.2
As	Strong	0.9
Se	Weak	2.6

Species	Category	Signal-to-noise ratio
Pb	Strong	7.6
Ba	Weak	0.0
Ca	Weak	10.0
Sb	Weak	0.5
Chrysene	Weak	5.9
Benzo[b]Fluorathene	Weak	8.4
Indeno[1,2,3-cd]Pyrene	Weak	4.0
Dibenzo[a,h]anthracence	Weak	0.1
C25	Weak	9.9
17ahop	Weak	1.3
Levoglucozan?		

Having set up the data input, the model is ready for base model runs. Base Model Run is the process that primary factor profiles and factor contributions are produced (EPA, 2014). In this practice, the number of runs was set as 100 times while the seed was set 12 as the starting point for each iteration but later was set as “random” to assess whether the found solution is a local or global minimum (EPA, 2014). The number of factors was set from three to seven to explore the solution which has the most reasonable physical meaning.

4.4 Modelling Results

4.4.1 Three factors

Figure 4.1 shows the factor profiles when three factors were set before the model run on Jinan's PM_{2.5}.

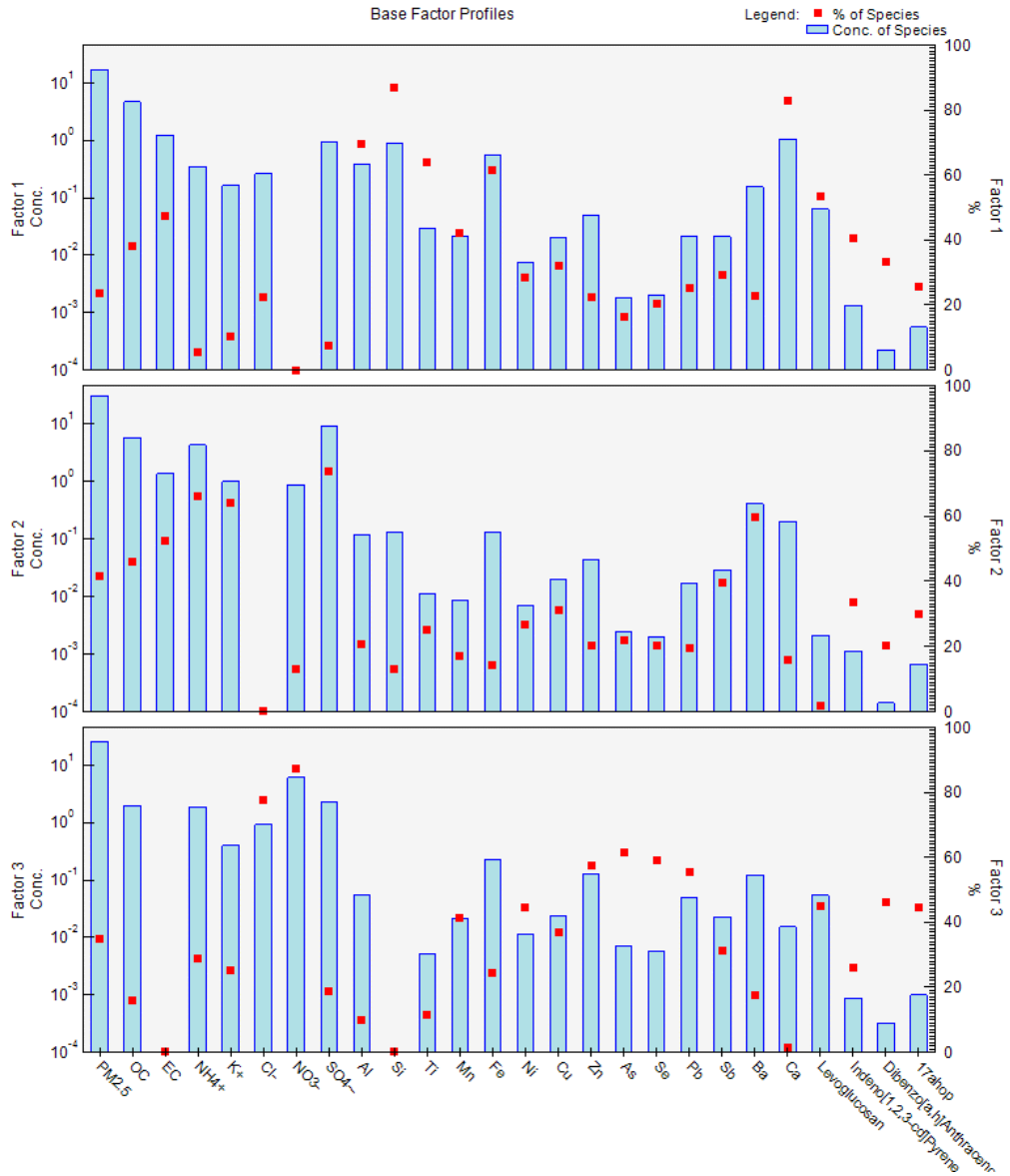


Figure 4-1 Factor profiles when three factors was set before the model run

According to the run Factor 1 is mainly characterised by Al, Si, Fe, and Ca. This could be due to the contribution from mineral dust contribution (Zíková et al. 2016). There are also many other species which also have high loadings such as OC, EC, organic molecular markers and trace metals. Therefore other sources have also contributed to this factor. In factor 2, the profile is mainly characterized by NH_4^+ , K^+ , SO_4^{2-} , Sb and Ba, which indicates the contribution from secondary sulphate formation and other fossil fuels combustion including traffic and biomass burning and coal combustion (Cheng et al. 2013) Zhang et al. 2007; Hopke 2016). Factor 3 is, however, characterised with high concentrations of Cl^- , NO_3^- and majority of trace metal and organic molecular markers. There is an also reasonable high content of K^+ , levoglucosan and NH_4^+ , indicating the possible emissions from secondary nitrate, industrial emission, fossil fuel combustions and biomass burning (Song et al. 2006). Therefore, three factors are not enough to explain all the sources for $\text{PM}_{2.5}$ in Jinan as some sources are mixed together in a single factor. In addition, the value of objective function Q, which is also known as the goodness-of-fit parameter, is large. However, the results still show that there is a strong signal that fossil fuel, mineral dust, secondary nitrate and sulphate, industrial and biomass burning could be the major sources for $\text{PM}_{2.5}$ in Jinan but they are not fully separated. This model run provides some preliminary suggestions on the existence of main sources in Jinan.

4.4.2 Four factors

For four factors PMF model run, the number of runs and seed number has not been changed as well as the species selection and its corresponding S/N categories. Only the number of factors was set to four. The Q value and Q-Robust were reduced to 1471.2 and 1485.1, respectively, which is a significant decrease compared to the previous results (2265.3 and 2320.0). However, in the residual analysis, OC, SO_4^{2-} and NO_3^- are not entirely

normal distributed and with relatively big scaled residuals, which means poorer species model fit.

Here are the factor profiles in this model run (See Figure 4-2). According to the profile plot, factor one is mainly characterised by NH_4^+ , K^+ and SO_4^{2-} . The total mass of NH_4^+ , K^+ and SO_4^{2-} are 71.9 %, 58.0% and 73.2%, respectively, in this factor. However, there is a minor contribution by levoglucosan but none of Cl^- from this factor. The K^+ may still come from biomass burning in the form of aged particles where KCl has been transformed to K_2SO_4 (Jing et al. 2017). Alternatively, it might due to other sources such as soil dust (Pachon et al, 2013). Hence, secondary sulphate and possible biomass burning could be the major contributors for this factor.

The second factor is mainly characterised with mineral dust tracers including Al, Si, Ti, Fe and Ca etc. Therefore, it can be verified that this is mineral dust source (Viana et al. 2008).

In the third factor, it is mainly characterised with high contribution of OC (66.3%), EC (78.6%) and organic molecular markers including Indeno[1,2,3-cd]pyrene, Dibenzo[a,h]anthracene and 17 α -hopane. These tracers imply that the influence from the vehicle exhaust mainly. Meanwhile, there is also some relatively high contribution from trace metals such as Cu, As and Ba. This could be due to the contribution mainly from vehicle exhaust or other fossil fuel combustion such as coal burning (Huang et al., 2014).

In the fourth factor, the main contribution comes from Cl^- , NO_3^- , Ni, Zn, As, Se, Pb and levoglucosan. The Cl^- may either from biomass burning or from coal combustion-related sources such as coal-burning power plant (Song et al. 2006; Cheng et al. 2013). The high loading of levoglucosan further suggests that the influence from biomass burning is significant. In addition, Ni, Zn, As and Pb may also come from coal burning or other

industrial sources. While NO_3^- is generally with respect to secondary nitrate. Also, considering some minor contribution of K^+ , this factor might be also a mixture of secondary nitrate, coal combustion, industry and some biomass burning contribution.

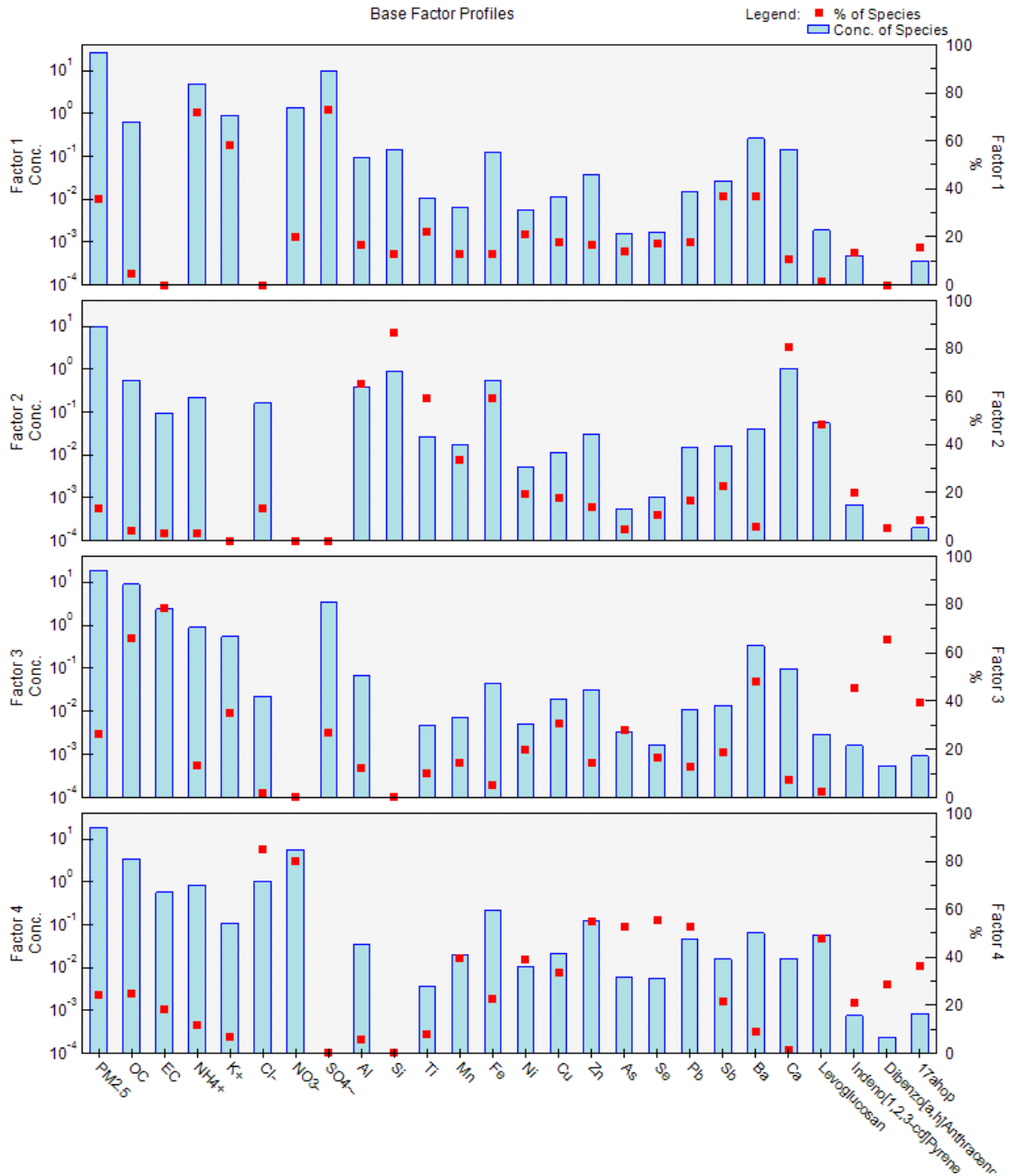


Figure 4-2 Factor profiles when four factors was set before the model run

4.4.3 Five factors

Again, for five factors PMF model run, the number of runs and seed number has not been changed as well as the species selection and its corresponding S/N categories. Only the number of factors was set to five to check if more sources can be continuously separated and lower the Q value. The Q value and Q-Robust continue reducing to 905.4 and 905.5, respectively, which implies an even better simulation. However, in the residual analysis, NO_3^- remains non-normal distributed and with relatively big scaled residuals.

According to the factor profile below on Figure 4-3, factor one is marked as NH_4^+ , and NO_3^- only, which is primary secondary nitrate. Factor two and four are also more clarified by OM, EC, Indeno[1,2,3-cd]pyrene, Dibenzo[a,h]anthracene, 17 α -hopane and Al, Si, Ti, Ca. They can be confirmed as the mixture of vehicle exhaust and mineral dust.

Factor three is more refined and clearer. The major markers are NH_4^+ (54.3%) and SO_4^{2-} (69.6%), which indicates that this is the factor for secondary sulphate. However, there is also some K^+ existed in this factor. As suggested earlier, it may be due to the aged particles from biomass burning emission or soil dust.

Factor five is mainly characterised by As, Cu, Zn, Mn, Ni and Pb. These could be due to different industrial sources including coal combustion, metallurgy, steel industry and oil combustion (Viana et al. 2008). The factor five is also characterised by Cl^- and levoglucosan, which implies the contribution from biomass burning (Simoneit et al. 1999b).

Therefore, secondary nitrate, vehicle exhaust and mineral dust have been identified at this stage.

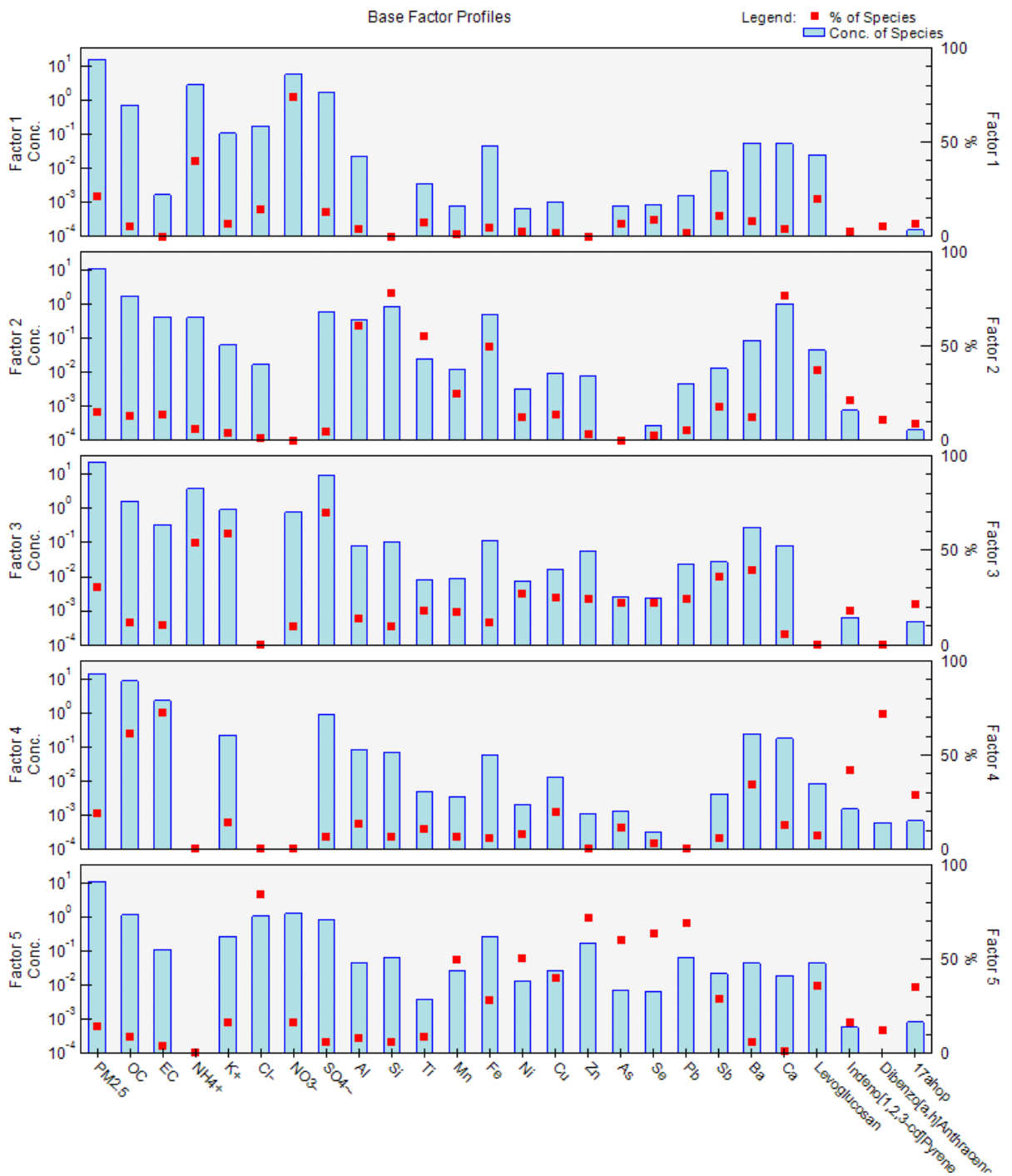


Figure 4-3 Factor profiles when five factors was set before the model run

4.4.4 Six factors

Regarding six factors PMF model run, The Q value and Q-Robust are both 666.4. The values have become the same, in the residual analysis, the residual distribution of all the

species are normally distributed with much less scaled residuals, indicating that the model has already tended to find out good fitting results.

In this model run, the chemical characterization for each specific source is clearer. The factor one is mainly characterized as NO_3^- and some NH_4^+ while other species' contribution is minor. Hence, it can be identified as secondary nitrate source. The second factor contains a reasonable amount of OC, SO_4^{2-} and marked by Ni, Zn, As, Se and Pb and also some Cl⁻. This factor could be interpreted as coal burning (Zhang et al. 2007; Hopke, 2016). The third factor mainly characterized by Cl⁻, Se levoglucosan, which indicates that this is the contribution from biomass burning. The factor four is characterized with the elements including Al, Si, Ti and Ca. So this is the factor for the $\text{PM}_{2.5}$ from mineral dust including soil, road re-suspended dust and maybe cement production too (Zíková et al. 2016). Hence, $\text{PM}_{2.5}$ in factor four could be mainly coming from coal burning mainly. The fifth factor is characterized as NH_4^+ , K^+ and SO_4^{2-} , this could be just due to secondary sulphate but whether the K^+ comes from biomass burning is still required some further analysis. The sixth factor is characterized by OM, EC, PAHs and α -hopane. This is the factor for vehicle exhaust sources (Cao et al. 2013; Wang et al. 2009).

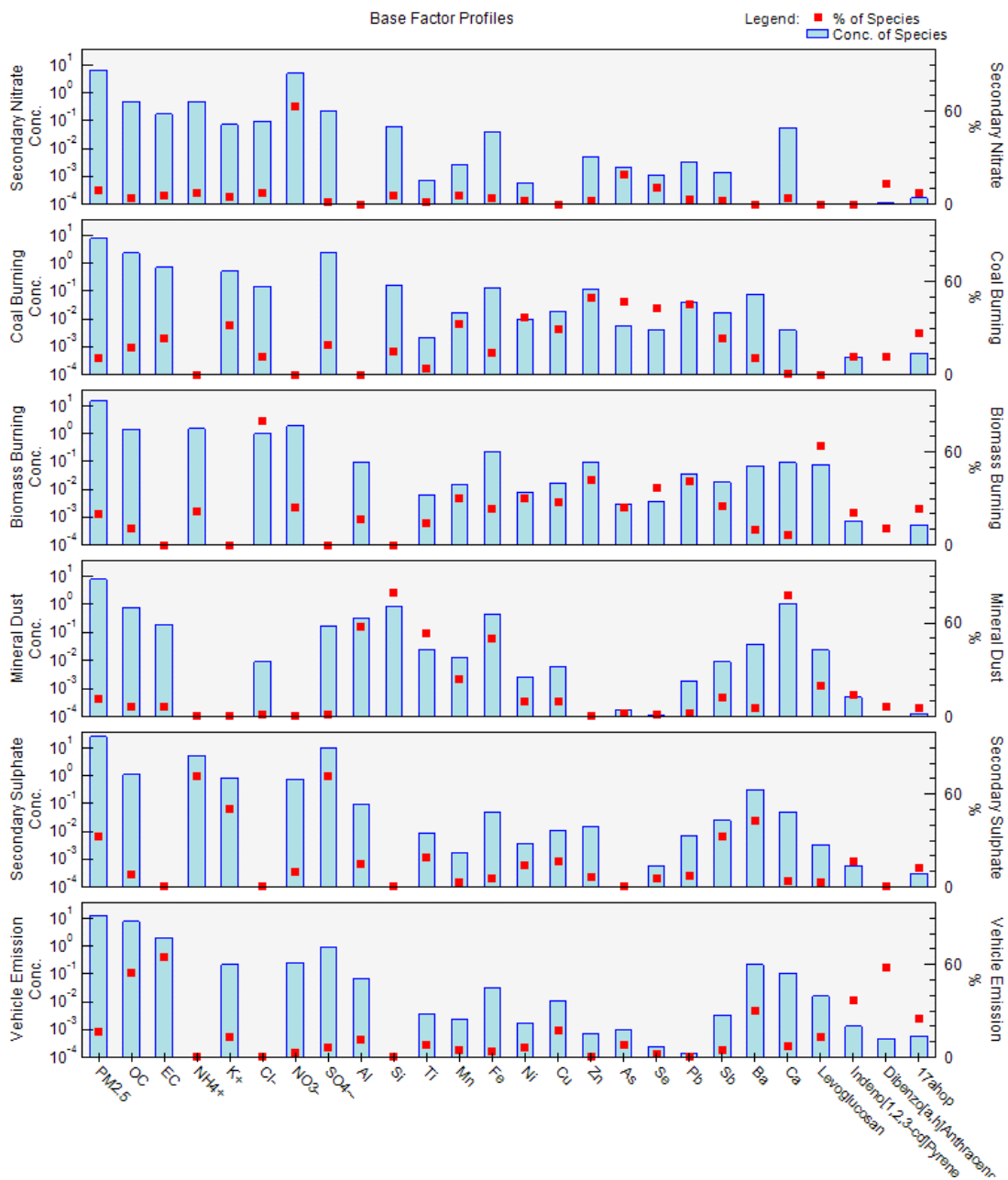


Figure 4-4 Factor profiles when six factors was set before the model run

4.4.5 Seven factors

The modelling results for seven factors have been also assessed in this study. The Q value and Q-Robust are both 509.5, which is even lower than the Q values that were obtained when there were six factors. All the selected species show good normal distributions. However, the source profiles for mineral dust seems to split up during the seven-factor

model run. Factor 1, 2, 4, 5 and 6 are very similar to the biomass burning, vehicle emission, secondary sulphate and secondary nitrate in the previous model run, respectively. However, both factor 3 and factor 7 are seems based on the emission from mineral dust. Factor 3 is mainly characterised by Al, Si, Ti, Fe and Ca while factor 7 is mainly marked by Al.



Figure 4-5 Factor profiles when seven factors was set before the model run

The G-Space plot shows that there is a clear edge existed according to Figure 4-6. There is also some correlation between two factors, which implies the rotation and separation factors in this result.

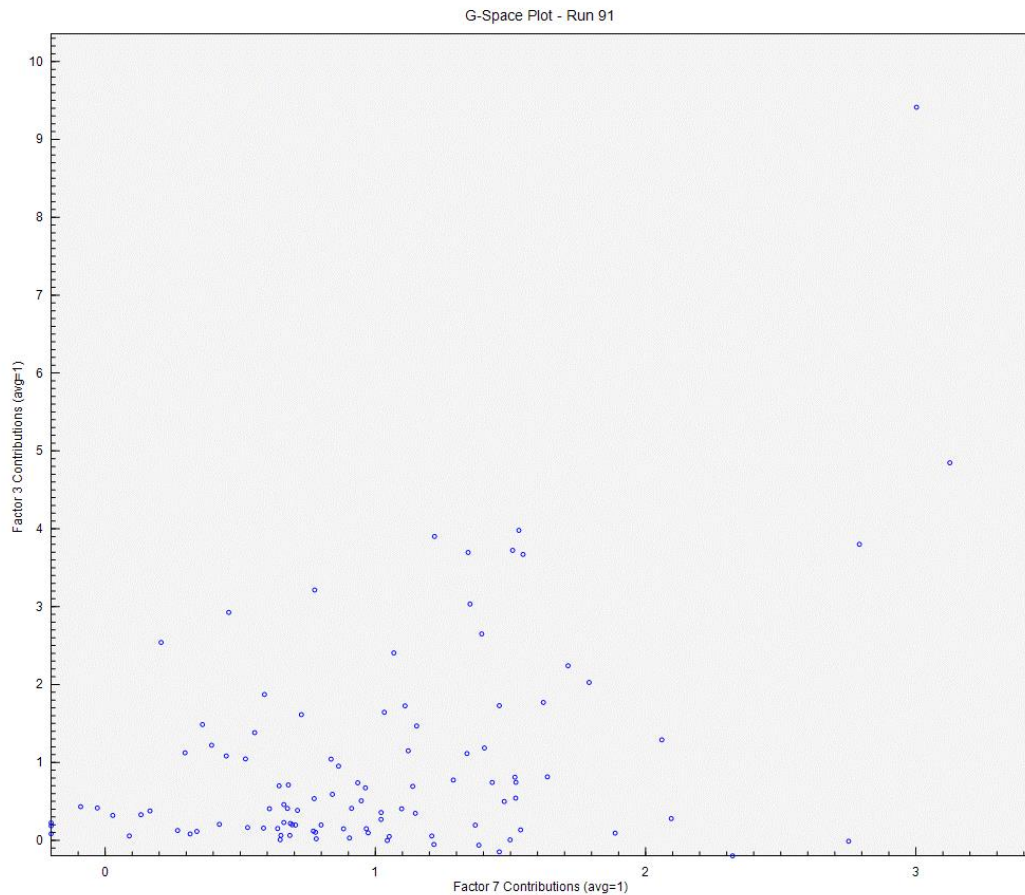


Figure 4-6: G-space plot of factor 3 and factor 7.

To sum up, though the Q values and residual analysis have indicated that the seven-factor modelling run may have even better theoretically mathematical solutions, the source profiles start losing its physical meaning under the circumstance to the physical environment. Therefore the results for the seven-factor model run are excluded (Chen et al. 2010).

Furthermore, in order to apportion cooking emission, cholesterol has also been applied in the PMF model. However, cholesterol has very high loading in the biomass burning factor when six factors are set. One possible explanation is that levoglucosan and cholesterol may represent some cooking emission while it is released when the vegetable is fried in the cook (Zhao et al. 2015). However, the PMF failed to separate biomass burning and cooking emissions. Last but not the least, *n*-alkanes and some other molecular markers are not applied in the PMF modelling in the end as it will result in higher Q-value significantly. This might be due to the instability caused by too many chosen species for the modelling while the limited sample size ($n < 120$) is available (Zhang et al. 2009).

4.5 Discussions

4.5.1 Further Biomass Burning's Contribution Analysis

In Chapter three, some evidence has shown that there is potential biomass burning contribution to the PM_{2.5} as there is some extent of correlation between K⁺ and levoglucosan measured in the samples. However, most of K⁺ appeared in the secondary sulphate factor while the levoglucosan does not improve the modelling performance in the PMF modelling. Therefore, another approach is attempted to find out its contribution.

There could be three causes (or hypothesis). First of all, the biomass burning was far enough away from the sampling site so that the emitted chemicals is highly aged and transferred to secondary aerosols. For instance, K⁺ and Cl⁻ have been found as the main PM_{2.5} tracers of biomass burning as its emission is largely composed of K and Cl (Li et al. 2007). However, Cl⁻ may also come from other sources such as coal combustion while K can also come from coal combustion or soil dust in China (Yao et al. 2002; Zhao et al. 2010).

4.5.2 Biomass burning contribution estimation by other means

Another approach is applied to estimate the contribution of biomass burning. Based on the enrichment factor approach, the contribution of biomass burning to OC can be calculated as follows (Zhang et al. 2014):

$$\text{Biomass Burning's Contribution to OC (\%)} = \frac{[\text{levoglucosan/OC}]_{\text{ambient}}}{[\text{levoglucosan/OC}]_{\text{source}}} \times 100\% \quad (4.1)$$

Zhang et al. (2007) reported that levoglucosan accounts for 8.2% of cereal burning which is the major biomass burning in China. And the average value of levoglucosan to OC ratio in Jinan's sample is 40.35. The contribution of biomass burning to OC in Jinan is about 20.3%, which suggests that the impact from biomass burning is significant during sampling periods. Hence, the mass contribution of biomass burning to the total PM_{2.5} is 4.1%.

4.5.3 PMF Uncertainty Analysis

After the confirmation of initial factors, the assessment of rotational ambiguity and modelling uncertainty (error estimation) are preceded. In PMF v5.0, three methods for undertaking error estimation are provided including classical bootstrap (BS), displacement of factor elements (DISP) and bootstrap enhanced by displacement of factor elements (BS-DISP). All of these methods are suggested to use as they are a complement to each other (Paatero et al. 2014). The error estimation is attempted to find out the uncertainty of modelling results due to random error and any other error and it is helpful for the analyst to tell the potential rotational ambiguity too.

4.5.3.1 Time series of sources contribution

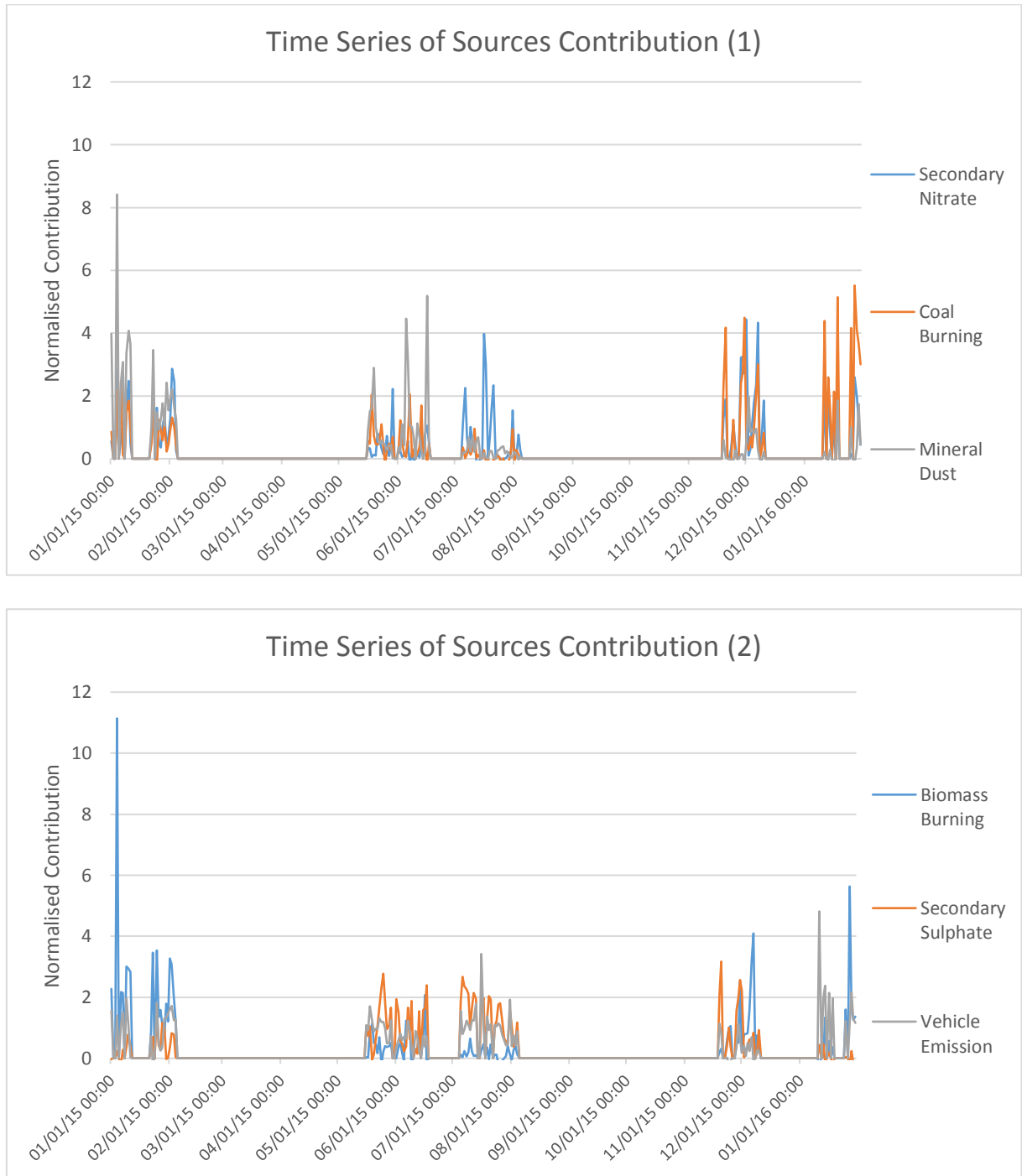


Figure 4-7 Time series of sources contribution during the sampling campaign

According to Figure 4-7, secondary nitrate has a steady contribution along the sampling campaign, which suggest that the influence by the vehicles emission is persistent. Coal

burning and mineral dust have shown more seasonal variation along this period. More contribution has been spotted in winter for coal burning but less contribution in summer while more mineral dust has found in later winter and early summer, which is consistent with expectation due to the more coal burning during the heating time. This could be due to the more frequent cold front system coming from Siberia bring more dust while passing by the Gobi dessert. Vehicle emission is also similar to secondary nitrate which has sustaining contribution along this period. However, biomass burning has much higher contribution during the winter than summer while more secondary sulphate is formed during the summer than winter.

4.5.3.1 Base model bootstrap Method (BS)

BS mainly focuses on evaluating the random errors but also partially evaluating the rotational ambiguity. In the summary of BS runs, if the base run is within the interquartile range box (IQR), the base run results are acceptable. Or any species with the base run outside the IQR should be evaluated as it means that even a small set of observation could result in the significant change of base run outcomes. BS is particularly useful for identifying the factors which are not very reproducible due to the poor solution or other causes such as wind direction or source activity etc. (Brown et al. 2015).

Having initialled the BS run, the BS box plots produced for each factor, which is shown below in Figure 4-8.

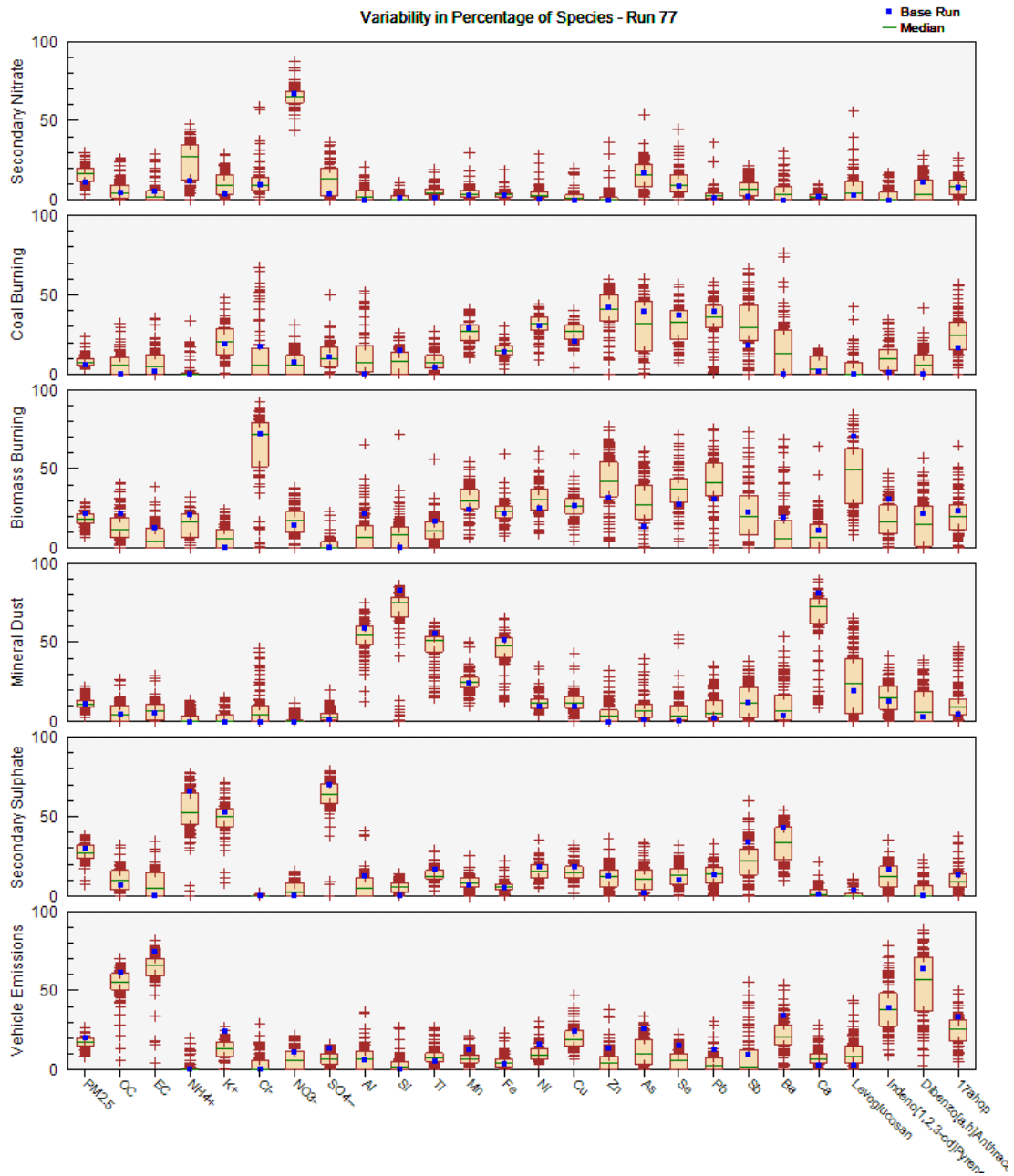


Figure 4-8 Uncertainties of each species contribution in each profile due to random error mainly

According to Figure 4-, the majority of species base run values are within the IQR in each factor. This is a positive sign that the random error for this factors simulation is not major. In addition, the bootstrap summary shows that the mapped factors are more than 80%. Therefore, it implies that the current number of factors may be suitable. However, there

are some base run results are out of IQR, indicating minor rotational ambiguity in the modelling outcome.

4.5.3.2 Base Model Displacement Error Estimation (DISP)

DISP is mainly used for assessing the rotational ambiguity for the PMF solution. The exploration of rotational ambiguity is assessed by evaluating the biggest range of source profile values without an appreciable increase in the Q-value. The details of how DISP works is explained in the “USEPA PMF v5.0 User Guide”, which will not be covered in this thesis. Overall, if factor swaps happen during the DISP diagnostics, this suggests that there is significant rotational ambiguity, which will be shown as the error code 6 in the DISP summary report. Meanwhile, the Q-value decrease should not be over 1%. Or it indicates that the current solution is not a global minimum, which will be shown as error code 9 in the DISP summary. DISP has been turn out as a good screening tool for solution swap assessment in other studies (Brown et al. 2015).

Here is the BS Summary:

```
0 0.000
0 0 0 0 0 0
0 2 0 0 0 2
0 14 8 0 3 7
0 22 15 0 5 10
```

This indicates that no factor swaps are found in any factors, which shows that there is no significant rotational ambiguity in this PMF solution. There is no Q-value decrease

(<1%), the solution can be considered as a global minimum. Consequently, it is not necessary to deploy rotation in the further analysis.

Finally, the linear correlation equation is $y = 0.94702 * x + 2.16852$, where the gradient is very close to 1 and $R^2 = 0.877$. The base model run has suggested that the modelled total variable perdition is matched with measurement data reasonably well (Figure 4.9).

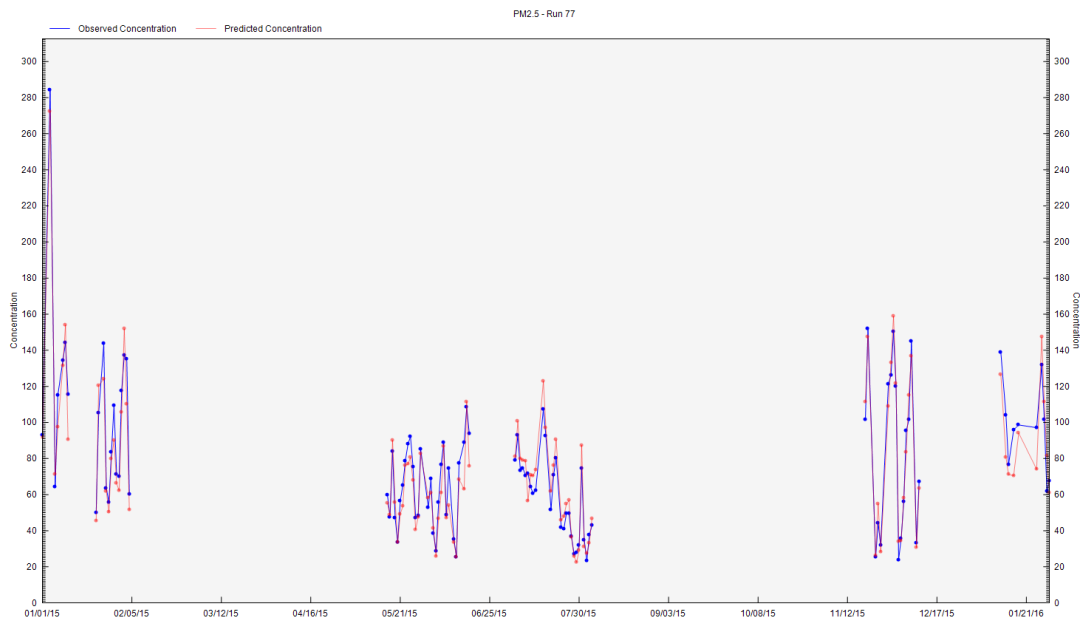


Figure 4-9 The Obs/Pred time series analysis of model run

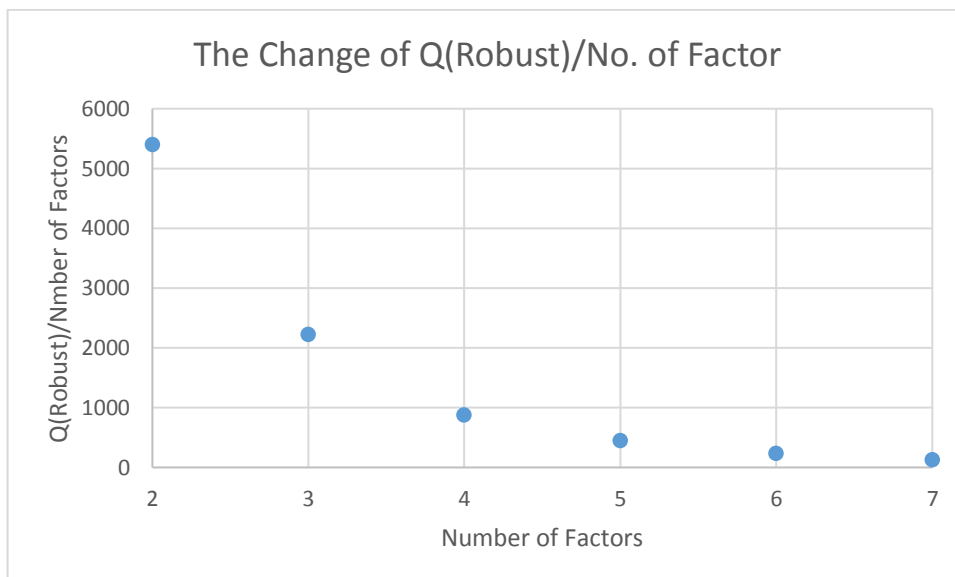


Figure 4-10 change of Q value to number of factors ratio against the number of factors

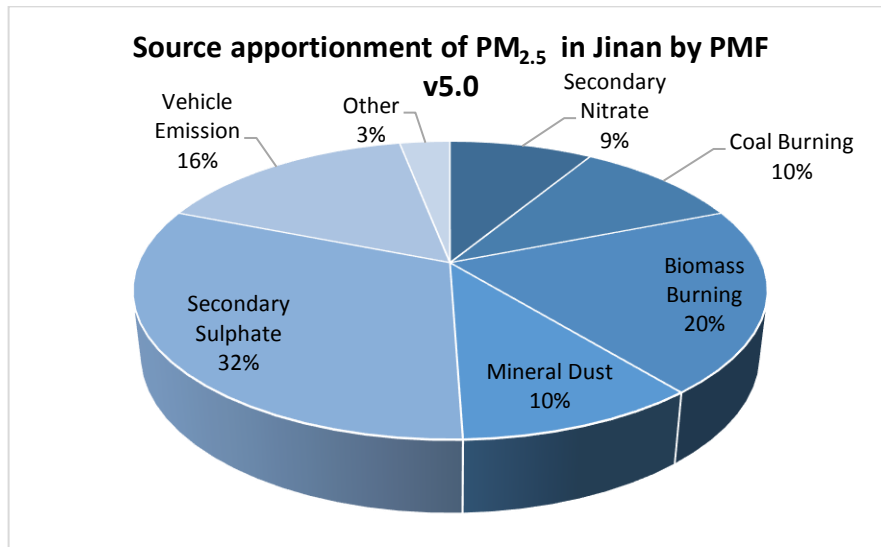
Figure 4-10 shows the change of Q values to number of factors ratio with respect to the increasing number of factors from two to seven. The decrease of the ratio is massive from two factors to five factors while the change is less significant from five to seven factors. This trend also suggest the results is relatively robust in terms of Q value.

4.6.3 Sources Contribution and Mass Closure

A convincing PMF modelling solution is achieved during the modelling progress and a couple of error diagnostics and other means of modelling results assessments have been applied to evaluate the quality of this model outcome. Six major sources have been identified including: Secondary Nitrate (9%), Secondary Sulphate (32%), Coal Combustion (10%), Mineral Dust (10%), Vehicle Exhaust (16%) and biomass burning (20%) etc. However, secondary sulphate and biomass burning could be overestimated and

coal combustion might be underestimated based on the discussion above. It is still worth comparing this result with mass closure for further evaluation.

a)



b)

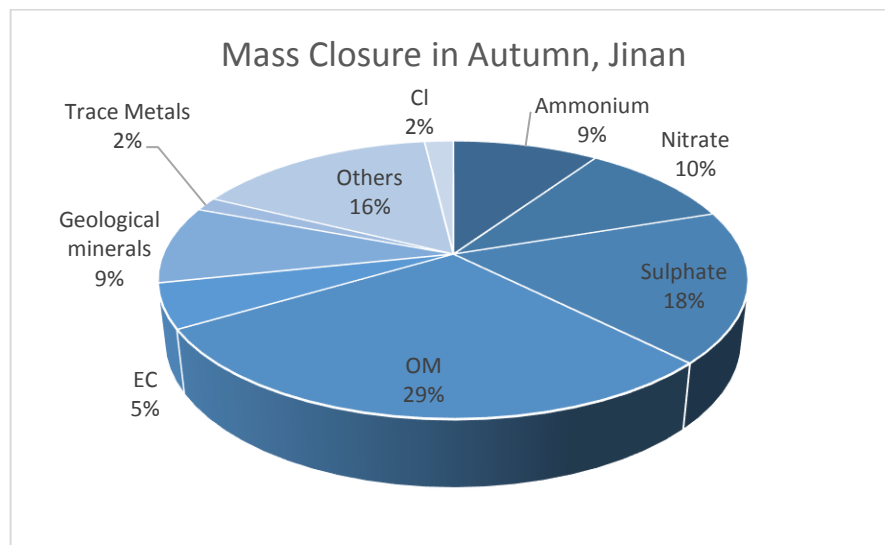


Figure 4-7 a) Source contribution modelled by PMF; b) mass closure analysis.

Figure 4-7 shows the results of both source apportionment analysis by PMF and Chemical Mass Analysis (CMA) which have been conducted in chapter three. In both analyses, the mineral dust accounts for 10% and 9%, respectively, which is fairly consistent with each other. In addition, the secondary inorganic aerosol (SIA), which is the sum of NH_4^+ , SO_4^{2-} and NO_3^- in CMC, is 36% while the SIA in PMF modelling result is 41%, which also have a acceptable agreement. But it seems that sulphate is overestimated by PMF while nitrate is underestimated. Overall, the results between PMF and CMC are still similar. The PMF modelling results should be compared with CMB results for further evaluation.

4.7 Conclusions

In summary, source apportionment by PMF modelling with organic molecular markers has been conducted. Six factors have been identified and their contributions to $\text{PM}_{2.5}$ in Jinan have been quantified too. The six major sources are Secondary Nitrate, Secondary Sulphate, Coal Combustion, Mineral Dust, Vehicle Exhaust, biomass burning and other sources, which accounts for 9%, 32%, 10%, 10%, 16%, 20%, 16% and 3% of $\text{PM}_{2.5}$ pollution in Jinan. Organic molecular markers turn out helpful while identifying fossil fuel burning sources such as coal combustion, biomass burning and vehicle exhaust in Jinan. Error estimation is conducted by BS and DISP. Neither significant rotational ambiguity nor any other major error has been found in this PMF modelling solution. The result is also comparable with CMC for quality control. This PMF model result is useful and helpful for the local policy maker and authority for their air pollution control in near future. But PMF seems overestimated the biomass burning significantly. For the further work, mannosan should be introduced for apportioning the biomass burning (Zhang et al. 2007). There is a couple of studies in China have reported that mannosan can be very helpful for apportioning the biomass burning in China and levoglucosan to mannosan ratio is a

reliable assessment to hardwood burning (Cheng et al. 2013). Further assessment is required to compare its results against CMB modelling results.

5 Chapter Five Chemical Mass Balance Modelling on Jinan's PM_{2.5} Dataset

Abstract

In this chapter, the modelling and performance of CMB models is discussed. The PM_{2.5} dataset is reorganised to meet the requirements of USEPA CMB v8.2 model input and the profiles of ambient PM_{2.5} emitted from the sources in China, are retrieved from the previous published literatures or provided by collaborators. CMB modelling showed that coal burning (16%), biomass burning (17%), metallurgy industry (11%), mineral dust (6%), petrol vehicles (8%), diesel vehicles (6%), secondary nitrate (13%), secondary sulphate (18%) and other (5%) are recognised as the major emission sources annually to PM_{2.5}, respectively, in Jinan. All model performance criteria were met for the annual average dataset. Regarding seasonal source apportionment results, the outcomes of winter and early summer also met the criteria but the summer and autumn have excessive value of χ^2 . This may be due to the change of sources contributing to PM_{2.5} in summer and/or poor representativeness of the source profiles are used under the context of this two seasons. Significant seasonal variation in the contributions to PM_{2.5} was observed for secondary sulphate, secondary nitrate and coal burning. On the other hand, the contribution of other sources such as soil dust and biomass burning to PM_{2.5} mass remains stable throughout the year. Model performance analysis suggested that chemical profiles of local PM_{2.5} sources are needed to improve the source apportionment of PM_{2.5} in Jinan.

5.1 Introduction

CMB is another receptor model tool which has been widely used for receptor modelling. Unlike PMF, CMB requires source profiles as data input in the model based on its model principles (Watson et al. 2002). However, there were limited source profile data about a decade ago so that modellers had to use the source profile dataset elsewhere such the USEPA SPECIATE database etc. in China (Pei et al. 2016). There are two major issues using non-local profiles. First of all, the chemical compositions of same type of sources may differ in the different place and its difference could be huge (Pei et al. 2016). In addition, some profiles presented in the USEPA SPECIATE are old and have limited quantified species in the profile. Furthermore, lacking of uncertainty data of each measured specie is another problem. All of these issues may result in wrong results and errors after obsolete profiles are applied.

However, there are still some studies using CMB models to apportion the PM in China and more source profiles of major particle sources data gradually available in the recent years, which is very helpful for the future CMB modelling in China (Han et al. 2014; Kong et al. 2011; Zhang et al. 2007). For example, Bi et al. (2007) firstly applied CMB for apportioning the sources' contribution to PM_{10} in Jinan with mineral dust samples that are collected and measured in local urban area. In this chapter, the sources profiles of $PM_{2.5}$ collected in Jinan, Tianjin, Xiamen have been employed for the $PM_{2.5}$ dataset obtained from Jinan. Though there is no source profile is characterised in this project due to limited time and budget, the latest published and/or measured $PM_{2.5}$ profile in China have been applied in the CMB modelling. Both annual and seasonal source apportionment have been studied. The results reveal that coal combustion, industrial boilers, vehicle exhaust and secondary nitrate and sulphate are the major sources in Jinan. Meanwhile, how important

the local source profile has been addressed by the sensitivity test. It turns out that though the profiles from other places in China do fit better than other source profiles, for example USEPA SPECIATE and SPECIEUROPE during the practice, the profiles measured in or near Jinan recently still cannot fully represent the local PM_{2.5} chemical characteristics. The establishment of the local profiles are still essential for the local source apportionment by CMB modelling.

5.2 Methodology

5.2.1 Chemical Mass Balance Model

The mathematics of CMB model has already explained in the Chapter Two. In short, it is based on the equation derived from the principle of mass conservation of individual chemical (or markers) between the emission source and the receptor site, which is similar as PMF. However, as the model is conceived for one sampler per site and there is not residual term (Belis et al. 2013). The set of equations is then solved with variance-weighted least square under the USEPA CMB environment.

5.2.2 Sampling and Chemical Analysis

The details of sampling and chemical analysis of PM_{2.5} samples in Jinan has described in the previous chapter, which is not repeated here.

5.2.3 Model Parameters and Settings and Evaluation Criteria

In CMB, both the chemical species concentration and its corresponding uncertainty and source profile with the measurement uncertainty are compulsory. The species concentration dataset is identical as the one used in PMF models except that it was reformatted for the CMB model input format requirement. Due to the limited time and resources in this project, the source profiles that are used in the model run are collected via

data mining from the published literatures where all of them are the profiles established for the local sources in China.

The species used in the CMB are: OC and EC, water soluble ions including NH_4^+ , K^+ , Cl^- , NO_3^- , SO_4^{2-} and trace elements including Al, Si, Ti, V, Cr, Mn, Fe, Ni, Cu, Zn, Pb, Na, Mg and Ca. In CMB, the following performance measures have been established to assess the how well the model has performed, which is consist of the following parameters: 1) R-square value (r^2); 2) chi-square value (χ^2); 3) t-stat value and 4) Calculated/Measured Ratio (C/M) (USEPA, 2004).

5.3 Source Profiles Used in the Modelling

There is plenty of literature regarding the source profiles study in China have been examined for finding the appropriate source profiles dataset. Some profiles are also provided by the collaborator (College of Environmental Science and Engineering, NKU). The types of source profiles include road dust, soil dust, cement production, diesel vehicle exhaust, petrol vehicle exhaust, vehicle exhaust, including both petrol and diesel emission), biomass burning (general), wheat straw burning, wood burning, corn burning, secondary sulphate, secondary nitrate, coal burning, power plant emission, metallurgic plant, steel plant (Hao, 2008; Zhang et al. 2016). The profiles with correct particle size fraction (i.e. $\text{PM}_{2.5}$) and detailed total mass concentration and corresponding uncertainty to each measured species will be taken into the account. If the source was sampled in or near Jinan, it will be prioritized. Here are the details of the profiles used in the CMB model.

Table 5-1 Mass concentrations of source profiles that used in the CMB modelling

Sources Mass Concentration (% in mass)									
Species	Diesel	Petrol	Biomass Burning	Sec. Sulphate	Sec. Nitrate	Soil Dust (Tianjin)	Metallurgy	Soil Dust (Xiamen)	Coal Burning
OC	54.4	54.4	40.0	0.0	0.0	8.9	14.4	7.6	12.0
EC	19.4	6.3	3.0	0.0	0.0	1.2	3.5	0.2	9.1
Na⁺	0.9	3.3	1.0	0.0	0.0	0.0	0.0	0.0	0.0
NH₄⁺	0.3	0.0	1.0	22.5	27.3	1.1	6.6	2.0	3.1
K⁺	0.0	0.0	10.0	0.0	0.0	0.2	3.6	0.1	0.0
Mg²⁺	0.1	0.3	0.2	0.0	0.0	0.0	0.0	0.0	0.0
Ca²⁺	0.5	2.5	0.0	0.0	0.0	0.0	0.0	0.0	0.0
Cl⁻	1.2	5.4	17.1	0.0	0.0	0.4	12.5	0.3	1.8
NO₃⁻	1.4	1.5	0.3	0.0	77.5	0.4	2.1	0.3	1.0
SO₄²⁻	0.5	0.0	2.2	72.7	0.0	4.1	8.6	0.6	23.0
Al	0.0	0.5	0.0	0.0	0.0	3.8	4.6	4.2	4.6
Si	0.7	0.0	0.0	0.0	0.0	5.8	4.4	7.0	4.3
Ti	0.0	0.0	0.0	0.0	0.0	0.1	0.6	0.1	0.3
V	0.0	0.0	0.0	0.0	0.0	0.0	0.0	0.0	0.0
Cr	0.0	0.0	0.0	0.0	0.0	0.1	0.2	0.2	0.0
Mn	0.0	0.0	0.0	0.0	0.0	0.1	0.2	0.1	0.0
Fe	0.0	0.6	0.0	0.0	0.0	3.0	5.1	3.6	2.0
Co	0.1	0.3	0.0	0.0	0.0	0.0	0.0	0.0	0.0
Ni	0.0	0.0	0.0	0.0	0.0	0.0	0.1	0.0	0.0

Cu	0.0	0.0	0.0	0.0	0.0	0.7	0.1	1.0	0.1
Zn	0.0	0.1	0.0	0.0	0.0	0.1	2.0	0.1	1.5
As	0.2	0.1	0.0	0.0	0.0	0.0	0.0	0.0	0.1
Mo	0.0	0.0	0.0	0.0	0.0	0.0	0.0	0.0	0.0
Pb	0.0	0.0	0.0	0.0	0.0	0.0	0.0	0.0	1.1
Na	0.0	0.0	0.0	0.0	0.0	0.6	1.4	0.6	3.5
Mg	0.0	0.0	0.0	0.0	0.0	2.0	2.0	1.7	0.3
K	0.0	0.6	15.5	0.0	0.0	0.8	5.8	0.9	3.2
Ca	0.0	0.0	0.0	0.0	0.0	8.5	3.1	7.9	1.6

Note: The source profiles are available at : 1) Diesel vehicles, petrol vehicles, soil dust, metallurgy by Zhang, N. et al., 2016.; 2)Coal burning by Hao, J.M. et al. (2008); 3) soil dust and biomass burning by Dr Shi Guoliang, College of Environmental Science and Engineering, NKU (personal communication).

Table 5-2 Mass concentration uncertainties of source profiles that used in the CMB modelling (% mass)

Species	Diesel	Petrol	Biomass Burning	Sec. Sulphate	Sec. Nitrate	Soil Dust (Tianjin)	Metallurgy	Soil Dust ()	Coal Burning
OC	6.99	18.73	4.11	0.00	0.00	2.08	9.48	2.67	3.74
EC	6.23	4.29	1.21	0.00	0.00	0.56	2.57	0.25	5.10
Na ⁺	1.12	4.32	0.67	0.00	0.00	0.00	0.00	0.00	0.00
NH ₄ ⁺	0.18	0.00	0.85	0.24	0.32	0.51	6.16	0.98	1.06
K ⁺	0.00	0.00	4.52	0.00	0.00	0.08	2.82	0.05	0.00
Mg ²⁺	0.15	0.30	0.03	0.00	0.00	0.00	0.00	0.00	0.00
Ca ²⁺	0.27	0.32	0.00	0.00	0.00	0.00	0.00	0.00	0.00
Cl ⁻	1.29	6.06	6.86	0.00	0.00	0.17	13.64	0.16	0.73
NO ₃ ⁻	0.78	1.28	0.20	0.00	0.39	0.20	1.77	0.17	0.71
SO ₄ ²⁻	0.46	0.00	0.23	0.39	0.00	2.37	4.04	0.34	4.43
Al	0.03	0.61	0.00	0.00	0.00	2.81	4.02	1.06	1.70
Si	1.28	0.00	0.00	0.00	0.00	4.92	3.12	2.02	1.58
Ti	0.00	0.00	0.00	0.00	0.00	0.07	0.50	0.04	0.14
V	0.00	0.00	0.00	0.00	0.00	0.00	0.00	0.00	0.01
Cr	0.00	0.00	0.00	0.00	0.00	0.07	0.05	0.21	0.01
Mn	0.01	0.02	0.01	0.00	0.00	0.07	0.24	0.03	0.00
Fe	0.02	0.06	0.00	0.00	0.00	2.10	4.33	1.43	0.45
Co	0.05	0.11	0.00	0.00	0.00	0.00	0.00	0.00	0.00
Ni	0.00	0.01	0.00	0.00	0.00	0.00	0.03	0.00	0.01
Cu	0.00	0.01	0.00	0.00	0.00	0.51	0.04	0.25	0.04

Species	Diesel	Petrol	Biomass Burning	Sec. Sulphate	Sec. Nitrate	Soil Dust (Tianjin)	Metallurgy	Soil Dust ()	Coal Burning
Zn	0.01	0.01	0.00	0.00	0.00	0.23	4.10	0.10	0.32
As	0.21	0.11	0.00	0.00	0.00	0.01	0.00	0.02	0.02
Mo	0.00	0.00	0.00	0.00	0.00	0.00	0.00	0.00	0.00
Pb	0.02	0.01	0.00	0.00	0.00	0.00	0.00	0.00	0.41
Na	0.00	0.00	0.00	0.00	0.00	0.18	0.76	0.22	0.20
Mg	0.00	0.00	0.00	0.00	0.00	0.94	1.52	1.08	0.09
K	0.04	0.27	4.01	0.00	0.00	0.69	6.42	0.30	0.76
Ca	0.01	0.03	0.00	0.00	0.00	3.08	2.47	5.01	0.39

Note: The source profiles are available at : 1)Zhang, N. et al., 2016. Development of source profiles and their application in source apportionment of PM_{2.5} in Xiamen, China. *Frontiers of Environmental Science & Engineering*, 10(5), p.17.; 2) Hao, J.M. et al. (2008) The physical and chemical characterisation of combustion sources. Beijing: China Science Press.; 3) Dr Shi Guoliang, College of Environmental Science and Engineering, NKU.

5.3.1 Soil dust

The soil dust profile was provided by College of Environmental Science and Engineering, NKU. The 100g of surface soil dust was collected in the exposed field at north, south, east and west side of city as well as along the direction of prevailing wind. Chemicals include OC and EC, water soluble ions and trace metal elements, which have been analysed by Sunset thermal/optical analyser, IC and ICP-MS in the laboratory. Its chemical mass concentration and uncertainty has been shown above in Table 5-1 and Table 5-2 and it is also illustrated in Figure 5-1 below.

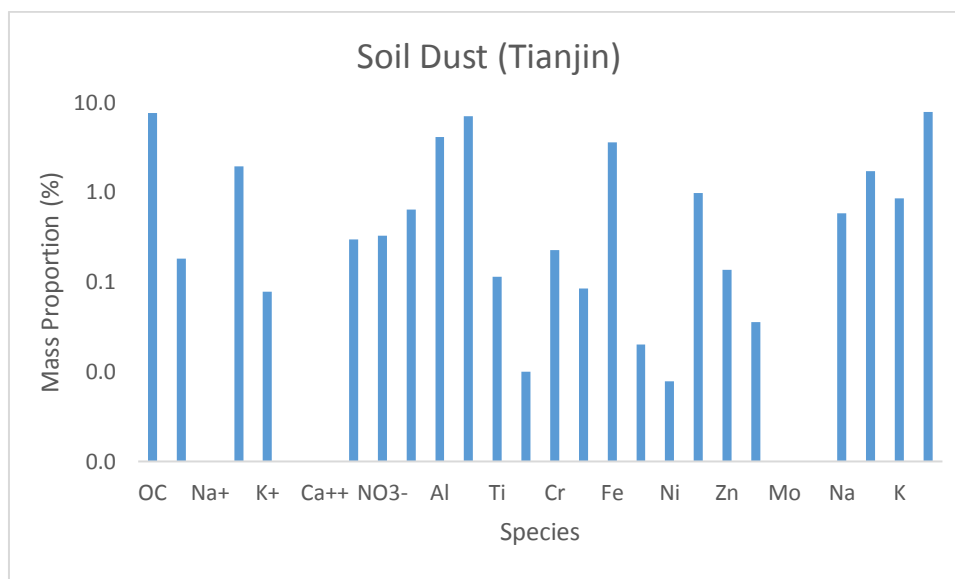


Figure 5-1 Chemical characterisation of soil profile in Tianjin, Northern China (Provided by College of Environmental Science and Engineering, NKU).

The soil profile is mainly marked by OC, Al, Si, Fe and Ca. This is similar to the soil profiles reported by other studies (Pant, 2014). It is also similar to the factor profile of mineral dust apportioned by PMF where Al, Si, Fe, Ti and Ca are the primary components. The high amount of OC in the soil dust might come from the organic matter from soil or anthropogenic contamination (Soane, 1990).

5.3.2 Biomass Burning

The biomass burning profile is cited from the study reported by Zhang et al. (2016) where the straw samples were well-burned and its emitted particles collected on the both quartz and Teflon filter for chemical analysis. The OC and EC, water-soluble ions and trace metals were analysed by Sunset Thermal/optical analyser, IC and XRF (Zhang et al. 2016).

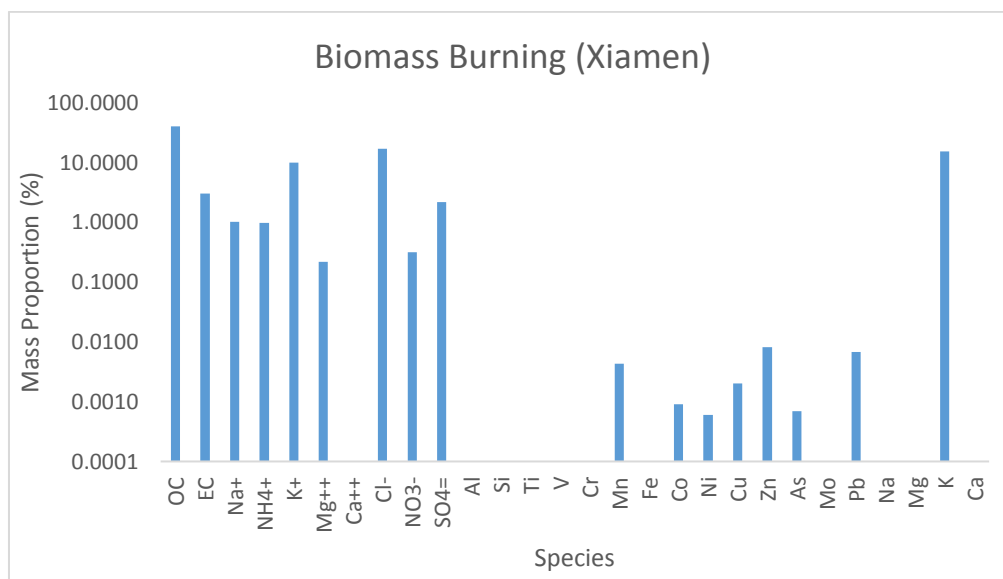


Figure 5-2 Chemical characterisation of biomass burning profile in Xiamen, Eastern China (Zhang et al. 2016).

According to Figure 5-2, the biomass burning is characterized by K^+ and Cl^- except OC as well as considerable amount of EC and sulphate. Other species, however, they are only accounting for minor constituent from biomass emission.

5.3.3 Coal burning

Coal burning is massively used as a thermal power supplier in different kinds of industrial boilers in China. One of the major issues about these boilers is that it has not been mechanized and automated and limited measures have been taken to remove the dust before the emission (Hao et al., 2008). In this study, the boiler profiles cited from Hao et al. (2008)'s work has been used for CMB modelling. The samples were collected from eight different boilers in China and the average value is being used for representing more broadly and realistic coal burning emission. The coal burning is marked by sulphate and other trace element, water-soluble ions including NH_4^+ , SO_4^{2-} , Al, Si, Fe, OC and EC.

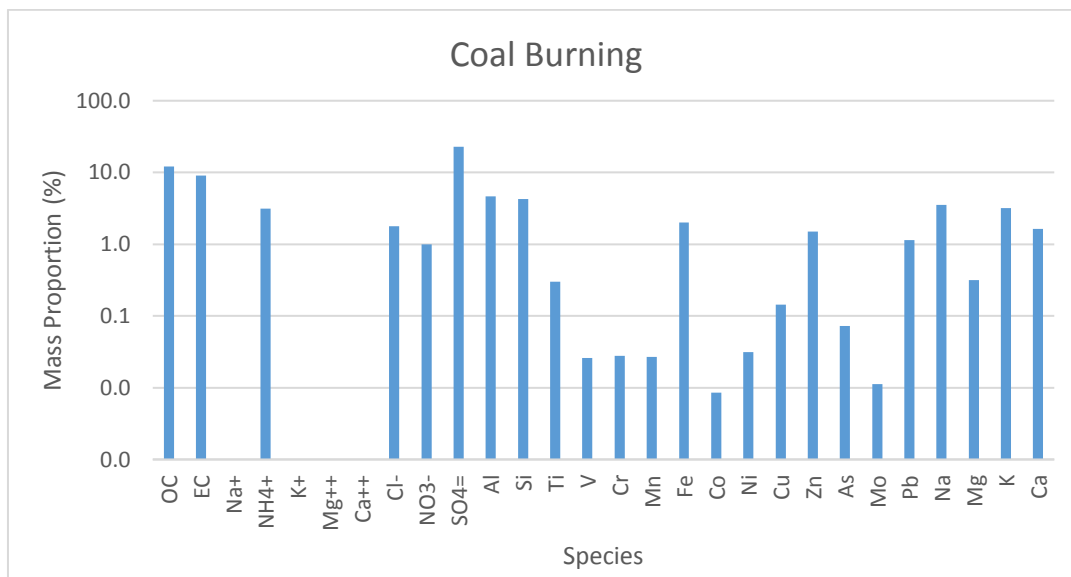


Figure 5-3 Chemical characterisation of coal burning profile China (Hao, 2008).

5.3.4 Secondary sulphate and nitrate

The secondary sulphate and nitrate are considered in the form of pure ammonium nitrate and ammonium sulphate (Zhang et al. 2016).

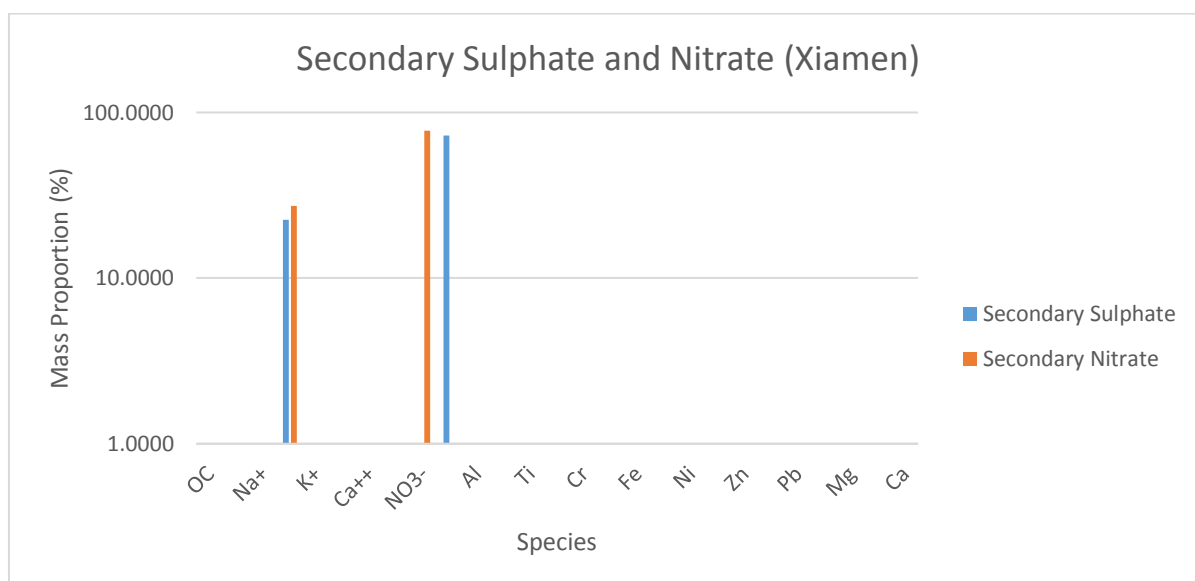


Figure 5-4 Source profile of secondary sulphate and nitrate (Zhang et al. 2016).

5.3.5 Diesel and petrol vehicle emissions

The vehicle exhaust profiles, including petrol and diesel vehicle emissions were collected at kerb side in Xiamen (Zhang et al. 2016). Chemicals include OC and EC, water-soluble ions and trace metal elements, which have been analysed by Sunset thermal/optical analyser, IC and ICP-MS (hang et al. 2016).

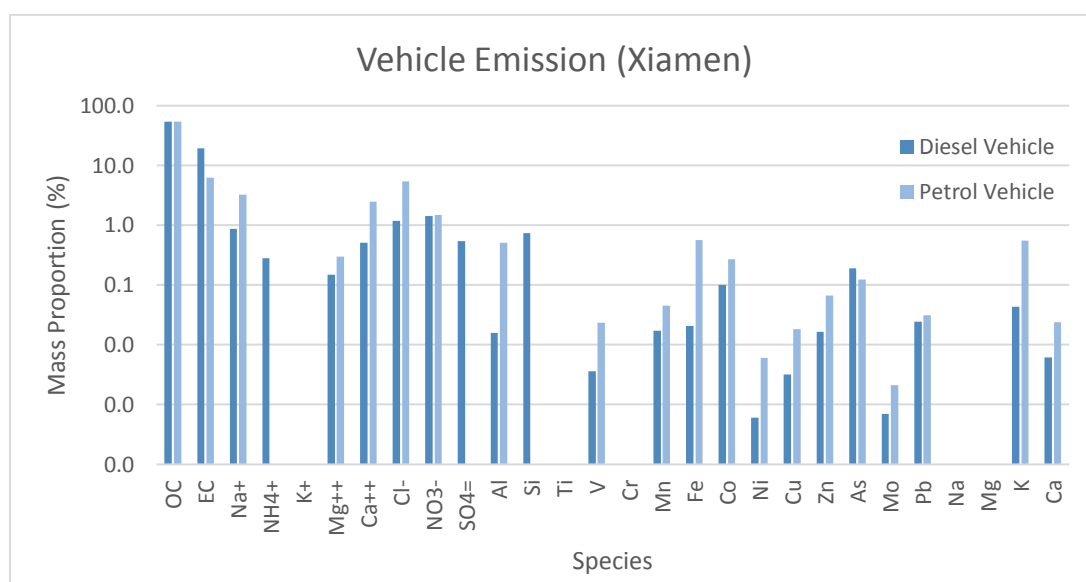


Figure 5-5 Chemical characterisation of vehicle exhaust profile in Xiamen, Eastern China.

The key components in both diesel and petrol vehicle emission are the exceptionally high amount of OC and EC from the emission, which both contribute more than 67% of total mass.

5.3.6 Metallurgic Plant

As Jinan is a highly industrialized city where played an important role in metallurgy, especially the iron and steel production. The metallurgic plant profile is chosen as data input in the CMB model. The metallurgic plant profile is also provided by College of Environmental Science and Engineering, NKU with same chemical analytical methods.

The PM_{2.5} of steel production plant emission was directly collected by DEKATI Electrical Low Pressure Impactor Sampler (ELPI®+) at the end of stack after the de-dusting.

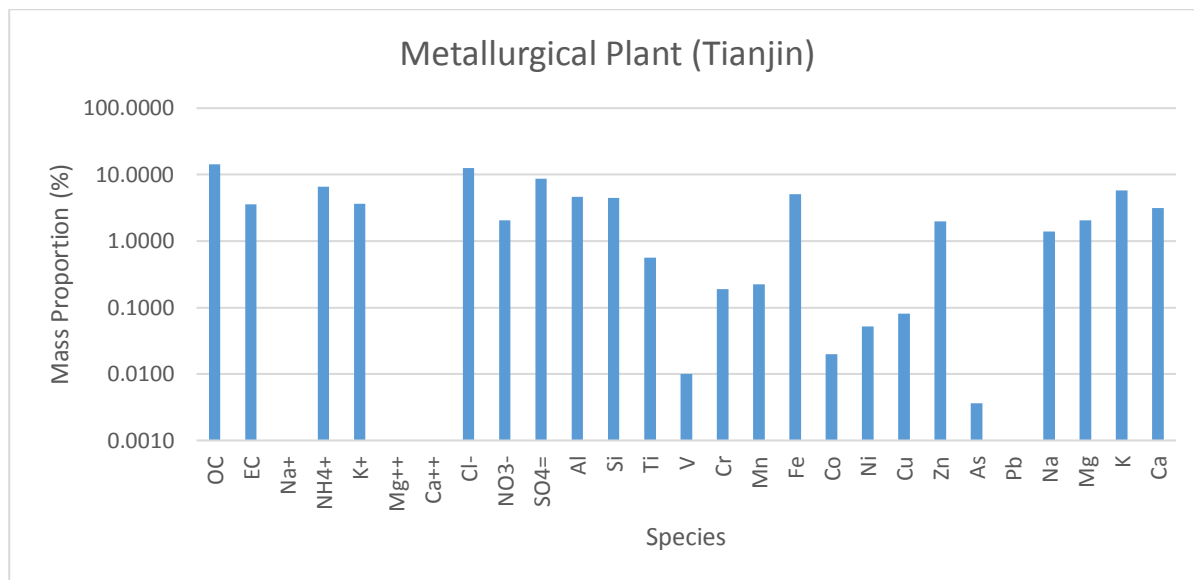


Figure 5-6 Chemical characterisation of metallurgic plant profile in Jinan, Northern China (Provided by College of Environmental Science and Engineering, NKU).

The chemical characteristics of metallurgy is more complex where is the no exceptionally high amount of any measured species but many components such as OC, Cl⁻, SO₄²⁻, Fe and K etc. These tracers can be also found in other sources such as biomass burning, soil dust and coal combustion. It suggests that it is highly complicated to industrial emission in terms of its chemical components.

5.3.7 The rejected source profiles

Table 5-3 the list of rejected profiles that have been used during the receptor modelling in CMB (% mass)

Species	CNG Vehicles	Fugitive Dust	Secondary Sulphate	Secondary Nitrate	Soil Dust (Jinan)	Road Dust (Jinan)	Coal Burning (Jinan)	Vehicle Exhaust (Jinan)	Vehicle Exhaust (Tianjin)	Mineral Dust (Tianjin)	Coal Burning (Tianjin)	Power Plant Emission (Tianjin)	Biomass Burning (Tianjin)	Wheat Straw Burning	Wood Burning	Corn residual burning
OC	35.262	5.3496	21.1	2.79	2.099734	10.23858	17.44875	37.42424	37.05	8.906901	19.52423	15.92389	53.07	41.96	40.24	37.7
EC	7.339	0.266	0.00197	1.87	2.221503	5.058115	3.959023	30.66667	30.36	1.207399	1.369084	2.90437	5.355	3.7	43.7	3.2
Na+	4.764	0.3823	0	0	0	0	0	0	0	0	0	0	0	0	0	0
NH4+	0	0.0196	11.1	9.82	0	0	0	2.444444	2.42	1.131024	4.952211	13.03148	0	4.14	0.37	3.17
K+	0	0.355	0	0	0	0	0	0	0	0.159883	1.618542	0.403172	12.22	4.08	3.58	9.08
Mg++	0.3022	0.114	0	0	0	0	0	0	0	0	0	0	0	0	0	0
Ca++	6.367	3.5508	0	0	0	0	0	0	0	0	0	0	0	0	0	0
Cl-	3.1986	0.1975	0	0	0.251099	0.48762	0.693528	0.888889	0.88	0.442407	4.271816	7.638745	7.125	8.11	4.74	17.02
NO3-	4.8542	0.1086	0.0188	53.2	0.085316	0.309089	0.110364	1.727273	1.71	0.44482	1.599974	2.292617	0.155	0.06	0.28	0.18
SO4=	0	0.4438	19.1	0.161	0.57685	5.470556	4.488694	8.656566	8.57	4.149322	31.44806	29.34889	0.72	7.8	1.09	2.43
Al	0	2.7185	0.223	0.0288	13.01393	11.21945	21.99526	3.686869	3.65	3.768147	3.487126	9.130542	0.66	0.008	0.203	0.015
Si	0.9923	4.5315	0.321	0.0103	51.27101	25.29202	26.72326	7.292929	7.22	5.815203	3.406073	6.397073	0.34	1.072	0.633	1.997
Ti	0	0.2084	0.0187	0.00826	1.185499	0.887826	1.60403	0.020202	0.02	0.106017	0.17854	0.344745	0.015	0.0011	0.004	0.0018
V	0.081	0.0039	0	0	0.028891	0.019479	0.029468	0.010101	0.01	0.01	0.01	0.01	0.01	0.0001	0.0001	0.0001
Cr	0	0.0046	0	0	0.120993	0.163882	0.073764	0.021212	0.02	0.113731	0.082822	0.973092	0.045	0.0001	0.0011	0.0004
Mn	0.1349	0.0691	0	0	0.259631	0.143115	0.092908	4.666667	4.26	0.090546	0.040814	0.138435	0.01	0.0002	0.0009	0.0005
Fe	0.2789	2.7181	0.00187	0.00308	9.016699	6.745549	5.53809	0.010101	0.01	3.035101	1.318774	4.053995	0.42	0.001	0.014	0.007
Co	0.7825	0.0063	0	0	0.061854	0.025274	0.026653	0.010101	0.02	0.02	0.02	0.02	0.02	0	0	0
Ni	0.0259	0.0014	0.00375	0.00435	0	0	0	0.020202	0.01	0.006448	0.038209	0.611434	0.025	0.0001	0.0002	0.0003
Cu	0	0.0056	0.0174	0.0193	0.033932	0.035899	0.035662	0.060606	0.06	0.699923	0.073744	0.137744	0.01	0	0	0
Zn	0.1608	0.0352	0.0318	0.0723	0.106257	0.228758	0.115807	0	0	0.145667	0.362148	0.122568	0.085	0.0323	0.0787	0.0142
As	0.5275	0.0005	0	0	0	0	0	0	0	0.016604	0.063684	0.003889	0.003889	0.0003	0.0003	0.0002
Mo	0.0461	0.0003	0	0	0	0	0	0	0	0	0	0	0	0	0	0

Species	CNG Vehicles	Fugitive Dust	Secondary Sulphate	Secondary Nitrate	Soil Dust (Jinan)	Road Dust (Jinan)	Coal Burning (Jinan)	Vehicle Exhaust (Jinan)	Vehicle Exhaust (Tianjin)	Mineral Dust (Tianjin)	Coal Burning (Tianjin)	Power Plant Emission (Tianjin)	Biomass Burning (Tianjin)	Wheat Straw Burning	Wood Burning	Corn residual burning
Pb	0.2001	0.0118	0.0252	0.0206	0.016869	0.014489	0.020646	0	0	0	0	0	0	0.0108	0.0066	0.0073
Na	0	0	0	0	3.805659	2.008597	0.991818	1.050505	1.04	0.600276	3.533556	0.895628	0.015	0.284	0.752	0.263
Mg	0	0	0	0	3.646468	3.722592	0.973737	0.090909	0.09	1.955369	0.863182	2.060929	0.16	0.006	0.011	0.005
K	0.0888	0.11239	0	0	3.835519	2.339901	1.291313	0.878788	0.87	0.798883	1.15471	0.363252	9.53	4.156	3.058	8.341
Ca	0	8.1701	0	0	8.362289	25.5884	5.915657	0.010101	0.01	8.535827	3.127555	3.767364	3.82	0.036	0.047	0.017

Other source profiles have also been used for the modelling process. However, the results do not meet the model's robustness requirement and criteria where r^2 and χ^2 are out of the range or more than 120% of mass have been explained.

5.4 Modelling Results and Model Performance

5.4.1 Annual source apportionment of $PM_{2.5}$ in Jinan

For the model setup, OC and EC, water-soluble ions including NH_4^+ , K^+ , Cl^- , NO_3^- , SO_4^{2-} and trace elements including Al, Si, Ti, V, Mn, Fe, Ni, Cu, Zn, Pb, Na, Mg and Ca have been chosen from the source profiles as input for the CMB modelling. On the other hand, the $PM_{2.5}$ and species concentration dataset is the same as what was input in PMF model. But it has been reformatted with respect to CMB requirement and annual average concentration is calculated for $PM_{2.5}$ apportionment throughout the sampling period in Jinan. In addition, Britt and Luecke function, which allows the source profiles used in the fit calculation to vary, is not selected and in use as it is not a fully tested method (USEPA, 2014) but source elimination is selected.

The modelling result is shown below in Figure 5-7.

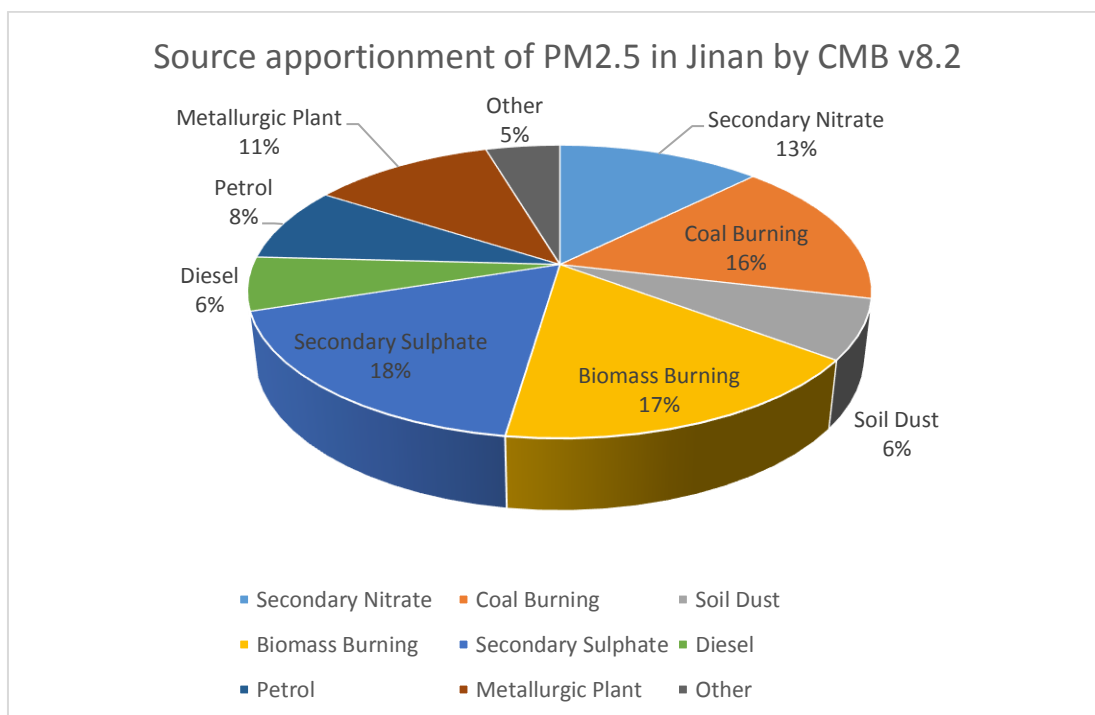


Figure 5-7 PM_{2.5} apportionment by CMB v8.2 in Jinan coupled with the PM_{2.5} profiles from China

According to Figure 5-7, secondary sulphate is found as one of the greatest contributors in Jinan, which is account for 18% of total PM_{2.5} mass. This is very likely to due to a large amount of precursor gases emitted from coal burning where have high intensity of coal combustion (Zhang et al. 2016). Meanwhile, CMB model suggests that the emission from coal burning accounts for 16% of the total PM_{2.5} mass. In addition, secondary nitrate accounts for 13% of the total PM_{2.5} mass in Jinan, which is another major source of fine particles. The CMB model also apportioned both petrol and diesel vehicles emissions successfully, where petrol vehicle contributes 8% and diesel vehicle contributes 6% of PM_{2.5} in Jinan annually. On the other hand, biomass burning is apportioned in CMB, which accounts for 17% of total PM_{2.5} mass. This is about three times greater than the estimation by levoglucosan enrichment factor analysis. This might be due to the differences between the real source profiles for the local biomass burning and the profile that used in this model.

As none of single biomass burning has worked including wood burning, wheat burning and corn burning, it is likely that the biomass burning in Jinan is consist of a few different biomass. Another possibility is that the biomass burning is away from the receptor so that the emitted chemicals have been massively aged (Li, et al., 2016). Finally, soil dust and metallurgic plant also have significant contribution to fine particles in Jinan, which are 6 and 11%.

The model performance is taken into account by the parameters mentioned above. The r^2 and χ^2 are 0.97 and 0.79, respectively. This suggests that the source contribution estimates explain the observation well with the fitting source profiles and species. In addition, C/M and R/U ratio for each species used in the CMB are all within the range of 0.75-1.5 and -2-2, respectively. This implies the CMB model run reproduced the individual ambient concertation by source contribution estimate well too. In summary, the profiles used in this CMB model run works reasonably for the $PM_{2.5}$ concentration dataset in terms of modelling performance criteria. It is a convinced result showing the impact to $PM_{2.5}$ by the major sources in Jinan.

5.4.2 Seasonal variation of source contributions to $PM_{2.5}$ in Jinan.

The average of seasonal $PM_{2.5}$ and individual species concentration were also used as input in the CMB models to assess the contributions of major sources during the different seasons. Model performance wise, the profile works fine in winter, early summer and autumn. The r^2 and χ^2 ranges between 0.90 to 0.96 and 1.29 to 1.94, respectively. The mass percentage is between 80.0 to 118%. However, the source profiles do not work well for summer season where its mass percentage is up to almost 120%, and χ^2 is over 2.0. The autumn has also experienced excessive χ^2 value. According to Figure 5-8, soil dust and coal burning remains

stable throughout the year. It implies that Jinan might be suffered by the coal burning related sources all year round. Meanwhile there is the relatively significant seasonal variations suggested by secondary sulphate and nitrate as well as biomass burning. As biomass burning is highly dependent on location and time (Yu et al. 2013; Yang et al. 2013), it is likely that more straws of wheat and corns were burn during the late early summer and autumn near Jinan. In addition, there is the particularly high percentage of nitrate in autumn (18%). However, the vehicle exhaust emission is down to 5% in autumn and there is 16% of unresolved $PM_{2.5}$ mass in this season. One possible explanation is that the some extra nitrate might be due to long-range transport with more complex contribution by other sources (Ge et al. 2017). Moreover, secondary sulphate formation was largely depressed during the winter in Jinan. This could be due to low RH and very low photochemical activity during the winter in Jinan so that there are not enough oxidants such as OH and H_2O_2 formation in favour of SO_2 conversion and aqueous phase oxidation is also limited. Therefore, the high amount of sulphate in winter may be more likely coming from the primary emission (Wang et al. 2014; Zheng et al. 2015).

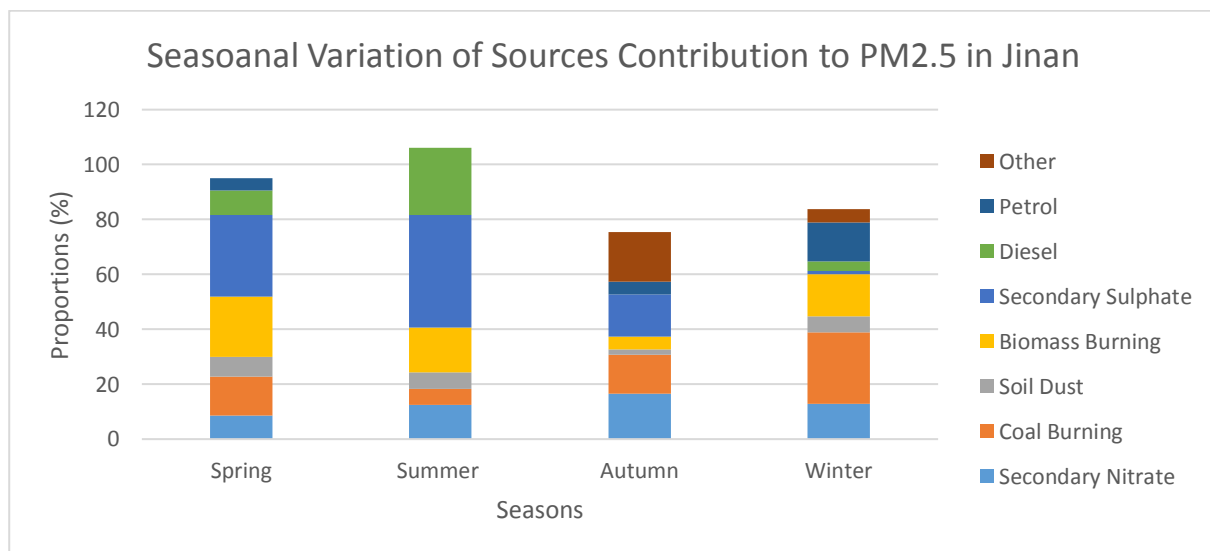


Figure 5-8 Seasonal variations of source contributions to $PM_{2.5}$ in Jinan.

5.4 Comparison between CMB modelling result and mass closure analysis

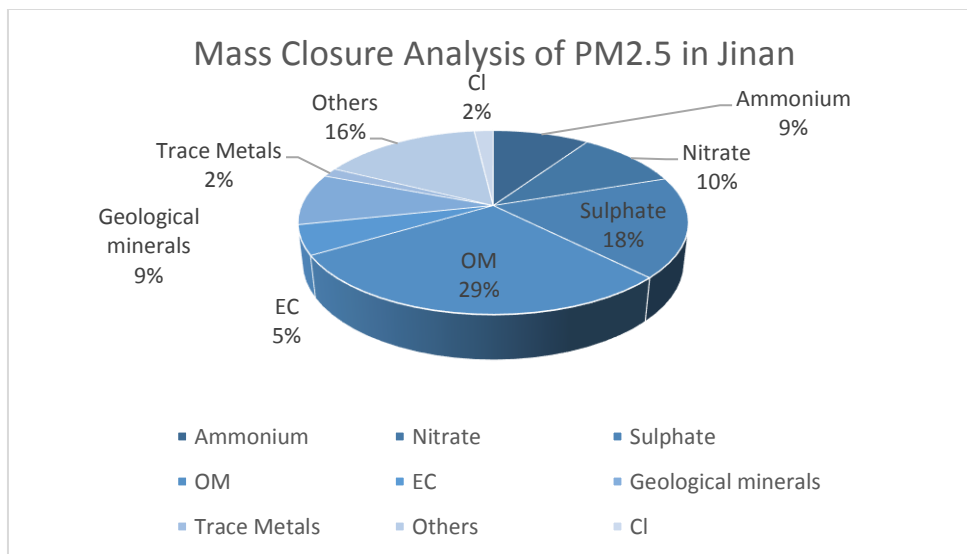


Figure 5-9 Annual PM_{2.5} Mass Closure analysis in Jinan

Figure 5-9 shows the results from Chemical Mass Analysis (CMC) which have been conducted in chapter three. In CMB, the annual soil dust accounts for 6% while the geological minerals accounts for 9%, respectively. Again, the CMB shows some good agreement with CMC since soil dust is part of the whole geological minerals and it is the major components of geological minerals in urban area. In addition, the secondary sulphate and nitrate in CMC are 17% and 10% while the result in CMB model is 15% and 12%. Since the profiles of secondary sulphate and nitrate have considered the contribution of secondary ammonium, CMB seems underestimate the impact from the secondary inorganic aerosols but still with some good agreement in terms of sulphate to nitrate ratio. Similar to the outcomes from PMF, it is possible that the biomass burning in CMB have taken into account some of SIA since secondary sulphate and nitrate will be formed quickly after the emission (Simoneit 2002) and there is considerable amount of nitrate, sulphate

and ammonium in the biomass burning profile. Overall, the results between CMB and CMC are similar.

5.5 Further work

There are two major improvements can be done based on the current work. Firstly, the local PM_{2.5} source profiles establishment is critical for source apportionment of PM_{2.5} by CMB in Jinan. It is also critical for PMF factors assessments. However, there is still a lack of PM_{2.5} source profiles in Jinan have been published. The profiles database (e.g. such as USEPA SPECIATE) establishment is highly recommended for the major cities in China and the database should be well-maintained and updated for the air quality assessments and source apportionments study.

Secondly, the source apportionment of PM_{2.5} and OC should be conducted by the profiles consists of more organic molecular markers. For example, Zheng et al. (2005) firstly apportioned the sources of OM and PM_{2.5} in Beijing by using CMB model with profiles which consists of large number of organic molecular markers. Though most of profiles are from USEPA database decade ago, there are also a couple of study specified the source profiles in terms of organic molecular markers have been established in China (Wang et al. 2008; He et al. 2006; Zhao et al. 2015; Zhang et al. 2007). A separate CMB modelling based on pure organic molecular markers can also be conducted for the PM_{2.5} dataset in Jinan for assisting the judgement of modelling results. The source apportionment of OC can be also helpful to assess the impact of SOC (Gelencser, A. et al., 2007).

5.6 Conclusion

In summary, source apportionment by CMB modelling with PM_{2.5} profiles collected in China has been conducted. Annually, eight major sources have been identified including

secondary Nitrate (13%), secondary sulphate (18%), coal burning t (16%), biomass burning (17%), metallurgic plant (11%), soil dust (6%), petrol vehicle emission (8%) and diesel vehicle emission (6%). 4% of total $PM_{2.5}$ mass has not been resolved. There are significant seasonal variations for a couple of sources including secondary sulphate and nitrate, and coal burning while the contribution from soil dust are more stable throughout the year. The CMB model works well with provided source profiles where all the modelling performance parameters meet the criteria. However, the establishment of local source profiles are still required. The CMB suggests that Jinan is suffered by industrial emission, biomass burning, vehicles emission and secondary inorganic aerosols massively. The results from CMB and PMF models should be further compared.

6 Chapter Six PMF and CMB Modelling Results Comparison

Abstract

In this chapter, the results generated by PMF and CMB on PM_{2.5} dataset of Jinan have been compared. Most of the sources have similar results annually except secondary sulphate where it might be overestimated by PMF model. There is more similarity on SIA and vehicle emission but greater differences in biomass burning, coal burning and mineral dust in terms of seasonal variation. The results of Jinan in this study is also compared with the previous study in Jinan and Beijing. Some significant similarity of PM_{2.5} pollution is found in both cities.

6.1 Introduction

There have been quite a few of inter-comparison of receptor models for PM source apportionment since both CMB and PMF have been introduced in China and elsewhere. Song et al. (2006; 2007) firstly compared the source apportionment results by a variety of receptor models including CMB, PMF and UNIMIX for the PM_{2.5} in Beijing where emissions from coal combustion and biomass burning have a good agreement. Another study has also focused on their applications for some certain study area and discussed the pros and cons to both CMB and PMF and what could be the best practice to evaluate the results from multiple modelling. For example, Querol et al. (2008) employed both PMF and CMB to apportioning the emission of PM₁₀ from the industry at an industrial urban background site. Querol et al. (2008) found that PMF might be more capable of identifying the origin of certain elements, e.g. using for industrial sources, while CMB is adept in

apportioning more sources depending on the available local experimental source profiles. Ke et al. (2008) compared the modelling results of PM_{2.5} source apportionment at Atlanta, GA, United States. Ke et al. (2008) found that CMB is powerful when apportioning the sources with clear and unique markers, e.g. wood combustion and vice versa. Both PMF and CMB were performing less well while apportioning the motor vehicle exhaust as diesel and petrol emission as it is hard to split due to their similar carbonaceous fractions (Ke, Liu, Wang, Armistead G. Russell, et al. 2008).

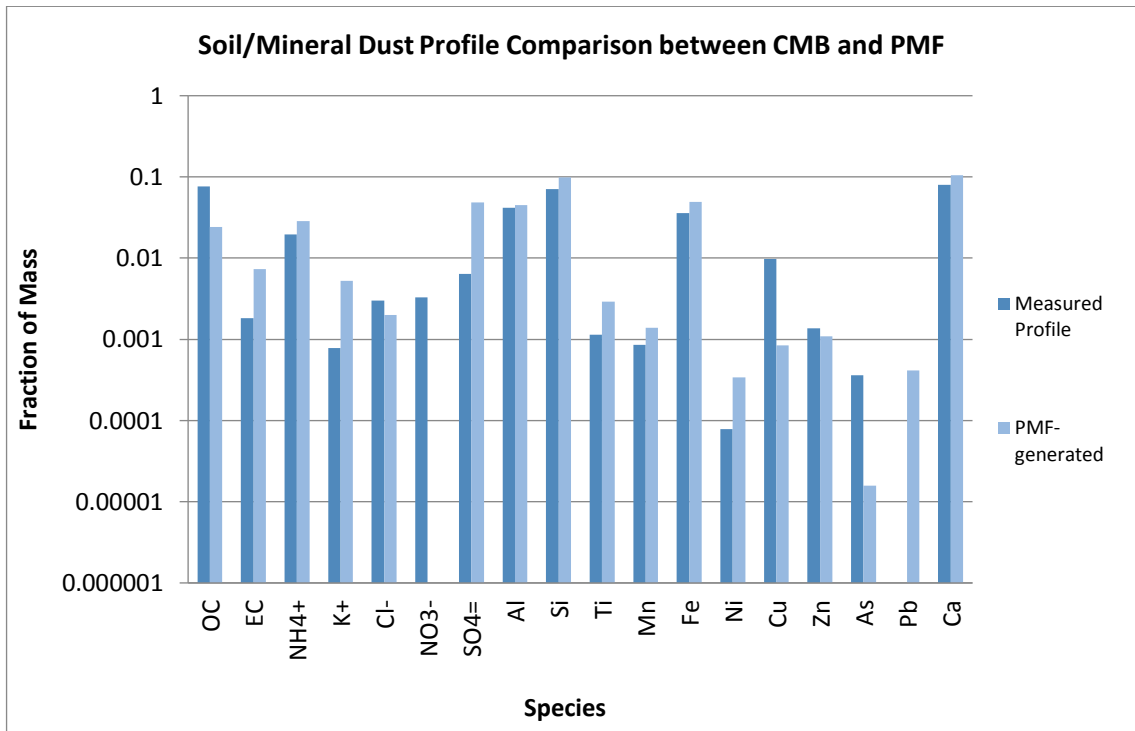
One of the key benefits of source apportionments by multiple methods is that it helps to assess the uncertainties in the modelling results and evaluate what could be a more robust interpretation of the results (Lee et al. 2008). However, there is not many case study on multiple receptor modelling on PM_{2.5} recently in China and there is lack of multiple receptor modelling for PM_{2.5} in Jinan in particular. In this chapter, the results between CMB and PMF on Jinan's PM_{2.5} are compared. In addition, the results are also compared with other similar source apportionments in Jinan and other northern Chinese cities. The similarity of the results and the causes of the differences will be discussed.

6.2 The PMF and CMB results comparison in this study

6.2.1 Profile Comparison

The PMF-generated profiles (or factor profiles) and measured profiles that used in CMB have been compared. There are six common sources have been apportioned by both receptor models, which are secondary nitrate, secondary sulphate, biomass burning, coal burning, mineral/soil dust and vehicle emissions. Overall, soil and mineral dust, secondary sulphate and nitrate and vehicle exhaust show good agreement in terms of profiles where biomass burning has more differences.

a)



b)

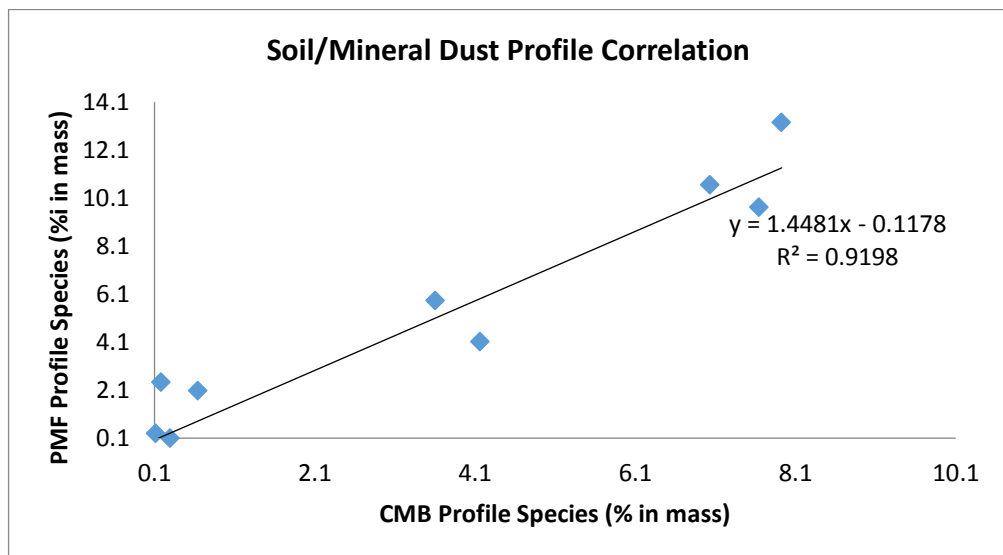
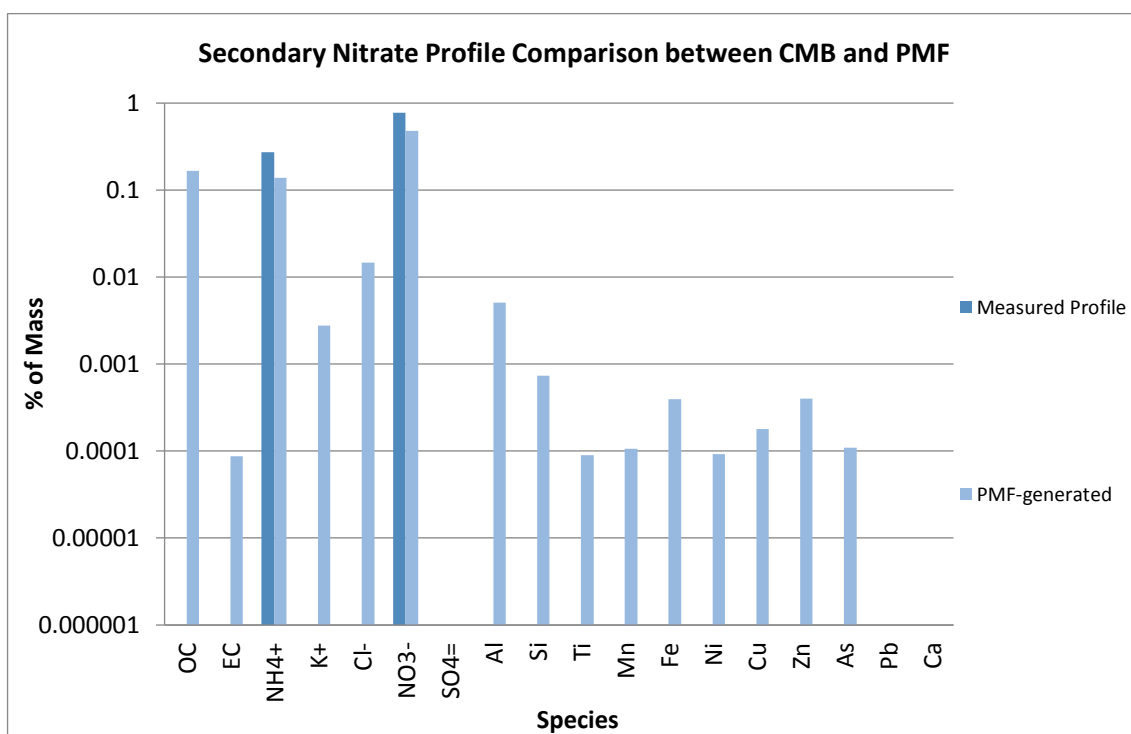


Figure 6-1 a) source (or factor) profiles of soil or mineral dust comparison (Provided by College of Environmental Science and Engineering, NKU); b) species abundances correlations between measured and PMF-generated profiles for soil/mineral dust

First of all, Figure 6-1 shows the comparison between the soil dust profile used in CMB and PMF-generated profile representing mineral dust. Both profiles are rich in Al, Si, Fe and Ca, which drives the contribution to these two sources. Both Ca and Si have high

abundances in these profiles and they have a similar amount in each profile. Therefore there is a good correlation between the measured and PMF-generated profiles ($r^2 = 0.92$). However, the gradient is about 1.44 which suggests that there is less other constituents that has been derived by PMF. This may result in more uncertainty in the PMF results. On the other hand, as CMB suggests that the contribution by soil dust accounts for 6% to $PM_{2.5}$ in Jinan while PMF suggests that the contribution by mineral dust is 10%. It might also imply that soil dust could be one of the major contributors to the mineral dust in Jinan too.

a)



b)

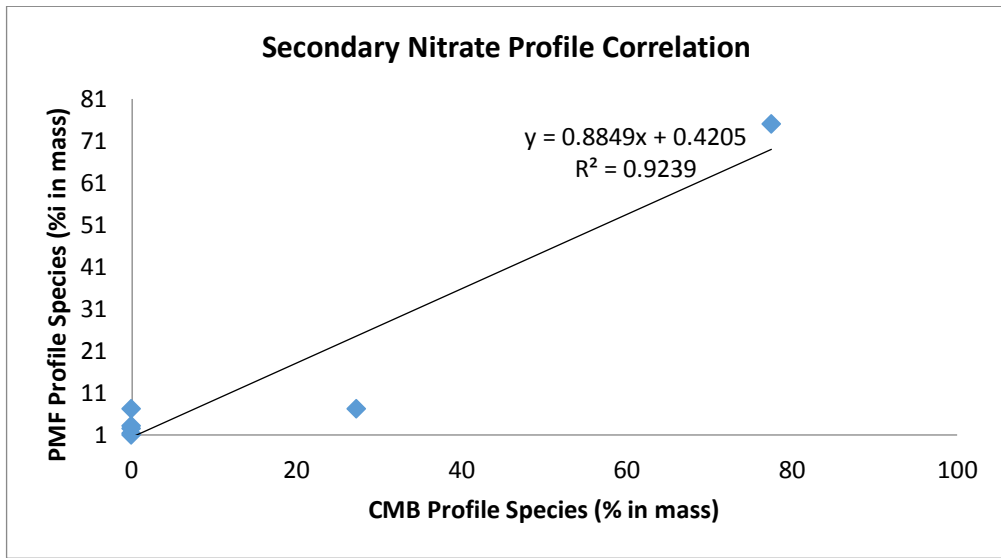
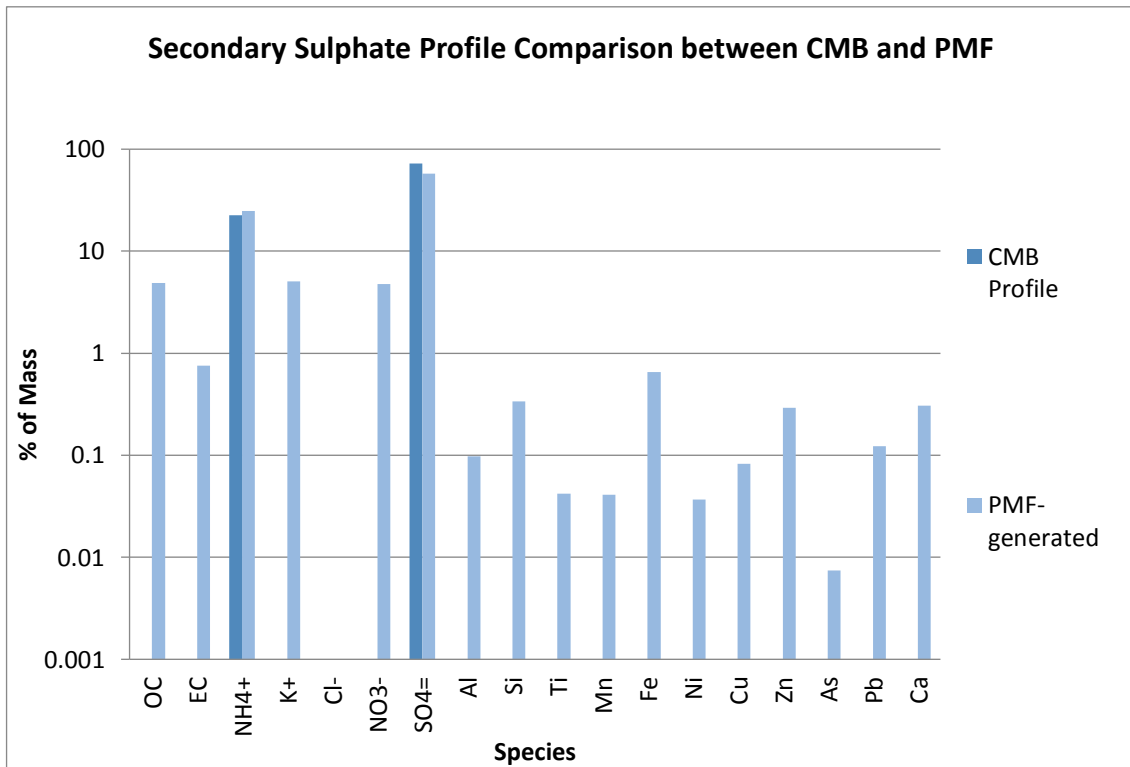


Figure 6-2 a) source (or factor) profiles of secondary nitrate comparison (Zhang et al. 2016) species abundances correlations between measured and PMF-generated profiles for secondary nitrate

a)



b)

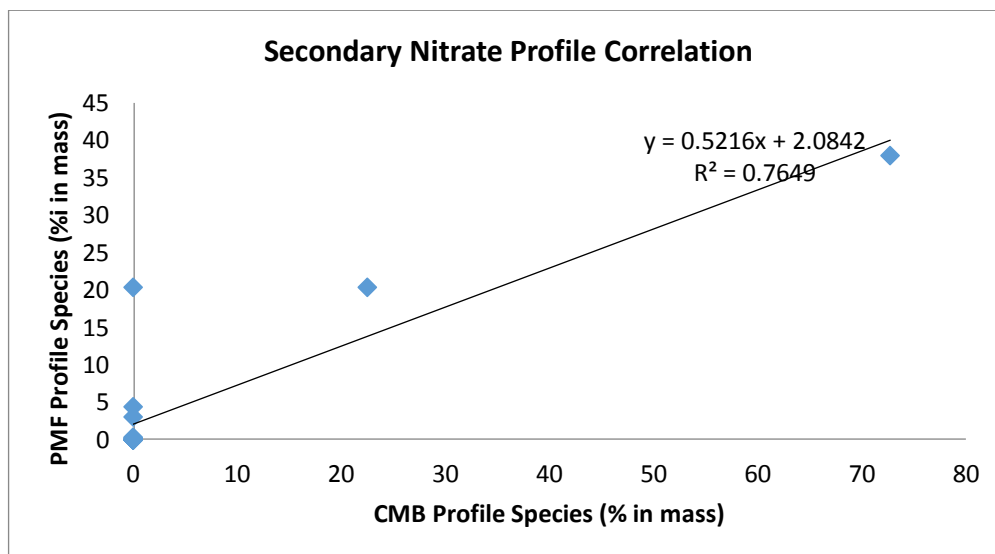
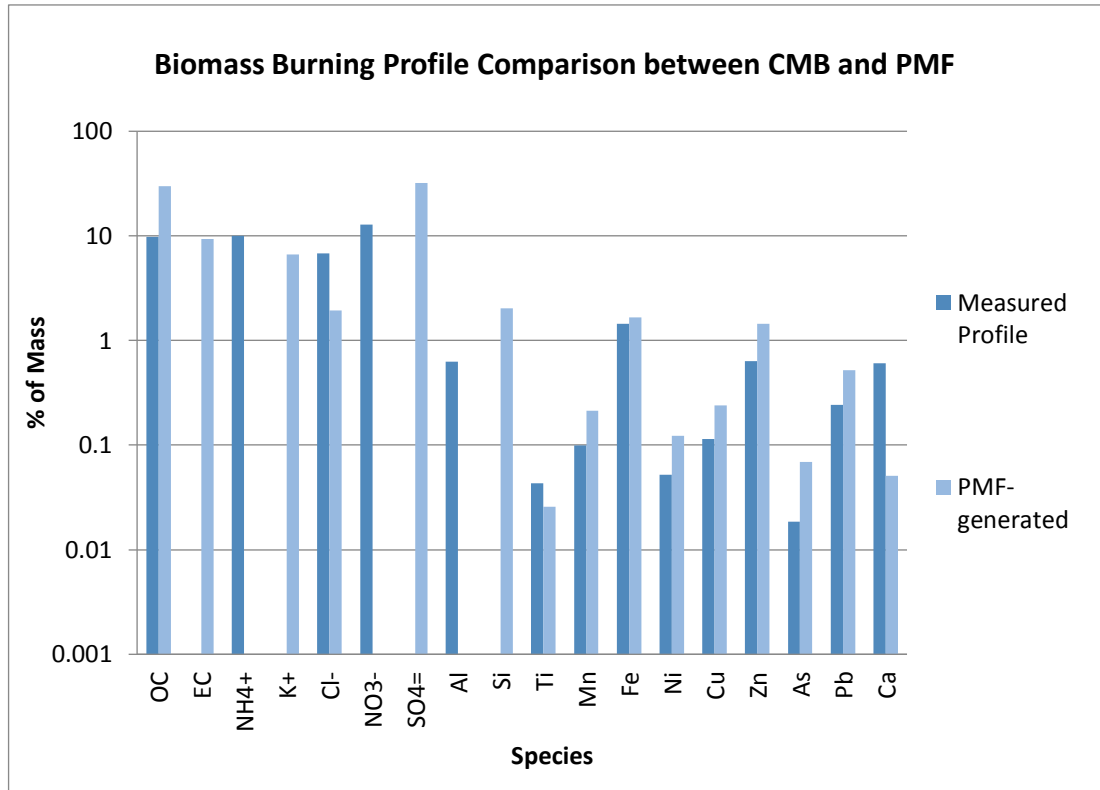


Figure 6-3 a) source (or factor) profiles of secondary sulphate comparison (Zhang et al. 2016); b) species abundances correlations between measured and PMF-generated profiles for secondary sulphate

Figure 6-2 and Figure 6-3 show us the comparisons between the secondary nitrate and sulphate profiles used in CMB and PMF-generated profiles representing secondary nitrate and sulphate, respectively. In CMB, both secondary nitrate and secondary sulphate are considered as pure NH_4NO_3 and $(\text{NH}_4)_2\text{SO}_4$, respectively (Zhang et al. 2016). However, there is a significant amount of OC suggested in both secondary nitrate and sulphate profiles generated by PMF, implying the influence of the SOA formation during the secondary nitrate and sulphate formation (Lee et al. 2008). In addition, the molar ratios of ammonium to nitrate and ammonium to sulphate in the PMF-generated profiles are 1.05 and 2.42, respectively. These suggest that the nitrate and sulphate have been highly neutralized in the ambient air and they are mainly in the form of NH_4NO_3 and $(\text{NH}_4)_2\text{SO}_4$, which is the reason why the measured profiles and PMF-generated profiles have a good correlation (Tian et al. 2013). High loading of OC and trace elements in both factor profiles also suggest that there

could also be some influence from the secondary organic aerosol and some covariance with other sources including coal combustion and traffic emissions (Zíková et al. 2016).

a)



b)

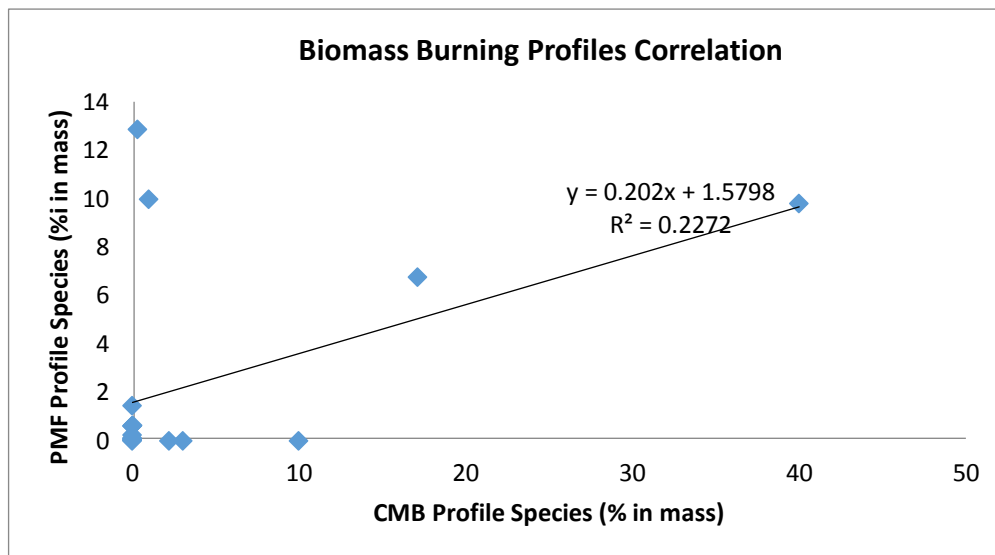
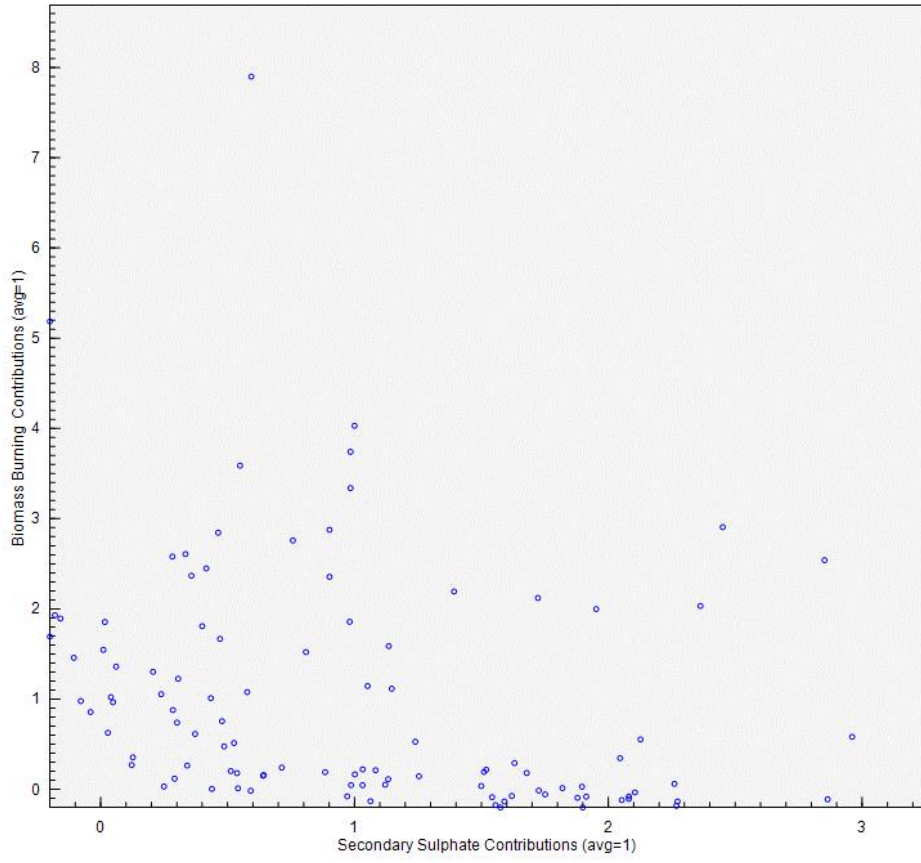


Figure 6-4 a) source (or factor) profiles of biomass burning comparison (Zhang et al. 2016); b) species abundances correlations between measured and PMF-generated profiles for biomass burning emissions.

In Figure 6-4, the biomass burning profile and measured biomass burning profiles have been compared. There are great disagreements on these profiles than other comparisons. The main differences occur between the loadings of EC, NH_4^+ , NO_3^- and SO_4^{2-} , though more agreements have been found between trace metals. This probably due to the PMF-generated profiles represent more complex sources rather than the biomass burning only. The Biomass burning factor apportioned by PMF may have the impact from the secondary sulphate and coal burning. This is suggested by the G-plot in Figure 6-5 below. Figure 6-5 implies that the biomass burning and secondary sulphate have some correlation to some extent and this may result in some rotational ambiguity which makes the PMF biomass profile differs even more than measured biomass burning profile. There is a similar trend between biomass burning and coal burning too.

a)

G-Space Plot - Run 77



b)

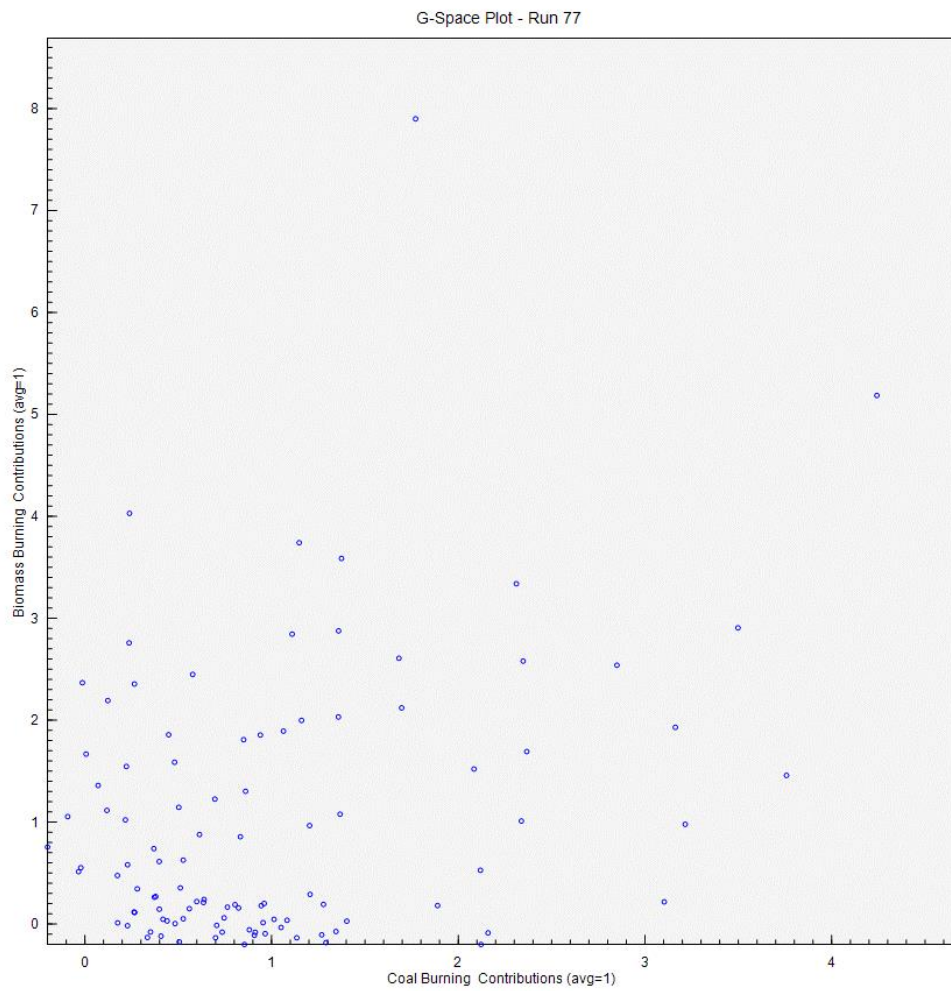
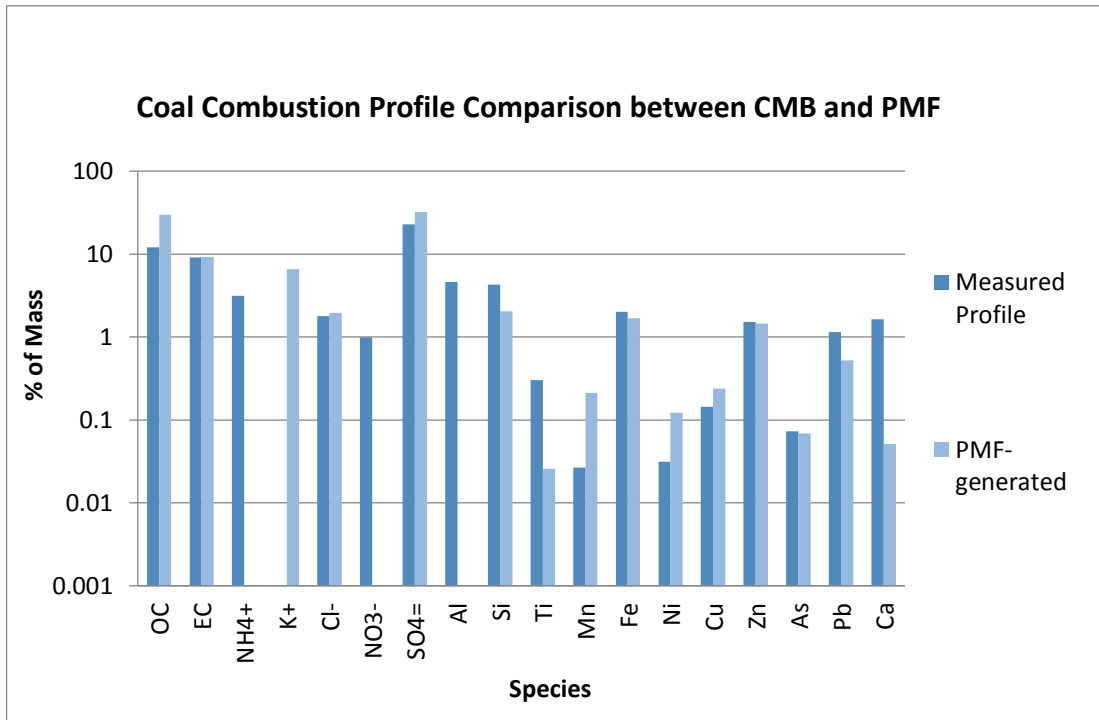


Figure 6-5 a) correlation between PMF modelled biomass burning and measured biomass burning profile; b) G-plot between PMF modelled biomass burning and secondary sulphate; PMF modelled biomass burning and coal burning.

a)



b)

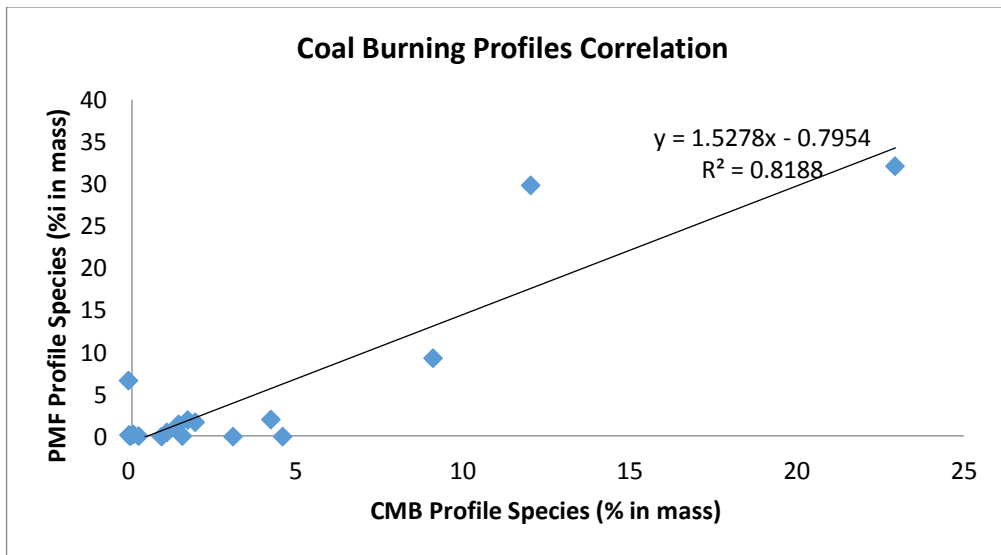
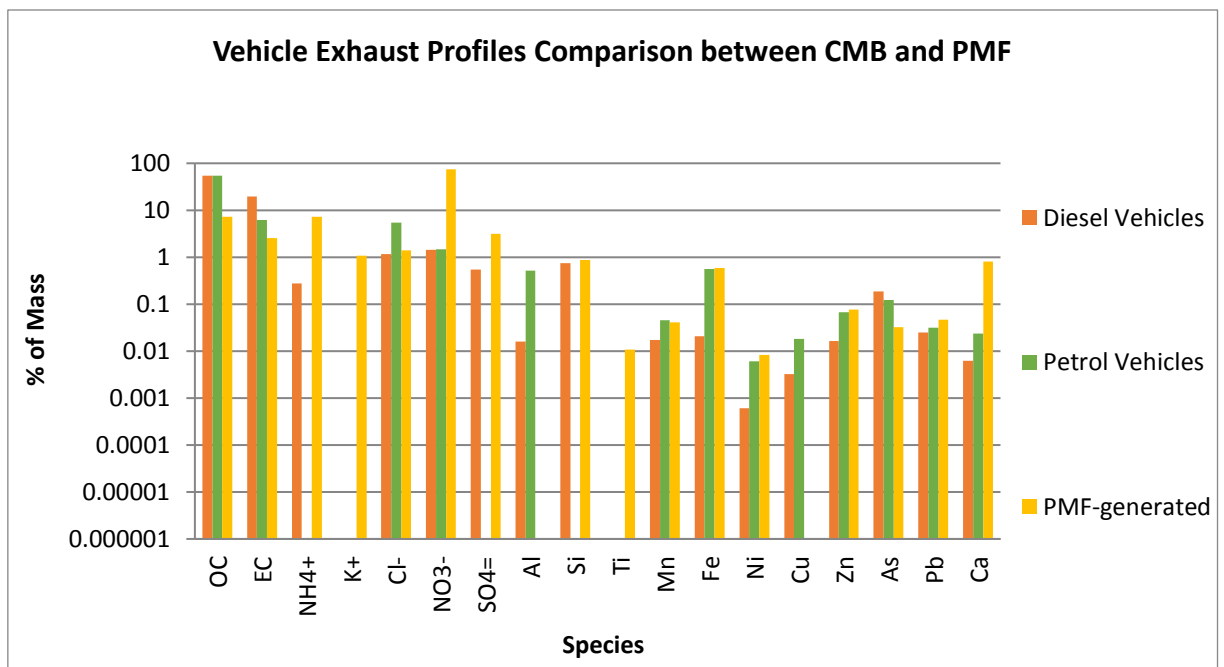


Figure 6-6 a) source (or factor) profiles of coal burning comparison; b) species abundances correlations between measured and PMF-generated profiles for coal burning

The coal burning emission profile and measured coal burning profiles have been compared. The PMF coal burning factor and CMB profiles show some good agreement in OC and EC as well as Cl⁻, Fe and NH₄⁺. However, the PMF-generated profile failed to recreate the

existence of Al, which is unrealistic (Zhang et al. 2016). Therefore the correlation between these two profiles is relatively poorer than secondary inorganic aerosols. In addition, Se is another one of the most influential markers which helps for the source identification except Cl. But Se is not helpful in the CMB modelling which also implies the importance of developing local profiles. There is still some room to optimize on apportioning this source. Overall, PMF generates similar profiles compared to the measured source profile that used in CMB. Both models also suggest similar mass contribution of coal burning emission to the PM_{2.5} in Jinan. Therefore, another good agreements have achieved

a)



b)

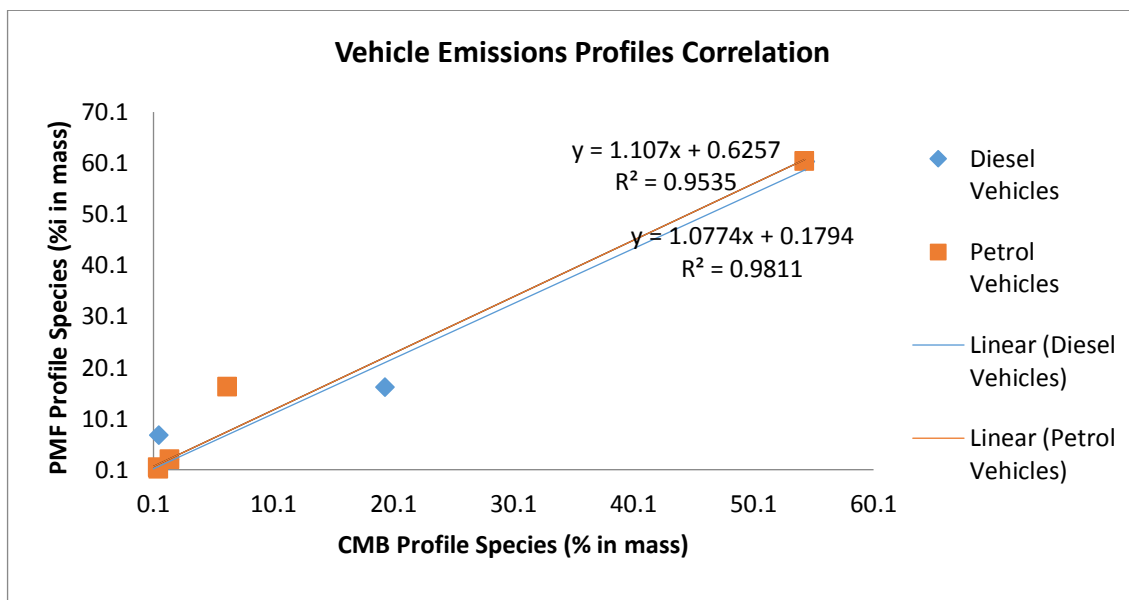


Figure 6-7 a) source (or factor) profiles of petrol car/vehicle exhaust comparison; b) species abundances correlations between measured and PMF-generated profiles for petrol car/vehicle exhaust

Figure 6-7 shows that there is a good agreement between the profiles of vehicle exhaust used in CMB and PMF. This is largely due to the agreements on OC and EC where OC is a very important marker of vehicle exhaust (Zhang et al. 2016). However, some differences still remain. For example, the PMF-generated profile suggests more Al, Fe and Ca contribution, implying the importance of road dust (Viana et al. 2008). In addition, there is much more NO_3^- in CMB measured profile where suggest greater influence from the tailpipe.

6.2.2 Annual Source Contribution

The inter-comparison of CMB and PMF on sources contribution is presented here. The annual and seasonal source contribution apportioned by both models are compared. As discussed before, both models have shown the similar number and type of emissions sources, which is the foundation for a useful comparison (Lee et al. 2008).

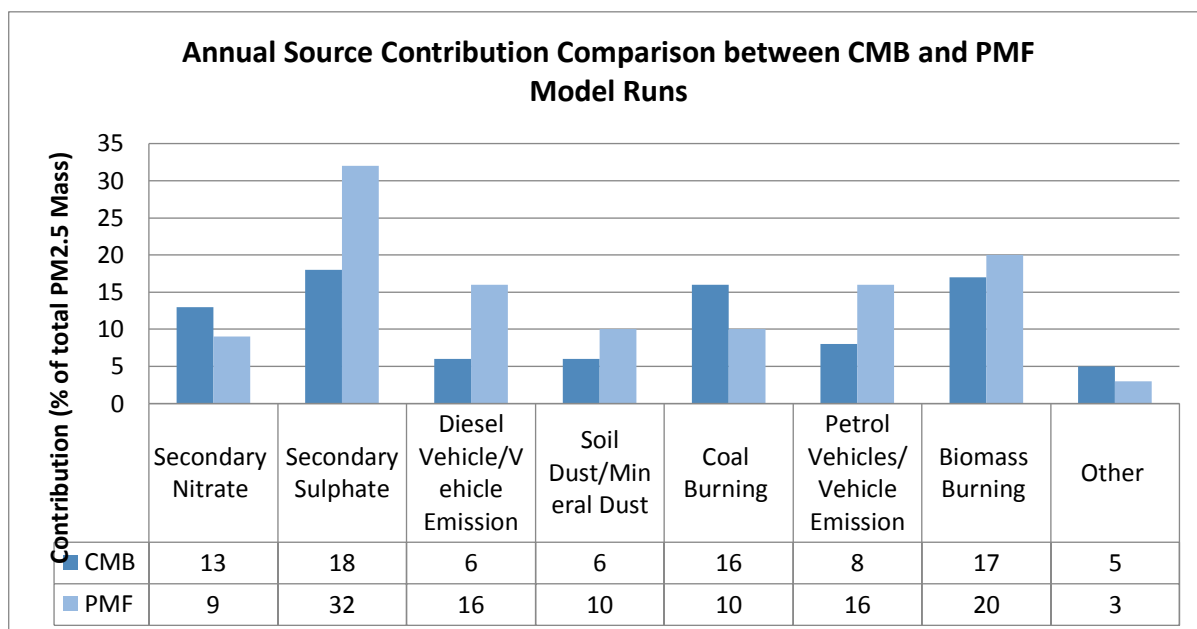


Figure 6-8 the comparison of source apportionment of PM_{2.5} results by CMB and PMF model run

Figure 6-8 summarizes the contribution from all the sources identified in both CMB and PMF. Overall, most of the sources have similar contributions except secondary sulphate and coal burning. Regarding SIA, the secondary nitrate estimation is 13 and 9% in CMB and PMF, respectively. However, CMB suggests the contribution of secondary sulphate is only 18% in Jinan but this figure is almost doubled in PMF. According to mass closure analysis, the sulphate contributes to 17% of total sampled PM_{2.5} mass. Hence, PMF might overestimate the secondary sulphate in the modelling. On the other hand, the coal burning has less contribution suggested by PMF than CMB. It is likely that the PMF's secondary sulphate factors have considered some other contributions from SOA formation and other primary emissions such as coal burning. This is supported by their factor profiles that there is some amount of OC appearing in these two profiles.

Moreover, the secondary formation of biomass burning may also contribute to the mass of SIA, particularly the secondary sulphate in this study, which may result in overestimation.

There could be some portion of K^+ contribute the factor profile of secondary sulphate in factor profile and this could be coming from the biomass burning, which is supported by the G-plot (See Figure 6-9). The clear edge suggest that there is correlation between biomass burning and secondary sulphate too. By using levoglucosan, 4% of mass contribution to $PM_{2.5}$ by biomass is estimated only. Furthermore, the primary emission of KCl may have been almost transferred to K_2SO_4 and KNO_3 by heterogeneous reactions during the long-range transportation from rural area near Jinan to urban Jinan (Li et al. 2010).

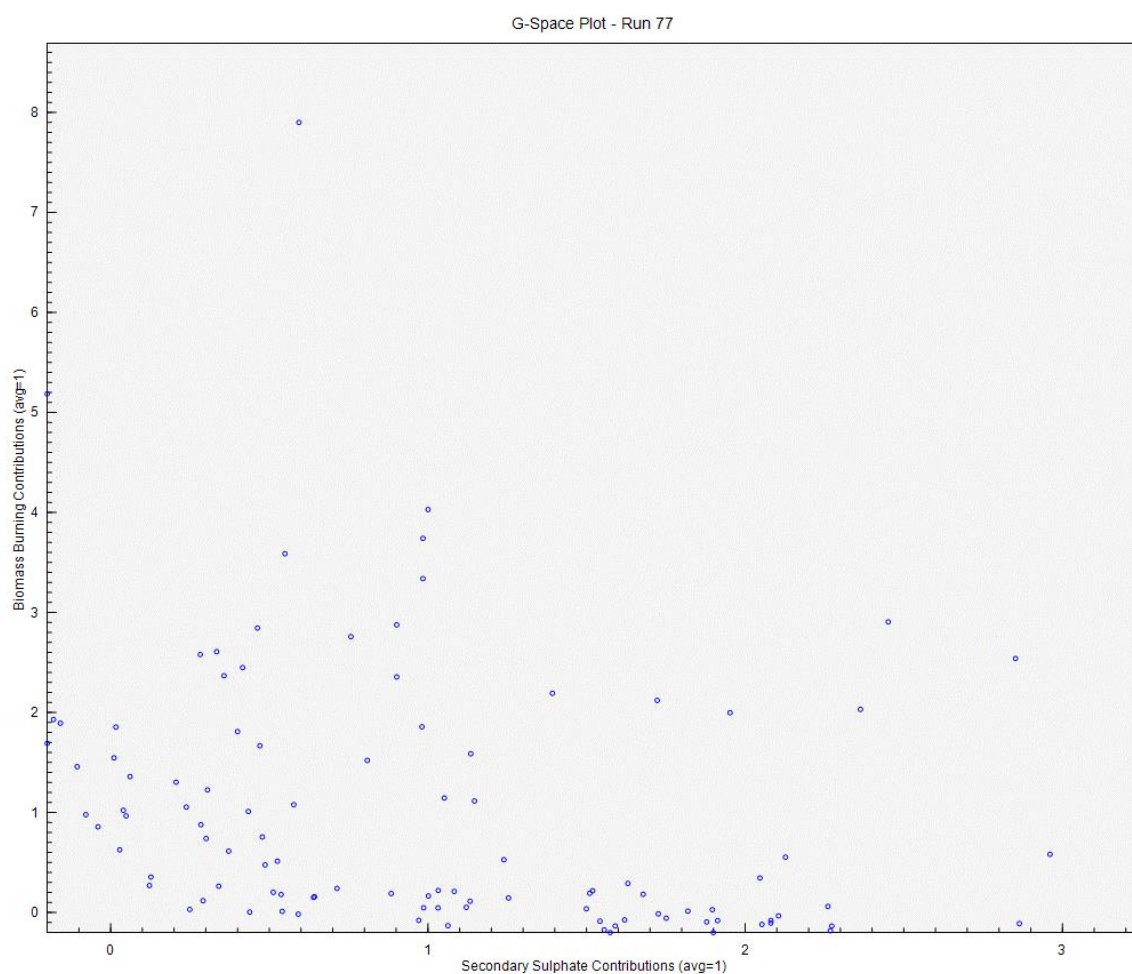


Figure 6-9 the G-plot of biomass burning against secondary sulphate factor

Regarding, vehicle exhaust, CMB has similar estimation against PMF if diesel and petrol emission are summed up. Meanwhile, the contribution of soil dust from CMB is also similar to PMF. As discussed earlier, both factors have shown good correlation between CMB and PMF results. Therefore the agreements on these two factors are high. On the other hand, biomass burning also achieved similar contribution in both models. But K^+ and Cl^- are mainly driving this source in CMB while Cl^- and levoglucosan mainly drive the biomass burning factor in PMF, which is a big difference. Regarding coal burning, the source contributions in both models are close too. The agreements on annual contribution is good in this study.

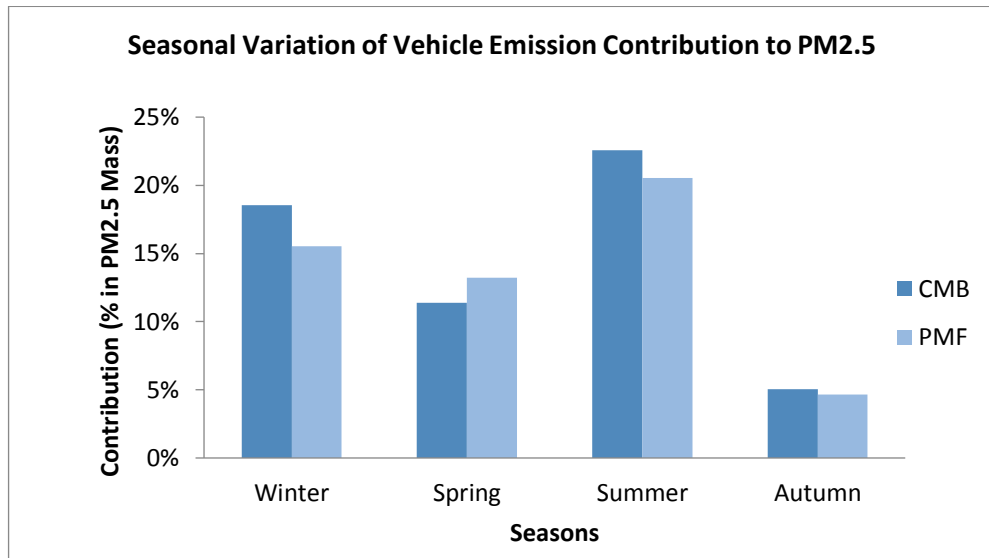
6.2.2 Seasonal Source Contribution and Daily Source Contribution

Except the overall annual source contributions have been compared, the seasonal and daily variation has been also discussed. Both Table 6-1 and Figure 6-10 present the seasonal variations of sources contribution apportioned by two different models. For the convenience, P1 and P5 is combined together to represent winter period.

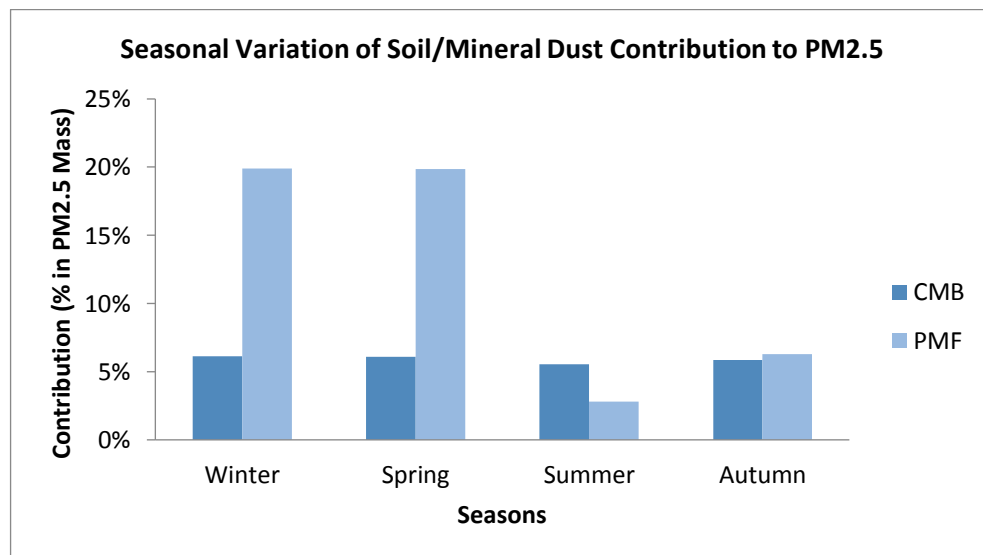
Table 6-1 Seasonal Source Apportionment of PM_{2.5} in Jinan by both CMB and PMF

Sources	Winter		Early summer		Summer		Autumn	
	CMB	PMF	CMB	PMF	CMB	PMF	CMB	PMF
Petrol Vehicle Emission	15%	16%	4%	13%	0%	21%	5%	5%
Biomass Burning	16%	22%	19%	4%	15%	1%	14%	26%
Coal Burning Power Station	27%	13%	12%	20%	5%	12%	16%	14%
Diesle Vehicle Emission	4%	16%	8%	13%	23%	21%	0%	5%
Secondary Sulphate	1%	4%	25%	21%	37%	27%	17%	18%
Secondary Nitrate	13%	11%	7%	9%	11%	16%	18%	27%
Metallurgic Plant	13%	0%	19%	0%	3%	0%	5%	0%
Soil Dust	6%	20%	6%	20%	6%	3%	6%	6%
Other	5%	0%	0%	0%	0%	0%	20%	0%

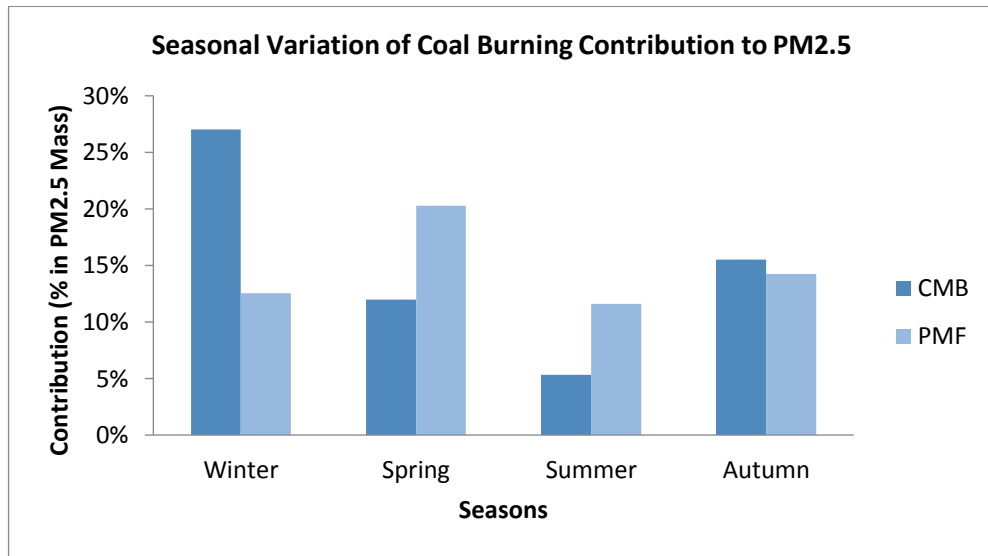
a)



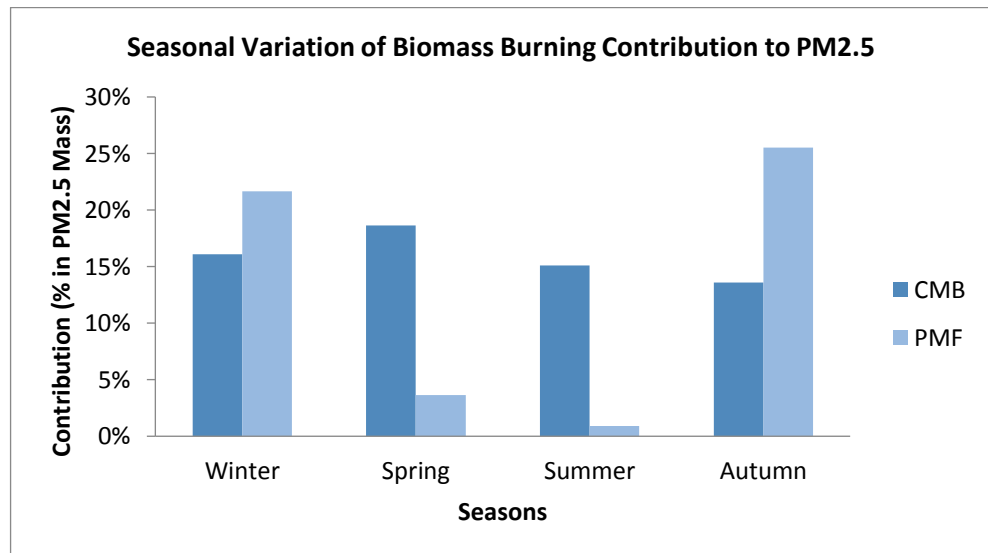
b)



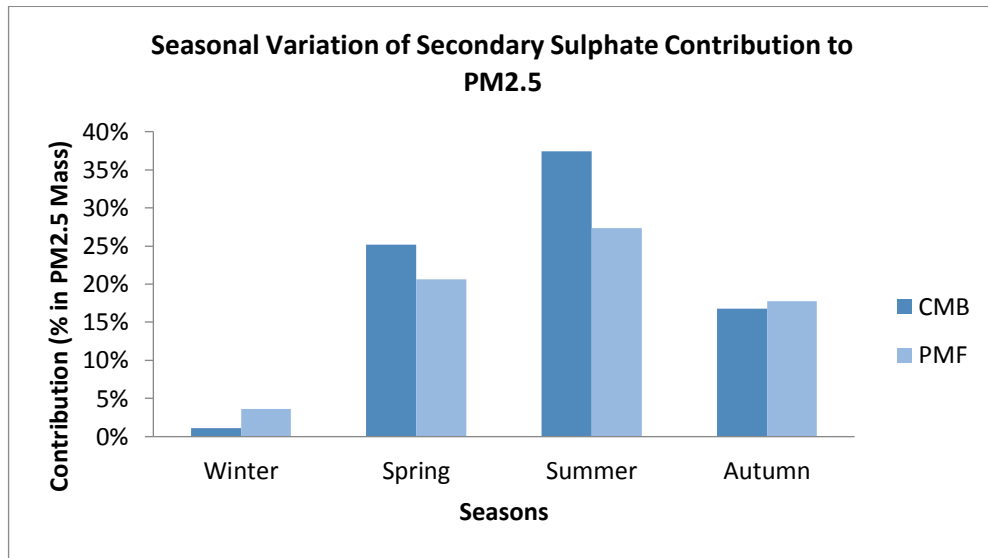
c)



d)



e)



f)

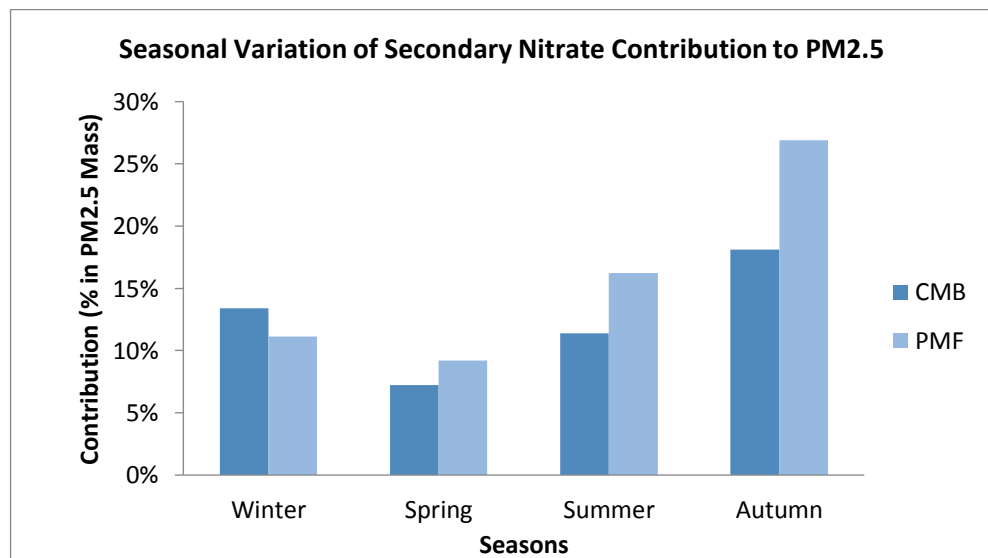


Figure 6-10 a) – f) Comparison of seasonal variations of PM_{2.5} apportionments for vehicle emission, soil/mineral dust, coal burning, industrial emission, secondary sulphate and secondary nitrate, respectively, by CMB and PMF.

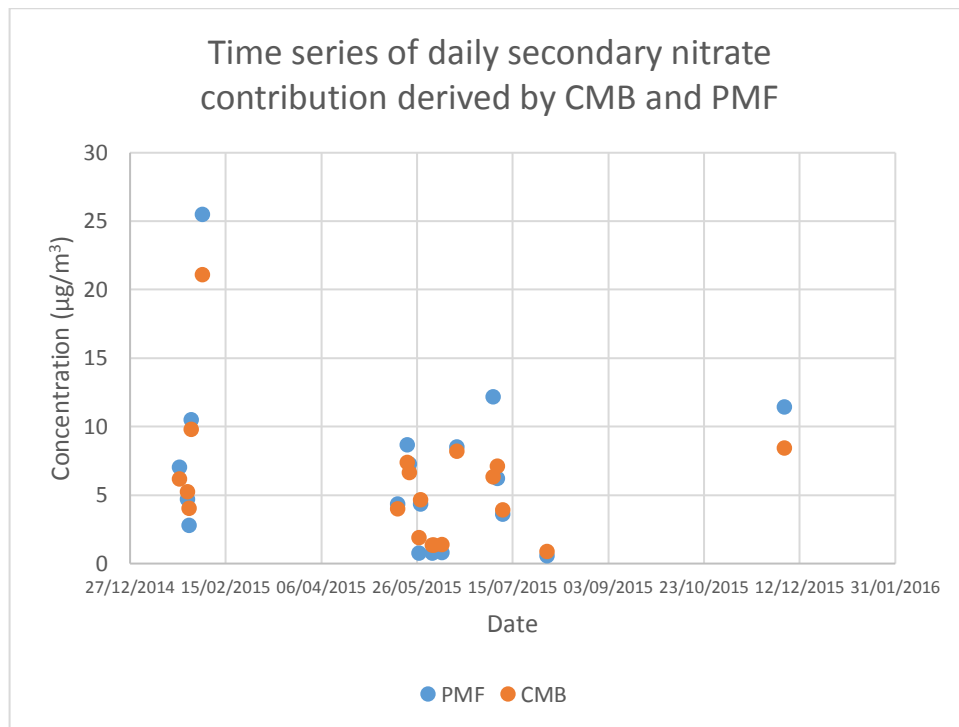
As mentioned in Chapter 5, the CMB modelling for summer has poor performance and the sources contribution have been overestimated. Apart from it, both models show some good agreement overall in four seasons, particularly for vehicle emission and SIA. However, there are some major differences for soil and mineral dust, coal burning and biomass burning. For instance, there is a stable contribution to PM_{2.5} from soil dust in Jinan but the mineral dust varied in different seasons. The mineral dust has greater emission in winter and early summer but the much smaller contribution in summer and autumn by PMF. This could be due to the sources of mineral dust in winter and early summer is more complex. Some study suggests that there is also a significant amount of Al, Fe, Si in the particles that left after coal combustion process (Kong et al. 2011; Pei et al. 2016). Hence, the mineral dust may therefore affect by coal-burning too in winter and autumn. This may also explain why there is less coal burning contribution than the expectation in autumn by PMF. ($\mu\text{g}/\text{m}^3$)

Meanwhile, CMB estimates that there is greater emission from coal burning in winter and autumn but less emission in early summer and summer. Compared to CMB, PMF suggests that the contribution from these sources is much more stable throughout the year. The trend by CMB is relatively closer to the expectation since more coal has been burnt during winter and autumn for domestic heating in north China. The difference might suggest that the coal burning profile used in CMB fit the real coal combustion profiles in Jinan well. Finally, there are a few common issues on seasonal variations of secondary sulphate, nitrate and vehicle emissions although they are similar to each other from both modelling simulations. It seems that both CMB and PMF underestimated the vehicle emission in autumn while secondary nitrate and sulphate have been overestimated in autumn

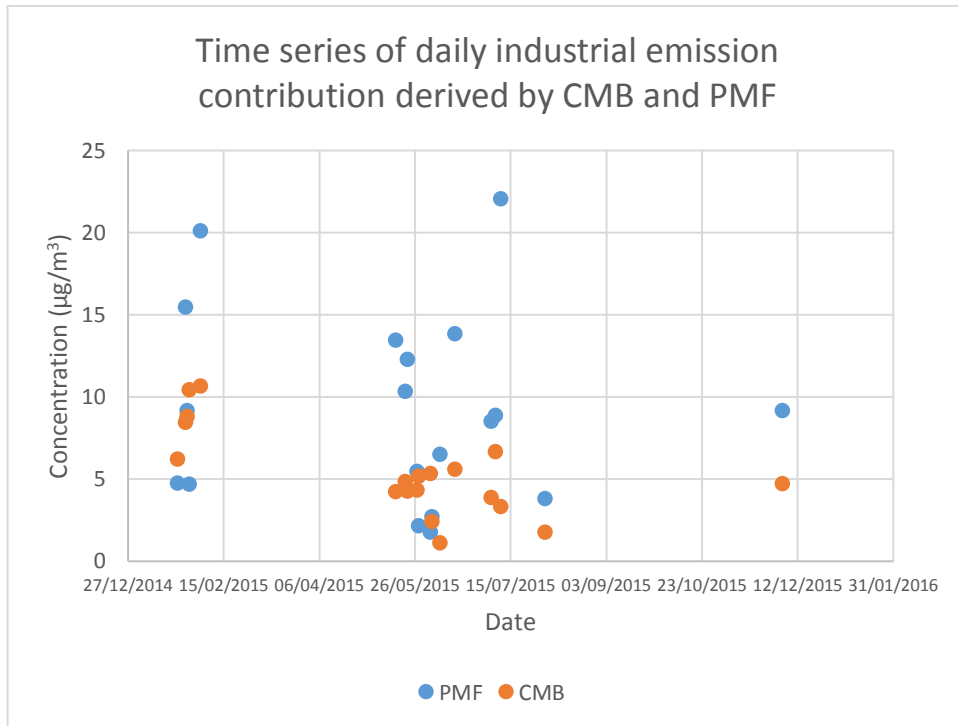
massively. The reason that results in this outcomes may be due to both model leave relatively large portion of unresolved $PM_{2.5}$ mass in the outcome.

On the other hand, figure 6-11 shows the comparison of results between PMF and CMB in terms of daily variation.

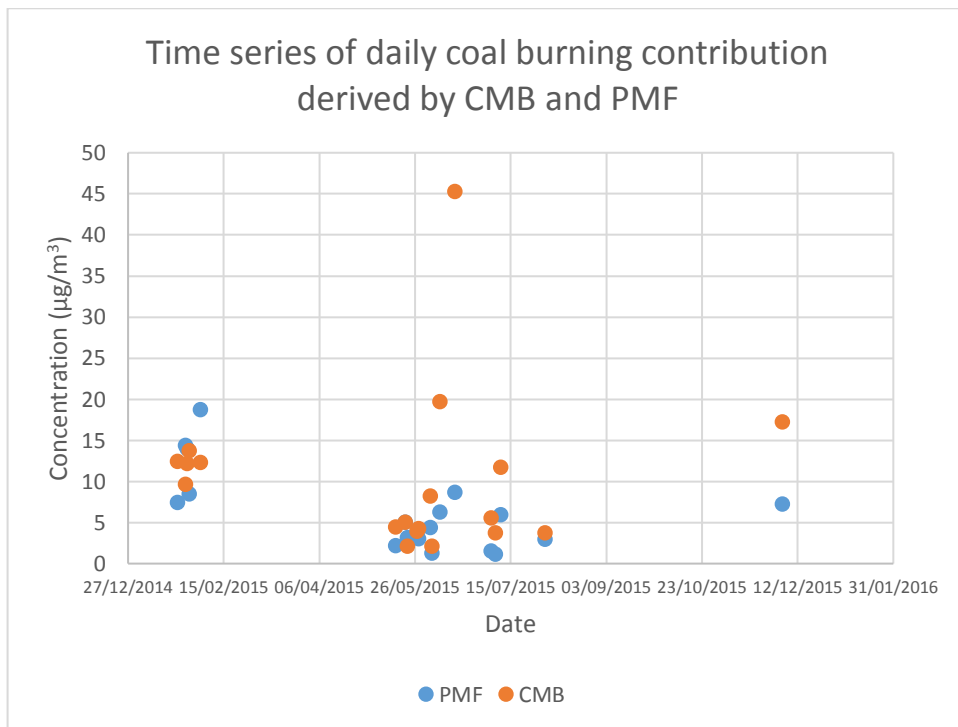
a)



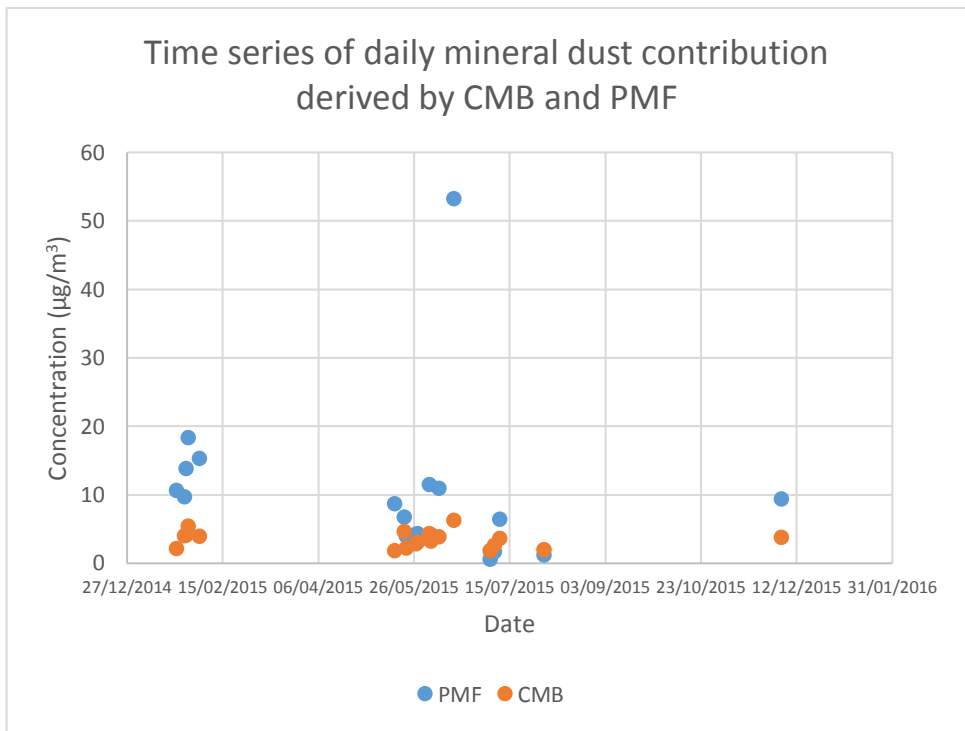
b)



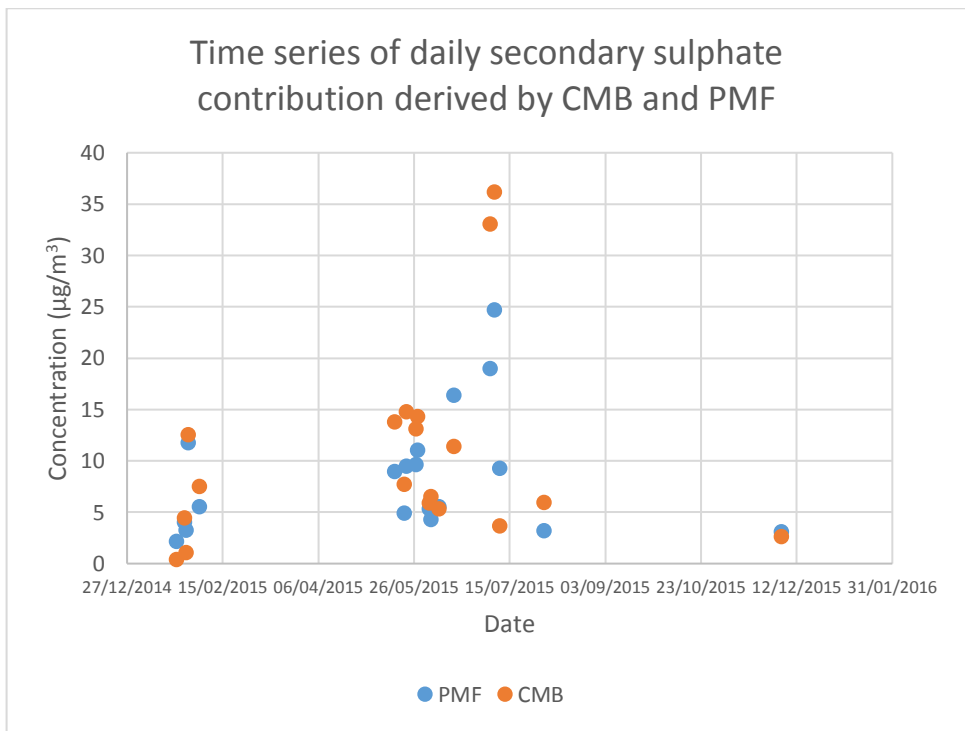
c)



d)



e)



f)

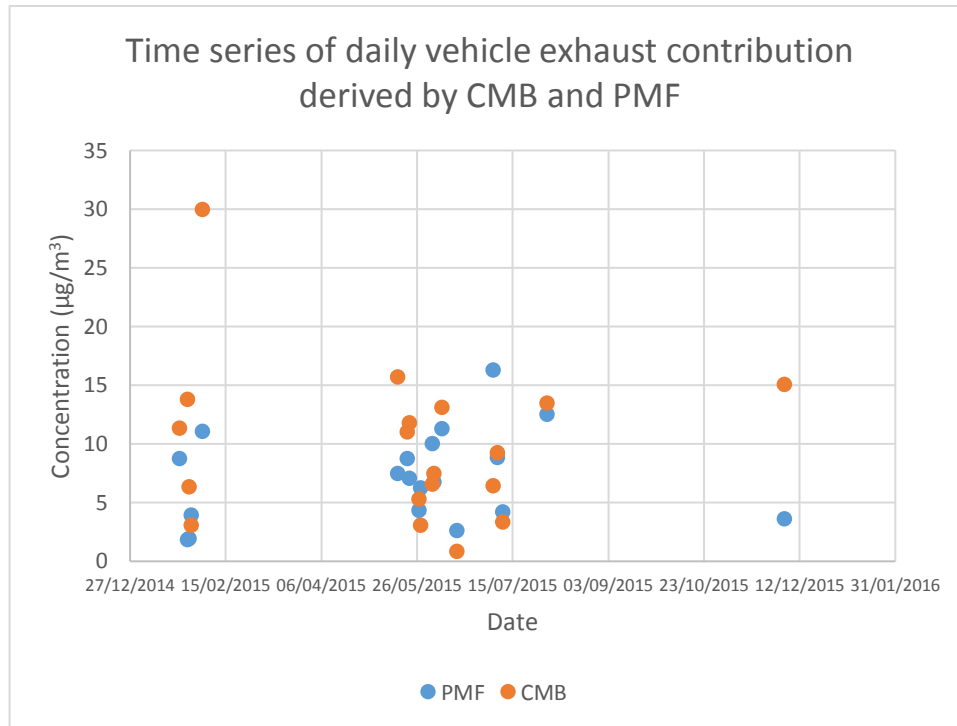


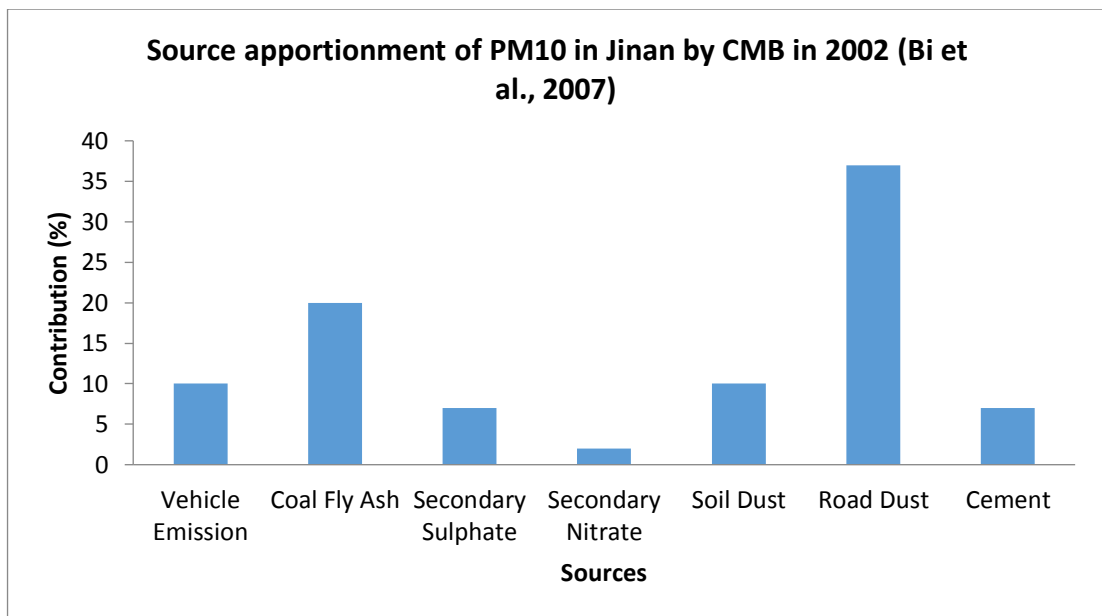
Figure 6-11 a)– f) Comparison of daily variations of PM_{2.5} apportionments for vehicle emission, soil/mineral dust, coal burning, industrial emission, secondary sulphate and secondary nitrate, respectively, by CMB and PMF.

Only selected data has been considered as CMB may fail to apportion some part of daily input. This could be due to the significant change of sources in some particular day or the variations of source activity. Among all of these sources, secondary nitrate has shown the greatest agreement at daily level. Secondary sulphate and vehicle emission are also simulated by CMB and PMF with similar results. However, CMB seems overestimate the coal burning contribution during the summer. In addition, CMB may also underestimate the contribution by mineral dust. This might because that there are more sources rather than soil affect the PM_{2.5}. The greatest differences occur on industrial emission. This could be due to the complexity of industrial activity in Jinan while there are many other sources rather than metal works itself in the city.

6.3 The Receptor Modelling results comparison between other studies in Jinan

As mentioned in Chapter one, there is a couple case study has discussed the sources of PM in Jinan. Though the majority of source identification have not employed receptor models yet, Bi et al. (2007) and Yang et al. (2013) used CMB and PMF to apporioned the PM₁₀ and PM_{2.5} in Jinan.

a)



b)

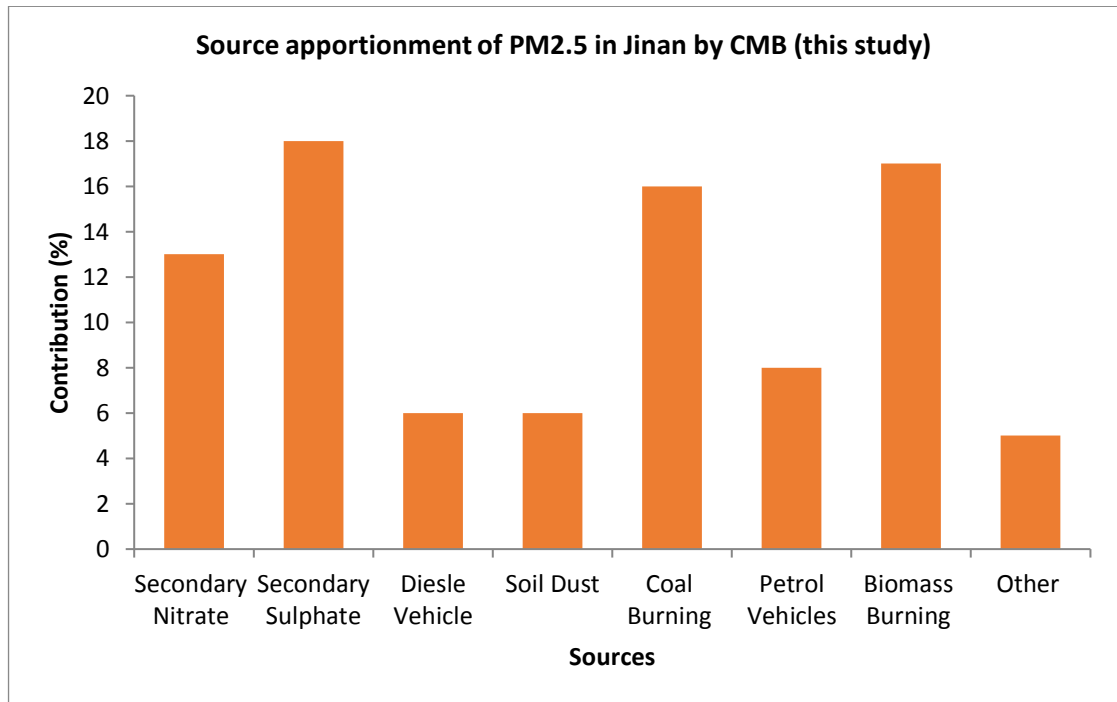


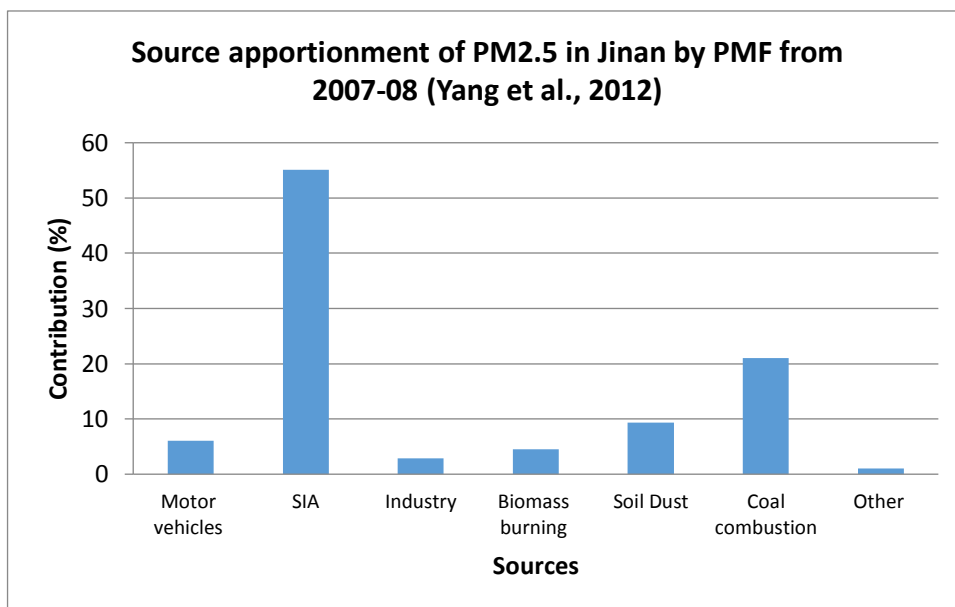
Figure 6-11 a) Source apportionment of PM₁₀ by CMB in 2002 (Bi et al. 2007); b) Source apportionment of PM_{2.5} by CMB in this study.

Figure 6-11 compares the CMB results between the PM₁₀ source apportionment in 2002 and this study. The two source apportionment provides very different results. The dominant contribution in PM₁₀ is mineral dust where the sum of soil dust, road dust and cement is more than half of total PM₁₀ mass. In addition, secondary sulphate and nitrate contribute only 10% of the total PM₁₀ mass in Jinan. On the contrary, the secondary sulphate and nitrate have become the major contributor in PM_{2.5} while soil dust contributes less than 10% in PM_{2.5}. This suggests the SIA plays a much greater role in PM_{2.5} rather than PM₁₀, which is consistent with the fact that more secondary aerosol formation is also an emerging trend in China's fine particle pollution today elsewhere in northern China (Huang et al. 2014).

However, the contribution from coal burning and vehicle emission is similar between PM₁₀ and PM_{2.5}, which suggests that coal burning and vehicle emission is both important in PM₁₀

and $PM_{2.5}$. Size distribution of different sources particles could be one of the major causes that result in these differences.

a)



b)

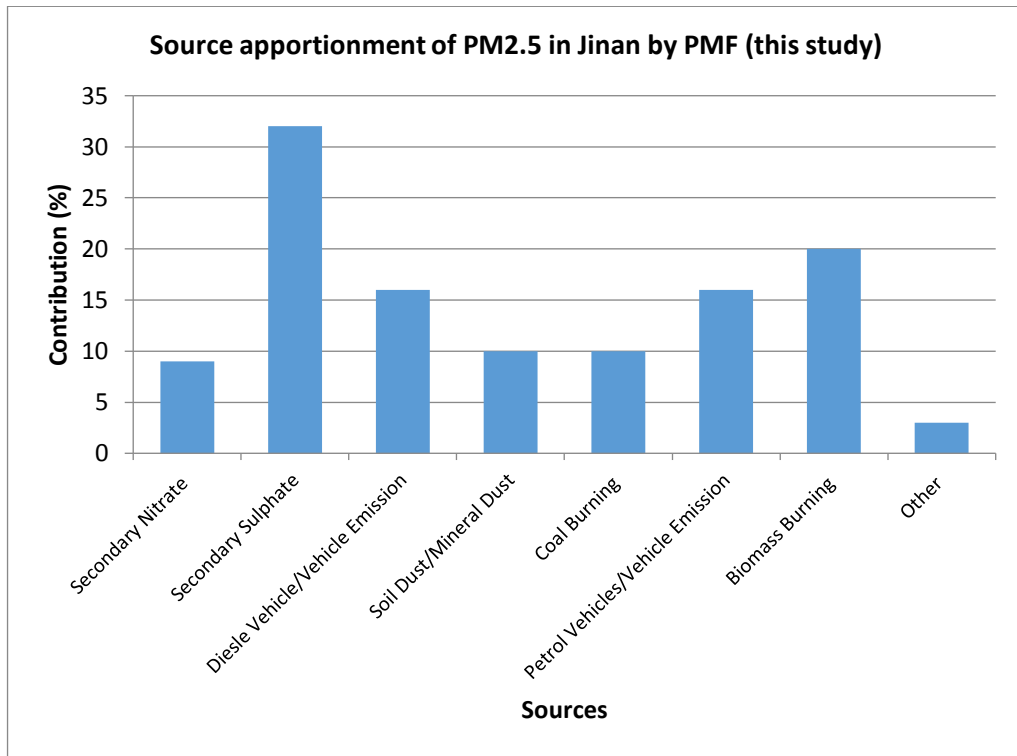


Figure 6-12 a) Source apportionment of PM_{2.5} by PMF in 2002 (Yang et al., 2012); b) Source apportionment of PM_{2.5} by PMF in this study.

Figure 6-12 on the other hand, compares the PM_{2.5} source apportionment of PMF by two different studies. There are more agreements between PMF modelling as well as the CMB modelling results in this study and previous PMF modelling by Yang et al. (2007). Both results show that there is a massive amount of secondary inorganic aerosol formation. The increase in mineral dust and vehicle emission is as expected since mineral dust represents other Al, Si, Fe and Ca rich sources and there is much more vehicles on the road today. However, the PMF modelling in this study has shown much higher biomass burning contribution but much lower coal burning contribution to PM_{2.5}. Further work needs to be done to investigate the causes of this difference including the local biomass burning profile establishment.

6.4 The similarity and difference of PM_{2.5} sources between Jinan and Beijing

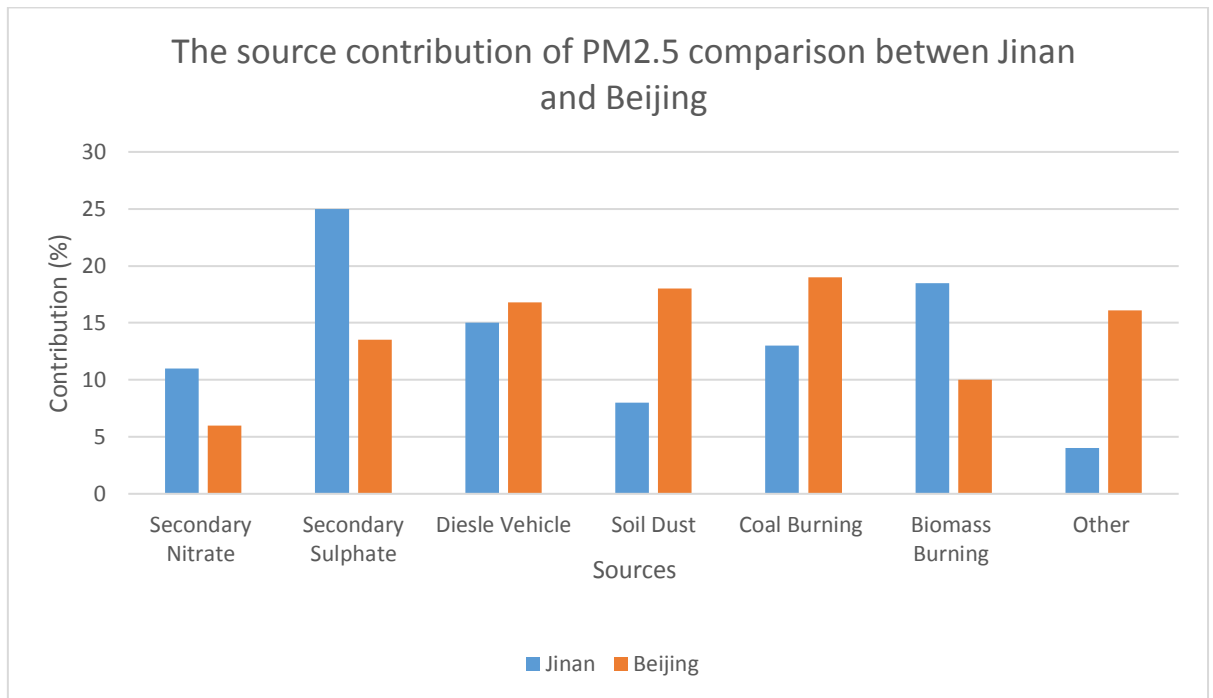


Figure 6-13 the PM_{2.5} source contribution in Jinan compared with source contributions to PM_{2.5} in Beijing from 2005-2014 based on the reviewed literature. Sources: (Okuda et al. 2004; Zheng et al. 2005; Zhang et al. 2007; Wang et al. 2009; Zhang et al. 2013; Huang et al. 2014; Liu et al. 2014; Huang et al. 2014;; Song et al. 2006a; Song et al. 2006b; Wang et al. 2008;)

Figure 6-13 illustrates the similarity and differences between the source contribution of PM_{2.5} in Jinan and Beijing. Both cities lie in North China Plain (NCP) and they are only about 400 km away. According to Figure 6-13, Jinan has greater impact on PM_{2.5} by secondary sulphate, nitrate and biomass burning. This is the common issue of PM_{2.5} pollution in northern China today (Huang et al. 2014). However, Beijing suffered more mineral dust than Jinan and this is likely due to its location where Beijing is closer to Gobi desert and the sandstorm may still play the role for the PM_{2.5} (Liu et al. 2014). The impact from traffic is pretty similar in this two cities. Overall, there is a considerable similarity of PM_{2.5} pollution in both cities. Since secondary aerosol formation is an regional issue (Guo

et al. 2013), the mitigation of $PM_{2.5}$ should be cooperated and conducted under an even bigger framework and expand the Beijing-Tianjin-Hebei mitigation strategy (Wang et al. 2015).

6.5 Conclusion

In this chapter, the results of CMB and PMF modelling results for Jinan have been compared. Some good agreements have been found in the comparison. Both models identify the secondary nitrate, secondary sulphate, vehicle exhaust, mineral/soil dust and biomass burning sources. Secondary nitrate and sulphate and vehicle emissions have shown the best agreements. The chemical mass closure also reveals that the estimation of SIA and mineral dust from CMB are relatively close. However, PMF may overestimate the contribution from secondary sulphate and underestimate the contribution from the coal burning. Unfortunately, the similarities between each model at seasonal and daily scale are getting worse. This is probably due to not only the source profiles that used in CMB are not representative enough but also relatively big errors remain in PMF. Meanwhile, the source apportionment results of Jinan and Beijing are also compared. Both cities are suffered by the similar contribution of secondary sulphate, secondary nitrate and coal burning. Overall, both models are good at evaluate the secondary nitrate in this case study. Other sources including mineral dust and general vehicle emissions can also be reasonably simulated. However, there are more difficulties while assessing the contribution by industrial and biomass burning, especially for PMF. It is more likely that CMB may apportion these two sources when the proper source profile is provided. In addition, the source profile by different industrial activity could be completely different while there is lots of secondary aerosol formation during the biomass burning process. More careful and

sophisticated measures are required when apportioning the contribution by these two source.

7 Chapter Seven Conclusion

This study and thesis present the source apportionment of PM_{2.5} in Jinan by different receptor models. The major sources that contribute the PM_{2.5} have been identified by CMB and PMF models separately. The similarity and differences of modelling results have been compared and the potential causes have also been discussed. This is first work that analyses the sources of PM_{2.5} using different receptor models for the same dataset and sampling campaign period in Jinan.

As a highly urbanised and industrial megacity, Jinan has suffered severe air pollution for more than two decades. By 2007, Cheng et al. (2011) suggested the annual mean PM_{2.5} concentration is 148.71 µg·m³. In this study, a sampling station consist of one four-channel small volume PM_{2.5} sampler (TH-16A PM Sampler), one medium volume sampler (TH-150F Automatic Medium Volume Sampler) and weather station was set up on the roof of lecture theatre building at central campus of Shandong University in central Jinan to find out the latest PM_{2.5} level. In total, 120 days of sampling have been conducted in Jinan where 103 samples of total 120 samples are available for whole measured chemical species. After the sampling, the samples have been stored in the freezer at -20 °C and brought back to Birmingham by the heat insulated foam box with commercial ice pack. Water-soluble ions (including Na⁺, NH₄⁺, K⁺, Mg²⁺, Ca²⁺, Cl⁻, NO₃⁻, SO₄²⁻, PO₄³⁻ and C₂O₂²⁻) was measured Dionex ICS 500 and Dionex ICS 2000. Trace metals (including Ag, Cd, In, Sn, Sb, Te, I, Rh, Ti, V, Cr, Mn, Fe, Co, Ni, Cu, La, Ce, Sm, Eu, Tb, Hf, Ba, Pr, Nd, Gd, Dy, Ho, Er, Tm, Yb, Lu, Ge, Zn, Ga, As, Se, Br, Rb, Sr, Y, Zr, Nb, Mo, W, Ir, Au, Hg, Pb, Pd, Pt, Tl, U, Cs, Bi, Na, Mg, Al, Si, P, S, Cl, K, Ca, Sc) have been measured by the

Thermo Scientific ARL™ QUANT'X EDXRF Spectrometer at the University of Massachusetts, Amherst in U.S.A.. The OC and EC were measured by the Sunset Laboratory Thermo-Optical Carbon Aerosol Analyser where EUSAAR2 (European Supersites for Atmospheric Aerosol Research) protocol is applied. The molecular markers including n-Alkanes, hopanes, PAHs, levoglucosan and cholesterol, however, have been extracted from the sample paper first and then analysed by GC-MS.

The physical and chemical analysis of Jinan's samples suggests that the annual mean concentration of PM_{2.5} is 79.3 µg·m⁻³, where the mean concentration during the five sampling periods (Winter-1, Early summer, Summer, Autumn and Winter-2) are 122.1, 57.4, 53.9, 97.7 and 82.1 µg·m⁻³. The average concentration of PM_{2.5} throughout the year is still much higher than both national guidance (PM_{2.5} annual mean concentration: 70 µg·m⁻³) and WHO guidance (15 µg·m⁻³) at annual level according to this periods mean. Both winter and autumn are the most polluted period which is about 1.5 – 2.2 times greater than late early summer and summer. However, the mean concentration in this study is lower than the mean concentration reported in 2007 (Cheng et al. 2011), implies that some measures on controlling the emissions in Jinan might be effective. This is thanks to the declining contribution from secondary inorganic aerosols. But there is also some other changes in terms of chemical composition. According to the mass closure analysis, organic matter (OM) dominates the PM_{2.5} compositions, which accounts for 35% of total PM_{2.5} mass throughout the year. This weights much more mass than the study reported earlier (Cheng et al. 2011; Yang et al. 2013). Except OM, secondary inorganic aerosols including ammonium, sulphate and nitrate are the other dominant chemicals, which accounts for 36% of total PM_{2.5} mass. In addition, EC, geological minerals, trace metal, chloride and rest of chemical species are accounted 5, 9, 1, 2 and 12 % of total PM_{2.5} mass.

Except the inorganics, the organic molecular markers (OMM) have also been measured and quantified including PAHs (retene, BaAnt, Chr, BbPyr, BaPyr, Ipyre, DBahAnt, BghiPer and COR), n-alkanes (C₂₄ to C₃₄), hopanes (17 α (H)-22,29,30-Trisnorhopane (C_{27 α}), 17 α ,21 β (H)-30-norhopane (C_{29 $\alpha\beta$}), 17 α (H),21 β (H)-Hopane (C_{30 $\alpha\beta$}), 22S-17 α (H),21 β (H)-30-Homohopane(C_{31 $\alpha\beta$ S}) and 22R-17 α (H),21 β (H)-30-Bishomohopane (C_{31 $\alpha\beta$ R})), and sterols (levoglucosan and cholesterol). These OMM are helpful and useful to tell the impact from fossil fuel combustion (including coal and vehicle emission), plantation, and biomass burning and cooking. Both PAHs and n-alkanes suggest that Jinan is suffered from the emission from coal burning related emission while hopanes indicate that the impact from traffic is significant. In summer, the natural PM_{2.5} source such as plant wax are also remarkable in Jinan. Moreover, levoglucosan imply that the biomass burning can contribute up to 4% of total PM_{2.5} mass in Jinan. Levoglucosan and cholesterol also imply the impact from cooking too.

In this project, both positive matrix factorisation (PMF) and chemical mass balance (CMB) have been applied for the receptor modelling to apportion the sources contribution to PM_{2.5}. In the PMF model run, PM_{2.5}, OC, EC, NH₄⁺, K⁺, Cl⁻, NO₃⁻, SO₄²⁻, Al, Si, Ti, Mn, Fe, Ni, Cu, Zn, As, Se, Pb, Ba, Ca, Sb, chrysene, benzo[b]fluorathene, indeno[1,2,3-cd]anthracene, dibenzo[a,h]anthracene and 17 α (H),21 β (H)-Hopane have been evaluated as suitable chemical species input and chosen for the model run. The six major sources are Secondary Nitrate, Secondary Sulphate, Coal Combustion, Mineral Dust, Vehicle Emission, Biomass Burning and other sources, which accounts for 9%, 32%, 10%, 10%, 16%, 20%, 12% and 3% of PM_{2.5} pollution in Jinan. OMM turns out helpful to identify the sources in PMF modelling to provide greater confidence, particularly for the vehicle exhaust and biomass burning. In addition, Error estimation is conducted by BS,

DISP and BS-DISP too. Neither significant rotational ambiguity nor any other major error has been found in this PMF modelling solution. The result is also comparable with chemical mass closure (CMC) for quality control and the results between the CMC and PMF have good agreements on mineral dust and secondary nitrate. But there is still covariance between some certain sources, which should be concerned while interpreting the factor profiles while resolved by the model. PMF also overestimate the contribution by secondary sulphate in the model run.

On the other hand, source apportionment by CMB modelling with PM_{2.5} profiles collected in China has been conducted in the meantime. Annually, eight major sources have been identified including Secondary Nitrate (13%), Secondary Sulphate (18%), coal burning (16%), metallurgic plant (11%), soil dust (6%), petrol vehicle emission (8%), diesel vehicle emission (6%) and biomass burning (17%) and 5% of total PM_{2.5} mass has not been resolved. There are significant seasonal variations for a couple of sources including secondary sulphate and nitrate, vehicle emission and coal burning throughout the year. The CMB model works well with provided source profiles where all the modelling performance parameters meet the criteria. However, the model performance is getting worse at seasonal and daily source apportionment level. The local source profiles are still required for more accurate CMB modelling. On the other hand, it might be more difficult for PMF to apportion the biomass burning as it will share some sulphate loading with secondary sulphate. PMF is also struggling identity for the industrial sources well as its composition varies massively from different type of industrial emissions. On the contrary, CMB could be a better option to tackle biomass burning and industrial emission if the local profiles are provided.

Overall, during the receptor modelling, PMF and CMB do show some reasonable agreements for in terms of modelling results in Jinan, especially the SIA, vehicle emission and coal burning. It is also found that Jinan and its nearby city Beijing share the very similar pollution by SIA and coal burning too.

Further work is required to further improve the receptor modelling and the source apportionment of $PM_{2.5}$ overall. For PMF and CMB modelling, longer period of sampling is recommended, which is particularly helpful to optimize the results quality of PMF as bigger sample population is preferred by the model. An another sampling site at rural background is also recommended for a better understanding of primary $PM_{2.5}$ emission and secondary formation within the city. Size-resolved sampling by e.g. MOUDI or CMS including SMPS can be also helpful to understand the portion of the secondary aerosol formation and distinguish the sources further. In addition, there is strong need to establish the local source profiles for CMB in order to achieve a more accurate modelling outcome, especially on daily and seasonal temporal scale. The profile including OMM for CMB can be also very helpful to apportion the sources in much more details than PMF. Other methods incorporating the back trajectories techniques including potential source contribution (PSCF), conditional probability function (CPF) should be used to have better understanding the impact by the long-range transport. High-resolution satellite image and remote sensing can be also deployed for tacking biomass burning emission.

In summary, both PMF and CMB should be applied in the future source apportionment case study for a more robust modelling. This work can be also helpful for the local authority to mitigate the $PM_{2.5}$ pollution in Jinan.

References

- Abdel-Shafy, H.I. & Mansour, M.S.M., 2015. A review on polycyclic aromatic hydrocarbons: Source, environmental impact, effect on human health and remediation. *Egyptian Journal of Petroleum*, 25(1), pp.107–123. Available at: <http://www.sciencedirect.com/science/article/pii/S1110062114200237>.
- Adam Reff, S.I.E.& P.V.B., 2012. Receptor Modeling of Ambient Particulate Matter Data Using Positive Matrix Factorization: Review of Existing Methods. *Journal of the Air & Waste Management Association*, 57(2), pp.146–154.
- Amato, F. et al., 2016. AIRUSE-LIFE + : a harmonized PM speciation and source apportionment in five southern European cities. , pp.3289–3309.
- Amato, F. et al., 2012. Emission factors from road dust resuspension in a Mediterranean freeway. *Atmospheric Environment*, 61, pp.580–587. Available at: <http://dx.doi.org/10.1016/j.atmosenv.2012.07.065>.
- Andra's Gelencse'r David Simpson, Asuncio'n Sa'nchez-Ochoa, Anne Kasper-Giebl, Hans Puxbaum, Alexandre Caseiro, Casimiro Pio, and Michel Legrand, B.M., 2007. Source apportionment of PM_{2.5} organic aerosol over Europe: Primary/secondary, natural/anthropogenic, and fossil/biogenic origin. *JOURNAL OF GEOPHYSICAL RESEARCH*, 112, pp.1–12.
- Belis, C.A. et al., 2013. Critical review and meta-analysis of ambient particulate matter source apportionment using receptor models in Europe. *Atmospheric Environment*, 69.

- Belis, C. a. et al., 2015. A new methodology to assess the performance and uncertainty of source apportionment models in intercomparison exercises. *Atmospheric Environment*, 119, pp.35–44. Available at: <http://linkinghub.elsevier.com/retrieve/pii/S1352231015302478>.
- Bi, X. et al., 2007a. Source apportionment of PM₁₀ in six cities of northern British Virgin Islands and northern China. *Atmospheric Environment*, 41(5), pp.903–912.
- Bi, X. et al., 2007b. Source apportionment of PM₁₀ in six cities of northern China. *Atmospheric Environment*, 41(5), pp.903–912.
- Brown, S.G. et al., 2015. Methods for estimating uncertainty in PMF solutions: Examples with ambient air and water quality data and guidance on reporting PMF results. *Science of the Total Environment*, 518–519, pp.626–635. Available at: <http://dx.doi.org/10.1016/j.scitotenv.2015.01.022>.
- Bullock, K.R. et al., 2008. Evaluation of the CMB and PMF models using organic molecular markers in fine particulate matter collected during the Pittsburgh Air Quality Study. , 42, pp.6897–6904.
- Cao, G.L. et al., 2011. Emission inventories of primary particles and pollutant gases for China. *Chinese Science Bulletin*, 56(8), pp.781–788.
- Cao, J.J. et al., 2013. Characteristics and sources of carbonaceous aerosols from Shanghai, China. *Atmospheric Chemistry and Physics*, 13(2), pp.803–817.
- Cao, J.J. et al., 2005. Characterization and source apportionment of atmospheric organic and elemental carbon during fall and winter of 2003 in Xi'an, China. *Atmospheric Chemistry and Physics Discussions*, 5(3), pp.3561–3593.

- Cao, J.J. et al., 2008. Size-differentiated source profiles for fugitive dust in the Chinese Loess Plateau. *Atmospheric Environment*, 42(10), pp.2261–2275.
- Caseiro, A. et al., 2009. Wood burning impact on PM10 in three Austrian regions. *Atmospheric Environment*, 43(13), pp.2186–2195. Available at: <http://dx.doi.org/10.1016/j.atmosenv.2009.01.012>.
- Cass, G.R., 1998. Organic molecular tracers for particulate air pollution sources. *TrAC - Trends in Analytical Chemistry*, 17(6), pp.356–366.
- Castro, L.M. et al., 1999. Carbonaceous aerosol in urban and rural European atmospheres: Estimation of secondary organic carbon concentrations. *Atmospheric Environment*, 33(17), pp.2771–2781.
- Chan Yao, X., C., 2008. Air pollution in mega cities in China. *Atmospheric Environment*, 42(2008), p.43.
- Chemistry, A., Atmospheric, P. & Techniques, M., 2013. Biomass burning contribution to Beijing aerosol *Biogeosciences*. , pp.7765–7781.
- Chen, F., Hu, W. & Zhong, Q., 2013. Emissions of particle-phase polycyclic aromatic hydrocarbons (PAHs) in the Fu Gui-shan Tunnel of Nanjing, China. *Atmospheric Research*, 124, pp.53–60.
- Chen, J. et al., 2016. A review of biomass burning: Emissions and impacts on air quality, health and climate in China. *Science of The Total Environment*, 579(November 2016), pp.1000–1034. Available at: <http://dx.doi.org/10.1016/j.scitotenv.2016.11.025>.
- Chen, L.W.A. et al., 2010. Toward effective source apportionment using positive matrix

- factorization: experiments with simulated PM_{2.5} data. *Journal of the Air & Waste Management Association* (1995), 60(1), pp.43–54.
- Cheng, S. et al., 2011. Evaluating PM_{2.5} ionic components and source apportionment in Jinan, China from 2004 to 2008 using trajectory statistical methods. *Journal of environmental monitoring: JEM*, 13(6), pp.1662–71. Available at: <http://www.ncbi.nlm.nih.gov/pubmed/21505680>.
- Cheng, Y. et al., 2013. Biomass burning contribution to Beijing aerosol. *Atmospheric Chemistry and Physics*, 13(15), pp.7765–7781.
- Cheng, Y. et al., 2016. Reactive nitrogen chemistry in aerosol water as a source of sulfate during haze events in China. *Science Advances*, 2(12), pp.e1601530–e1601530. Available at: <http://advances.sciencemag.org/cgi/doi/10.1126/sciadv.1601530>.
- Chow, J.C. et al., 2015. Mass reconstruction methods for PM_{2.5}: a review. *Air Quality, Atmosphere & Health*, pp.243–263. Available at: <http://link.springer.com/10.1007/s11869-015-0338-3>.
- Crippa, M. et al., 2014. Organic aerosol components derived from 25 AMS data sets across Europe using a consistent ME-2 based source apportionment approach. *Atmospheric Chemistry and Physics*, 14(12), pp.6159–6176.
- Dai, W. et al., 2013a. Chemical composition and source identification of PM_{2.5} in the suburb of Shenzhen, China. *Atmospheric Research*, 122, pp.391–400.
- Dai, W. et al., 2013b. Chemical composition and source identification of PM_{2.5} in the suburb of Shenzhen, China. *Atmospheric Research*, 122, pp.391–400. Available at: <http://dx.doi.org/10.1016/j.atmosres.2012.12.004>.

- Dameng, L., Shaopeng, G. & Xianghua, A., 2008. Distribution and source apportionment of polycyclic aromatic hydrocarbons from atmospheric particulate matter PM_{2.5} in Beijing. *Advances in Atmospheric Sciences*, 25(2), pp.297–305. Available at: <http://dx.doi.org/10.1007/s00376-008-0297-9>.
- Fabretti, J. et al., 2009. Elemental characterization and source identification of PM_{2.5} using Positive Matrix Factorization: The Malraux road tunnel, Nice, France. *Atmospheric Research*, 94(2), pp.320–329. Available at: <http://dx.doi.org/10.1016/j.atmosres.2009.06.010>.
- Feng, Y.C. et al., 2007. Source apportionment of ambient total suspended particulates and coarse particulate matter in urban areas of Jiaozuo, China. *Journal of the Air & Waste Management Association*, 57(5), pp.561–575.
- Fitzgerald, J.W., 1991. REVIEW ARTICLE MARINE AEROSOLS: A REVIEW., 25(3), pp.533–545.
- Fu, P. et al., 2008. Organic molecular compositions and temporal variations of summertime mountain aerosols over Mt. Tai, North China Plain. *Journal of Geophysical Research Atmospheres*, 113(19), pp.1–20.
- Gao, X.M. et al., 2011. Semi-continuous measurement of water-soluble ions in PM_{2.5} in Jinan, China: Temporal variations and source apportionments. *Atmospheric Environment*, 45(33), pp.6048–6056.
- Ge, X. et al., 2017. Aerosol characteristics and sources in Yangzhou, China resolved by offline aerosol mass spectrometry and other techniques. *Environmental Pollution*, 225, pp.74–85. Available at: <http://dx.doi.org/10.1016/j.envpol.2017.03.044>.

- Ge, X. et al., Characteristics and Formation Mechanisms of Fine Particulate Nitrate in Typical Urban Areas in China. , pp.1–12.
- Geng, N.B. et al., 2013. PM_{2.5} in an industrial district of Zhengzhou, China: Chemical composition and source apportionment. *Particuology*, 11(1), pp.99–109.
- Guo, H. et al., 2009. Receptor modeling of source apportionment of Hong Kong aerosols and the implication of urban and regional contribution. *Atmospheric Environment*, 43(6), pp.1159–1169.
- Guo, S. et al., 2013. Quantitative evaluation of emission controls on primary and secondary organic aerosol sources during Beijing 2008 Olympics. *Atmospheric Chemistry and Physics*, 13(16), pp.8303–8314.
- Han, B. et al., 2011. Source apportionment of ambient PM₁₀ in urban areas of Wuxi, China. *Frontiers of Environmental Science and Engineering in China*, 5(4), pp.552–563.
- Han, J. et al., 2014. Chemical Characterizations of PM₁₀ Profiles for Major Emission Sources in Xining, Northwestern China. *Aerosol and Air Quality Research*, 14(3), pp.1017–1027.
- Harrison, R.M. et al., 2012. Estimation of the Contributions of Brake Dust , Tire Wear , and Resuspension to Nonexhaust Traffic Particles Derived from Atmospheric Measurements.
- He, L.Y. et al., 2006. Chemical characterization of fine particles from on-road vehicles in the Wutong tunnel in Shenzhen, China. *Chemosphere*, 62(10), pp.1565–1573.

- He, L.Y. et al., 2004. Measurement of emissions of fine particulate organic matter from Chinese cooking. *Atmospheric Environment*, 38(38), pp.6557–6564.
- He, L.Y. et al., 2011. Submicron aerosol analysis and organic source apportionment in an urban atmosphere in Pearl River Delta of China using high-resolution aerosol mass spectrometry. *Journal of Geophysical Research-Atmospheres*, 116, p.15.
- Hedberg, E. et al., 2006. Is levoglucosan a suitable quantitative tracer for wood burning? Comparison with receptor modeling on trace elements in Lycksele, Sweden. *Journal of the Air & Waste Management Association* (1995), 56(12), pp.1669–78. Available at: <http://www.ncbi.nlm.nih.gov/pubmed/17195486>.
- Ho, K.F. et al., 2006. Source apportionment of PM_{2.5} in urban area of Hong Kong. *JOURNAL OF HAZARDOUS MATERIALS*, 138(1), pp.73–85.
- Hopke, P., 1991. Introduction to Receptor Modeling. *Chemometrics and Intelligent Systems*, 10, p.24.
- Hopke, P.K., 2016. A Review of Receptor Modeling Methods for Source Apportionment. *Journal of the Air & Waste Management Association*, 2247(January), p.10962247.2016.1140693. Available at: <http://www.tandfonline.com/doi/full/10.1080/10962247.2016.1140693>.
- Hopke, P.K., 2003. Recent developments in receptor modeling. *Journal of Chemometrics*, 17(5), pp.255–265.
- Hou, X.M. et al., 2008. Emission of fine organic aerosol from traditional charcoal broiling in China. *Journal of Atmospheric Chemistry*, 61(2), pp.119–131.

- Hu, J. et al., 2012. Seasonal variation and source apportionment of PAHs in TSP in the atmosphere of Guiyang, Southwest China. *Atmospheric Research*, 118, pp.271–279.
- Hu, X. et al., 2013. Size Distribution and Source Apportionment of Airborne Metallic Elements in Nanjing, China. *AEROSOL AND AIR QUALITY RESEARCH*, 13(6), p.1796+.
- Hua, Y. et al., 2015. Characteristics and source apportionment of PM_{2.5} during a fall heavy haze episode in the Yangtze River Delta of China. *Atmospheric Environment*, 123, pp.380–391. Available at: <http://dx.doi.org/10.1016/j.atmosenv.2015.03.046>.
- Huang, B. et al., 2013. Chemical composition, diurnal variation and sources of PM_{2.5} at two industrial sites of South China. *Atmospheric Pollution Research*, 4(3), pp.298–305. Available at: <http://dx.doi.org/10.5094/APR.2013.033>.
- Huang, L. et al., 2011. Chemical characteristics and source apportionment of PM₁₀ during a brown haze episode in Harbin, China. *Particuology*, 9(1), pp.32–38. Available at: <http://dx.doi.org/10.1016/j.partic.2010.07.022>.
- Huang, R.-J. et al., 2014. High secondary aerosol contribution to particulate pollution during haze events in China. *Nature*, 514(7521), pp.218–222. Available at: <http://dx.doi.org/10.1038/nature13774>.
- Huang, R.J. et al., 2014. High secondary aerosol contribution to particulate pollution during haze events in China. *Nature*, 514(7521), pp.218–222.
- Huang, X.F. et al., 2014. Source apportionment and secondary organic aerosol estimation of PM_{2.5} in an urban atmosphere in China. *Science China-Earth Sciences*, 57(6), pp.1352–1362.

iastate (2018) Station data and MetData. Available at:
http://mesonet.agron.iastate.edu/sites/windrose.phtml?network=WI_ASOS&station=CWA [Accessed on 15th of March, 2018]

Jiang, Y.L. et al., 2009. The sources and seasonal variations of organic compounds in PM_{2.5} in Beijing and Shanghai. *Journal of Atmospheric Chemistry*, 62(3), pp.175–192.

Jing, B. et al., 2017. Hygroscopic properties of potassium chloride and its internal mixtures with organic compounds relevant to biomass burning aerosol particles. *Scientific Reports*, (January), pp.1–11. Available at: <http://dx.doi.org/10.1038/srep43572>.

Jinxia Gu Daowen Han, Lujian Hou, S. Du, Jing Yi Guanghui Liu, Bin Han, J.X. & Bai, G.Y. & Z.-P., 2014. Major chemical compositions, possible sources, and mass closure analysis of PM_{2.5} in Jinan, China. *Air Qual Atmos Health*, 7, pp.251–262.

Ke, L., Liu, W., Wang, Y., Russell, A.G., et al., 2008. Comparison of PM_{2.5} source apportionment using positive matrix factorization and molecular marker-based chemical mass balance. *Science of the Total Environment*, 394(2–3), pp.290–302.

Ke, L., Liu, W., Wang, Y., Russell, A.G., et al., 2008. Comparison of PM_{2.5} source apportionment using positive matrix factorization and molecular marker-based chemical mass balance. , 94.

Kong, S. et al., 2011. Characterization of PM₁₀ source profiles for fugitive dust in Fushun—a city famous for coal. *Atmospheric Environment*, 45(30), pp.5351–5365. Available at: <http://dx.doi.org/10.1016/j.atmosenv.2011.06.050>.

Kong, S. et al., 2012. Chemical compositions and sources of atmospheric PM₁₀ in heating,

- non-heating and sand periods at a coal-based city in northeastern China. *J Environ Monit*, 14(3), pp.852–865.
- Kong, S. et al., 2010. Receptor modeling of PM_{2.5}, PM₁₀ and TSP in different seasons and long-range transport analysis at a coastal site of Tianjin, China. *Science of the Total Environment*, 408(20), pp.4681–4694. Available at: <http://dx.doi.org/10.1016/j.scitotenv.2010.06.005>.
- Kong, S. et al., 2014. Similarities and differences in PM_{2.5}, PM₁₀ and TSP chemical profiles of fugitive dust sources in a coastal oilfield city in China. *Aerosol and Air Quality Research*, 14(7), pp.2017–2028.
- Lee, S. et al., 2008. Source apportionment of PM_{2.5} : Comparing PMF and CMB results for four ambient monitoring sites in the southeastern United States. , 42, pp.4126–4137.
- Lei, C. et al., 2004. Study of PM_{2.5} in Beijing suburban site by neutron activation analysis and source apportionment. *Journal of Radioanalytical and Nuclear Chemistry*, 261(1), pp.87–94.
- Li, H. et al., 2016. Chemical characterization and source apportionment of PM_{2.5} aerosols in a megacity of Southeast China. *Atmospheric Research*, 181, pp.288–299. Available at: <http://dx.doi.org/10.1016/j.atmosres.2016.07.005>.
- Li, J. et al., 2014. Chemical characteristics and source apportionment of PM_{2.5} during the harvest season in eastern China's agricultural regions. *ATMOSPHERIC ENVIRONMENT*, 92, pp.442–448.
- Li, J. et al., 2006. Source seasonality of polycyclic aromatic hydrocarbons (PAHs) in a

- subtropical city, Guangzhou, South China. *Science of the Total Environment*, 355(1–3), pp.145–155.
- Li, J.D. et al., 2010. Chemical compositions and source apportionment of atmospheric PM10 in suburban area of Changsha, China. *Journal of Central South University of Technology*, 17(3), pp.509–515.
- Li, L. et al., 2016. Economic evaluation of the air pollution effect on public health in China's 74 cities. *SpringerPlus*, 5(1).
- Li, T.C. et al., 2013. Physicochemical Characteristics and Source Apportionment of Atmospheric Aerosol Particles in Kinmen-Xiamen Airshed. *Aerosol and Air Quality Research*, 13(1), pp.308–323.
- Li, W. et al., 2016. A review of single aerosol particle studies in the atmosphere of East Asia: Morphology, mixing state, source, and heterogeneous reactions. *Journal of Cleaner Production*, 112(January 2013), pp.1330–1349. Available at: <http://dx.doi.org/10.1016/j.jclepro.2015.04.050>.
- Li, W., Peng, Y. & Bai, Z., 2010. Distributions and sources of n-alkanes in PM2.5 at urban, industrial and coastal sites in Tianjin, China. *Journal of Environmental Sciences*, 22(10), pp.1551–1557. Available at: [http://dx.doi.org/10.1016/S1001-0742\(09\)60288-6](http://dx.doi.org/10.1016/S1001-0742(09)60288-6).
- Li, W.J., Shao, L.Y. & Buseck, P.R., 2010. and Physics Haze types in Beijing and the influence of agricultural biomass burning. , pp.8119–8130.
- Li, X. et al., 2007. Particulate and trace gas emissions from open burning of wheat straw and corn stover in China. *Environmental Science and Technology*, 41(17), pp.6052–

6058.

- Li, X. et al., 2013. Seasonal variation and source apportionment of organic and inorganic compounds in PM_{2.5} and PM₁₀ particulates in Beijing, China. *Journal of Environmental Sciences*, 25(4), pp.741–750. Available at: <http://www.sciencedirect.com/science/article/pii/S1001074212601211>.
- Li, Y.J. et al., 2017. Real-time chemical characterization of atmospheric particulate matter in China: A review. *Atmospheric Environment*, 158, pp.270–304. Available at: <http://dx.doi.org/10.1016/j.atmosenv.2017.02.027>.
- Liang, C.S. et al., 2016. Review on recent progress in observations, source identifications and countermeasures of PM_{2.5}. *Environment International*, 86, pp.150–170. Available at: <http://dx.doi.org/10.1016/j.envint.2015.10.016>.
- Lin, L., Lee, M.L. & Eatough, D.J., 2010. Review of Recent Advances in Detection of Organic Markers in Fine Particulate Matter and Their Use for Source Apportionment. *Journal of the Air & Waste Management Association (Air & Waste Management Association)*, 60(1), pp.3–25. Available at: <http://10.0.12.83/1047-3289.60.1.3%5Cnhttp://search.ebscohost.com/login.aspx?direct=true&db=a9h&AN=47331727&site=ehost-live>.
- Liu, B. et al., 2016. Chemical composition and source apportionment of ambient PM_{2.5} during the non-heating period in Taian, China. *Atmospheric Research*, 170, pp.23–33. Available at: <http://dx.doi.org/10.1016/j.atmosres.2015.11.002>.
- Liu, D. et al., 2013. The Use of Levoglucosan and Radiocarbon for Source Apportionment of PM_{2.5} Carbonaceous Aerosols at a Background Site in East China. *Environmental*

- Science & Technology, 47(18), pp.10454–10461.
- Liu, G. et al., 2015. Chemical composition and source apportionment of the ambient PM_{2.5} in Hangzhou, China. *Particuology*, 18, pp.135–143. Available at: <http://dx.doi.org/10.1016/j.partic.2014.03.011>.
- Liu, G.Q. et al., 2010. A source study of atmospheric polycyclic aromatic hydrocarbons in Shenzhen, South China. *Environmental Monitoring and Assessment*, 163(1–4), pp.599–606.
- Liu, Q. et al., 2014. Chemical characteristics and source apportionment of PM₁₀ during Asian dust storm and non-dust storm days in Beijing. *Atmospheric Environment*, 91, pp.85–94. Available at: <http://dx.doi.org/10.1016/j.atmosenv.2014.03.057>.
- Long, S. et al., 2014. Characteristics of secondary inorganic aerosol and sulfate species in size-fractionated aerosol particles in Shanghai. *Journal of Environmental Sciences*, 26(5), pp.1040–1051. Available at: [http://dx.doi.org/10.1016/S1001-0742\(13\)60521-5](http://dx.doi.org/10.1016/S1001-0742(13)60521-5).
- Ma, J.Z. et al., 2012. A review of atmospheric chemistry research in China: Photochemical smog, haze pollution, and gas-aerosol interactions. *Advances in Atmospheric Sciences*, 29(5), pp.1006–1026.
- Ma, W.L. et al., 2010. Seasonal variations of sources of polycyclic aromatic hydrocarbons (PAHs) to a northeastern urban city, China. *Chemosphere*, 79(4), pp.441–447. Available at: <http://dx.doi.org/10.1016/j.chemosphere.2010.01.048>.
- Masiol, M. et al., 2017. Sources of Submicrometre Particles Near a Major International Airport. *Atmospheric Chemistry and Physics Discussions*, (April), pp.1–61. Available

at: <http://www.atmos-chem-phys-discuss.net/acp-2017-150/>.

Miller, M.S., Friedlander, S.K. & Hidy, G.M., 1972. A chemical element balance for the Pasadena aerosol. *Journal of Colloid And Interface Science*, 39(1), pp.165–176.

Ni, T., Han, B. & Bai, Z., 2012. Source Apportionment of PM10 in Four Cities of Northeastern China. *Aerosol and Air Quality Research*, 12(4), pp.571–582.

Ni, T.R., Han, B. & Bai, Z.P., 2012. Source Apportionment of PM10 in Four Cities of Northeastern China. *Aerosol and Air Quality Research*, 12(4), pp.571–582.

Okuda, T. et al., 2004. Daily concentrations of trace metals in aerosols in Beijing, China, determined by using inductively coupled plasma mass spectrometry equipped with laser ablation analysis, and source identification of aerosols. *Science of the Total Environment*, 330(1–3), pp.145–158.

Paatero, P. et al., 2014. Methods for estimating uncertainty in factor analytic solutions. *Atmospheric Measurement Techniques*, 7(3).

Paatero, P. & Hopke, P.K., 2003. Discarding or downweighting high-noise variables in factor analytic models. *Analytica Chimica Acta*, 490(1–2), pp.277–289.

Paatero, P. & Tapper, U., 1993. Analysis of different modes of factor analysis as least squares fit problems. *Chemometrics and Intelligent Laboratory Systems*, 18(2), pp.183–194.

Paatero, P. & Tappert, U., 1994. Positive Matrix Factorization : A non-negative factor model with optimal utilization of error estimates of data values. *Environmetrics*, 5(April 1993), pp.111–126.

- Pachon, J.E. et al., 2013. Revising the use of potassium (K) in the source apportionment of PM_{2.5}. *Atmospheric Pollution Research*, 4(1), pp.14–21. Available at: <http://linkinghub.elsevier.com/retrieve/pii/S1309104215303962>.
- Pant, P., 2014. RECEPTOR MODELLING STUDIES OF AIRBORNE PARTICULATE MATTER IN THE UNITED KINGDOM AND INDIA by PALLAVI PANT Submitted to the University of Birmingham in partial fulfilment for the ., (September).
- Pant, P. & Harrison, R.M., 2013. Estimation of the contribution of road traffic emissions to particulate matter concentrations from field measurements: A review. *Atmospheric Environment*, 77, pp.78–97. Available at: <http://dx.doi.org/10.1016/j.atmosenv.2013.04.028>.
- Pant, P., Yin, J. & Harrison, R.M., 2014. Sensitivity of a Chemical Mass Balance model to different molecular marker traffic source profiles. *Atmospheric Environment*, 82, pp.238–249. Available at: <http://dx.doi.org/10.1016/j.atmosenv.2013.10.005>.
- Pei, B. et al., 2016. Emissions and source profiles of PM_{2.5} for coal-fired boilers in the Shanghai megacity, China. , 7, pp.1–8.
- Pernigotti, D., Belis, C. a. & Spanó, L., 2016. SPECIEUROPE: The European data base for PM source profiles. *Atmospheric Pollution Research*, 7(2), pp.307–314.
- Pui, D.Y.H., Chen, S.C. & Zuo, Z.L., 2014. PM_{2.5} in China: Measurements, sources, visibility and health effects, and mitigation. *Particuology*, 13, pp.1–26.
- Qiao, T. et al., 2016. Simultaneous monitoring and compositions analysis of PM₁ and PM_{2.5} in Shanghai: Implications for characterization of haze pollution and source

apportionment. *Science of the Total Environment*, 557–558, pp.386–394. Available at: <http://dx.doi.org/10.1016/j.scitotenv.2016.03.095>.

Qiu, L.M. et al., 2012. Source Apportionment of Ambient PM₁₀ in the Urban Area of Longyan City, China: a Comparative Study Based on Chemical Mass Balance Model and Factor Analysis Method. *Chemical Research in Chinese Universities*, 28(2), pp.204–208.

Querol, X. et al., 2008. Inter-comparison of receptor models for PM source apportionment : Case study in an industrial area. , 42, pp.3820–3832.

Querol, X. et al., 2006. Speciation and sources of atmospheric aerosols in a highly industrialised emerging mega-city in Central China. *Journal of Environmental Monitoring*, 8(10), pp.1049–1059.

Reff, a, Eberly, S.I. & Bhave, P. V, 2007. Receptor modeling of ambient particulate matter data using positive matrix factorization: review of existing methods. *J Air Waste Manag Assoc*, 57(February), pp.146–154.

Rogge, W.F. et al., 1993. Sources of Fine Organic Aerosol .4. Particulate Abrasion Products From Leaf Surfaces of Urban Plants. *Environmental Science & Technology*, 27, pp.2700–2711.

Schkolnik, G. et al., 2005. A new method for the determination of levoglucosan, methylerythritol and related compounds and its application for rainwater and smoke samples. *Environmental Science & Technology*, 39(8), pp.2744–2752.

Seguel A., R., Morales S., R.G.E. & Leiva G., M.A., 2009. Estimations of primary and secondary organic carbon formation in PM_{2.5} aerosols of Santiago City, Chile.

- Atmospheric Environment, 43(13), pp.2125–2131.
- Senlin, L. et al., 2007. Chemical elements and their source apportionment of PM₁₀ in Beijing urban atmosphere. *Environmental Monitoring and Assessment*, 133(1–3), pp.79–85.
- Shen, Z. et al., 2010. Characteristics of traffic-related emissions: A case study in roadside ambient air over xi'an, China. *Aerosol and Air Quality Research*, 10(3), pp.292–300.
- Simoneit, B.R., 1999. A review of biomarker compounds as source indicators and tracers for air pollution. *Environmental science and pollution research international*, 6(3), pp.159–169.
- Simoneit, B.R.T., 2002. Biomass burning - A review of organic tracers for smoke from incomplete combustion,
- Simoneit, B.R.T. et al., 1999a. Levoglucosan, a tracer for cellulose in biomass burning and atmospheric particles. *Atmospheric Environment*, 33(2), pp.173–182. Available at: <http://www.sciencedirect.com/science/article/pii/S1352231098001459>.
- Simoneit, B.R.T. et al., 1999b. Levoglucosan, a tracer for cellulose in biomass burning and atmospheric particles. *Atmospheric Environment*, 33(2), pp.173–182.
- Simoneit, B.R.T. et al., 1991. Molecular marker study of extractable organic matter in aerosols from urban areas of China. *Atmospheric Environment Part A, General Topics*, 25(10), pp.2111–2129.
- Solomon, P. a. et al., 1989. Chemical Characteristics of PM₁₀ Aerosols Collected in the Los Angeles Area. *Japca*, 39(2), pp.154–163. Available at:

<http://www.tandfonline.com/doi/abs/10.1080/08940630.1989.10466515>.

Song, Y., Zhang, Y., et al., 2006. Source apportionment of PM_{2.5} in Beijing by positive matrix factorization. *Atmospheric Environment*, 40(8), pp.1526–1537.

Song, Y. et al., 2007. Source apportionment of PM_{2.5} in Beijing in 2004. *Journal of Hazardous Materials*, 146(1–2), pp.124–130.

Song, Y., Xie, S., et al., 2006. Source apportionment of PM_{2.5} in Beijing using principal component analysis/absolute principal component scores and UNMIX. *Science of the Total Environment*, 372(1), pp.278–286.

Sun, Y. et al., 2005. Chemical composition of dust storms in Beijing and implications for the mixing of mineral aerosol with pollution aerosol on the pathway. *Journal of Geophysical Research Atmospheres*, 110(24), pp.1–11.

Sun, Y. et al., 2004. The air-borne particulate pollution in Beijing - Concentration, composition, distribution and sources. *Atmospheric Environment*, 38(35), pp.5991–6004.

Taiwo, A.M., Harrison, R.M. & Shi, Z., 2014. A review of receptor modelling of industrially emitted particulate matter. *Atmospheric Environment*, 97, pp.109–120. Available at: <http://dx.doi.org/10.1016/j.atmosenv.2014.07.051>.

Tao, J. et al., 2017. Source apportionment of PM_{2.5} at urban and suburban areas of the Pearl River Delta region, south China - With emphasis on ship emissions. *Science of the Total Environment*, 574, pp.1559–1570. Available at: <http://dx.doi.org/10.1016/j.scitotenv.2016.08.175>.

- Tao, J. et al., 2014. PM_{2.5} pollution in a megacity of southwest China: source apportionment and implication. *Atmos. Chem. Phys.*, 14, pp.8679–8869.
- Tian, Y.Z. et al., 2013. Long-term variation of the levels, compositions and sources of size-resolved particulate matter in a megacity in China. *Science of the Total Environment*, 463–464, pp.462–468. Available at: <http://dx.doi.org/10.1016/j.scitotenv.2013.06.055>.
- Urban, R.C. et al., 2012. Use of levoglucosan, potassium, and water-soluble organic carbon to characterize the origins of biomass-burning aerosols. *Atmospheric Environment*, 61, pp.562–569. Available at: <http://dx.doi.org/10.1016/j.atmosenv.2012.07.082>.
- Viana, M. et al., 2008. Source apportionment of particulate matter in Europe: A review of methods and results. *Journal of Aerosol Science*, 39(10), pp.827–849.
- Wählin, P., Berkowicz, R. & Palmgren, F., 2006. Characterisation of traffic-generated particulate matter in Copenhagen. *Atmospheric Environment*, 40(12), pp.2151–2159.
- Wang, F. et al., 2014. Environmental Science Processes & Impacts. *Environmental Science: Processes & Impacts*, 17(2011), pp.197–205. Available at: <http://dx.doi.org/10.1039/C4EM00570H>.
- Wang, G. et al., 2006. Molecular, seasonal and spatial distributions of organic aerosols from fourteen Chinese cities. *Environmental Science and Technology*, 40(15), pp.4619–4625.

- Wang, G. et al., 2016. Persistent sulfate formation from London Fog to Chinese haze. Proceedings of the National Academy of Sciences, p.201616540. Available at: <http://www.pnas.org/lookup/doi/10.1073/pnas.1616540113>.
- Wang, G. et al., 2009. Size-distributions of n-hydrocarbons, PAHs and hopanes and their sources in the urban, mountain and marine atmospheres over East Asia. Atmospheric Chemistry and Physics Discussions, 9(3), pp.13859–13888.
- Wang, G. et al., 2015. Source apportionment and seasonal variation of PM_{2.5} carbonaceous aerosol in the Beijing-Tianjin-Hebei Region of China. ENVIRONMENTAL MONITORING AND ASSESSMENT, 187(3).
- Wang, H. et al., 2008. Long-term monitoring and source apportionment of PM_{2.5}/PM₁₀ in Beijing, China. Journal of Environmental Sciences, 20(11), pp.1323–1327.
- Wang, H.L. et al., 2009. Characterization of PM(2.5)/PM(2.5-10) and source tracking in the juncture belt between urban and rural areas of Beijing. Chinese Science Bulletin, 54(14), pp.2506–2515.
- Wang, H.L. et al., 2008. Polycyclic aromatic hydrocarbons from rural household biomass burning in a typical Chinese village. Science in China, Series D: Earth Sciences, 51(7), pp.1013–1020.
- Wang, J. et al., 2016. Characterization of PM_{2.5} in Guangzhou, China: Uses of organic markers for supporting source apportionment. Science of the Total Environment, 550(97), pp.961–971. Available at: <http://dx.doi.org/10.1016/j.scitotenv.2016.01.138>.
- Wang, L. et al., 2013. Source apportionment of particulate pollutants in the atmosphere

- over the Northern Yellow Sea. *Atmospheric Environment*, 70, pp.425–434.
- Wang, L.T. et al., 2014. The 2013 severe haze over southern Hebei, China: model evaluation, source apportionment, and policy implications. *Atmospheric Chemistry and Physics*, 14(6), pp.3151–3173.
- Wang, Q. et al., 2009. Source apportionment of fine organic aerosols in Beijing. *Atmospheric Chemistry and Physics Discussions*, 9(2), pp.9043–9080.
- Wang, Q.Q. et al., 2015. Organic tracer-based source analysis of PM_{2.5} organic and elemental carbon: A case study at Dongguan in the Pearl River Delta, China. *Atmospheric Environment*, 118(AUGUST), pp.164–175.
- Wang, W. et al., 2011. Atmospheric concentrations and air-soil gas exchange of polycyclic aromatic hydrocarbons (PAHs) in remote, rural village and urban areas of Beijing-Tianjin region, North China. *Science of the Total Environment*, 409(15), pp.2942–2950.
- Wang, X.H. et al., 2006. Chemical composition and sources of PM₁₀ and PM_{2.5} aerosols in Guangzhou, China. *Environmental Monitoring and Assessment*, 119(1–3), pp.425–439.
- Wang, Y. et al., 2012. Source apportionment of airborne particulate matter using inorganic and organic species as tracers. *Atmospheric Environment*, 55, pp.525–532.
- Watson, J.G. et al., 2002. Receptor modeling application framework for particle source apportionment. , 49, pp.1093–1136.
- Wei, Z. et al., 2014. The 2013 severe haze over the Southern Hebei, China: PM_{2.5}

composition and source apportionment. *ATMOSPHERIC POLLUTION RESEARCH*, 5(4), pp.759–768.

WHO (2005) WHO Air quality guidelines for particulate matter, ozone, nitrogen dioxide and sulfur dioxide : global update 2005 : summary of risk assessment. Available at: <http://apps.who.int/iris/handle/10665/69477> [Accessed on 26th of June, 2016]

Wu, B. et al., 2016. Characterization of the chemical composition of PM_{2.5} emitted from on-road China III and China IV diesel trucks in Beijing, China. *Science of the Total Environment*, 551–552, pp.579–589.

Wu, G. et al., 2013. Chemical composition, mass closure and sources of atmospheric PM₁₀ from industrial sites in Shenzhen, China. *JOURNAL OF ENVIRONMENTAL SCIENCES-CHINA*, 25(8), pp.1626–1635.

Wu, L. et al., 2009. Secondary organic carbon quantification and source apportionment of PM₁₀ in Kaifeng, China. *Journal of Environmental Sciences*, 21(10), pp.1353–1362.

Xiao, R. et al., 2011. Characterization and source apportionment of submicron aerosol with aerosol mass spectrometer during the PRIDE-PRD 2006 campaign. *Atmospheric Chemistry and Physics*, 11(14), pp.6911–6929.

Xu, P. et al., 2011. Aerosol size distributions in urban Jinan: Seasonal characteristics and variations between weekdays and weekends in a heavily polluted atmosphere. *Environmental Monitoring and Assessment*, 179(1–4), pp.443–456.

Yang, B. et al., 2013. Science of the Total Environment Source apportionment of polycyclic aromatic hydrocarbons in soils of Huanghuai Plain , China : Comparison of three receptor models. *Science of the Total Environment*, The, 443, pp.31–39.

Available at: <http://dx.doi.org/10.1016/j.scitotenv.2012.10.094>.

Yang, L. et al., 2012. Airborne fine particulate pollution in Jinan, China: Concentrations, chemical compositions and influence on visibility impairment. *Atmospheric Environment*, 55, pp.506–514. Available at: <http://dx.doi.org/10.1016/j.atmosenv.2012.02.029>.

Yang, L. et al., 2013. Source identification and health impact of PM_{2.5} in a heavily polluted urban atmosphere in China. *Atmospheric Environment*, 75, pp.265–269. Available at: <http://dx.doi.org/10.1016/j.atmosenv.2013.04.058>.

Yao, L. et al., 2016. Sources apportionment of PM_{2.5} in a background site in the North China Plain. *Science of the Total Environment*, 541, pp.590–598. Available at: <http://dx.doi.org/10.1016/j.scitotenv.2015.09.123>.

Yao, Q. et al., 2009. Studies on formation and control of combustion particulate matter in China: A review. *ENERGY*, 34(9), pp.1296–1309.

Yao, X. et al., 2002. The water-soluble ionic composition of PM_{2.5} in Shanghai and Beijing, China. *Atmospheric Environment*, 36(26), pp.4223–4234.

Ye, Z. et al., 2017. Chemical characterization of fine particulate matter in Changzhou, China, and source apportionment with offline aerosol mass spectrometry. *Atmospheric Chemistry and Physics*, 17(4), pp.2573–2592.

Yin, J. et al., 2015. Receptor modelling of fine particles in southern England using CMB including comparison with AMS-PMF factors. , pp.2139–2158.

Yin, J. et al., 2010. Source apportionment of fine particles at urban background and rural

- sites in the UK atmosphere. *Atmospheric Environment*, 44(6), pp.841–851.
- Yu, L. et al., 2013. Characterization and source apportionment of PM_{2.5} in an urban environment in Beijing. *Aerosol and Air Quality Research*, 13(2).
- Yuan, Z.B. et al., 2009. Source analysis of volatile organic compounds by positive matrix factorization in urban and rural environments in Beijing. *Journal of Geophysical Research-Atmospheres*, 114, p.14.
- Yuesi, W. et al., 2014. Mechanism for the formation of the January 2013 heavy haze pollution episode over central and eastern China. , 57(1), pp.14–25.
- Zhang, D., Liu, J. & Li, B., 2014. Tackling air pollution in China-What do we learn from the great smog of 1950s in London. *Sustainability (Switzerland)*, 6(8), pp.5322–5338.
- Zhang, N. et al., 2016. Development of source profiles and their application in source apportionment of PM_{2.5} in Xiamen, China. *Frontiers of Environmental Science & Engineering*, 10(5), p.17. Available at: <http://link.springer.com/10.1007/s11783-016-0879-1>.
- Zhang, Q. et al., 2014. Chemical profiles of urban fugitive dust over Xi'an in the south margin of the Loess Plateau, China. *Atmospheric Pollution Research*, 5(August), pp.421–430. Available at: <http://search.ebscohost.com/login.aspx?direct=true&AuthType=ip,uid&db=eih&AN=97137545&site=ehost-live>.
- Zhang, R. et al., 2013. Chemical characterization and source apportionment of PM_{2.5} in Beijing: Seasonal perspective. *Atmospheric Chemistry and Physics*, 13(14), pp.7053–7074.

- Zhang, T. et al., 2014. Characterization and seasonal variations of levoglucosan in fine particulate matter in Xi'an, China. *Journal of the Air & Waste Management Association*, 64(11), pp.1317–1327. Available at: <http://www.tandfonline.com/doi/abs/10.1080/10962247.2014.944959>.
- Zhang, T. et al., 2008. Identification and estimation of the biomass burning contribution to Beijing aerosol using levoglucosan as a molecular marker. *Atmospheric Environment*, 42(29), pp.7013–7021.
- Zhang, W. et al., 2007. Source apportionment for urban PM10 and PM2.5 in the Beijing area. *Chinese Science Bulletin*, 52(5), pp.608–615.
- Zhang, Y. et al., 2008. Characteristics of particulate carbon emissions from real-world Chinese coal combustion. *Environmental Science and Technology*, 42(14), pp.5068–5073.
- Zhang, Y. et al., 2015. Chemical characterization of PM2.5 emitted from on-road heavy-duty diesel trucks in China. *Atmospheric Environment*, 122, pp.885–891. Available at: <http://dx.doi.org/10.1016/j.atmosenv.2015.07.014>.
- Zhang, Y. et al., 2015. Source apportionment of elemental carbon in Beijing, China: insights from radiocarbon and organic marker measurements. *Environmental Science & Technology*, p.150626152257002. Available at: <http://pubs.acs.org/doi/abs/10.1021/acs.est.5b01944>.
- Zhang, Y. et al., 2009a. Source apportionment of primary and secondary organic aerosols using positive matrix factorization (PMF) of molecular markers. *Atmospheric Environment*, 43(34), pp.5567–5574.

- Zhang, Y. et al., 2009b. Source apportionment of primary and secondary organic aerosols using positive matrix factorization (PMF) of molecular markers. *Atmospheric Environment*, 43(34), pp.5567–5574. Available at: <http://dx.doi.org/10.1016/j.atmosenv.2009.02.047>.
- Zhang, Y.-L. et al., 2014. Radiocarbon-Based Source Apportionment of Carbonaceous Aerosols at a Regional Background Site on Hainan Island, South China. *ENVIRONMENTAL SCIENCE & TECHNOLOGY*, 48(5), pp.2651–2659.
- Zhang, Y.L. et al., 2015. Fossil vs. non-fossil sources of fine carbonaceous aerosols in four Chinese cities during the extreme winter haze episode of 2013. *Atmospheric Chemistry and Physics*, 15(3), pp.1299–1312.
- Zhang, Y.L. et al., 2012. Radiocarbon-based source apportionment of elemental carbon and organic carbon at a regional background site on Hainan Island, South China. , 12(2005), p.10841.
- Zhang, Y.X. et al., 2009. Sensitivity of a molecular marker based positive matrix factorization model to the number of receptor observations. *Atmospheric Environment*, 43(32), pp.4951–4958. Available at: <http://dx.doi.org/10.1016/j.atmosenv.2009.07.009>.
- Zhang, Y.X. et al., 2007. Source profiles of particulate organic matters emitted from cereal straw burnings. *Journal of Environmental Sciences-China*, 19(2), pp.167–175.
- Zhao, M. et al., 2015. Chemical characterization, the transport pathways and potential sources of PM_{2.5} in Shanghai: Seasonal variations. *Atmospheric Research*, 158–159, pp.66–78. Available at:

<http://www.sciencedirect.com/science/article/pii/S0169809515000447>.

Zhao, Q. et al., 2010. Dust storms come to Central and Southwestern China, too: implications from a major dust event in Chongqing. *Atmospheric Chemistry and Physics*, 10(6), pp.2615–2630.

Zhao, X. et al., 2015. Composition profiles of organic aerosols from Chinese residential cooking: Case study in urban Guangzhou, south China. *Journal of Atmospheric Chemistry*, 72(1), pp.1–18.

Zheng, G.J. et al., 2015. Exploring the severe winter haze in Beijing : the impact of synoptic weather , regional transport and heterogeneous reactions. , pp.2969–2983.

Zheng, M. et al., 2005. Seasonal trends in PM_{2.5} source contributions in Beijing, China. *Atmospheric Environment*, 39(22), pp.3967–3976. Available at: <http://linkinghub.elsevier.com/retrieve/pii/S1352231005003389>.

Zheng, M. et al., 2005. Seasonal trends in PM_{2.5} source contributions in Beijing, China. *Atmospheric Environment*, 39(22), pp.3967–3976.

Zhou, S.Z. et al., 2012. Formation of secondary organic carbon and long-range transport of carbonaceous aerosols at Mount Heng in South China. *Atmospheric Environment*, 63, pp.203–212.

Zíková, N. et al., 2016. On the source contribution to Beijing PM_{2.5} concentrations. *Atmospheric Environment*, 134, pp.84–95.

郑玫 et al., 2014. 中国pm_{2.5}来源解析方法综述. *北京大学学报(自然科学版)*, 50(6), pp.1141–1154. [Zheng et al. (2014) Source apportionment of PM_{2.5} in China: a

review. Acta Scientiarum Naturalium Universitatis Pekinensis 50(6), PP.1141-1154]